frontiers | Research Topics

Novel phenotyping and risk stratification strategies for heart failure

Edited by
Jeffrey Shi Kai Chan, Ying Liu, Ana Ciobanu, Tong Liu and Aggeliki Gkouziouta

Published in
Frontiers in Cardiovascular Medicine

ISSN 1664-8714
ISBN 978-2-83251-376-7
DOI 10.3389/978-2-83251-376-7

About Frontiers

Frontiers is more than just an open access publisher of scholarly articles: it is a pioneering approach to the world of academia, radically improving the way scholarly research is managed. The grand vision of Frontiers is a world where all people have an equal opportunity to seek, share and generate knowledge. Frontiers provides immediate and permanent online open access to all its publications, but this alone is not enough to realize our grand goals.

Frontiers journal series

The Frontiers journal series is a multi-tier and interdisciplinary set of open-access, online journals, promising a paradigm shift from the current review, selection and dissemination processes in academic publishing. All Frontiers journals are driven by researchers for researchers; therefore, they constitute a service to the scholarly community. At the same time, the *Frontiers journal series* operates on a revolutionary invention, the tiered publishing system, initially addressing specific communities of scholars, and gradually climbing up to broader public understanding, thus serving the interests of the lay society, too.

Dedication to quality

Each Frontiers article is a landmark of the highest quality, thanks to genuinely collaborative interactions between authors and review editors, who include some of the world's best academicians. Research must be certified by peers before entering a stream of knowledge that may eventually reach the public - and shape society; therefore, Frontiers only applies the most rigorous and unbiased reviews. Frontiers revolutionizes research publishing by freely delivering the most outstanding research, evaluated with no bias from both the academic and social point of view. By applying the most advanced information technologies, Frontiers is catapulting scholarly publishing into a new generation.

What are Frontiers Research Topics?

Frontiers Research Topics are very popular trademarks of the *Frontiers journals series*: they are collections of at least ten articles, all centered on a particular subject. With their unique mix of varied contributions from Original Research to Review Articles, Frontiers Research Topics unify the most influential researchers, the latest key findings and historical advances in a hot research area.

Find out more on how to host your own Frontiers Research Topic or contribute to one as an author by contacting the Frontiers editorial office: frontiersin.org/about/contact

Novel phenotyping and risk stratification strategies for heart failure

Topic editors

Jeffrey Shi Kai Chan — Cardiovascular Analytics Group, Hong Kong, SAR China
Ying Liu — Dalian Medical University, China
Ana Ciobanu — Carol Davila University of Medicine and Pharmacy, Romania
Tong Liu — Tianjin Medical University, China
Aggeliki Gkouziouta — Onassis Cardiac Surgery Center, Greece

Citation

Chan, J. S. K., Liu, Y., Ciobanu, A., Liu, T., Gkouziouta, A., eds. (2023). *Novel phenotyping and risk stratification strategies for heart failure*.
Lausanne: Frontiers Media SA. doi: 10.3389/978-2-83251-376-7

Table of contents

frontiers | Frontiers in Cardiovascular Medicine

TYPE Editorial
PUBLISHED 05 January 2023
DOI 10.3389/fcvm.2022.1115991

OPEN ACCESS

EDITED AND REVIEWED BY
Emma Birks,
University of Kentucky, United States

*CORRESPONDENCE
Jeffrey Shi Kai Chan
✉ jeffreychan.dbs@gmail.com

SPECIALTY SECTION
This article was submitted to Heart Failure and Transplantation, a section of the journal Frontiers in Cardiovascular Medicine

RECEIVED 04 December 2022
ACCEPTED 21 December 2022
PUBLISHED 05 January 2023

CITATION
Chan JSK, Ciobanu A, Liu Y, Gkouziouta A and Liu T (2023) Editorial: Novel phenotyping and risk stratification strategies for heart failure. *Front. Cardiovasc. Med.* 9:1115991. doi: 10.3389/fcvm.2022.1115991

Editorial: Novel phenotyping and risk stratification strategies for heart failure

Jeffrey Shi Kai Chan[1]*, Ana Ciobanu[2,3], Ying Liu[4], Aggeliki Gkouziouta[5] and Tong Liu[6]

[1]Heart Failure and Structural Heart Disease Research Unit, Cardiovascular Analytics Group, Hong Kong, Hong Kong SAR, China, [2]Faculty of Medicine, Carol Davila University of Medicine and Pharmacy, Bucharest, Romania, [3]Department of Internal Medicine and Cardiology, Theodor Burghele Clinical Hospital, Bucharest, Romania, [4]Heart Failure and Structural Cardiology Division, The First Affiliated Hospital of Dalian Medical University, Dalian, Liaoning, China, [5]Onassis Cardiac Surgery Center, Athens, Greece, [6]Tianjin Key Laboratory of Ionic-Molecular Function of Cardiovascular Disease, Department of Cardiology, Tianjin Institute of Cardiology, Second Hospital of Tianjin Medical University, Tianjin, China

KEYWORDS

heart failure, phenotype, risk stratification, epidemiology, pathophysiology

Editorial on the Research Topic
Novel phenotyping and risk stratification strategies for heart failure

Since its designation as an emerging epidemic in 1997, heart failure (HF) has remained a major public health problem (1). With an estimated 64.3 million people living with HF worldwide, it is a common cause of hospitalizations and contributes significantly to healthcare costs, morbidity, and mortality (2). Although recent decades have seen massive leaps in the understanding and management of HF, much remains to be explored and the frontiers of HF research continue to be pushed, as is evident from the 15 excellent articles presented in this Research Topic.

Pathophysiological understanding is critically important in all medical conditions, and HF is no exception. Here, Meng et al. presented a prospective cohort of 84 consecutive patients with acute decompensation of HF who, compared to 83 patients without HF, had higher $CD4^+/CD8^+$ expression of T cell immunoglobulin and mucin domain-containing protein 3 (Tim-3), a unique inhibitory co-receptor expressed on the surface of immune cells and mediates immune tolerance; Tim-3 expression was also independently associated with major adverse cardiac and cerebrovascular events. These highlighted the importance of inflammation in acute decompensation of HF. Meanwhile, Li N. et al. provided a comprehensive review of the role of RNA binding motif protein 20 (RBM20) and other splicing factors in titin isoform ratio modification, myocardial stiffness, and thus pathophysiology of HF with preserved ejection fraction (HFpEF). Aside from pathophysiological insights, the authors suggested that RBM20 may be a therapeutic target for mitigating myocardial stiffness in HFpEF, which, given the relative paucity of efficacious treatments for HFpEF (3), may be an exciting prospect warranting further exploration.

These recent advances in our pathophysiological understanding of HF also implied new opportunities to better characterize HF, with recent years having seen many novel risk factors and diagnostic tools being identified (4–7). Knowing that the diagnosis and workup of HFpEF is particularly challenging (8), Lau et al. provided a concise but informative summary of the role of cardiac magnetic resonance imaging in the assessment of HFpEF, which should be useful for both clinicians and researchers alike. However, the term "HFpEF" also points to the issue of phenotyping: even though left ventricular ejection fraction has been the most common way of classifying HF phenotypes, it may be a relatively insensitive marker of myocardial function, may not adequately reflect myocardial dysfunction, and has considerable temporal variability and operator dependency, amongst other limitations (9). Thus, alternative means of classifying and phenotyping HF have been extensively explored and remain an active area of research. Here, Sun et al. summarized studies that used clustering analysis for discovering new HF phenotypes. They found that patients from Africa, South America, and South and West Asia were under-represented, and that studies with a large number of clustering variables tended to have small sample sizes which may be statistically detrimental. There was also an under-exploration of functional outcomes as endpoints, and a lack of exploration of genomic and proteomic data, which may represent new opportunities for further studies.

Amongst those diagnosed with HF, prognostication remains to be of much clinical interest. In prospective multicentre cohort study of 4,305 Chinese patients with HF, Ge et al. found an inverse association between lean body mass and mortality, but none between fat mass and mortality. This relates to the contentious "obesity paradox", a phenomenon where obese patients were observed to have lower mortality, contrary to common expectation (10). While some had raised the possibility of such "paradox" being a spurious association arising from collider bias (11), others have shown that collider bias only explains such "paradox" partially (12). In the case of HF, frailty/sarcopenia or cardiorespiratory fitness were possible confounders that could constitute collider bias. In this study by Ge et al., a higher lean body mass could be seen as a surrogate for the absence of sarcopenia, and collider bias was unlikely to have affected the findings. Overall, this study furthered our understanding of the interactions between body composition and HF outcomes.

Meanwhile, Zhao et al. showed, in a retrospective cohort study of 170 patients with myocarditis, that higher levels of N-terminal pro-hormone brain natriuretic peptide (NT-proBNP) were independently associated with higher risk of major adverse cardiovascular events (MACE), and that NT-proBNP was superior to left ventricular EF in predicting 30-day death or heart transplantation. In another biomarker study, Zong et al. studied 956 Chinese patients with HF and 485 without HF, and found that high levels of trimethyllysine (TML), a precursor to trimethylamine N-oxide (TMAO) which is a metabolic product of intestinal microorganisms, was independently associated with HF and positively correlated with levels of NT-proBNP. Furthermore, higher levels of TML was associated with the composite outcome of cardiovascular mortality and HF hospitalization amongst patients with HF. On a related note, Li X. et al. showed in a systematic review and meta-analysis of 10 observational studies with 13,425 patients that higher levels of TMAO were associated with MACE and mortality in HF; significant heterogeneity was observed for both outcomes, which was not unexpected given the observational nature of included studies and the varying definitions of elevated TMAO. Overall, these two latter studies gave insights into gut microbiota metabolites as novel prognosticators in HF, and had potential implications in gut-heart interactions that may contribute to the pathophysiology of HF. The mechanisms underlying the above observations remained to be elucidated, highlighting the importance of gut microbiota as a new frontier in HF research and a potential treatment target in HF.

While most treatments of HF are pharmacological, recent years have seen a number of devices emerging as promising therapeutic options. Here, Miyagi et al. reviewed novel device-based approaches to left atrial pressure relief, highlighting both the potential and limitations of this new frontier in personalized HFpEF management. This personalized approach to HF management was echoed by Guo et al., who explored associations between single-nucleotide polymorphisms of low-density lipoprotein receptor-related protein 6 (LRP6) and risks of sudden cardiac death and mortality, finding that the A allele of rs2302684 was associated with increased risks of these endpoints. Such finding has potential implications for personalized sudden cardiac death risk stratification and polygenic risk scores in HF. Combining genetic data with other markers, such as electrocardiographic and echocardiographic measurements (5, 13–15), may also improve predictive power.

Two studies also explored the effects of non-cardiovascular comorbidities and complications. In a retrospective, propensity score-matched cohort of 4,328 patients with HF without thyroid disease, Wang C. et al. found that a low FT3/FT4 ratio was associated with higher risks of all-cause and cardiovascular mortality. This adds to our understanding of the intricate interactions between thyroid and HF and suggests that clinicians may consider working up patients with HF and without overt thyroid diseases for subclinical thyroid dysfunction. On the other hand, Zhong et al. studied 100 patients with myocardial infarction in a case-control study, finding that low baseline hemoglobin was an independent risk factor for in-hospital post-myocardial infarction gastrointestinal bleeding, and that low hemoglobin and Kilip class IV were independent risk factors for in-hospital mortality in those who had such bleeding. These findings may aid clinicians in risk stratification of hospitalized patients with myocardial infarction.

Last but definitely not least, three studies delved into more specific populations with or at risk of HF for which evidence has been relatively scarce. In a retrospective cohort study of 306 Chinese patients with lung cancer, Ren et al. demonstrated that atrial cardiomyopathy was prevalent regardless of histological subtypes, and that atrial cardiomyopathy was associated with worse survival. With recent advancements in the understanding of cancer therapy-related cardiotoxicity (16–22), these are important findings that will facilitate risk stratification and management of patients with lung cancer. Grupper et al., on the other hand, studied 59 consecutive patients implanted with the HeartMate3 left ventricular assist device (LVAD) in a prospective cohort study, observing that a diastolic plateau, which is a sign observed during right heart catheterization and is typically associated with constrictive or restrictive pathologies, was associated with increased risks of adverse cardiovascular events. With right heart failure being the major cause of morbidity and mortality in patients receiving LVAD (23), these findings give insights into the haemodynamic effects of LVAD and may facilitate clinicians in the risk stratification of patients receiving LVAD. Meanwhile, Wang S. et al. described in great detail the presentation, phenotype, genetic mutations, investigation findings, and outcome of 29 Chinese patients with hereditary transthyretin amyloid cardiomyopathy. Hereditary transthyretin amyloid cardiomyopathy is likely underdiagnosed (24), and with the emergence of several novel, evidence-based treatments (25–27), this study was a timely contribution to our understanding of these patients.

To conclude, the 15 excellent articles in this Research Topic explored various aspects of HF research, with particular emphasis on phenotyping and risk stratification. We believe that these are valuable contribution to the literature that will better our understanding and management of HF in the years to come.

Author contributions

All authors listed have made a substantial, direct, and intellectual contribution to the work and approved it for publication.

Conflict of interest

The authors declare that the research was conducted in the absence of any commercial or financial relationships that could be construed as a potential conflict of interest.

Publisher's note

References

1. Roger VL. Epidemiology of heart failure. *Circ Res.* (2021) 128:1421–34. doi: 10.1161/CIRCRESAHA.121.318172

2. Groenewegen A, Rutten FH, Mosterd A, Hoes AW. Epidemiology of heart failure. *Eur J Heart Fail.* (2020) 22:1342–56. doi: 10.1002/ejhf.1858

3. Wintrich J, Kindermann I, Ukena C, Selejan S, Werner C, Maack C, et al. Therapeutic approaches in heart failure with preserved ejection fraction: past, present, and future. *Clin Res Cardiol.* (2020) 109:1079–98. doi: 10.1007/s00392-020-01633-w

4. Lakhani I, Wong MV, Hung JKF, Gong M, Waleed K, Bin Xia Y, et al. Diagnostic and prognostic value of serum C-reactive protein in heart failure with preserved ejection fraction: a systematic review and meta-analysis. *Heart Fail Rev.* (2021) 26:1141–50. doi: 10.1007/s10741-020-09927-x

5. Wang W, Mu G, Liu C, Xie J, Zhang H, Zhang X, et al. A novel three-dimensional and tissue doppler echocardiographic index for diagnosing and prognosticating heart failure with preserved ejection fraction. *Front Cardiovasc Med.* (2022) 9:822314. doi: 10.3389/fcvm.2022.822314

6. Li X, Chan JSK, Guan B, Peng S, Wu X, Lu X, et al. Triglyceride-glucose index and the risk of heart failure: Evidence from two large cohorts and a mendelian randomization analysis. *Cardiovasc Diabetol.* (2022) 21:1–12. doi: 10.1186/s12933-022-01658-7

7. Chan JSK, Satti DI, Lee YHA, Hui JMH, Lee TTL, Chou OHI, et al. High visit-to-visit cholesterol variability predicts heart failure and adverse cardiovascular events: a population-based cohort study. *Eur J Prev Cardiol.* (2022). doi: 10.1093/eurheartj/ehab849.153

8. Ho JE, Redfield MM, Lewis GD, Paulus WJ, Lam CSP. Deliberating the diagnostic dilemma of heart failure with preserved ejection fraction. *Circulation.* (2020) 142:1770–80. doi: 10.1161/CIRCULATIONAHA.119.041818

9. Marwick TH. Ejection fraction pros and cons: JACC state-of-the-art review. *J Am Coll Cardiol.* (2018) 72:2360–79. doi: 10.1016/j.jacc.2018.08.2162

10. Horwich TB, Fonarow GC, Clark AL. Obesity and the obesity paradox in heart failure. *Prog Cardiovasc Dis.* (2018) 61:151–6. doi: 10.1016/j.pcad.2018.05.005

11. Banack HR, Kaufman JS. Does selection bias explain the obesity paradox among individuals with cardiovascular disease? *Ann Epidemiol.* (2015) 25:342–9. doi: 10.1016/j.annepidem.2015.02.008

12. Sperrin M, Candlish J, Badrick E, Renehan A, Buchan I. Collider Bias Is Only a Partial Explanation for the Obesity Paradox. *Epidemiology.* (2016) 27:525. doi: 10.1097/EDE.0000000000000493

13. Chan JSK, Zhou J, Lee S, Li A, Tan M, Leung KSK, et al. Fragmented QRS is independently predictive of long-term adverse clinical outcomes in asian patients hospitalized for heart failure: a retrospective cohort study. *Front Cardiovasc Med.* (2021) 8:1634. doi: 10.3389/fcvm.2021.738417

14. Chan JSK, Lau DHH, Fan Y, Lee AP-W. Age-related changes in left ventricular vortex formation and flow energetics. *J Clin Med.* (2021) 10:3619. doi: 10.3390/jcm10163619

15. Bazoukis G, Garcia-Zamora S, Çinier G, Lee S, Gul EE, Álvarez-García J, et al. Association of electrocardiographic markers with myocardial fibrosis as assessed by cardiac magnetic resonance in different clinical settings. *World J Cardiol.* (2022) 14:483–95. doi: 10.4330/wjc.v14.i9.483

16. Duraes AR, de Souza Lima Bitar Y, Neto MG, Mesquita ET, Chan JS, Tse G, et al. Effectiveness of sacubitril-valsartan in patients with cancer therapy-related

cardiac dysfunction: a systematic review of clinical and preclinical studies. *Minerva Med.* (2022) 113:551–7. doi: 10.23736/S0026-4806.22.08029-6

17. Zhou J, Lee S, Lakhani I, Yang L, Liu T, Zhang Y, et al. Adverse Cardiovascular Complications following prescription of programmed cell death 1 (PD-1) and programmed cell death ligand 1 (PD-L1) inhibitors: a propensity-score matched Cohort Study with competing risk analysis. *Cardio-oncology (London, England).* (2022) 8:1–22. doi: 10.1186/s40959-021-00128-5

18. Chan JSK, Lakhani I, Lee TTL, Chou OHI, Lee YHA, Cheung YM, et al. Cardiovascular outcomes and hospitalizations in Asian patients receiving immune checkpoint inhibitors: a population-based study. *Curr Probl Cardiol.* (2022) 48:101380. doi: 10.1016/j.cpcardiol.2022.101380

19. Chan JSK, Tang P, Ng K, Dee EC, Lee TTL, Chou OHI, et al. Cardiovascular risks of chemo-immunotherapy for lung cancer: A population-based cohort study. *Lung Cancer.* (2022) 174:67–70. doi: 10.1016/j.lungcan.2022.10.010

20. Lyon AR, López-Fernández T, Couch LS, Asteggiano R, Aznar MC, Bergler-Klein J, et al. 2022 ESC Guidelines on cardio-oncology developed in collaboration with the European Hematology Association (EHA), the European Society for Therapeutic Radiology and Oncology (ESTRO) and the International Cardio-Oncology Society (IC-OS). *Eur Heart J.* (2022) 43:4229–361. doi: 10.1093/eurheartj/ehac244

21. Chan JSK, Tang P, Hui JMH, Lee YHA, Dee EC, Ng K, et al. Association between duration of gonadotrophin-releasing hormone agonist use and cardiovascular risks: A population-based competing-risk analysis. *Prostate.* (2022) 82:1477–80. doi: 10.1002/pros.24423

22. Song W, Zheng Y, Dong M, Zhong L, Bazoukis G, Perone F, et al. Electrocardiographic features of immune checkpoint inhibitor-associated myocarditis. *Curr Probl Cardiol.* (2022) 48:101478. doi: 10.1016/j.cpcardiol.2022.101478

23. Frankfurter C, Molinero M, Vishram-Nielsen JKK, Foroutan F, Mak S, Rao V, et al. Predicting the Risk of Right Ventricular Failure in Patients Undergoing Left Ventricular Assist Device Implantation: A Systematic Review. *Circ Hear Fail.* (2020) 13:E006994. doi: 10.1161/CIRCHEARTFAILURE.120.006994

24. Damy T, Costes B, Hagège AA, Donal E, Eicher JC, Slama M, et al. Prevalence and clinical phenotype of hereditary transthyretin amyloid cardiomyopathy in patients with increased left ventricular wall thickness. *Eur Heart J.* (2016) 37:1826–34. doi: 10.1093/eurheartj/ehv583

25. Maurer MS, Schwartz JH, Gundapaneni B, Elliott PM, Merlini G, Waddington-Cruz M, et al. Tafamidis Treatment for Patients with Transthyretin Amyloid Cardiomyopathy. *N Engl J Med.* (2018) 379:1007–16. doi: 10.1056/NEJMoa1805689

26. Benson MD, Waddington-Cruz M, Berk JL, Polydefkis M, Dyck PJ, Wang AK, et al. Inotersen Treatment for Patients with Hereditary Transthyretin Amyloidosis. *N Engl J Med.* (2018) 379:22–31. doi: 10.1056/NEJMoa1716793

27. Adams D, Gonzalez-Duarte A, O'Riordan WD, Yang C-C, Ueda M, Kristen A V, et al. Patisiran, an RNAi Therapeutic, for Hereditary Transthyretin Amyloidosis. *N Engl J Med.* (2018) 379:11–21. doi: 10.1056/NEJMoa1716153

frontiers in Cardiovascular Medicine

ORIGINAL RESEARCH
published: 04 February 2022
doi: 10.3389/fcvm.2021.815595

LRP6 Polymorphisms Is Associated With Sudden Cardiac Death in Patients With Chronic Heart Failure in the Chinese Han Population

Qi Guo[1†], *Yiwei Lai*[1†], *Jianmin Chu*[2], *Xuhua Chen*[2], *Mingyang Gao*[1], *Caihua Sang*[1], *Jianzeng Dong*[1], *Jielin Pu*[2,3*] and *Changsheng Ma*[1*]

[1] Department of Cardiology, National Clinical Research Center for Cardiovascular Diseases, Beijing Anzhen Hospital, Capital Medical University, Beijing, China, [2] State Key Laboratory of Cardiovascular Disease, National Center for Cardiovascular Disease, Fuwai Hospital, Chinese Academy of Medical Sciences and Peking Union Medical College, Beijing, China, [3] Department of Cardiology, Shanghai East Hospital, Tongji University, Shanghai, China

OPEN ACCESS

Edited by:
Tong Liu,
Tianjin Medical University, China

Reviewed by:
Jinzhu Hu,
Nanchang University, China
Anuradha Kalyanasundaram,
The Ohio State University, United States

***Correspondence:**
Jielin Pu
jielinpudf@sina.com
Changsheng Ma
chshma@vip.sina.com

[†] *These authors have contributed equally to this work and share first authorship*

Specialty section:
This article was submitted to Heart Failure and Transplantation, a section of the journal Frontiers in Cardiovascular Medicine

Received: *15 November 2021*
Accepted: *15 December 2021*
Published: *04 February 2022*

Citation:
Guo Q, Lai Y, Chu J, Chen X, Gao M, Sang C, Dong J, Pu J and Ma C (2022) LRP6 Polymorphisms Is Associated With Sudden Cardiac Death in Patients With Chronic Heart Failure in the Chinese Han Population. Front. Cardiovasc. Med. 8:815595. doi: 10.3389/fcvm.2021.815595

Low-density lipoprotein receptor-related protein 6 (LRP6) plays a critical role in cardiovascular homeostasis. The deficiency of *LRP6* is associated with a high risk of arrhythmias. However, the association between genetic variations of *LRP6* and sudden cardiac death (SCD) remains unknown. This study aims to explore the association between common variants of *LRP6* and the prognosis of chronic heart failure (CHF) patients. From July 2005 to December 2009, patients with CHF were enrolled from 10 hospitals in China. The single-nucleotide polymorphism (SNP) rs2302684 was selected for the evaluation of the effect of *LRP6* polymorphisms on the survival in patients with CHF. A total of 1,437 patients with CHF were finally included for the analysis. During a median follow-up of 61 months (range 0.4–129 months), a total of 546 (38.0%) patients died, including 201 (36.8%) cases with SCD and 345 (63.2%) cases with non-SCD. Patients carrying A allele of rs2302684 had an increased risk of all-cause death (adjusted HR 1.452, 95% CI 1.189–1.706; $P < 0.001$) and SCD (adjusted HR 1.783, 95% CI 1.337–2.378; $P < 0.001$). Therefore, the SNP rs2302684 T>A in *LRP6* indicated higher risks of all-cause death and SCD in patients with CHF. *LRP6* could be added as a novel predictor of SCD and might be a potential therapeutic target in the prevention of SCD in the CHF population.

Keywords: LRP6, single-nucleotide polymorphism, chronic heart failure, prognosis, sudden cardiac death

INTRODUCTION

Chronic heart failure (CHF), which may be caused by ischemic cardiomyopathy (ICM) or non-ischemic cardiomyopathy (NICM), is one of the chief causes of morbidity and mortality worldwide (1, 2). It currently affects more than five million Americans and the prevalence is expected to increase by 25% within the next 15 years (3). This heart failure pandemic is also evident in Asia and China (4). The predominant modes of death in CHF patients are pump failure and sudden cardiac death (SCD) (5). Sudden cardiac death, caused by malignant ventricular tachycardia (VT) or ventricular fibrillation (VF), remains a primary cause of mortality in patients with CHF (6). Therefore, the prediction and prevention of SCD play critical roles in the management of the

CHF population. So far, even several factors have been known as potential predictors of SCD, including biomarkers, hemodynamic status, and electrophysiological parameters, the sensitivity and specificity are not powerful (7).

Low-density lipoprotein (LDL) receptor-related protein 6 (LRP6) is a single-pass transmembrane protein, which contains four extracellular epidermal growth factor-like repeats and three LDL receptor repeats (8). It is recognized as a coreceptor for the Wnt signaling cascade and plays a critical role in regulating Wnt signaling (9, 10). Work to date has identified that dysregulated Wnt signaling conduces to a high incidence of arrhythmias associated with various forms of heart disease (11). Furthermore, accumulating evidence reveals the significant effect of LRP6 on cardiovascular health and homeostasis (12). Additionally, LRP6 was mainly allocated within the gap junction of cardiomyocytes (13). However, the potential relation between genetic variations of *LRP6* and SCD has not yet been reported in previous studies. In the present study, we examined the association between common variants of *LRP6* and the prognosis in patients with CHF.

MATERIALS AND METHODS

Study Population

From July 2005 to December 2009, patients with CHF were enrolled from 10 hospitals in China. Details for the cohort have been described previously (9, 14–16). Inclusion criteria include: (a) CHF caused by ICM or idiopathic dilated cardiomyopathy (DCM); (b) classification of the New York Heart Association (NYHA) was II–IV with optimizing drug therapy; and (c) left ventricular ejection fraction (LVEF) $\leq$50% in ICM or $\leq$45% in DCM (9, 14–16). Ischemic cardiomyopathy was diagnosed as $\geq$70% luminal stenosis of one or more major coronary arteries diagnosed by coronary angiography with a myocardial infarction history at least 3 months before the enrolment. DCM was diagnosed consistently with the guidelines of familial DCM (17). Excluded criteria include: (a) pacemaker dependency; (b) unable to perform the genotyping; and (c) pregnancy, terminal illnesses, or other uncontrollable system diseases (9, 14–16).

The study was approved by the Ethics Committee of Beijing Anzhen Hospital and Fuwai Hospital (Beijing, China), and complied with the principles of the Declaration of Helsinki. Written informed consent was obtained from all the enrolled patients who reported themselves as Chinese Han nationality.

Endpoint Evaluation

All the participants were followed up periodically until August 2017 during regular outpatient clinics or by transtelephonic visits. The endpoints included all-cause death, SCD (ICD appropriate discharge was regarded as SCD), and non-SCD (NSCD) (heart transplantation was regarded as non-SCD). Sudden cardiac death was defined as an unexpected death within 1 h of onset of acute symptoms attributable to cardiac causes or an unwitnessed death of someone last seen in a stable condition in 24 h without evidence of non-cardiac causes (7). If there were discrepancies between the first two reviewers, the event was adjudicated by a third investigator to provide the final classification.

Abbreviations: CHF, chronic heart failure; DCM, dilated cardiomyopathy; ICM, ischemic cardiomyopathy; LRP6, low-density lipoprotein receptor-related protein 6; LVEF, left ventricular ejection fraction; PCR, polymerase chain reactions; SCD, sudden cardiac death.

Tag Single-Nucleotide Polymorphisms Selection

Tag single-nucleotide polymorphisms (SNPs) were selected by the pairwise tagging method from the HapMap CHB databank (HapMap Data Rel 24 PhaseII, Nov08, on NCBI B36 assembly, dbSNP b126) via the tag SNPs' online software (http://hapmap.ncbi.nlm.nih.gov/cgi-perl/gbrowse/hapmap24_B36/#search). Common variants were defined as a minor allele frequency (MAF) $>$ 0.05, with a linkage disequilibrium (LD) measure r^2 threshold of 0.8. Forty-three tag SNPs that covered the entire *LRP6* gene were selected. To reduce the false-positive caused by multiple tests, with 43 candidate SNPs, $P < 0.001$ was considered statistically significant for SNP selection. Polymerase chain reactions (PCRs) were performed firstly in 100 subjects with CHF. There were no significant associations between SNPs and clinical endpoints other than the SNP rs2302684 T>A. Thus, rs2302684 was finally selected to perform the PCRs in the whole study population for the analysis.

Genotyping in CHF Population

Genomic DNA was extracted from peripheral blood leukocytes of the participants and stored at −70°C after determination of absorbance at 260 nm followed by Picogreen analysis (Molecular Probes, Eugene, Oegon, USA) (18).

Primers were designed by Primer Premier 5.0 software as follows: forward TTGATGATGCTCCTGTAA and reverse TATTCTTGGCCTTGTTCT (328 bp). PCR amplification was performed with the Geneamp PCR system 9700 (Applied Biosystems). An initial 4 min cycle at 94°C was followed by 35 thermal cycles at 94°C for 30 s, 47°C for 30 s, and 72°C for 30 s, and ended with a 10 min extension at 72°C. Each reaction mixture (30 μl) contained 3 μl 10× PCR buffer, 0.5 μl dNTP-mix (10 mmol/L), 0.5 μl of each primer (10 μmol/L), 0.5 μl Taq polymerase (5 U/μl; Takara Bio), 1 μl genomic DNA (50 ng/μl), and 24 μl double-distilled H_2O.

PCR products were sequenced after purification by ABI 3130XL DNA Analyzer System (Applied Biosystems, USA). Repeat genotyping was carried out in 95 (5.0%) random duplicate samples to affirm the reproducibility was 100% (**Figure 1**).

Statistical Analysis

Continuous variables were presented as the mean ± SD and compared by Student's test. Categorical variables were presented as numbers and percentages and compared by chi-square analysis. A *P*-value of $<$ 0.05 was considered statistically significant. Linkage disequilibrium of rs2302684 was analyzed by Haploview4.2, and Hardy-Weinberg equilibrium of alleles was analyzed by chi-square analysis with 1 degree of freedom. Survival analysis was performed in CHF patients. Cox proportional hazards models were performed under three different models (dominant, recessive, additive models) to evaluate the effects of genotype on survival. Kaplan-Meier curve

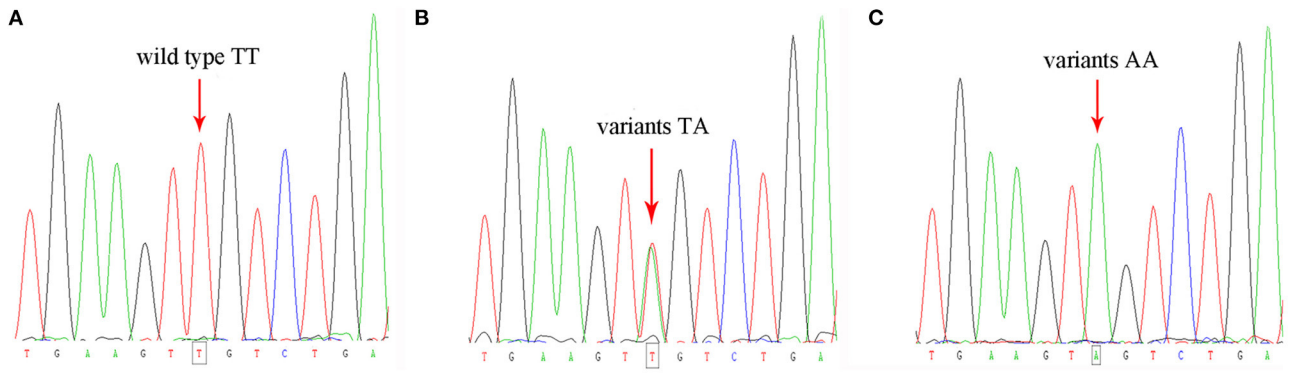

FIGURE 1 | Genotyping of the studied population showing the wild type **(A)** and the variants of rs2302684 T>A **(B,C)**.

was applied to describe survival freedom from events and multivariate cox proportional hazards models were used to adjust for confounding factors. The covariates were selected according to clinical significance and baseline data, including age, sex, NYHA levels, LVEF, ischemic etiology, and other variables with a *P*-value of < 0.2 in the baseline. Statistical analyses were conducted using the IBM SPSS 26.0 software.

RESULTS

Clinical Characteristics of the Studied Population

A total of 1,437 patients (age 60.55 ± 11.98 years, 1,134 males) with CHF were finally enrolled for the analysis, including 957 patients with ICM and 480 patients with DCM. The mean LVDD of the participants was 63.27 ± 9.77 mm, and the mean LVEF was 36.04 ± 8.80%. Among them, 43.0% of patients had the NYHA function of level II, 32.6% of patients had the NYHA function of level III, and the other 24.4% patients had the NYHA function of level IV. The mean BMI of the participants was 24.84 ± 3.84 kg/m^2. The clinical characteristics were summarized in **Table 1**.

In the studied CHF population, 443 patients (age 61.41 ± 11.79 years, 340 males) carried A allele of SNP rs2302684. The patients carrying A allele of SNP rs2302684 comprised a larger percentage of patients with ICM than those carrying the wild type of TT (71.6 vs. 64.4%, $P = 0.009$). Furthermore, CHF patients with A allele of rs2302684 had a tendency to the higher classification of NYHA level than those without (NYHA II, 38.8 vs. 44.9%; NYHA III, 33.2 vs. 32.4%; NYHA IV, 28 vs. 22.7%; $P = 0.047$). However, no significant differences were demonstrated in age, sex distribution, BMI, LVDD, LVEF, complications, the prevalence of arrhythmias, and medication between the patients with rs2302684 wild type of TT and those with A allele (**Table 1**).

Long-Term Follow-Up of the CHF Population

During a median follow-up of 61 months (range 0.4–129 months) in 1,437 participants with CHF, a total of 546 (38.0%) patients died, including 348 patients with ICM and 198 patients with DCM. Among them, 201 (36.8%) cases had SCD, including 129 cases with ICM and 72 cases with DCM. The rest of 345 (63.2%) cases had NSCD.

Associations of SNP Rs2302684 T>A and the Clinical Endpoints

The correlation of mortality and A allele of rs2302684 were analyzed by survival cox regression analysis in the CHF cohort under the dominant, recessive, and additive models, respectively. The effect of the A allele on mortality was significant under different models (**Table 2**). Under the dominant model, the risks of all-cause death (HR 1.45, 95% CI 1.21–1.73; $P < 0.001$) and SCD (HR 1.85, 95% CI 1.39–2.45; $P < 0.001$) increased significantly in patients with A allele of rs2302684. After adjusted for age, sex, ischemic etiology, NYHA levels, LVEF, BMI, and the use of β-blocker, the associations remained significant in all-cause death (HR 1.43, 95% CI 1.20–1.72; $P < 0.001$) and SCD (HR 1.80, 95% CI 1.34–2.40; $P < 0.001$). The Kaplan-Meier curves made under the dominant models were shown in **Figure 2**. Thus, SNP rs2302684 T>A indicated a higher risk of all-cause death and SCD but not NSCD in the CHF patients.

The effect of A allele of rs2302684 on the mortality endpoints was generally consistent across the selected subgroups, including different age (P for interaction = 0.268 for all-cause mortality and 0.189 for SCD), sex (P for interaction = 0.838 for all-cause mortality and 0.183 for SCD), and ischemic etiology (P for interaction = 0.473 for all-cause mortality and 0. 664 for SCD) (**Figure 3**).

DISCUSSION

Main Findings

In this prospective study of 1,437 patients with CHF in the Chinese Han nationality, the associations of SNP rs2302684 T>A in *LRP6* and long-term clinical endpoints were explored. The A allele of rs2302684 was recognized as an independent risk factor and predictor of all-cause death and SCD in the CHF population. To the best of our knowledge, this is the first study to show the association between common variants in *LRP6* gene with the different causes of mortality in patients with CHF.

TABLE 1 | Baseline characteristics of the studied population.

Clinical characteristics	CHF			
	ALL (*n* = 1,437)	**TT** (*n* = 994)	**TA+AA** (*n* = 443)	***P*-values**
Sex, *n* = Male (%)	1,134 (78.9)	794 (79.9)	340 (76.7)	0.203
Age (years)	60.55 ± 11.98	60.16 ± 12.05	61.41 ± 11.79	0.068
Etiology, *n* = ICM (%)	957 (66.6)	640 (64.4)	317 (71.6)	0.009
LVDD (mm)	63.27 ± 9.77	63.15 ± 9.57	63.55 ± 10.21	0.479
LVEF (%)	36.04 ± 8.80	36.26 ± 8.54	35.55 ± 9.36	0.157
NYHA, *n* (%)				0.047
I	0	0	0	–
II	618 (43.0%)	446 (44.9)	172 (38.8)	–
III	469 (32.6%)	322 (32.4)	147 (33.2)	–
IV	350 (24.4%)	226 (22.7)	124 (28)	–
BMI (kg/m^2)	24.84 ± 3.84	24.72 ± 3.80	25.10 ± 3.91	0.085
Hypertension, *n* (%)	723 (50.3)	493 (49.6)	230 (51.9)	0.45
Hyperlipidemia, *n* (%)	353 (24.6)	249 (25.1)	104 (23.5)	0.566
Diabetes, *n* (%)	361 (25.1)	245 (24.6)	116 (26.2)	0.579
QRS durations (ms)	110.45 ± 52.48	110.74 ± 53.36	109.80 ± 50.51	0.755
AF/AFL, *n* (%)	214 (14.9)	151 (15.2)	63 (14.2)	0.692
PVC/NSVT, *n* (%)	114 (7.9)	72 (7.2)	42 (9.5)	0.179
VT/VF, *n* (%)	43 (3.0)	27 (2.7)	16 (3.6)	0.452
Medications, *n* (%)				
β-blocker	1077 (74.9)	733 (73.7)	342 (77.2)	0.184
ACEI	992 (69.0)	686 (69.0)	309 (69.8)	0.828
Diuretic	1055 (73.4)	720 (72.4)	333 (75.2)	0.309
Aldosterone antagonists	1066 (74.2)	738 (74.2)	328 (74.0)	0.987
ICD, *n* (%)	37 (2.6)	24 (2.4)	13 (2.9)	0.693

AF, atrial fibrillation; AFL, atrial flutter; BMI, body mass index; CHF, chronic heart failure; DCM, dilated cardiomyopathy; ICM, ischemic cardiomyopathy; LVDD, left ventricular end-diastolic diameter; LVEF, left ventricular ejection fraction; NSVT, non-sustainable ventricular tachycardia; NYHA, New York Heart Association; PVC, premature ventricular contraction; VT, ventricular tachycardia; VF, ventricular fibrillation.
M ± SD for normally distributed data and n (%) for categoric variables.

TABLE 2 | Associations of SNP rs2302684 T>A and clinical endpoints of the studied population.

Models	Dominant (TA + AA compared with TT)			Recessive (AA compared with TT + TA)			Additive models
	TT	**AA + TA**	**HR (95% CI)**	**TT + TA**	**AA**	**HR (95% CI)**	**HR (95% CI)**
All cause death	361	185		521	25		
Unadjusted			1.45 (1.21–1.73)			1.83 (1.22–2.73)	1.40 (1.21–1.63)
Adjusted*			1.43 (1.20–1.72)			1.87 (1.25–2.79)	1.39 (1.20–1.62)
SCD	121	80		189	12		
Unadjusted			1.85 (1.39–2.45)			2.36 (1.3–4.23)	1.71 (1.36–2.14)
Adjusted*			1.80 (1.34–2.40)			2.34 (1.33–4.29)	1.68 (1.33–2.12)
NSCD	240	105		332	13		
Unadjusted			1.25 (0.99–1.57)			1.51 (0.87–2.64)	1.23 (1.01–1.50)
Adjusted*			1.24 (0.98–1.57)			1.54 (0.88–2.69)	1.23 (1.01–1.50)

CHF, chronic heart failure; HR: NSCD, non-sudden cardiac death; SCD, sudden cardiac death.
**Adjusted for: age, sex, BMI, NYHA class, ejection fraction, ischemic etiology, non-sustained ventricular arrhythmias, use of beta-blocker.*

LRP6 and Wnt Signal Regulation

The human *LRP6* gene, which is located in chromosome 12 p11–p13, has 150 kb in length with 23 exons (8, 19). It encodes a member of the low-density lipoprotein receptor family, which is composed of cell surface proteins that participate in receptor-mediated endocytosis of specific ligands (8, 19). *LRP6* gene

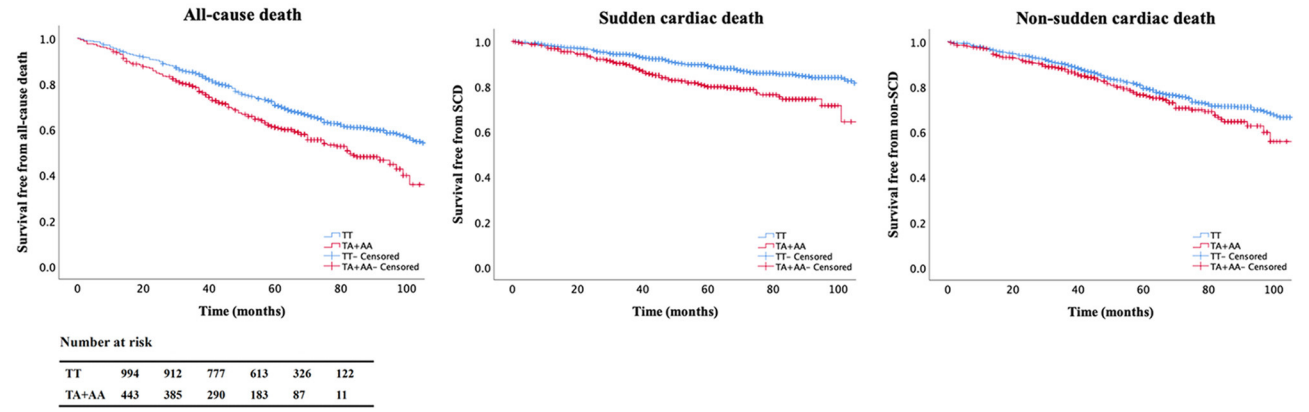

FIGURE 2 | Kaplan-Meier curves in the chronic heart failure (CHF) cohort. Patients carrying A allele of rs2302684 were more vulnerable to all-cause death and sudden cardiac death (SCD) than those without it. The table denotes the number of patients at risk for every 20 months of the follow-up.

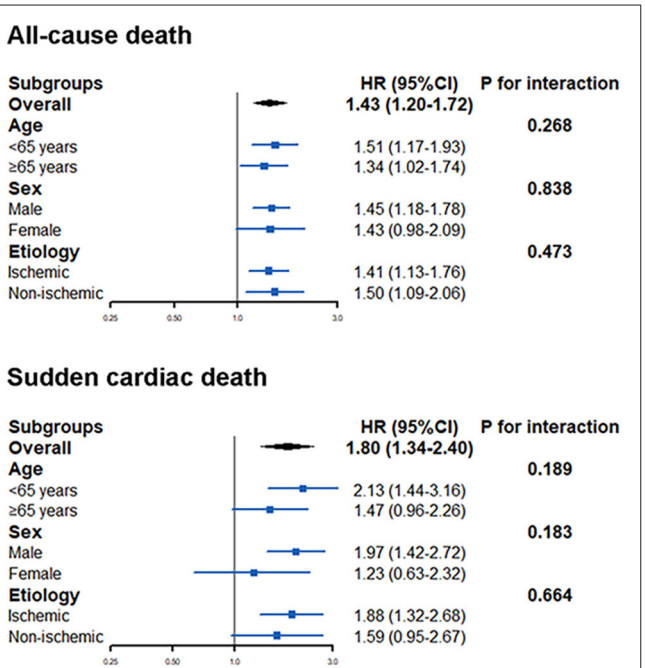

FIGURE 3 | The effect of A allele of rs2302684 on all-cause mortality and sudden cardiac death in different subgroups, including different ages, sex, and etiology.

is homologous to *LRP5* and has large extracellular domains consisting of four β-propeller motifs followed by three LDL ligand-binding domains, which regulate the binding process between Wnt secretory protein and frizzled family of receptors (10, 20). LRP6 function as coreceptors for Wnt ligands and thus play a central role in Wnt/β-catenin signaling involved in a wide variety of biologic processes (12, 21).

Wnts are a family of secreted glycoproteins that participate in activating several signaling pathways (22). It could bind to a class of Frizzled receptors or LRP6 to downregulate the glycogen synthase kinase-3β (GSK-3β) activity and to initiate the canonical Wnt/β-catenin signaling cascade (22). Wnt/β-catenin signaling is a crucial regulator of tissue development and homeostasis, especially in cardiac differentiation and development (11, 20). The conserved Wnt cascade has been confirmed to control the proliferation, differentiation and polarity of cells (23–25). Abnormal signaling disturbs tissue growth and function, which could lead to a number of debilitating and terminal diseases (20). Thus, alterations in the *LRP6* gene might affect Wnt/β-catenin signaling and lead to several human diseases including osteoporosis, Alzheimer's disease, coronary artery disease, and metabolic disease (20, 26–31).

LRP6 and Sudden Cardiac Death

Wnt signaling is critical in cardiac development and various cardiac pathologies, including cardiac hypertrophy and fibrosis, myocardial infarction, heart failure, and arrhythmias (30, 32, 33). It has been reported that abnormalities of Wnt signaling were an important cause of familial sudden death in patients with ARVC (34). Additionally, a recent genome-wide association study showed that WNT8A was associated with atrial fibrillation (35).

Mutations in *LRP6* could dysregulate Wnt signaling and have been associated with numerous human diseases (12, 20). The rs2302684 is an intron variant. No association has been reported between this tag SNP of *LRP6* and the prognosis of patients with CHF in the Chinese Han population. Our study revealed a close relationship between *LRP6* common variants and SCD in the CHF group. According to previous researches, the potential reasons for this relationship might have two aspects. On one hand, LRP6 serves as a scaffold protein that regulates the cardiac gap junction assembly. *LRP6* deficiency might impair the dynamics of connexin43 protein trafficking and stability, which disrupts gap junction formation and function. The proper functioning of gap junctions is essential in the generation and propagation of cardiac action potentials. Thus, the disrupting connexin43 expression or phosphorylation caused by *LRP6* deficiency impaired the electrical communication

in gap junctions and led to the initiation and maintenance of arrhythmias (33, 36, 37). It was reported that defective connexin43 gap junctions in *LRP6*-ablated mouse hearts induced VT and VF (13). On the other hand, many studies demonstrated that Wnt signaling was linked to cardiac fibrosis which could impede electrical wave propagation and potentially cause arrhythmias (38–40). Furthermore, a recent study reported that *LRP6* played an important role in keeping the integrity of the intercalated disk, on which the coordinated excitation and contractile performance of the myocardium were dependent, and the interaction between *LRP6* and connexin43 might be involved in this process (41). Therefore, *LRP6* variants might cause malignant arrhythmias and SCD via disturbing Wnt signaling pathways, as well as disrupting the function of gap junction and the intercalated disk of the myocardium.

LRP6 and CHF With Different Etiologies

It was reported that LRP6 was dramatically decreased in heart tissues with DCM (42). Additionally, *LRP6* is genetically linked to early coronary artery disease and hyperlipemia (20, 43, 44). It has been demonstrated that mutant *LRP6* was associated with atherosclerosis. The underlying mechanism might be as follows: firstly, LRP6 is critical in LDL receptor-mediated LDL uptake, which is significant in atherosclerosis; secondly, LRP6 plays an important role in metabolic regulation, including lipid homeostasis and glucose metabolism, thus it is associated with atherosclerosis; lastly, mutant *LRP6* could trigger atherosclerosis by activating platelet-derived growth factor (PDGF)-dependent vascular smooth muscle cell differentiation (31, 45). Considering the close relationship of *LRP6*, DCM, and atherosclerosis, we analyzed the association of *LRP6* with the mortality endpoints in different etiologies of CHF. In our study, the effect of rs2302684 A allele in *LRP6* on the mortality endpoint was consistent in patients with different CHF reasons, including ICM and DCM. Therefore, we found that *LRP6* variants were associated with a higher risk of all-cause death and SCD in the CHF cohort attributed to both ICM and DCM.

Study Limitations

There are several limitations to the study. The lack of functional research in this work is one of the limitations. In this study, we only found the association between the SNP of *LRP6* and SCD in CHF patients via gene tests, however, the exact mechanism of how the SNP affects the heart is still unknown. We only speculate the possible mechanism according to existing studies, and we still need further functional studies to explore the underlying mechanism in our future work. Additionally, ICD recordings were not collected in the present cohort, and only a limited number of patients had a history of ventricular arrhythmias (VAs). Therefore, we are not able to deepen our investigation about the association between VAs and the SNP of interest.

CONCLUSIONS

The study firstly demonstrated that *LRP6* rs2302684 polymorphism is associated with increased risks of all-cause death and SCD in CHF patients in the Chinese Han population. Therefore, *LRP6* could be regarded as an independent risk factor and a novel predictor of SCD, and it might provide a potential therapeutic target in SCD prevention.

DATA AVAILABILITY STATEMENT

The datasets presented in this article are not readily available because the hospital does not permit the authors to publicize the database. Requests to access the datasets should be directed to the corresponding author/s.

ETHICS STATEMENT

The studies involving human participants were reviewed and approved by Anzhen Hospital and Fuwai Hospital. The patients/participants provided their written informed consent to participate in this study.

AUTHOR CONTRIBUTIONS

QG, YL, JP, and CM is responsible for the conception and design of the study. QG conducted the selection of the SNP. QG and MG conducted the telephone interview. JC and XC conducted the in-person interview. QG and YL was responsible for the statistical analysis and drafted the manuscript. JD and CS revised it critically for important intellectual content. JP and CM critically appraised the manuscript and approved the final version. All authors have the access to all of the data, read the manuscript, and agreed to be accountable for all aspects of the work.

FUNDING

This work was supported by the National Key Research and Development Program of China (2016YFC0900901) to CM and the National Basic Research Program of China (2013CB531105) to JP.

REFERENCES

1. Lloyd-Jones D, Adams R, Carnethon M, De Simone G, Ferguson TB, Flegal K, et al. Heart disease and stroke statistics—2009 update: a report from the American Heart Association Statistics Committee and Stroke Statistics Subcommittee. *Circulation.* (2009) 119:e21–181. doi: 10.1161/CIRCULATIONAHA.108.191261
2. Roger VL, Weston SA, Redfield MM, Hellermann-Homan JP, Killian J, Yawn BP, et al. Trends in heart failure incidence and survival in a community-based population. *JAMA.* (2004) 292:344–50. doi: 10.1001/jama.292.3.344
3. Go AS, Mozaffarian D, Roger VL, Benjamin EJ, Berry JD, Blaha MJ, et al. Executive summary: heart disease and stroke statistics—2014 update: a report from the American Heart Association. *Circulation.* (2014) 129:399–410. doi: 10.1161/01.cir.0000442015.53336.12

4. Shimokawa H, Miura M, Nochioka K, Sakata Y. Heart failure as a general pandemic in Asia. *Eur J Heart Fail.* (2015) 17:884–92. doi: 10.1002/ejhf.319
5. Korngold EC, Januzzi JL Jr, Gantzer ML, Moorthy MV, Cook NR, Albert CM. Amino-terminal pro-B-type natriuretic peptide and high-sensitivity C-reactive protein as predictors of sudden cardiac death among women. *Circulation.* (2009) 119:2868–76. doi: 10.1161/CIRCULATIONAHA.108.832576
6. Linde C, Daubert C. Cardiac resynchronization therapy in patients with New York Heart Association class I and II heart failure: an approach to 2010. *Circulation.* (2010) 122:1037–43. doi: 10.1161/CIRCULATIONAHA.109.923094
7. European Heart Rhythm A, Heart Rhythm S, Zipes DP, Camm AJ, Borggrefe M, Buxton AE, et al. ACC/AHA/ESC 2006 guidelines for management of patients with ventricular arrhythmias and the prevention of sudden cardiac death: a report of the American College of Cardiology/American Heart Association Task Force and the European Society of Cardiology Committee for Practice Guidelines (Writing Committee to develop guidelines for management of patients with ventricular arrhythmias and the prevention of sudden cardiac death). *J Am Coll Cardiol.* (2006) 48:e247–346. doi: 10.1016/j.jacc.2006.07.010
8. Brown SD, Twells RC, Hey PJ, Cox RD, Levy ER, Soderman AR, et al. Isolation and characterization of LRP6, a novel member of the low density lipoprotein receptor gene family. *Biochem Biophys Res Commun.* (1998) 248:879–88. doi: 10.1006/bbrc.1998.9061
9. Pinson KI, Brennan J, Monkley S, Avery BJ, Skarnes WC. An LDL-receptor-related protein mediates Wnt signalling in mice. *Nature.* (2000) 407:535–8. doi: 10.1038/35035124
10. Tamai K, Semenov M, Kato Y, Spokony R, Liu C, Katsuyama Y, et al. LDL-receptor-related proteins in Wnt signal transduction. *Nature.* (2000) 407:530–5. doi: 10.1038/35035117
11. Ai Z, Fischer A, Spray DC, Brown AM, Fishman GI. Wnt-1 regulation of connexin43 in cardiac myocytes. *J Clin Invest.* (2000) 105:161–71. doi: 10.1172/JCI7798
12. Kang S. Low-density lipoprotein receptor-related protein 6-mediated signaling pathways and associated cardiovascular diseases: diagnostic and therapeutic opportunities. *Hum Genet.* (2020) 139:447–59. doi: 10.1007/s00439-020-02124-8
13. Li J, Li C, Liang D, Lv F, Yuan T, The E, et al. LRP6 acts as a scaffold protein in cardiac gap junction assembly. *Nat Commun.* (2016) 7:11775. doi: 10.1038/ncomms11775
14. Pei J, Li N, Chen J, Li X, Zhang Y, Wang Z, et al. The predictive values of beta1-adrenergic and M2 muscarinic receptor autoantibodies for sudden cardiac death in patients with chronic heart failure. *Eur J Heart Fail.* (2012) 14:887–94. doi: 10.1093/eurjhf/hfs082
15. Liu X, Pei J, Hou C, Liu N, Chu J, Pu J, et al. A common NOS1AP genetic polymorphism, rs12567209 G>A, is associated with sudden cardiac death in patients with chronic heart failure in the Chinese Han population. *J Card Fail.* (2014) 20:244–51. doi: 10.1016/j.cardfail.2014.01.006
16. Yu H, Pei J, Liu X, Chen J, Li X, Zhang Y, et al. Calcium channel autoantibodies predicted sudden cardiac death and all-cause mortality in patients with ischemic and nonischemic chronic heart failure. *Dis Markers.* (2014) 2014:796075. doi: 10.1155/2014/796075
17. Fatkin D. members of the CCGDCWG. Guidelines for the diagnosis and management of familial dilated cardiomyopathy. *Heart Lung Circ.* (2011) 20:691–3. doi: 10.1016/j.hlc.2011.07.008
18. Ran Y, Chen J, Li N, Zhang W, Feng L, Wang R, et al. Common RyR2 variants associate with ventricular arrhythmias and sudden cardiac death in chronic heart failure. *Clin Sci (Lond).* (2010) 119:215–23. doi: 10.1042/CS20090656
19. Houston DW, Wylie C. Cloning and expression of Xenopus Lrp5 and Lrp6 genes. *Mech Dev.* (2002) 117:337–42. doi: 10.1016/s0925-4773(02)00205-8
20. Joiner DM, Ke J, Zhong Z, Xu HE, Williams BO. LRP5 and LRP6 in development and disease. *Trends Endocrinol Metab.* (2013) 24:31–9. doi: 10.1016/j.tem.2012.10.003
21. Kokubu C, Heinzmann U, Kokubu T, Sakai N, Kubota T, Kawai M, et al. Skeletal defects in ringelschwanz mutant mice reveal that Lrp6 is required for proper somitogenesis and osteogenesis. *Development.* (2004) 131:5469–80. doi: 10.1242/dev.01405
22. Dieckmann M, Dietrich MF, Herz J. Lipoprotein receptors–an evolutionarily ancient multifunctional receptor family. *Biol Chem.* (2010) 391:1341–63. doi: 10.1515/BC.2010.129
23. Dierick H, Bejsovec A. Cellular mechanisms of wingless/Wnt signal transduction. *Curr Top Dev Biol.* (1999) 43:153–90. doi: 10.1016/s0070-2153(08)60381-6
24. Kikuchi A. Regulation of beta-catenin signaling in the Wnt pathway. *Biochem Biophys Res Commun.* (2000) 268:243–8. doi: 10.1006/bbrc.1999.1860
25. Miller JR, Hocking AM, Brown JD, Moon RT. Mechanism and function of signal transduction by the Wnt/beta-catenin and Wnt/Ca2+ pathways. *Oncogene.* (1999) 18:7860–72. doi: 10.1038/sj.onc.1203245
26. Mani A, Radhakrishnan J, Wang H, Mani A, Mani MA, Nelson-Williams C, et al. LRP6 mutation in a family with early coronary disease and metabolic risk factors. *Science.* (2007) 315:1278–82. doi: 10.1126/science.1136370
27. Alberti KG, Eckel RH, Grundy SM, Zimmet PZ, Cleeman JI, Donato KA, et al. Harmonizing the metabolic syndrome: a joint interim statement of the International Diabetes Federation Task Force on Epidemiology and Prevention; National Heart, Lung, and Blood Institute; American Heart Association; World Heart Federation; International Atherosclerosis Society; and International Association for the Study of Obesity. *Circulation.* (2009) 120:1640–5. doi: 10.1161/CIRCULATIONAHA.109.192644
28. De Ferrari GV, Papassotiropoulos A, Biechele T, Wavrant De-Vrieze F, Avila ME, Major MB, et al. Common genetic variation within the low-density lipoprotein receptor-related protein 6 and late-onset Alzheimer's disease. *Proc Natl Acad Sci USA.* (2007) 104:9434–9. doi: 10.1073/pnas.0603523104
29. Cheng SL, Ramachandran B, Behrmann A, Shao JS, Mead M, Smith C, et al. Vascular smooth muscle LRP6 limits arteriosclerotic calcification in diabetic LDLR$^{-/-}$ mice by restraining noncanonical Wnt signals. *Circ Res.* (2015) 117:142–56. doi: 10.1161/CIRCRESAHA.117.306712
30. Guo J, Li Y, Ren YH, Sun Z, Dong J, Yan H, et al. Mutant LRP6 impairs endothelial cell functions associated with familial normolipidemic coronary artery disease. *Int J Mol Sci.* (2016) 17:1173. doi: 10.3390/ijms17071173
31. Liu W, Mani S, Davis NR, Sarrafzadegan N, Kavathas PB, Mani A. Mutation in EGFP domain of LDL receptor-related protein 6 impairs cellular LDL clearance. *Circ Res.* (2008) 103:1280–8. doi: 10.1161/CIRCRESAHA.108.183863
32. Basheer WA, Harris BS, Mentrup HL, Abreha M, Thames EL, Lea JB, et al. Cardiomyocyte-specific overexpression of the ubiquitin ligase Wwp1 contributes to reduction in Connexin 43 and arrhythmogenesis. *J Mol Cell Cardiol.* (2015) 88:1–13. doi: 10.1016/j.yjmcc.2015.09.004
33. Dawson K, Aflaki M, Nattel S. Role of the Wnt-Frizzled system in cardiac pathophysiology: a rapidly developing, poorly understood area with enormous potential. *J Physiol.* (2013) 591:1409–32. doi: 10.1113/jphysiol.2012.235382
34. Gollob MH, Blier L, Brugada R, Champagne J, Chauhan V, Connors S, et al. Recommendations for the use of genetic testing in the clinical evaluation of inherited cardiac arrhythmias associated with sudden cardiac death: Canadian Cardiovascular Society/Canadian Heart Rhythm Society joint position paper. *Can J Cardiol.* (2011) 27:232–45. doi: 10.1016/j.cjca.2010.12.078
35. Ellinor PT, Lunetta KL, Albert CM, Glazer NL, Ritchie MD, Smith AV, et al. Meta-analysis identifies six new susceptibility loci for atrial fibrillation. *Nat Genet.* (2012) 44:670–5. doi: 10.1038/ng.2261
36. Jansen JA, van Veen TA, de Jong S, van der Nagel R, van Stuijvenberg L, Driessen H, et al. Reduced Cx43 expression triggers increased fibrosis due to enhanced fibroblast activity. *Circ Arrhythm Electrophysiol.* (2012) 5:380–90. doi: 10.1161/CIRCEP.111.966580
37. Burstein B, Comtois P, Michael G, Nishida K, Villeneuve L, Yeh YH, et al. Changes in connexin expression and the atrial fibrillation substrate in congestive heart failure. *Circ Res.* (2009) 105:1213–22. doi: 10.1161/CIRCRESAHA.108.183400
38. Ye B, Ge Y, Perens G, Hong L, Xu H, Fishbein MC, et al. Canonical Wnt/beta-catenin signaling in epicardial fibrosis of failed pediatric heart allografts with diastolic dysfunction. *Cardiovasc Pathol.* (2013) 22:54–7. doi: 10.1016/j.carpath.2012.03.004
39. Duan J, Gherghe C, Liu D, Hamlett E, Srikantha L, Rodgers L, et al. Wnt1/betacatenin injury response activates the epicardium and

cardiac fibroblasts to promote cardiac repair. *EMBO J.* (2012) 31:429–42. doi: 10.1038/emboj.2011.418
40. Laeremans H, Rensen SS, Ottenheijm HC, Smits JF, Blankesteijn WM. Wnt/frizzled signalling modulates the migration and differentiation of immortalized cardiac fibroblasts. *Cardiovasc Res.* (2010) 87:514–23. doi: 10.1093/cvr/cvq067
41. Wang X, Zou Y, Li Y, Chen Z, Yin C, Wang Y, et al. Lipoprotein receptor-related protein 6 is required to maintain intercalated disk integrity. *Genes Cells.* (2019) 24:789–800. doi: 10.1111/gtc.12727
42. Chen Z, Li Y, Wang Y, Qian J, Ma H, Wang X, et al. Cardiomyocyte-restricted low density lipoprotein receptor-related protein 6 (LRP6) deletion leads to lethal dilated cardiomyopathy partly through Drp1 signaling. *Theranostics.* (2018) 8:627–43. doi: 10.7150/thno.22177
43. Xu S, Cheng J, Chen YN Li K, Ma ZW, Cen JM, et al. The LRP6 rs2302685 polymorphism is associated with increased risk of myocardial infarction. *Lipids Health Dis.* (2014) 13:94. doi: 10.1186/1476-511X-13-94
44. Clevers H, Nusse R. Wnt/beta-catenin signaling and disease. *Cell.* (2012) 149:1192–205. doi: 10.1016/j.cell.2012.05.012
45. Go GW. Low-density lipoprotein receptor-related protein 6 (LRP6) is a novel nutritional therapeutic target for hyperlipidemia, non-alcoholic fatty liver disease, and atherosclerosis. *Nutrients.* (2015) 7:4453–64. doi: 10.3390/nu7064453

Conflict of Interest: The authors declare that the research was conducted in the absence of any commercial or financial relationships that could be construed as a potential conflict of interest.

Publisher's Note: All claims expressed in this article are solely those of the authors and do not necessarily represent those of their affiliated organizations, or those of the publisher, the editors and the reviewers. Any product that may be evaluated in this article, or claim that may be made by its manufacturer, is not guaranteed or endorsed by the publisher.

frontiers in Cardiovascular Medicine

SYSTEMATIC REVIEW
published: 16 February 2022
doi: 10.3389/fcvm.2022.817396

Trimethylamine N-Oxide in Heart Failure: A Meta-Analysis of Prognostic Value

*Xingxing Li[1], Zongjing Fan[2], Jie Cui[2], Dong Li[2], Jinjin Lu[2], Xiaoyun Cui[2], Liandi Xie[2], Yang Wu[2], Qian Lin[3] and Yan Li[2]**

[1] Second Clinical School of Medicine, Beijing University of Chinese Medicine, Beijing, China, [2] Department of Cardiology, Dongfang Hospital, Beijing University of Chinese Medicine, Beijing, China, [3] Department of Cardiology, Dongzhimen Hospital, Beijing University of Chinese Medicine, Beijing, China*

Objective: The present study aimed to explore the prognostic value of trimethylamine N-oxide (TMAO) in heart failure (HF).

Methods: PubMed, Excerpta Medica Database (EMBASE), Cochrane Library, Web of Science, Wanfang Database, SINOMED, China Science and Technology Journal Database (VIP), and China National Knowledge Infrastructure (CNKI) were searched up to June 1, 2021. Studies recording the major adverse cardiovascular events (MACEs) or all-cause mortality in HF patients and their circulating TMAO concentrations were included. Meta-analysis was performed using Stata 13.0.

Results: Ten articles (12 studies) involving 13,425 participants from 2014 to 2021 were considered. Compared to low-level TMAO, elevated TMAO was correlated with MACEs and all-cause mortality in HF (RR: 1.28, 95% CI: 1.17, 1.39, $P < 0.0001$, random-effects model and RR: 1.35, 95% CI: 1.28, 1.42, $P < 0.0001$, random-effects model, respectively). Consistent results were obtained in all examined subgroups as well as in the sensitivity analysis.

Conclusion: Elevated TMAO may be an adverse prognostic indicator in patients with HF.

Systematic Review Registration: https://www.crd.york.ac.uk/prospero/display_record.php?RecordID=267208

Keywords: heart failure, trimethylamine N-oxide, major adverse cardiovascular events, all-cause mortality, meta-analysis

OPEN ACCESS

Edited by:
Tong Liu,
Tianjin Medical University, China

Reviewed by:
Xin Hai,
First Affiliated Hospital of Harbin Medical University, China
Rajesh H. Amin,
Auburn University, United States
Hailan Zhu,
Southern Medical University, China

****Correspondence:***
Yan Li
15801434320@163.com

Specialty section:
This article was submitted to Heart Failure and Transplantation, a section of the journal Frontiers in Cardiovascular Medicine

Received: *18 November 2021*
Accepted: *19 January 2022*
Published: *16 February 2022*

Citation:
Li X, Fan Z, Cui J, Li D, Lu J, Cui X, Xie L, Wu Y, Lin Q and Li Y (2022) Trimethylamine N-Oxide in Heart Failure: A Meta-Analysis of Prognostic Value. Front. Cardiovasc. Med. 9:817396. doi: 10.3389/fcvm.2022.817396

INTRODUCTION

Heart failure (HF) is an increasing public health problem worldwide (1). Evidence from epidemiological studies has shown that approximately 64.3 million people worldwide suffer from HF (2). Patients with HF usually experience the following malignant disease cycle: "hospitalization-improvement-discharge-rehospitalization" (3). Despite recent advances in the diagnosis and treatment of HF, patient mortality remains high (4, 5), suggesting that many risk factors for HF remain unexplored.

Intestinal microorganisms are involved in the occurrence and progression of many diseases (6). Recent studies have revealed the associations between human gut microbes and HF (7, 8). As one of the metabolic products in intestinal microorganisms, trimethylamine N-oxide (TMAO) has been demonstrated to promote the development of HF and is an important risk factor for patients with HF (9). Schuett et al. (10) followed more than 4,000 patients with HF for 9.7 years; and they

reported that after excluding factors, such as body weight, smoking, hypertension, diabetes, and atrial fibrillation, high levels of TMAO are associated with all-cause mortality in patients with HF. TMAO aggravates HF by damaging vascular endothelial function, affecting mitochondrial metabolism, and promoting myocardial fibrosis (11, 12). Owing to the limited sample size, further evaluation is still needed.

Therefore, the present systematic review and meta-analysis aimed to explore the prognostic value of TMAO in HF. To our knowledge, this is the first study to include data from around the world describing the association between TMAO and HF.

METHODS

Study Registration

This meta-analysis was performed in accordance with the recommendations of the Preferred Reporting Items for Systematic Reviews (PRISMA) statement (13). The review protocol was registered at PROSPERO as CRD42021267208.

Search Strategy

We searched the following 4 English electronic databases and 3 Chinese literature databases for studies published from inception to June 1, 2021: PubMed, Excerpta Medica Database (EMBASE), Cochrane Library, Web of Science, Wanfang database, SINOMED, VIP database, and China National Knowledge Infrastructure (CNKI). In addition, there was no restriction for language. Taking PubMed as an example, the details of the search strategy are shown in **Table 1**. This work was completed by two independent reviewers (ZF and JC), and in cases where they disagreed, a third individual (LX) was consulted. Moreover, manual retrieval was performed on Baidu Academic, Google Academic, books, impurities, and conference materials to obtain all the materials related to this study as comprehensively as possible. We also screened the references of the included papers, full texts, and bibliographies of all potential articles, including relevant reviews and meta-analyses, to identify additional eligible studies.

TABLE 1 | Search strategy in the PubMed database.

Number	Search terms
#1	Heart failure [Mesh]
#2	(Cardiac Failure [Title/Abstract]) OR (Heart Decompensation [Title/Abstract])) OR (Decompensation, Heart [Title/Abstract])) OR (Heart Failure, Right-Sided [Title/Abstract])) OR (Heart Failure, Right Sided [Title/Abstract])) OR (Right-Sided Heart Failure [Title/Abstract])) OR (Right Sided Heart Failure [Title/Abstract])) OR (Myocardial Failure [Title/Abstract])) OR (Congestive Heart Failure [Title/Abstract])) OR (Heart Failure, Congestive [Title/Abstract])) OR (Heart Failure, Left-Sided [Title/Abstract])) OR (Heart Failure, Left Sided [Title/Abstract])) OR (Left-Sided Heart Failure [Title/Abstract])) OR (Left Sided Heart Failure [Title/Abstract])
#3	#1OR#2
#4	("trimethylamine N-oxide" [Mesh])
#5	(trimethyloxamine [Title/Abstract]) OR (trimethylammonium oxide [Title/Abstract]) OR (TMAO [Title/Abstract]) OR (trimethylamine oxide [Title/Abstract])
#6	#4OR#5
#7	#3AND#6

Inclusion and Exclusion Criteria

To prevent bias, the inclusion criteria were prespecified as follows: (a) the subjects were patients with HF; (b) prospective cohort; (c) major adverse cardiac events (MACEs), including cardiovascular mortality, MI, cardiovascular hospitalization or revascularization, in addition to all-cause mortality were reported; and (d) hazard ratio (HR)/relative risk (RR) and 95% CI were reported.

Studies were excluded if any of the following criteria were observed: (a) duplications; (b) lack of data on TMAO levels and heart failure; or (c) case reports, animal trials, review articles, systematic reviews, meta-analyses, commentaries, editorials, or meeting abstracts.

Data Extraction

All data were independently extracted by two reviewers (DL and JL), and disagreements were resolved by discussion. If necessary, a third author (XC) was involved. Study information of the included studies was recorded, including the first author, publication year, participant characteristics, sample size, region, circulating TMAO concentration, duration of follow-up, adjusted risk factors, and outcome assessment.

Quality Assessment

Two authors (XC and LX) independently assessed the methodological quality of the included studies. The Newcastle-Ottawa quality assessment scale (NOS) was used to evaluate the risk of bias based on study group selection, group comparability, and ascertainment of exposure or outcome (14). The maximum score of this scale is 9 points, and studies with a score $\geq$7 are rated as high quality (15).

Data Synthesis and Statistical Analysis

The data were analyzed with Stata (version 13.0) (16). RRs and 95% CIs were used to estimate the combined effects. The overall effect was calculated by a Z-test, and $P < 0.05$ (2-tailed) was defined as statistically significant. Potential heterogeneity was evaluated by Cochran Q and I^2 statistics (17). A fixed-effect model was employed when heterogeneity was low ($P \geq 0.05$, $I^2 \leq 50\%$) (18). However, when high heterogeneity occurred ($P < 0.05$, $I^2 > 50\%$), we further analyzed its potential sources from the following three aspects: clinical heterogeneity, methodological heterogeneity, and statistical heterogeneity. We evaluated clinical heterogeneity first. If there was evident clinical heterogeneity, subgroup analysis was performed. If clinical heterogeneity was evident and subgroup analysis could not be conducted, descriptive analysis was only used. After excluding clinical and methodological heterogeneity, statistical heterogeneity was considered, and a random-effect model was used (19). A funnel chart, Egger's, and Begg's test were constructed to evaluate publication bias (19). Publication bias will be adjusted by the method of trim and filling.

We performed sensitivity analyses to evaluate reliable results. The methods included changing the type of analysis methods (random-effects model or fixed-effects model), eliminating each of the included studies one by one, and then combining the effect quantities.

Ethics

Because patient privacy was not involved in the present study, ethical approval was not needed.

RESULTS

Literature Search and Screening

The search of 8 databases identified 396 articles for further evaluation (129 from CNKI, 23 from WANFANG, 13 from VIP, 36 from SINOMED, 55 from PubMed, 6 from the Cochrane Library, 114 from Embase, and 20 from the Web of Science), of which 190 were removed after review due to duplicate records. After reading the titles and abstracts, 178 were excluded for various reasons. Finally, only 10 studies (10, 20–28) met the inclusion criteria after screening full texts. **Figure 1** shows the detailed process of the study selection process.

Study Characteristics and Quality Assessment

Ten articles (12 studies) involving 13,425 participants from 2014 to 2021 were included in the present study. Most trials were performed in Europe (3 in the UK, 1 in Norway, 1 in Germany, and 1 in other); however, trials were also performed in the United States (2 trials) and Asia (2 in China). Only three studies (23, 24, 28) included patients with acute HF; all others included patients with chronic HF. Three studies were multicenter, and the others were single-center. The follow-up duration ranged from 1 to 9.7 years with a median follow-up of 3.4 years. The average age of the patients ranged from 57 to 78 years old. Most trials had more males than females. Baseline TMAO levels were reported in all included studies. All the studies reported data on MACEs or all-cause mortality. All observational studies were adjusted for multiple potential confounding factors, and more than half of the studies were rated as "good" quality. The characteristics of the included studies are listed in **Table 2**.

Primary Outcome: The Association Between TMAO Level and MACEs in Patients With HF

Five cohort studies with a total of 8,716 participants reported an association of MACEs with TMAO levels (RR: 1.28; 95% CI: 1.17, 1.39; $P < 0.0001$; $I^2 = 56.1\%$; P-heterogeneity = 0.058; random-effects model; **Figure 2**). This result indicated that a high circulating TMAO concentration was associated with a greater risk of MACEs in patients with HF. Due to the high heterogeneity, subgroup analysis was implemented. The subgroup analysis did not affect the results (**Figure 3**).

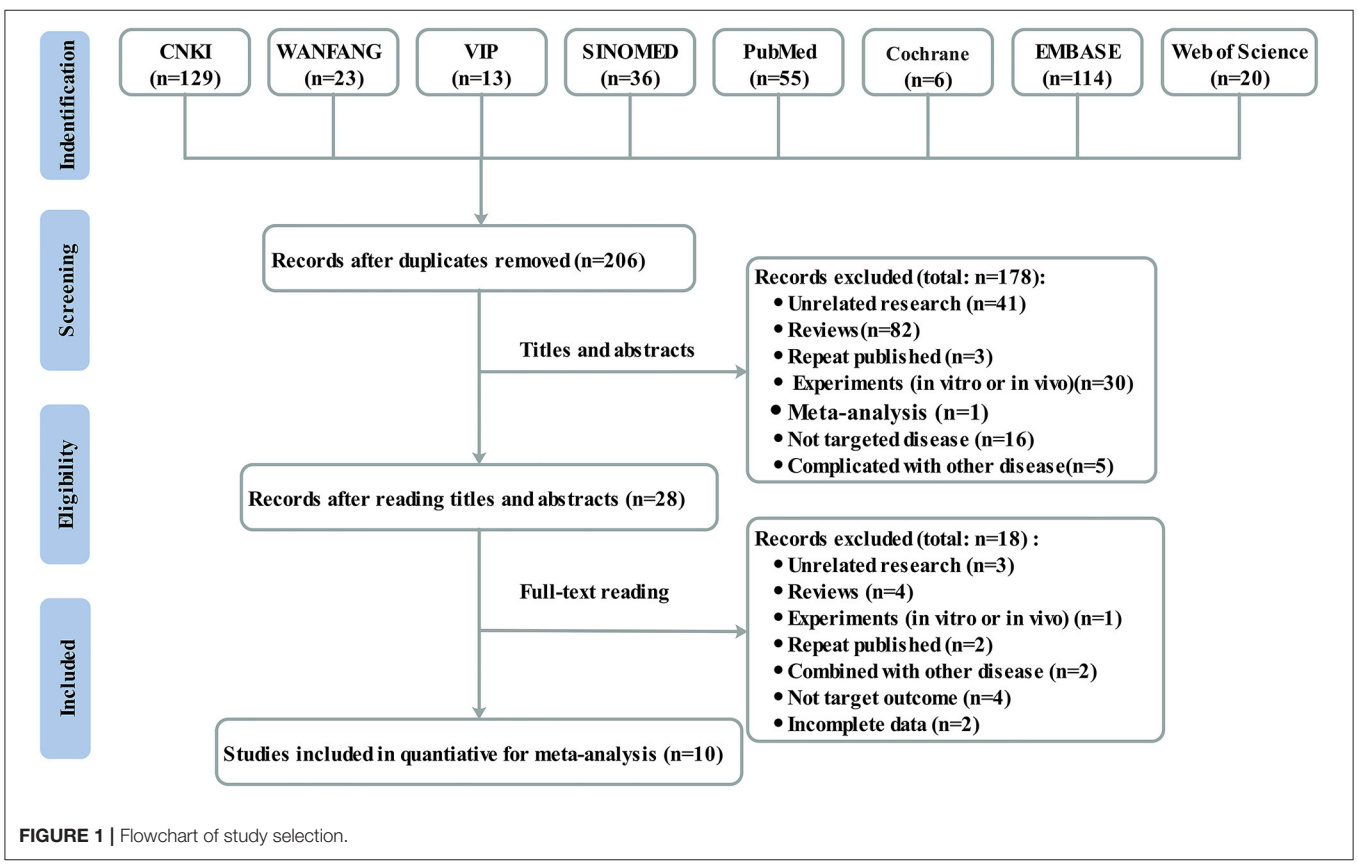

FIGURE 1 | Flowchart of study selection.

TABLE 2 | Characteristics of the selected studies and quality assessment.

References	Location	HF type	Scale	Follow-up, years	Participants (male, %)	Age, years	TMAO level (umol/L)	Outcome	Adjusted risk factors	Study quality
Tang et al. (20)	USA	Chronic	Single center	5	720 (59)	66 ± 10	5.0 (3.0, 8.5)	All-cause mortality	Yes	8
Tang et al. (21)	USA	Chronic	Single center	5	112 (75)	57 ± 14	5.8 (3.6, 12.1)	All-cause mortality	Yes	8
Trøseid et al. (22)	Norway	Chronic	Single center	5.2	155 (83)	57 ± 11	NA	All-cause mortality	Yes	7
Suzuki and Heaney (23)	UK	Acute	Single center	1	972 (61)	78 (69–84)	5.6 (3.4, 10.5)	All-cause mortality	Yes	6
Schuett et al. (10)	Germany	Chronic	Single center	9.7	2,490 (NA)	63 ± 10	4.73 (3.4, 6.82)/4.73 (3.22, 6.85)	All-cause mortality	Yes	6
Liu (24)	China	Acute	Single center	1	64 (67)	70 ± 14	6.56 ± 11.83	All-cause mortality	Yes	6
Suzuki et al. (25)	European	Chronic	Multicenter	1	2,234 (74)	70 (61–78)	5.9 (3.6, 10.8)	All-cause mortality; MACE	Yes	8
Suzuki et al. (25)	European	Chronic	Multicenter	2	2,234 (74)	70 (61–78)	5.9 (3.6, 10.8)	All-cause mortality; MACE	Yes	8
Suzuki et al. (25)	European	Chronic	Multicenter	3	2,234 (74)	70 (61–78)	5.9 (3.6, 10.8)	All-cause mortality; MACE	Yes	8
Salzano et al. (26)	UK	Chronic	Single center	5	196 (49)	73 (67–78)	7.0 (4.2, 12.5)	All-cause mortality	Yes	6
Zhou et al. (27)	China	Chronic	Multicenter	1.8	1,208 (689)	73 (64–80)	4.5 (2.83, 7.92)	All-cause mortality, MACE	Yes	7
Israr et al. (28)	UK	Acute	Single center	1	806 (61)	78 (69–84)	10.2 (5.8, 18.7)	All-cause mortality; MACE	Yes	6

USA, the United States; UK, United Kingdom.

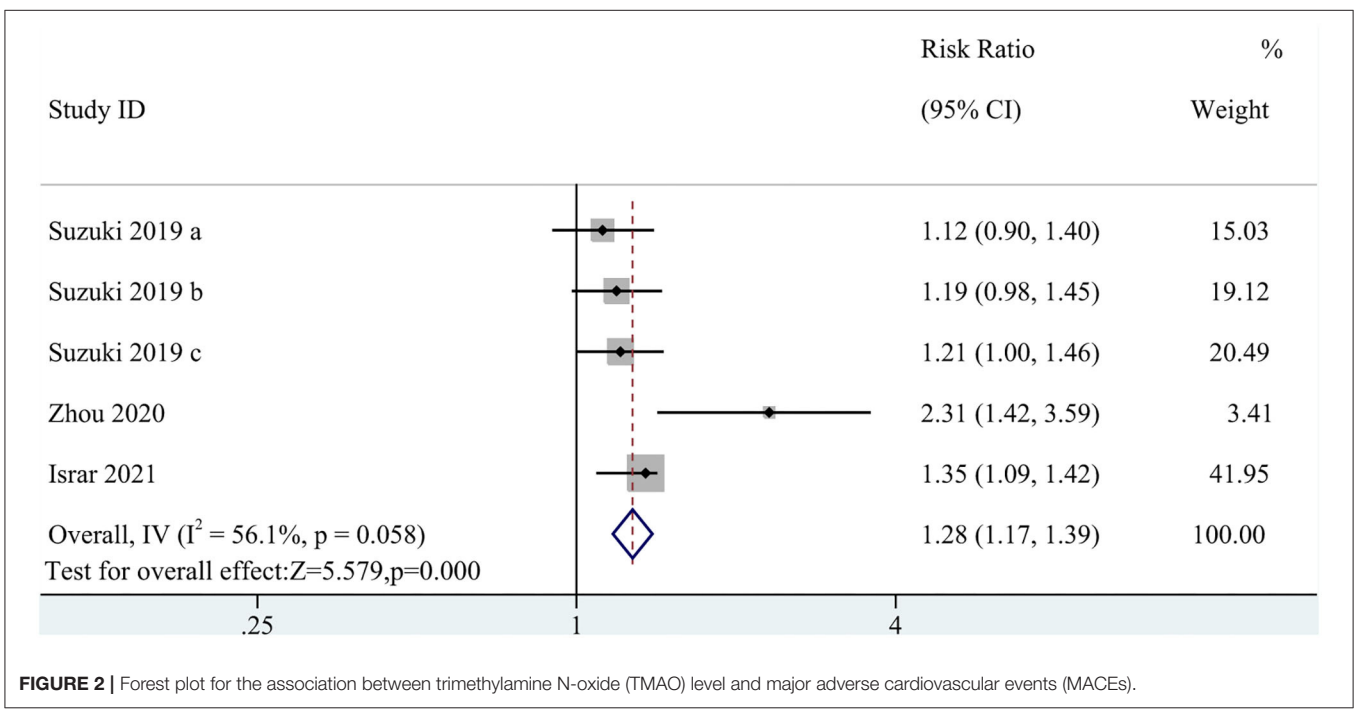

FIGURE 2 | Forest plot for the association between trimethylamine N-oxide (TMAO) level and major adverse cardiovascular events (MACEs).

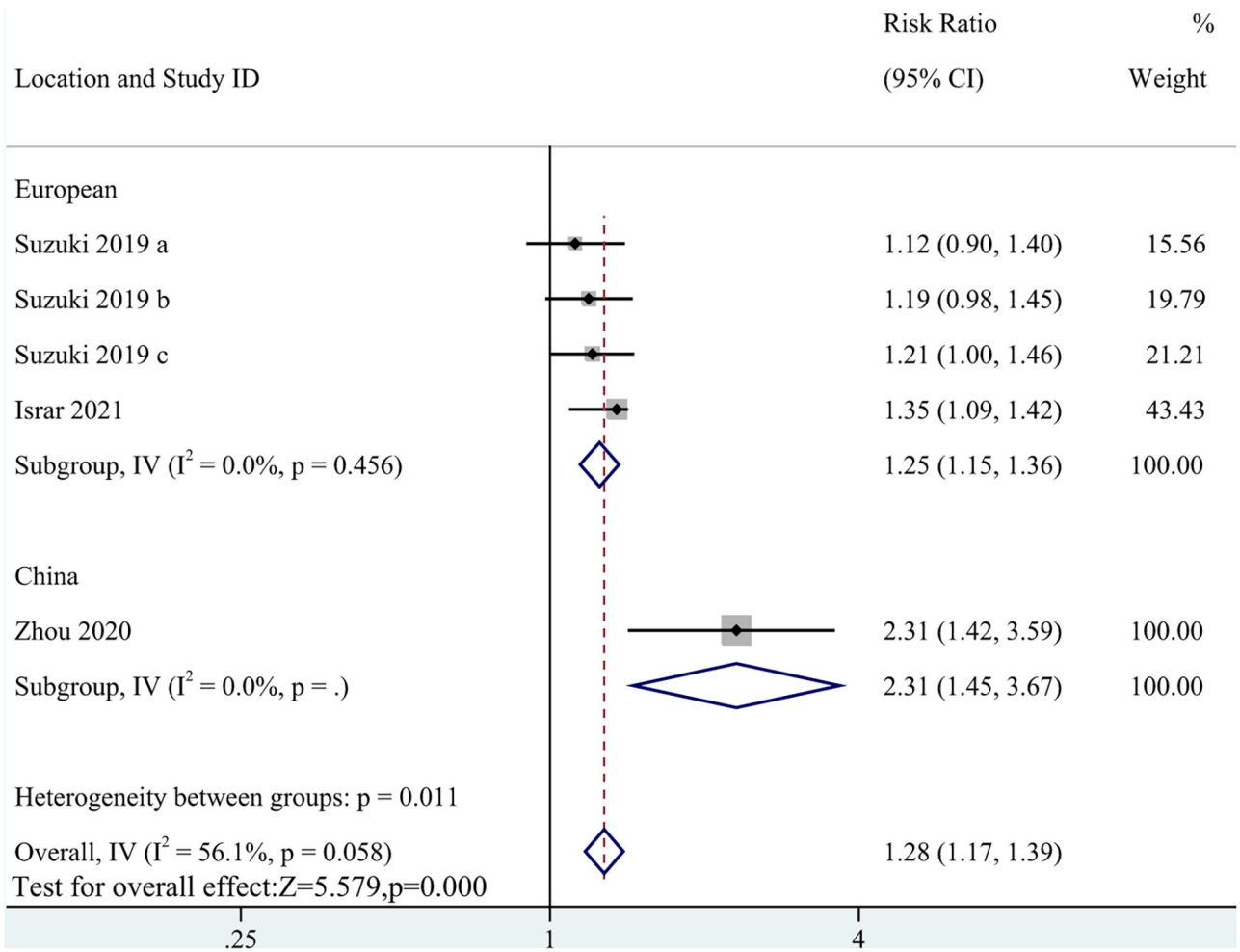

FIGURE 3 | Subgroup analysis for the association between TMAO level and MACEs.

Secondary Outcome: The Association Between TMAO Level and All-Cause Mortality in Patients With HF

The pooled analysis comparing the all-cause mortality in HF patients with high and low circulating TMAO concentrations involved all included studies (RR: 1.35; 95% CI: 1.28, 1.42; $P < 0.0001$; $I^2 = 56.5\%$; P-heterogeneity = 0.008; random-effects model; **Figure 4**). The results showed that the risk of all-cause mortality was greater with higher circulating TMAO concentrations among patients with HF. Considering significant heterogeneity, we performed subgroup analysis based on study characteristics to explore the potential sources of heterogeneity (**Table 3**). Seven items, including study scale, location, HF type, sample size, age, follow up, and study quality, were included in the subgroup analysis to evaluate the impact on heterogeneity. In general, the results were not influenced by these factors, indicating that the meta-analysis result was stable.

Publication Bias Analysis

For the relationship between TMAO and MACEs in the present study, the funnel plot appeared asymmetric (**Figure 5A**), but further Egger's and Begg's tests demonstrated that there was no publication bias ($P = 0.922$ for Egger's test and $P = 0.462$ for Begg's test). In addition, the funnel plot and Egger's test all indicated potential publication bias for the relationship between TMAO and all-cause mortality ($P = 0.017$ for Egger's test; **Figure 5B**). Although publication bias existed, the results of trim-and-fill method suggested that the meta-analysis results were robust (RR: 0.251; 95% CI: 0.11, 0.392; $P < 0.001$ for MACEs; RR: 0.257; 95% CI: 0.153, 0.36; $P < 0.001$ for all-cause mortality; **Figure 6**).

Sensitivity Analysis

Sensitivity analyses were performed to assess whether the results of this meta-analysis were stable. The results showed that no obvious effect was found after deleting the studies

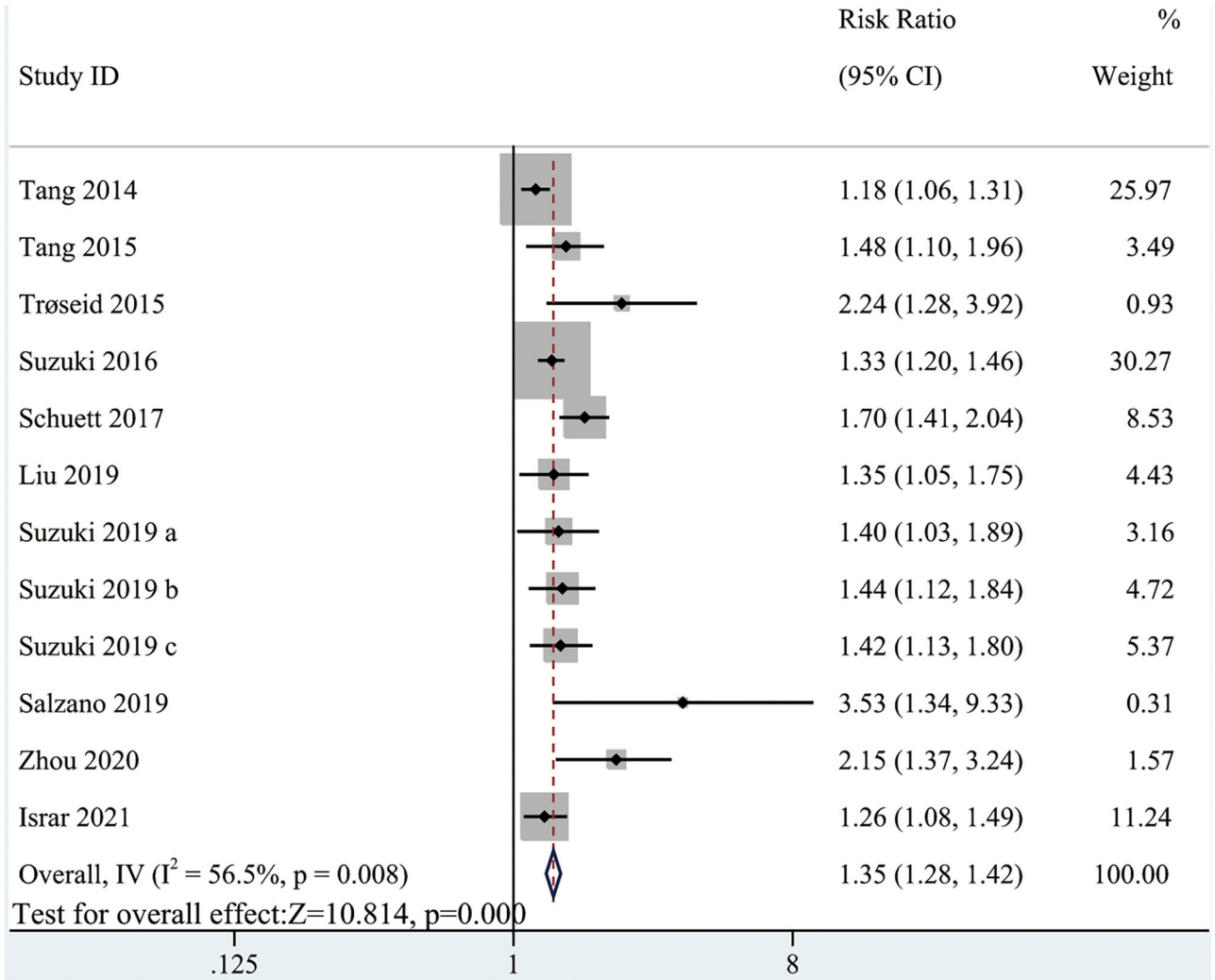

FIGURE 4 | Forest plot for the association between TMAO level and all-cause mortality.

one by one, which suggested that the study results were credible (**Figure 7**).

DISCUSSION

At present, there are few reported meta-analyses on the relationship between TMAO and the poor prognosis of HF; the included studies are mainly from Europe and the United States, and there is a lack of data on Asian HF populations (29). With this background, we performed the first systematic review and meta-analysis involving studies from around the world to explore whether high levels of TMAO are related to the poor prognosis of HF patients. These 10 articles were published from 2014 to 2021, which reflected recent results about the role of circulating TMAO levels in predicting the poor prognosis of patients with HF. This systematic review and meta-analysis provided relatively reliable evidence that elevated TMAO is related to MACEs and all-cause mortality in patients with HF.

Trimethylamine N-oxide (TMAO) is a small odorless molecule (molecular mass of 75.11 g/mol) (30). Dietary choline, betaine, and L-carnitine are metabolized by intestinal microorganisms to generate trimethylamine (TMA), which is further converted to TMAO by hepatic flavin monooxygenase (FMO) (31, 32). Although TMAO can maintain normal physiological activities of the human body, high concentrations of TMAO may cause various cardiovascular diseases (33). Animal studies have shown that both choline supplementation (a precursor to TMAO production) and direct dietary TMAO supplementation increase the level of TMAO, exacerbating myocardial fibrosis and worsening cardiac function (34). Chen et al. (35) proposed that inhibitors of TMA formation reduce circulating TMAO levels in obese mice induced by Western diets, thereby preventing subsequent cardiac dysfunction. TMAO induces HF *via* multiple pathological mechanisms, including inflammation, mitochondrial dysfunction, oxygen-free radical production, and myocardial fibrosis (**Figure 8**) (36–40). There

TABLE 3 | Subgroup analysis for the association between TMAO level and all-cause mortality according to study characteristics.

Subgroups	Studies, *n*	Effects model	Over effect		Heterogeneity	
			RR (95% CI)	*P* value	I^2, %	*P* value
All	12	Random	1.35 (1.28, 1.42)	<0.0001	56.5	0.008
Scale						
Single-center	8	Fixed	1.32 (1.25, 1.40)	<0.0001	64.8	0.006
Multi-center	4	Random	1.49 (1.29, 1.71)	<0.0001	5.8	0.364
Location						
USA	2	Random	1.21 (1.19, 1.34)	<0.0001	52	0.149
European	8	Fixed	1.40 (1.31, 1.49)	<0.0001	47	0.067
Asia	2	Random	1.53 (1.22, 1.90)	<0.0001	69.8	0.069
HF type						
Chronic	9	Random	1.34 (1.28, 1.48)	<0.0001	67	0.002
Acute	3	Fixed	1.31 (1.21, 1.42)	<0.0001	0	0.834
Participants						
<900	6	Random	1.26 (1.16, 1.36)	<0.0001	55.9	0.045
≥900	6	Fixed	1.43 (1.32, 1.54)	<0.0001	44.1	0.112
Age						
<70	5	Random	1.33 (1.22, 1.44)	<0.0001	74.3	0.004
≥70	7	Fixed	1.36 (1.27, 1.46)	<0.0001	36.8	0.148
Follow up						
<5	7	Fixed	1.35 (1.26, 1.45)	<0.0001	0	0.449
≥5	5	Random	1.33 (1.22, 1.46)	<0.0001	79.4	0.001
Study quality						
Good	8	Random	1.32 (1.24, 1.40)	<0.0001	51.0	0.046
Fair	4	Random	1.43 (1.29, 1.67)	<0.0001	67.6	0.026

are many factors that affect the level of TMAO in the body, including diet, intestinal microbiota, sex, age, kidney function, weight, and drugs (31, 32, 41, 42). In the original studies included in this article, 7 were corrected for age, 5 were corrected for renal function, and 4 were corrected for sex and weight. At the same time, we conducted subgroup analyses of age, scale, location, HF type (chronic or acute), sample size, follow-up, and study quality to explore the potential sources of heterogeneity. Sensitivity analysis was also implemented. Fortunately, subgroup analyses and sensitivity analyses did not change the overall results. We obtained the same result as Li et al. (29), but our original studies were distributed in Europe, the United States, and Asia, which made up for the deficiency of their study. However, it is worth mentioning that we still cannot rule out the influence of diet, gut microbiota, and drugs on TMAO. Red meat, eggs, and sea fish are common sources of TMAO in the diet (31, 41, 43), thereby reminding nutritionists to pay attention to the nutritional benefits of these foods while not ignoring the adverse metabolites (such as TMAO) associated with these foods when formulating nutritional prescriptions for patients with cardiovascular disease.

The rapidly increasing population of patients with HF imposes a heavy social and economic burden. Our results encourage the exploration of interventions to reduce TMAO. At present, methods to reduce TMAO mainly remain in the stage of animal experiments, including 3,3-dimethyl-1-butanol, choline analogs (IMC and FMC), and betaine aldehyde (44–46). The method used to reduce TMAO in clinical is microbial-driven therapy, however, a meta-analysis showed the opposite conclusion (47).

Existing studies have revealed the key role of TMAO in HF. TMAO may participate in the occurrence and development of HF through a variety of mechanisms. However, related scientific research has just started, and only limited studies have revealed the connection between TMAO and HF. There are questions about the relationship between TMAO and HF. First, due to the lack of long-term monitoring of circulating TMAO concentration in patients before HF occurs, it is still difficult to determine whether a high level of TMAO is the triggering factor of HF. The above results provided preliminary evidence that TMAO predicts the poor prognosis of patients with HF. Our findings originated from clinical data, adding new direct evidence, which largely confirms the reliability of the association between high concentrations of TMAO and poor prognosis of HF. Second, TMAO reduction interventions remain in the laboratory stage, and there is no effective treatment in the clinic. Finally, the results of the dose-response relationship provided in the meta-analysis better present the relationship between different dose levels of exposure factors and outcomes, making the results more reliable. However, due to the lack of studies on the relationship between different concentrations of TMAO and the prognosis of HF, the dose-response relationship between TMAO and the poor prognosis of HF remain unknown.

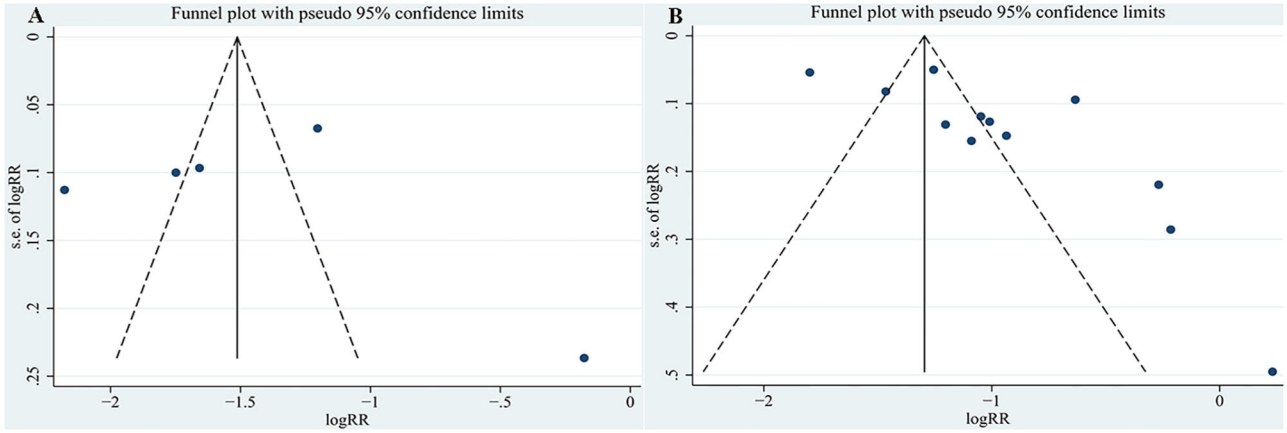

FIGURE 5 | Funnel plot for publication bias. **(A)** Funnel plot for publication bias of the association between TMAO level and MACEs; **(B)** Funnel plot for publication bias of the association between TMAO level and all-cause mortality.

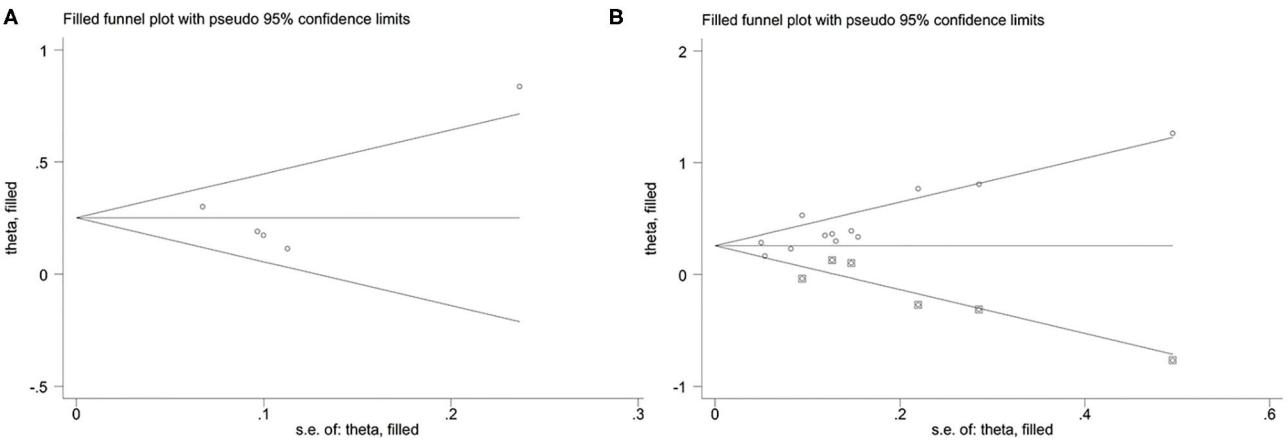

FIGURE 6 | Trim and fill method on MACEs **(A)** and all-cause mortality **(B)**.

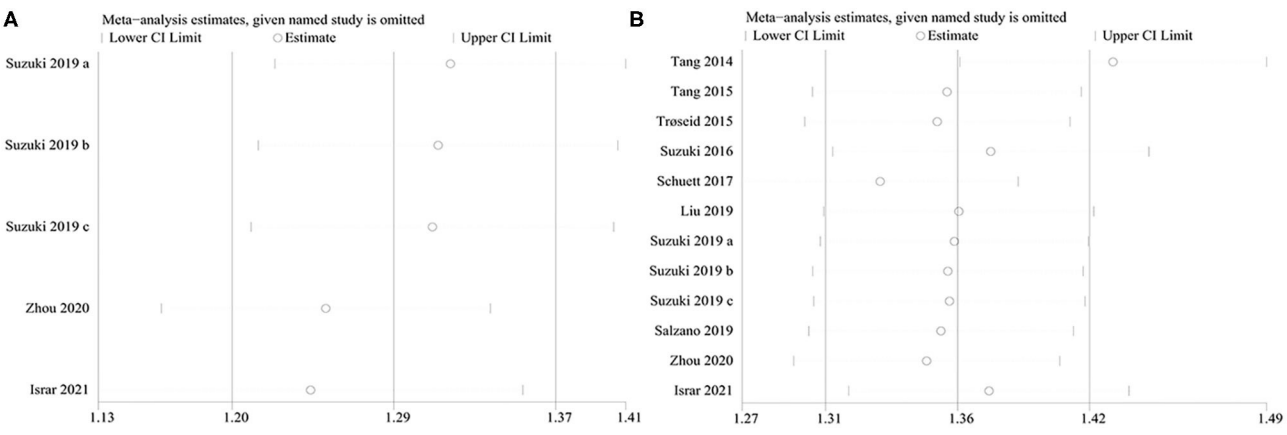

FIGURE 7 | The sensitivity analysis of the study. **(A)** The sensitivity analysis of the association between TMAO level and MACEs; **(B)** The sensitivity analysis of the association between TMAO level and all-cause mortality.

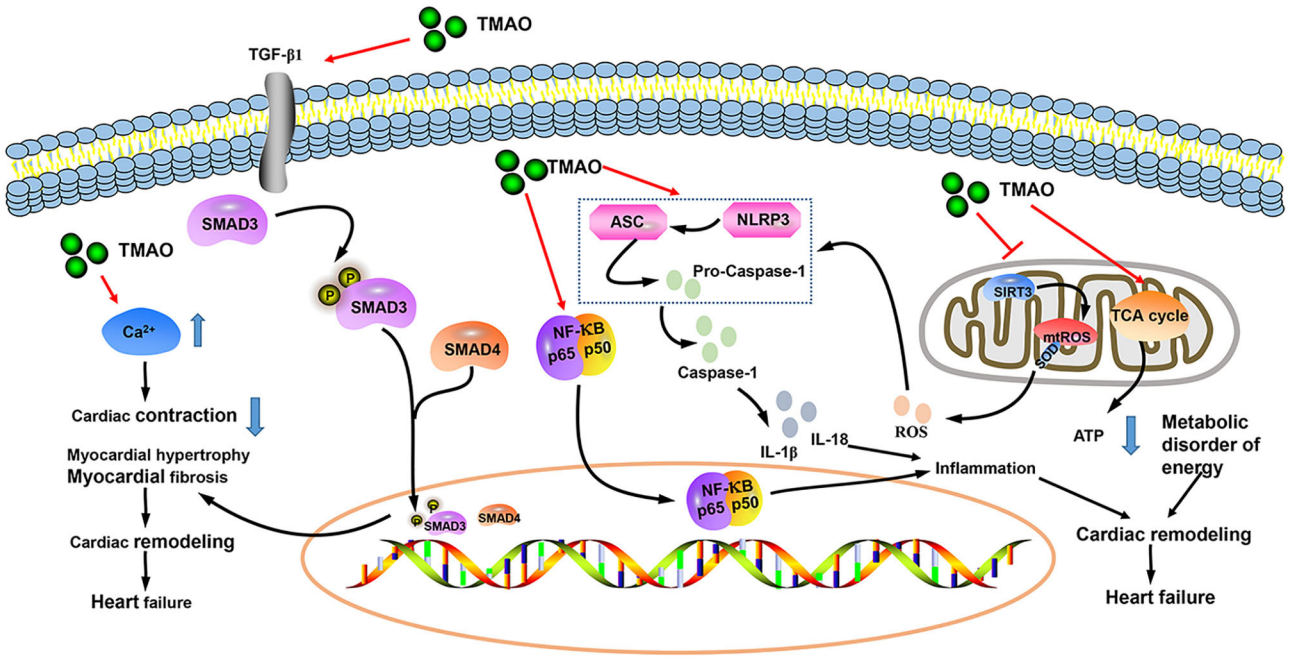

FIGURE 8 | Mechanism of TMAO exacerbating heart failure (HF) progression.

In the future, a large-scale prospective cohort should be further developed to explore the causal relationship between TMAO and HF, starting before the occurrence of HF. At the same time, the relationship between different concentrations of TMAO and the poor prognosis of patients with HF should be discussed. Prospective multicenter randomized controlled trials should be performed to further advance the understanding of TMAO from the laboratory to the clinic to treat patients with HF.

STRENGTHS AND LIMITATIONS

The present study clarified that TMAO is related to the poor prognosis of patients with HF. Moreover, more than 60 percent of the original studies were of high quality. The present study includes research from around the world, thereby allowing the research results to be widely promoted and overcoming the deficiencies of existing research to a certain extent. The detailed description of baseline characteristics also allowed identification of the source of heterogeneity.

However, the present study had several limitations. First, although we established rigorous inclusion criteria, some results indicated publication bias. Second, there was a lack of studies on the relationship between different concentrations of TMAO and MACE or all-cause death in HF, preventing a dose-response meta-analysis. Finally, we were unable to explore all the variables that influence TMAO levels, such as diet, environment, and medications.

CONCLUSION

The present study demonstrated that TMAO may be a risk factor for poor prognosis in patients with HF, but the underlying mechanism requires further investigation. Developing therapies that directly target TMAO may constitute a novel approach for preventing and treating HF.

DATA AVAILABILITY STATEMENT

The raw data supporting the conclusions of this article will be made available by the authors, without undue reservation.

AUTHOR CONTRIBUTIONS

XL and YL: conceptualization and writing original draft. YW and QL: project administration. ZF, JC, and DL: data management and data analysis. JL, XC, and LX: methodology and software application. XL, YL, and QL: writing review and editing and funding acquisition. All authors read and approved the final manuscript, critically reviewed the literature, and contributed to drafting the manuscript.

FUNDING

This work was supported by the Capital's Funds for Health Improvement and Research (Grant No. 2020-2-4201), National Natural Science Foundation of China (81973622), and Beijing University of Chinese Medicine 1166 Development Program for Junior Scientists (No. 030903010331).

REFERENCES

1. Tromp J, Bamadhaj S, Cleland JGF, Angermann CE, Dahlstrom U, Ouwerkerk W, et al. Post-discharge prognosis of patients admitted to hospital for heart failure by world region, and national level of income and income disparity (REPORT-HF): a cohort study. *Lancet Glob Health.* (2020) 8:e411–22. doi: 10.1016/S2214-109X(20)30004-8
2. Collaborators GDaIIaP. Global, regional, and national incidence, prevalence, and years lived with disability for 354 diseases and injuries for 195 countries and territories, 1990-2017: a systematic analysis for the Global Burden of Disease Study 2017. *Lancet.* (2018) 392:1789–858. doi: 10.1016/S0140-6736(18)32279-7
3. Savarese G, Sattar N, Januzzi J, Verma S, Lund LH, Fitchett D, et al. Empagliflozin is associated with a lower risk of post-acute heart failure rehospitalization and mortality. *Circulation.* (2019) 139:1458–60. doi: 10.1161/CIRCULATIONAHA.118.038339
4. Rossignol P, Hernandez AF, Solomon SD, Zannad F. Heart failure drug treatment. *Lancet.* (2019) 393:1034–44. doi: 10.1016/S0140-6736(18)31808-7
5. McDonagh TA, Metra M. 2021 ESC Guidelines for the diagnosis and treatment of acute and chronic heart failure. *Eur Heart J.* (2021). 42:3599–726. doi: 10.1093/eurheartj/ehab368
6. Sata Y, Marques FZ, Kaye DM. The emerging role of gut dysbiosis in cardio-metabolic risk factors for heart failure. *Curr Hypertens Rep.* (2020) 22:38. doi: 10.1007/s11906-020-01046-0
7. Tang WHW, Li DY, Hazen SL. Dietary metabolism, the gut microbiome, and heart failure. *Nat Rev Cardiol.* (2019) 16:137–54. doi: 10.1038/s41569-018-0108-7
8. Madan S, Mehra MR. Gut dysbiosis and heart failure: navigating the universe within. *Eur J Heart Fail.* (2020) 22:629–37. doi: 10.1002/ejhf.1792
9. Zhang Y, Wang Y, Ke B, Du J. TMAO: how gut microbiota contributes to heart failure. *Transl Res.* (2021) 228:109–25. doi: 10.1016/j.trsl.2020.08.007
10. Schuett K, Kleber ME, Scharnagl H, Lorkowski S, März W, Niessner A, et al. Trimethylamine-N-oxide and heart failure with reduced versus preserved ejection fraction. *J Am Coll Cardiol.* (2017) 70:3202–4. doi: 10.1016/j.jacc.2017.10.064
11. Ma G, Pan B, Chen Y, Guo C, Zhao M, Zheng L, et al. Trimethylamine N-oxide in atherogenesis: impairing endothelial self-repair capacity and enhancing monocyte adhesion. *Biosci Rep.* (2017) 37:BSR20160244. doi: 10.1042/BSR20160244
12. Chen ML, Zhu XH, Ran L, Lang HD, Yi L, Mi MT. Trimethylamine-N-Oxide induces vascular inflammation by activating the NLRP3 inflammasome through the SIRT3-SOD2-mtROS signaling pathway. *J Am Heart Assoc.* (2017) 6:e002238. doi: 10.1161/JAHA.117.006347
13. Shamseer L, Moher D, Clarke M, Ghersi D, Liberati A, Petticrew M, et al. Preferred reporting items for systematic review and meta-analysis protocols (PRISMA-P) 2015: elaboration and explanation. *BMJ.* (2015) 350:g7647. doi: 10.1136/bmj.g7647
14. Stang A. Critical evaluation of the Newcastle-Ottawa scale for the assessment of the quality of nonrandomized studies in meta-analyses. *Eur J Epidemiol.* (2010) 25:603–5. doi: 10.1007/s10654-010-9491-z
15. Zhou QP, Li XJ. C-reactive protein to albumin ratio in colorectal cancer: a meta-analysis of prognostic value. *Dose Response.* (2019) 17:1559325819889814. doi: 10.1177/1559325819889814
16. Higgins JP, Altman DG, Gøtzsche PC, Jüni P, Moher D, Oxman AD, et al. The Cochrane Collaboration's tool for assessing risk of bias in randomised trials. *BMJ.* (2011) 343:d5928. doi: 10.1136/bmj.d5928
17. Higgins JP, Thompson SG, Deeks JJ, Altman DG. Measuring inconsistency in meta-analyses. *BMJ.* (2003) 327:557–60. doi: 10.1136/bmj.327.7414.557
18. Lau J, Ioannidis JP, Schmid CH. Quantitative synthesis in systematic reviews. *Ann Intern Med.* (1997) 127:820–6. doi: 10.7326/0003-4819-127-9-199711010-00008
19. Borenstein M, Hedges LV, Higgins JP, Rothstein HR. A basic introduction to fixed-effect and random-effects models for meta-analysis. *Res Synth Methods.* (2010) 1:97–111. doi: 10.1002/jrsm.12
20. Tang WH, Wang Z, Fan Y, Levison B, Hazen JE, Donahue LM, et al. Prognostic value of elevated levels of intestinal microbe-generated metabolite trimethylamine-N-oxide in patients with heart failure: refining the gut hypothesis. *J Am Coll Cardiol.* (2014) 64:1908–14. doi: 10.1016/j.jacc.2014.02.617
21. Tang WH, Wang Z, Shrestha K, Borowski AG, Wu Y, Troughton RW, et al. Intestinal microbiota-dependent phosphatidylcholine metabolites, diastolic dysfunction, and adverse clinical outcomes in chronic systolic heart failure. *J Card Fail.* (2015) 21:91–6. doi: 10.1016/j.cardfail.2014.11.006
22. Trøseid M, Ueland T, Hov JR, Svardal A, Gregersen I, Dahl CP, et al. Microbiota-dependent metabolite trimethylamine-N-oxide is associated with disease severity and survival of patients with chronic heart failure. *J Intern Med.* (2015) 277:717–26. doi: 10.1111/joim.12328
23. Suzuki T, Heaney LM. Trimethylamine N-oxide and prognosis in acute heart failure. *Heart.* (2016) 102:841–8. doi: 10.1136/heartjnl-2015-308826
24. Liu YQH. *The Relationship Between Plasma Trimethylamine Oxide Level and Poor Prognosis in Patients With Acute Heart Failure*. Hunan: Nanhua University (2019).
25. Suzuki T, Yazaki Y, Voors AA, Jones DJL, Chan DCS, Anker SD, et al. Association with outcomes and response to treatment of trimethylamine N-oxide in heart failure: results from BIOSTAT-CHF. *Eur J Heart Fail.* (2019) 21:877–86. doi: 10.1002/ejhf.1338
26. Salzano A, Israr MZ, Yazaki Y, Heaney LM, Kanagala P, Singh A, et al. Combined use of trimethylamine N-oxide with BNP for risk stratification in heart failure with preserved ejection fraction: findings from the DIAMONDHFpEF study. *Eur J Prev Cardiol.* (2020) 27:2159–62. doi: 10.1177/2047487319870355
27. Zhou X, Jin M, Liu L, Yu Z, Lu X, Zhang H. Trimethylamine N-oxide and cardiovascular outcomes in patients with chronic heart failure after myocardial infarction. *ESC Heart Fail.* (2020) 7:188–93. doi: 10.1002/ehf2.12552
28. Israr MZ, Bernieh D, Salzano A, Cassambai S, Yazaki Y, Heaney LM, et al. Association of gut-related metabolites with outcome in acute heart failure. *Am Heart J.* (2021) 234:71–80. doi: 10.1016/j.ahj.2021.01.006
29. Li W, Huang A, Zhu H, Liu X, Huang X, Huang Y, et al. Gut microbiota-derived trimethylamine N-oxide is associated with poor prognosis in patients with heart failure. *Med J Aust.* (2020) 213:374–9. doi: 10.5694/mja2.50781
30. Bennett BJ, de Aguiar Vallim TQ, Wang Z, Shih DM, Meng Y, Gregory J, et al. Trimethylamine-N-oxide, a metabolite associated with atherosclerosis, exhibits complex genetic and dietary regulation. *Cell Metab.* (2013) 17:49–60. doi: 10.1016/j.cmet.2012.12.011
31. Jonsson AL, Bäckhed F. Role of gut microbiota in atherosclerosis. *Nat Rev Cardiol.* (2017) 14:79–87. doi: 10.1038/nrcardio.2016.183
32. Ma J, Li H. The role of gut microbiota in atherosclerosis and hypertension. *Front Pharmacol.* (2018) 9:1082. doi: 10.3389/fphar.2018.01082
33. Zhu Y, Li Q, Jiang H. Gut microbiota in atherosclerosis: focus on trimethylamine N-oxide. *Apmis.* (2020) 128:353–66. doi: 10.1111/apm.13038
34. Organ CL, Otsuka H, Bhushan S, Wang Z, Bradley J, Trivedi R, et al. Choline diet and its gut microbe-derived metabolite, trimethylamine N-Oxide, exacerbate pressure overload-induced heart failure. *Circ Heart Fail.* (2016) 9:e002314. doi: 10.1161/CIRCHEARTFAILURE.115.002314
35. Chen K, Zheng X, Feng M, Li D, Zhang H. Gut microbiota-dependent metabolite trimethylamine N-Oxide contributes to cardiac dysfunction in western diet-induced obese mice. *Front Physiol.* (2017) 8:139. doi: 10.3389/fphys.2017.00139
36. Li Z, Wu Z, Yan J. Gut microbe-derived metabolite trimethylamine N-oxide induces cardiac hypertrophy and fibrosis. *Lab Invest.* (2019) 99:346–57. doi: 10.1038/s41374-018-0091-y
37. Sun X, Jiao X, Ma Y, Liu Y, Zhang L, He Y, et al. Trimethylamine N-oxide induces inflammation and endothelial dysfunction in human umbilical vein endothelial cells via activating ROS-TXNIP-NLRP3 inflammasome. *Biochem Biophys Res Commun.* (2016) 481:63–70. doi: 10.1016/j.bbrc.2016.11.017
38. Seldin MM, Meng Y, Qi H, Zhu W, Wang Z, Hazen SL, et al. Trimethylamine N-Oxide promotes vascular inflammation through signaling of Mitogen-Activated Protein Kinase and Nuclear Factor-κB. *J Am Heart Assoc.* (2016) 5:e002767. doi: 10.1161/JAHA.115.002767
39. ML C, XH Z, L R, HD L, L Y, MT M. Trimethylamine-N-Oxide induces vascular inflammation by activating the NLRP3 inflammasome through the SIRT3-SOD2-mtROS signaling pathway. *J Am Heart Assoc.* (2017). 6:e002238. doi: 10.1161/JAHA.117.002238

40. Savi M, Bocchi L. Trimethylamine-N-Oxide (TMAO)-Induced impairment of cardiomyocyte function and the protective role of Urolithin B-Glucuronide. *Molecules.* (2018) 23:549. doi: 10.3390/molecules23030549
41. Janeiro MH, Ramírez MJ, Milagro FI. Implication of Trimethylamine N-Oxide (TMAO) in disease: potential biomarker or new therapeutic target. *Nutrients.* (2018) 10:1398. doi: 10.3390/nu10101398
42. Yang S, Li X, Yang F, Zhao R, Pan X, Liang J, et al. Gut microbiota-dependent marker TMAO in promoting cardiovascular disease: inflammation mechanism, clinical prognostic, and potential as a therapeutic target. *Front Pharmacol.* (2019) 10:1360. doi: 10.3389/fphar.2019.01360
43. Cho CE, Taesuwan S, Malysheva OV, Bender E, Tulchinsky NF, Yan J, et al. Trimethylamine-N-oxide (TMAO) response to animal source foods varies among healthy young men and is influenced by their gut microbiota composition: a randomized controlled trial. *Mol Nutr Food Res.* (2017) 61:1600324. doi: 10.1002/mnfr.201600324
44. Wang Z, Roberts AB, Buffa JA, Levison BS, Zhu W, Org E, et al. Non-lethal inhibition of gut microbial trimethylamine production for the treatment of atherosclerosis. *Cell.* (2015) 163:1585–95. doi: 10.1016/j.cell.2015.11.055
45. Roberts AB, Gu X, Buffa JA, Hurd AG, Wang Z, Zhu W, et al. Development of a gut microbe-targeted nonlethal therapeutic to inhibit thrombosis potential. *Nat Med.* (2018) 24:1407–17. doi: 10.1038/s41591-018-0128-1
46. Orman M, Bodea S, Funk MA. Structure-guided identification of a small molecule that inhibits anaerobic choline metabolism by human gut bacteria. *J Am Chem Soc.* (2019) 141:33–7. doi: 10.1021/jacs.8b04883
47. Miao L, Du J, Chen Z, Shi D, Qu H. Effects of microbiota-driven therapy on circulating Trimethylamine-N-Oxide Metabolism: a systematic review and meta-analysis. *Front Cardiovasc Med.* (2021) 8:710567. doi: 10.3389/fcvm.2021.710567

Conflict of Interest: The authors declare that the research was conducted in the absence of any commercial or financial relationships that could be construed as a potential conflict of interest.

Publisher's Note: All claims expressed in this article are solely those of the authors and do not necessarily represent those of their affiliated organizations, or those of the publisher, the editors and the reviewers. Any product that may be evaluated in this article, or claim that may be made by its manufacturer, is not guaranteed or endorsed by the publisher.

frontiers in Cardiovascular Medicine

ORIGINAL RESEARCH
published: 28 February 2022
doi: 10.3389/fcvm.2022.824628

Association of Lean Body Mass and Fat Mass With 1-Year Mortality Among Patients With Heart Failure

Yilan Ge[1], *Jiamin Liu*[1], *Lihua Zhang*[1], *Yan Gao*[1], *Bin Wang*[1], *Xiuling Wang*[1], *Jing Li*[1]* and *Xin Zheng*[1,2]*

[1] National Center for Cardiovascular Diseases, National Clinical Research Center for Cardiovascular Diseases, NHC Key Laboratory of Clinical Research for Cardiovascular Medications, State Key Laboratory of Cardiovascular Disease, Fuwai Hospital, Chinese Academy of Medical Sciences and Peking Union Medical College, Beijing, China, [2] National Clinical Research Center for Cardiovascular Diseases, Coronary Artery Disease Center, Fuwai Hospital, Chinese Academy of Medical Sciences, Shenzhen, China

OPEN ACCESS

Edited by:
Jeffrey Shi Kai Chan,
Cardiovascular Analytics Group,
Hong Kong SAR, China

Reviewed by:
Leonardo Roever,
Federal University of Uberlandia, Brazil
Sara Zand,
Taban Clinic, Iran
Peter H. Brubaker,
Wake Forest University, United States

***Correspondence:**
Xin Zheng
xin.zheng@fwoxford.org
Jing Li
jing.li@fwoxford.org

Specialty section:
This article was submitted to Heart Failure and Transplantation, a section of the journal Frontiers in Cardiovascular Medicine

Received: 29 November 2021
Accepted: 07 February 2022
Published: 28 February 2022

Citation:
Ge Y, Liu J, Zhang L, Gao Y, Wang B, Wang X, Li J and Zheng X (2022) Association of Lean Body Mass and Fat Mass With 1-Year Mortality Among Patients With Heart Failure. Front. Cardiovasc. Med. 9:824628. doi: 10.3389/fcvm.2022.824628

Background: Prior studies have found an unexplained inverse or U-shaped relationship between body mass index (BMI) and mortality in heart failure (HF) patients. However, little is known about the independent effects of each body component, i.e., lean body mass (LBM) and fat mass (FM), on mortality.

Methods: We used data from the China Patient-centered Evaluative Assessment of Cardiac Events-Prospective Heart Failure Study. LBM and FM were calculated using equations developed from the National Health and Nutrition Examination Survey. LBM and FM index, calculated by dividing LBM or FM in kilograms by the square of height in meters, were used for analysis. We used restricted cubic spline and Cox model to examine the association of LBM and FM index with 1-year all-cause mortality.

Results: Among 4,305 patients, median (interquartile range) age was 67 (57–76) years, 37.7% were women. During the 1-year follow-up, 691 (16.1%) patients died. After adjustments, LBM index was inversely associated with mortality in a linear way (*P*-overall association < 0.01; *P*-non-linearity $= 0.52$), but no association between FM index and mortality was observed (*P*-overall association $= 0.19$). Compared with patients in the 1st quartile of the LBM index, those in the 2nd, 3rd, and 4th quartiles had lower risk of death, with hazard ratio of 0.80 (95% CI 0.66–0.97), 0.65 (95% CI 0.52–0.83), and 0.61 (95% CI 0.45–0.82), respectively. In contrast, this association was not observed between FM index quartiles and mortality.

Conclusion: Higher LBM, not FM, was associated with lower 1-year mortality among HF patients.

Keywords: lean body mass, fat mass, body mass index, heart failure, mortality

INTRODUCTION

Obesity, as indexed by high body mass index (BMI), is a major risk factor for incident heart failure (HF) (1), and up to 60–80% of patients with HF are overweight or obese (2–4). However, in established HF, an unexpected inverse or *U*-shaped relation between BMI and mortality was consistently observed (2, 4–9). This paradoxical observation has been referred to as the "obesity paradox."

One of the possible reasons underlying this obesity paradox is the inaccuracy of BMI in estimating body fat, as BMI is an aggregate of lean body mass (LBM) and fat mass (FM), and LBM and FM may act differently on mortality (10–15). Therefore, understanding different contributions of body compositions may facilitate understanding obesity paradox and providing valuable information for obesity management to improve the prognosis of HF patients. Direct measurement of body composition is high-cost and requires sophisticated technologies, which limits its utilization in clinical practice. Therefore, to date, few studies, with relatively small sample size, have reported the effect of body composition among HF patients (16–19). There is a need to evaluate this association in a large population to assure adequate statistic power. A much more practical method of measuring body composition, which can be conducted in large-scale study, is the prediction equations derived from anthropometric measurement, and this method has been validated against dual-energy x-ray absorptiometry (14, 20). However, to our knowledge, the association between predicted LBM and FM by anthropometric equations with HF prognosis is scarcely explored. In addition, whether the age, sex, and comorbidities may modify the effect of body composition on mortality remain largely unknown, subgroup analysis is warranted to reveal more information.

Accordingly, using previously validated anthropometric equations to estimate LBM and FM, we evaluated the independent roles of LBM and FM in relation to all-cause mortality among patients hospitalized for HF in a large prospective cohort study.

METHODS

Study Design and Participants

The patients of this study were from a prospective cohort of acute HF, the China Patient-centered Evaluative Assessment of Cardiac Events-Prospective Heart Failure Study (China PEACE 5p-HF Study), which enrolled patients from 52 hospitals between 2016 and 2018 (21). We included patients aged 18 years or older who were hospitalized with a primary diagnosis of new-onset HF or decompensation of chronic HF; and excluded those who died during the index hospitalization ($n = 32$), or were lost to follow-up at 1 year after discharge ($n = 7$), or lacked information on height, waist circumference, or weight during hospitalization—these information was required to calculate predicted LBM and FM ($n = 563$), leaving 4,305 patients for analyses. All enrolled patients signed written informed consent. The China PEACE 5p-HF Study was approved by the Ethics Committees of Fuwai Hospital and all collaborating hospitals. The study was registered at www.clinicaltrials.gov (NCT02878811).

Anthropometric Measures

BMI was analyzed according to weight and height at discharge using the formula weight (kg)/(height in m)^2. Patients were stratified into the following categories recommended by the Working Group on Obesity in China according to BMI value: underweight (< 18.5 kg/m^2), normal weight (18.5–23.9 kg/m^2), overweight (24–27.9 kg/m^2), and obese (≥ 28 kg/m^2) (22).

LBM and FM were calculated using anthropometric prediction equations developed from the National Health and Nutrition Examination Survey (NHANES) (23), and the equations are shown in **Supplementary Table 1**. The high predictive ability for body compositions of these equations has been validated by several studies (14, 20). We calculated the LBM index (kg/m^2) and FM index (kg/m^2) using LBM and FM, respectively, in kilograms divided by the square of height in meters.

Data Collection

Detailed information on demographics, clinical characteristics, comorbidities, and discharge medications were obtained through abstraction of medical charts and in-person interviews during the index hospitalization. Left ventricular ejection fraction (LVEF) was measured during the index hospitalization by trained physicians with a standard protocol. Blood samples of enrolled patients were taken within 48 h of admission to perform analysis in the central laboratory.

Outcomes

The outcome of the study was all-cause death within 1 year after discharge. Information regarding patient survival status during 12 months of follow-up was collected from follow-up interviews, medical documents, and the national death cause database. All deaths were centrally adjudicated by trained clinicians.

Statistical Analysis

Continuous variables were expressed as mean ± SD or medians with interquartile range (IQR) and compared by the Kruskal-Wallis test. Categorical variables were presented as frequencies with percentages and compared by the χ^2-test.

The LBM index and FM index were categorized into sex-specific quartiles or were treated as continuous variables with the effect estimates for 1-SD increase. Cox proportional hazards models were used to estimate the hazard ratios (HRs) of the 1-year all-cause mortality associated with the LBM index and FM index. Separate Cox regression models were fitted with (1) model 1, no adjustment; (2) model 2, adjustment for age, sex, education level, systolic blood pressure at admission, heart rate at admission, NYHA class, LVEF, serum sodium, serum albumin, Hs-cTnT, NT-pro BNP, estimated glomerular filtration rate (eGFR), current smoking status, history of coronary heart disease, hypertension, chronic obstructive pulmonary disease,

anemia, valvular heart disease, diabetes mellitus, atrial fibrillation and prescription of angiotensin-converting enzyme inhibitors (ACEIs)/ angiotensin receptor blockers (ARBs), β-blockers, and mineralocorticoid receptor antagonists (MRAs); (3) model 3, the LBM or FM index was added to model 2 for mutual adjustment. In order to test linearity assumption between body composition indices and mortality, restricted cubic splines (RCS) were used in multivariable-adjusted models.

We conducted interaction and stratified analyses to evaluate the potential effect modification. We also performed several sensitivity analyses. First, we used different categories for the LBM and FM index (thirds or fifths). Second, we tested the robustness of our findings by using another body composition prediction equation developed from Chinese population (24). Third, due to the possible influence of reverse causation, we performed sensitivity analyses by excluding patients who might be in severe medical condition, including patients who died during the first 3 months of follow-up, or who had a BMI $<$ 18.5 kg/m^2.

All statistical analysis was performed by SAS version 9.4 (SAS Institute, Cary, NC, USA) and R programming language version 3.6.0 (R foundation for Statistical Computing, Vienna, Austria). All comparisons were two-sided, and statistical significance was defined as $P < 0.05$.

RESULTS

Population Characteristics

A total of 4,305 patients were included in the analysis. The median age of the study population was 67 (57–75) years, 37.3% were women, and 60.1% were overweight or obese patients. The median LBM indexes were 17.0 (15.5–18.5) and 13.9 (12.8–14.9) kg/m^2, and the median FM indexes were 6.6 (5.1–8.1) and 9.4 (7.6–11.3) kg/m^2 for men and women, respectively. **Table 1** shows the baseline characteristics of participants according to sex-adjusted LBM index quartiles**.** Patients with low LBM index were more likely to be older, have a lower level of education, and have a history of valvular heart disease, chronic obstructive pulmonary disease, and anemia; were less likely to have a history of metabolic syndrome, hypertension and diabetes mellitus; had lower levels of systolic blood pressure, LDL, TG, waist circumference, BMI, FM index, plasma sodium, and albumin; had higher level of HDL; had more severe HF (i.e., a higher proportion of NYHA functional classes III to IV and increased hs-cTnT and NT-proBNP levels); and were less likely to receive ACEIs/ARBs while more likely to receive MRAs.

Prognosis Analysis

During the 1-year follow-up, 691 patients (16.1%) died. In the multivariate model, higher BMI was found to be associated with a lower risk of death. With the normal BMI group (BMI 18.5- 24 kg/m^2) as a reference, HRs for BMI of $<$18.5, 24–28, and $\geq$28 kg/m^2 were 1.39 [95% confidence interval (CI) 1.10–1.76], 0.74 (95% CI 0.62–0.89), and 0.71 (95% CI 0.55–0.94), respectively ($p < 0.01$ for trend).

The cumulative incidence of death by each LBM and FM index quartile is described using the Kaplan-Meier method in **Figure 1**. A significantly higher 1-year mortality was observed among patients with LBM index in the 1st quartile (24.6%), compared with 17.5, 12.1, and 9.8% for those in the 2nd, 3rd, and 4th quartile, respectively. And the 1-year mortality rates among patients with FM index in the 1st, 2nd, 3rd, and 4th quartile were 23.2, 16.6, 13.2, and 10.8%, respectively (both log-rank $p < 0.01$).

Table 2 shows the association between the LBM index quartiles and mortality. The higher quartile of LBM index was associated with lower mortality in all models. In the fully adjusted model (model 3), LBM index was still negatively correlated with death risk. Compared with participants in the 1st LBM index quartile, the risk of death was lower for those in the 2nd quartile (HR 0.80, 95% CI 0.66–0.97), the 3rd quartile (HR 0.65, 95% CI 0.52–0.83), and the 4th quartile (HR 0.61, 95% CI 0.45–0.82).

Table 3 shows the association between the FM index quartiles and mortality. Higher FM index quartile was associated with better survival without adjusting for LBM index (models 1 and 2), while the protective effect of FM was no longer significant after adjusting for LBM index (model 3).

When accounting for LBM index and FM index as continuous covariates in the fully adjusted Cox model (model 3), each 1 SD increase in the LBM index decreased the risk of mortality (HR 0.77, 95% CI 0.67–0.84), while each 1 SD increase in the FM index did not decrease the risk of death (HR 0.95, 95% CI 0.83–1.09) (**Table 4**).

In the RCS analysis, LBM index was associated with mortality in a linear way, all-cause mortality decreased consistently with increasing LBM Index (P-overall association < 0.01; P-non-linearity $= 0.52$). However, no significant association between FM index and mortality was observed (P-overall association $=0.19$; P-non-linearity $= 0.22$) (**Figure 2**).

Figure 3 provides the results of the stratified analyses. The NYHA class modified the prognostic association of FM index and mortality (P-interaction $= 0.05$), higher FM index was strongly associated with poor prognosis among patients in NYHA II (HR 1.77, 95% CI 1.08–2.91), while associated with better survival among patients in NYHA III/IV (NYHA III: HR 0.87, 95% CI 0.68–1.00; NYHA IV: HR 0.82, 95% CI 0.63–0.99). No factor played an interactive role in the association between the LBM index and mortality.

Our results remained robust in several sensitivity analyses. The results did not change with the use of different categories for the LBM index and FM index (thirds or fifths) or with the use of prediction equations developed from Chinese population (**Supplementary Tables 2–4**). Analyses excluding patients who died during the first 3 months of follow-up or whose BMI was $<$18.5 kg/m^2 yielded consistent findings compared with the results of the primary multivariate analyses (**Supplementary Table 5**).

DISCUSSION

In this large prospective cohort of patients hospitalized for HF in China, we demonstrated that LBM index was inversely related

TABLE 1 | Baseline characteristics of patients hospitalized for HF among sex-adjusted lean body mass (LBM) index quartiles.

	Total	LBM index				
		The 1st quartile	The 2nd quartile	The 3rd quartile	The 4th quartile	*P*-value
N	**(*n* = 4,305)**	**(*n* = 1,075)**	**(*n* = 1,078)**	**(*n* = 1,076)**	**(*n* = 1,076)**	
Age, yr (IQR)	67 (57–75)	70 (62–78)	68 (60–76)	66 (56–74)	63 (51–72)	<0.01
Female, *n* (%)	1,607 (37.3)	401 (37.3)	403 (37.4)	401 (37.3)	402 (37.4)	1
High school education or above, *n* (%)	1,221 (28.4)	234 (21.8)	307 (28.5)	312 (29.0)	368 (34.2)	<0.01
Clinical features						
LVEF, % (IQR)	44.0 (33.0–57.0)	43.0 (32.0–56.0)	44.0 (33.0–57.0)	43.0 (33.0–56.0)	44.0 (34.0–58.0)	0.19
NYHA, *n* (%)						<0.01
NYHA II	632 (14.7)	120 (11.2)	158 (14.7)	191 (17.8)	163 (15.1)	
NYHA III	1,941 (45.1)	489 (45.5)	486 (45.1)	465 (43.2)	501 (46.6)	
NYHA IV	1,722 (40.0)	466 (43.3)	431 (40.0)	417 (38.8)	408 (37.9)	
Unknown	10 (0.2)	0 (0)	3 (0.3)	3 (0.3)	4 (0.4)	
HR, bpm/min (IQR)	85.0 (72.0–100.0)	85.0 (74.0–100.0)	84.0 (72.0–99.0)	84.0 (72.0–98.0)	86.0 (74.0–100.0)	0.05
SBP, mmHg (IQR)	130.0 (116.0–148.0)	127.0 (110.0–143.0)	130.0 (115.0–145.0)	130.0 (118.0–149.0)	134.0 (120.0–150.0)	<0.01
Albumin, g/L (IQR)	38.9 (35.9–41.9)	38.3 (35.2–41.2)	39.0 (35.7–41.8)	39.1 (36.3–42.3)	39.3 (36.5–42.5)	<0.01
Na, mmol/L (IQR)	140.0 (137.1–142.0)	139.3 (136.5–142.0)	140.0 (137.0–142.0)	140.0 (137.4–142.3)	140.9 (138.0–143.0)	<0.01
NT-proBNP, pg/mL (IQR)	1,423.0 (581.7–3,132.0)	2,126.5 (866.2–4,360.5)	1,667.0 (716.7–3,823.0)	1,237.0 (500.0–2,640.0)	970.1 (401.5–2,048.0)	<0.01
hs-cTnT, ng/L (IQR)	20.7 (12.4–38.2)	24.6 (14.7–46.8)	20.9 (12.7–39.2)	19.7 (11.7–36.2)	18.7 (11.1–34.0)	<0.01
eGFR, ml/min/1.73 m^2 (IQR)	68.2 (53.3–83.8)	66.9 (50.8–83.1)	66.5 (52.0–81.2)	69.6 (56.5–84.4)	68.9 (54.3–86.1)	<0.01
LDL, mmol/L (SD)	2.4±0.9	2.3±0.9	2.3±0.9	2.4±0.8	2.4±0.9	<0.01
TG, mmol/L (SD)	1.3±1.0	1.1±0.8	1.2±0.7	1.4±1.1	1.5±1.1	<0.01
HDL, mmol/L (SD)	1.1±0.3	1.2±0.4	1.1±0.4	1.1±0.3	1.0±0.3	<0.01
Waist circumference, cm (IQR)	89 (80–98)	84 (76–91)	87 (80–94)	90 (83–97)	96 (88–105)	<0.01
BMI, kg/m^2 (IQR)	24.0 (21.4–26.7)	19.6 (18.4–21.0)	22.6 (21.6–23.9)	25.1 (24.2–26.1)	29.0 (27.3–31.2)	<0.01
FM index, kg/m^2 (IQR)	7.5 (5.8–9.5)	5.8 (4.5–6.9)	7.3 (5.5–8.5)	8.2 (6.5–10.0)	10.2 (7.9–12.5)	<0.01
Smoking history, *n* (%)	1,102 (25.6)	265 (24.7)	282 (26.2)	286 (26.6)	269 (25.0)	0.7
Comorbidities, *n* (%)						
Metabolic syndrome	1,293 (30.0)	101 (9.4)	173 (16.0)	387 (36.0)	632 (58.7)	<0.01
Hypertension	2,512 (58.4)	520 (48.4)	607 (56.3)	641 (59.6)	744 (69.1)	<0.01
Cardiomyopathy	1,533 (35.6)	370 (34.4)	370 (34.3)	408 (37.9)	385 (35.8)	0.27
Atrial fibrillation	1,566 (36.4)	401 (37.3)	407 (37.8)	399 (37.1)	359 (33.4)	0.13
Valvular heart disease	695 (16.1)	213 (19.8)	197 (18.3)	161 (15.0)	124 (11.5)	<0.01
COPD	842 (19.6)	272 (25.3)	226 (21.0)	175 (16.3)	169 (15.7)	<0.01
Diabetes mellitus	1,360 (31.6)	268 (24.9)	319 (29.6)	382 (35.5)	391 (36.3)	<0.01
Anemia	960 (22.3)	321 (29.9)	275 (25.5)	201 (18.7)	163 (15.1)	<0.01
Coronary heart disease	2,476 (57.5)	619 (57.6)	640 (59.4)	631 (58.6)	586 (54.5)	0.1
Prior revascularization	707 (16.4)	159 (14.8)	188 (17.4)	190 (17.7)	170 (15.8)	0.22
Medications at discharge, *n* (%)						
ACEI/ARB	2,290 (53.2)	540 (50.2)	537 (49.8)	600 (55.8)	613 (57.0)	<0.01
β-blocker	2,602 (60.4)	630 (58.6)	640 (59.4)	678 (63.0)	654 (60.8)	0.17
MRA	2,766 (64.3)	730 (67.9)	677 (62.8)	674 (62.6)	685 (63.7)	0.03

LVEF, left ventricle ejection fraction; NYHA, New York Heart Association; HR, heart rate; SBP, systolic blood pressure; hs-cTnT, high sensitivity cardiac troponin T; NT-pro BNP, N-terminal brain natriuretic peptide precursor; eGFR, estimated glomerular filtration rate; BMI, body mass index; FM index, fat mass index; COPD, chronic obstructive pulmonary disease; ACEI, angiotensin-converting enzyme inhibitor; ARB, angiotensin receptor blocker; MRA, mineralocorticoid receptor antagonist.

to mortality, while FM index was not associated with the risk of death.

We expand on previous literatures in several respects. Firstly, this is the first large-scale, nationwide study to assess the association between body composition and mortality among HF patients. To date, only a limited number of studies have examined this relation, and the findings were inconsistent (16–19). Although these studies used a direct measurement of body composition, the lack of statistical power that resulted from the small sample size (198–418 patients) makes it impossible to draw firm conclusions. Our study used previously validated anthropometric equations to estimate LBM and FM (14, 20),

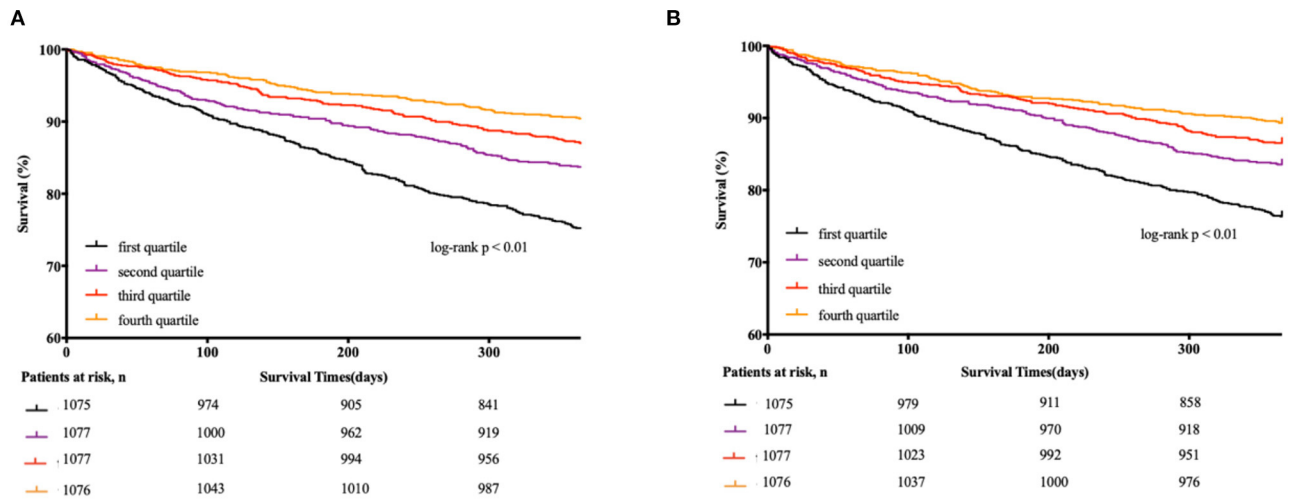

FIGURE 1 | Kaplan-Meier estimates of 1-year all-cause mortality according to quartiles of each body component. **(A)** Kaplan-Meier curve according to quartiles of LBM index for the all-cause mortality. **(B)** Kaplan-Meier curve according to quartiles of FM index for the all-cause mortality.

TABLE 2 | Hazard ratios (HR) for 1-year mortality of HF patients by lean body mass (LBM) index quartiles.

LBM index quartile	Model 1*		Model 2†		Model 3‡	
	HR (95%CI)	*P*-value	HR (95%CI)	*P*-value	HR (95%CI)	*P*-value
1	Ref.		Ref.		Ref.	
2	0.70 (0.58–0.84)	<0.01	0.79 (0.65–0.95)	0.01	0.80 (0.66–0.97)	0.03
3	0.48 (0.39–0.59)	<0.01	0.63 (0.51–0.79)	<0.01	0.65 (0.52–0.83)	<0.01
4	0.38 (0.30–0.47)	<0.01	0.57 (0.45–0.73)	<0.01	0.61 (0.45–0.82)	<0.01
p-value for trend	<0.01		<0.01		<0.01	

**Model 1: Unadjusted.*

†Model 2: Adjusted for age, sex, education level, systolic blood pressure at admission, heart rate at admission, NYHA class, LVEF, serum sodium, serum albumin, Hs-cTnT, NT-proBNP, eGFR, current smoking status, the history of coronary heart disease, hypertension, chronic obstructive pulmonary disease, anemia, valvular heart disease, diabetes mellitus, atrial fibrillation, the prescription of ACEI/ARB, β-blocker, and MRA.

‡Model 3: Adjusted using characteristics for Model 2 by adding FM index.

hence we could estimate the relation in a large-scale clinical epidemiological setting, and the further full adjustment for important covariates allows us to reveal robust conclusions.

Secondly, our study quantified the independent prognostic value of body constituents. Compared with previous studies, the mutual adjustment for LBM and FM in our study permits accurate analysis of the interplay of these variables' effects on survival. We found a survival benefit associated with high LBM that was independent of any effect of FM, while FM seems to be protective only if no adjustment was made for LBM. Prior studies evaluated the effect of fat on clinical outcomes without adjusting for muscle mass, and showed an protective effect of fat (16, 17, 25). Because higher FM in general is correlated with higher muscle mass (26), one could hypothesize that the lower mortality among patients with a high level of FM is a result of having large muscle mass. Accordingly, muscle mass could be a confounder when evaluating the association of FM and mortality, and it should be adjusted to tease out the independent effect of FM.

Thirdly, we present an in-depth analysis of the effect of body composition by stratified analyses, which has not been well-explored in previous studies. As shown in our study, the inverse association between LBM index and mortality was consistent in all subgroups. Increased muscle mass provides important metabolic benefits. Firstly, skeletal muscle is the primary target tissue for insulin-mediated glucose uptake, it has important role as an energy production and consumption system that influences the whole energy metabolism. Secondly, skeletal muscle could produce and secrete hundreds of myokines, like IL-15, BDNF and LIF, and these myokines were related with favorable changes in cardiometabolic profile, improved insulin sensitivity, anti-inflammation and antioxidant capacity (27, 28). Besides, muscle mass could indicate cardiorespiratory fitness to some extent (29), which is well-reported to be related with survival (30, 31). Hence, the result that muscle mass was universally favorable in all subgroups was not unexpected.

In addition, for the first time, we found that higher FM index exerts detrimental effect on mortality among HF patients

TABLE 3 | Hazard ratios (HR) for 1-year mortality of HF patients by fat mass (FM) index quartiles.

FM index quartile	Model 1*		Model 2†		Model 3‡	
	HR (95%CI)	*P*-value	HR (95%CI)	*P*-value	HR (95%CI)	*P*-value
1	Ref.		Ref.		Ref.	
2	0.70 (0.58–0.85)	<0.01	0.81 (0.67–0.99)	0.04	0.88 (0.72–1.08)	0.23
3	0.56 (0.45–0.69)	<0.01	0.74 (0.60–0.91)	<0.01	0.86 (0.69–1.08)	0.20
4	0.47 (0.38–0.59)	<0.01	0.69 (0.54–0.87)	<0.01	0.92 (0.70–1.21)	0.55
p-value for trend	<0.01		<0.01		0.44	

Model 1: Unadjusted.
†Model 2: Adjusted for age, sex, education level, systolic blood pressure at admission, heart rate at admission, NYHA class, LVEF, serum sodium, serum albumin, Hs-cTnT, NT-proBNP, eGFR, current smoking status, the history of coronary heart disease, hypertension, chronic obstructive pulmonary disease, anemia, valvular heart disease, diabetes mellitus, atrial fibrillation, the prescription of ACEI/ARB, β-blocker, and MRA.
‡Model 3: Adjusted using characteristics for Model 2 by adding LBM index.

TABLE 4 | Hazard ratios (HR) for 1-year mortality of HF patients according to a 1-SD increase in LBM index and FM index.

	Model 1*		Model 2†		Model 3‡	
	HR (95%CI)	*P*-value	HR (95%CI)	*P*-value	HR (95%CI)	*P*-value
LBM index	0.72 (0.67–0.79)	<0.01	0.75 (0.67–0.84)	<0.01	0.77 (0.67–0.84)	<0.01
FM index	0.74 (0.67–0.81)	<0.01	0.82 (0.73–0.92)	<0.01	0.95 (0.83–1.09)	0.50

Model 1: Unadjusted.
†Model 2: Adjusted for age, sex, education level, systolic blood pressure at admission, heart rate at admission, NYHA class, LVEF level, serum sodium, serum albumin, Hs-cTnT, NT-proBNP, estimated glomerular filtration rate, current smoking status, the history of coronary heart disease, hypertension, chronic obstructive pulmonary disease, anemia, valvular heart disease, diabetes mellitus, atrial fibrillation, the prescription of ACEI/ARB, β-blocker, and MRA.
‡Model 3: Adjusted using characteristics for Model 2 by adding FM index or LBM index.

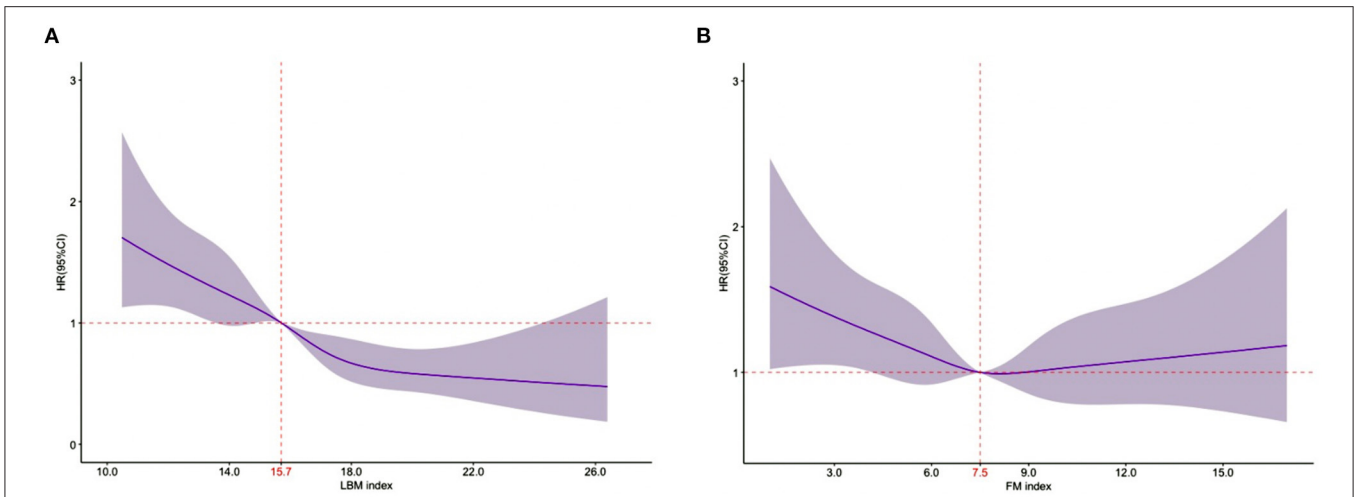

FIGURE 2 | Relationship of the LBM index and the FM index with 1-year all-cause mortality using restricted cubic splines. **(A)**. Relationship between LBM index and 1-year all-cause mortality [the reference point was 15.7 (median); *P*-overall association < 0.01; *P*-non-linearity = 0.52]. **(B)**. Relationship between FM index and 1-year all-cause mortality [the reference point was 7.5 (median); *P*-overall association = 0.19; *P*-non-linearity = 0.22]. **(A,B)** represent the results of multivariate analyses adjusted for age, sex, education level, systolic blood pressure at admission, heart rate at admission, NYHA class, LVEF level, serum sodium, serum albumin, hs-cTnT, NT-proBNP, eGFR, current smoking status, the history of coronary heart disease, hypertension, chronic obstructive pulmonary disease, anemia, valvular heart disease, diabetes mellitus, atrial fibrillation, the prescription of ACEI/ARB, β-blocker, MRA, and mutually adjust for FM index or LBM index.

in NYHA II, while it is associated with better survival in NYHA III/IV patients. The pathophysiologic mechanism of a relation between excess fat mass and increased mortality is well-established. Etiologic pathways include insulin resistance, inflammation and hormonal perturbations (32). Besides, obesity is an important risk factor for an expanding set of diseases,

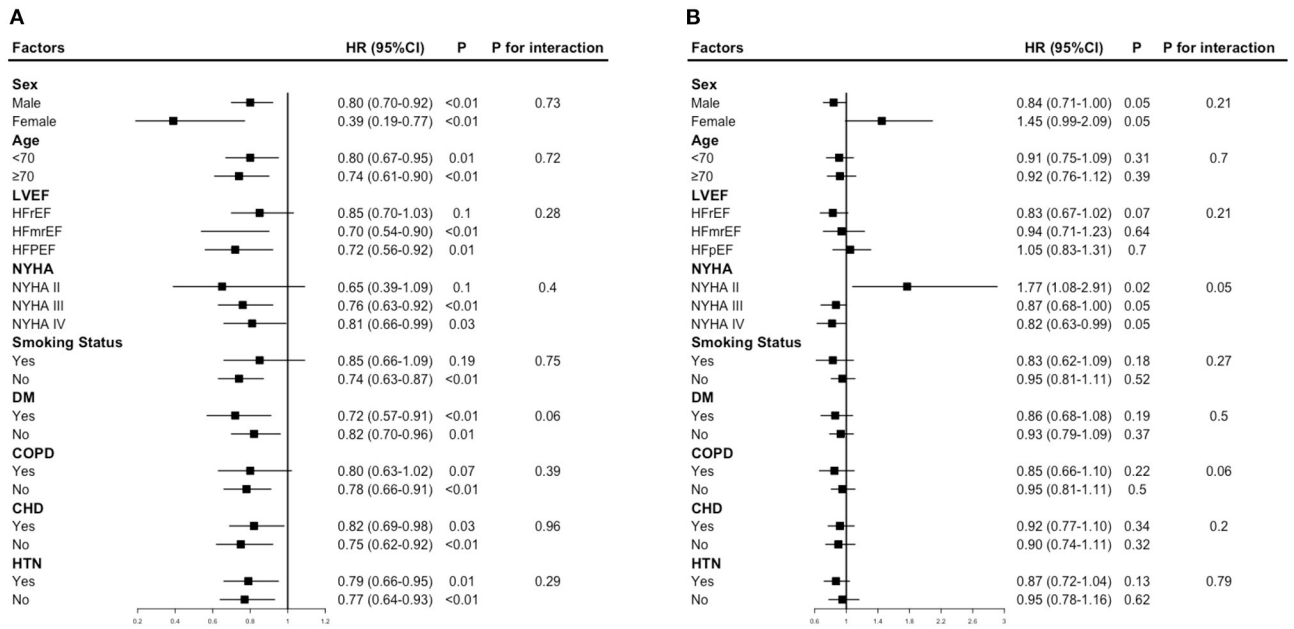

FIGURE 3 | Hazard ratios for mortality according to a 1 -SD increase in LBM index or FM index. **(A)** Hazard ratios per 1 standard deviation–increase in LBM index for mortality. **(B)** Hazard ratios per 1 standard deviation–increase in FM index for mortality. Each stratification was adjusted for all factors in model 3, except for the stratification factor itself.

including diabetes mellitus, cardiovascular disease, which were all related with poor clinical outcomes (33). However, a growing number of studies support a survival benefit of adipose tissue in critical illness (34). And our study also indicated that higher FM index correlate with better survival in NYHA III/IV patients. The HF patients in NYHA III/IV are highly likely to suffer from cachexia, which is a sign of poor prognosis. It is reported that the symptoms (dyspnea, gut oedema), the neurohormonal and inflammatory activation in critical illness induce marked depletion of fat mass through enhanced fat catabolism, facilitating the development of cachexia (35). In this regard, among NYHA III/IV patients, the patients with high fat mass were less likely to develop cachexia, and these patients might have better prognosis than patients with low fat mass (36). The pathophysiologic mechanisms linking adipose to survival benefit in critical illness were proposed to be related with energy reserves, anti-inflammatory mediators, endotoxin-binding lipoproteins, cardioprotective metabolic effects (34). Apart from the above, our study revealed that patients with a higher level of FM tend to exhibit a higher mortality in women, while exhibit a lower mortality in men (both marginally statistically significant). One study used waist-to-hip ratio to assess obesity, and the result was largely consistent with our finding (37). The mechanism behind this association and difference based on gender has be speculated to be related with different hormones level and fat distribution (38). More research is warranted to validate our findings, and the exact mechanism need to be further evaluated in future studies. Besides, the gender and disease severity might be taken into consideration when designing clinical trials targeting obesity management in HF.

Clinical Implications

Firstly, patients with the same BMI may have different body compositions and thus different risks of mortality. Therefore, measurement of body composition beyond total body mass should be incorporated in clinical assessments of HF patients to better identify patients at higher risk of death. Secondly, the predicted body composition indices estimated by anthropometric prediction equations, which are time-efficient and inexpensively measurable, can be integrated into routine clinical practice, especially in acute disease settings. Thirdly, in the era of precision medicine, the measurement of body composition could be used to formulate treatment recommendations. Patients with low muscle mass may benefit from more aggressive HF therapies, like β-blockers or ACEIs (39, 40), and additional treatment approaches to maintain or promote muscle mass through lifestyle modification (i.e., adequate protein supplementation, muscle-strengthening exercise) are important interventions to improve the clinical outcomes of HF patients (41–43). In addition, the recommendation of weight loss among obese HF patients should be considered more deliberately since the effect of fat mass might differ according to the disease severity.

Limitations

Several limitations should be acknowledged in the interpretation of this study. Firstly, this was an observational study, and although we adjusted for important clinical covariates affecting

prognosis, unmeasured or residual confounding factors may remain. Information on other prognostic factors, such as fitness ability and weight change, which may influence outcomes, was not available in this study. Secondly, using equations to calculate LBM and FM was not the most accurate way of measurements. However, the predictive ability for body compositions of these equations has been validated by other studies (14, 20). Besides, LBM and FM were analyzed in terms of categorical variables, making the exact value less important. Thirdly, reverse causality may in part be responsible for our observed associations. However, we minimized the potential for reverse causation due to advanced disease status by excluding patients who died within 3 months after discharge or with BMI < 18.5 kg/m^2, and the conclusions remained unchanged.

Future Directions

Firstly, further studies are needed to define the biologic mechanisms and relative importance of these mechanisms linking muscle mass to mortality, which would inform therapeutic approaches. Secondly, since the role of adipose tissue in HF prognosis is complex, more studies are warranted to evaluate the effect of different adipose tissue (visceral, subcutaneous, intermuscular, and intramuscular). Thirdly, few studies investigated the association between muscle-to-fat ratio and HF mortality, understanding how relative proportions of muscle mass and fat mass contribute to mortality will help identify which body composition phenotypes are optimal for survival in HF patients.

CONCLUSION

Among patients hospitalized for HF, increased LBM, but not FM, predicts a lower risk of mortality.

DATA AVAILABILITY STATEMENT

The original contributions presented in the study are included in the article/**Supplementary Materials**, further inquiries can be directed to the corresponding authors.

ETHICS STATEMENT

The studies involving human participants were reviewed and approved by the Ethics Committees of Fuwai Hospital and all collaborating hospitals. The patients/participants provided their written informed consent to participate in this study.

AUTHOR CONTRIBUTIONS

YG: concept, design, analysis, and drafting of the paper. JL, LZ, YG, BW, and XW: revision of the paper. XZ and JL: revision of the paper and responsible for the overall content as guarantor. All authors approved the submitted version of the manuscript.

FUNDING

This work was supported by the China Academy of Chinese Medical Sciences Innovation Fund for Medical Science (2021-12M-1-009), the National Key Technology R&D Program (2015BAI12B02) from the Ministry of Science and Technology of China, and the 111 Project from the Ministry of Education of China (B16005).

ACKNOWLEDGMENTS

We appreciate the multiple contributions by project teams at National Clinical Research Center for Cardiovascular Diseases in study design and implementations. We thank Harlan M. Krumholz from Yale University, Frederick A. Masoudi from the University of Colorado, John A. Spertus from University of Missouri, Xuyu Jin from the University of Oxford, and Christiane E. Angermann from Universitätsklinikum Würzburg for their instructive advice on study design. We are grateful to the grant support by the Chinese Government.

SUPPLEMENTARY MATERIAL

The Supplementary Material for this article can be found online at: https://www.frontiersin.org/articles/10.3389/fcvm.2022.824628/full#supplementary-material

REFERENCES

1. Kenchaiah S, Evans JC, Levy D, Wilson PW, Benjamin EJ, Larson MG, et al. Obesity and the risk of heart failure. *N Engl J Med.* (2002) 347:305–13. doi: 10.1056/NEJMoa020245
2. Kenchaiah S, Pocock SJ, Wang D, Finn PV, Zornoff LA, Skali H, et al. Body mass index and prognosis in patients with chronic heart failure: insights from the Candesartan in Heart failure: assessment of Reduction in Mortality and morbidity (CHARM) program. *Circulation.* (2007) 116:627–36. doi: 10.1161/CIRCULATIONAHA.106.679779
3. Horwich TB, Broderick S, Chen L, McCullough PA, Strzelczyk T, Kitzman DW, et al. Relation among body mass index, exercise training, and outcomes in chronic systolic heart failure. *Am J Cardiol.* (2011) 108:1754–9. doi: 10.1016/j.amjcard.2011.07.051
4. Kapoor JR, Heidenreich PA. Obesity and survival in patients with heart failure and preserved systolic function: a *U*-shaped relationship. *Am Heart J.* (2010) 159:75–80. doi: 10.1016/j.ahj.2009.10.026
5. Horwich TB, Fonarow GC, Hamilton MA, MacLellan WR, Woo MA, Tillisch JH. The relationship between obesity and mortality in patients with heart failure. *J Am Coll Cardiol.* (2001) 38:789–95. doi: 10.1016/S0735-1097(01)01448-6
6. Curtis JP, Selter JG, Wang Y, Rathore SS, Jovin IS, Jadbabaie F, et al. The obesity paradox: body mass index and outcomes in patients with heart failure. *Arch Intern Med.* (2005) 165:55–61. doi: 10.1001/archinte.165.1.55

7. Padwal R, McAlister FA, McMurray JJ, Cowie MR, Rich M, Pocock S, et al. The obesity paradox in heart failure patients with preserved versus reduced ejection fraction: a meta-analysis of individual patient data. *Int J Obes.* (2014) 38:1110–4. doi: 10.1038/ijo.2013.203
8. Lin GM, Li YH, Yin WH, Wu YW, Chu PH, Wu CC, et al. The obesity-mortality paradox in patients with heart failure in Taiwan and a collaborative meta-analysis for East Asian patients. *Am J Cardiol.* (2016) 118:1011–8. doi: 10.1016/j.amjcard.2016.06.056
9. Sharma A, Lavie CJ, Borer JS, Vallakati A, Goel S, Lopez-Jimenez F, et al. Meta-analysis of the relation of body mass index to all-cause and cardiovascular mortality and hospitalization in patients with chronic heart failure. *Am J Cardiol.* (2015) 115:1428–34. doi: 10.1016/j.amjcard.2015.02.024
10. Lavie CJ, De Schutter A, Patel DA, Romero-Corral A, Artham SM, Milani RV. Body composition and survival in stable coronary heart disease: impact of lean mass index and body fat in the "obesity paradox". *J Am Coll Cardiol.* (2012) 60:1374–80. doi: 10.1016/j.jacc.2012.05.037
11. Kruse NT, Buzkova P, Barzilay JI, Valderrabano RJ, Robbins JA, Fink HA, et al. Association of skeletal muscle mass, kidney disease and mortality in older men and women: the cardiovascular health study. *Aging.* (2020) 12:21023–36. doi: 10.18632/aging.202135
12. Eriksen CS, Kimer N, Suetta C, Møller S. Arm lean mass determined by dual-energy X-ray absorptiometry is superior to characterize skeletal muscle and predict sarcopenia-related mortality in cirrhosis. *Am J Physiol Gastrointest Liver Physiol.* (2021) 320:G729–40. doi: 10.1152/ajpgi.00478.2020
13. Seino S, Kitamura A, Abe T, Taniguchi Y, Yokoyama Y, Amano H, et al. Dose-response relationships between body composition indices and all-cause mortality in older Japanese adults. *J Am Med Dir Assoc*. (2020) 21:726–33.e4. doi: 10.1016/j.jamda.2019.11.018
14. Xing Z, Tang L, Chen J, Pei J, Chen P, Fang Z, et al. Association of predicted lean body mass and fat mass with cardiovascular events in patients with type 2 diabetes mellitus. *CMAJ.* (2019) 191:E1042–8. doi: 10.1503/cmaj.190124
15. Lin TY, Peng CH, Hung SC, Tarng DC. Body composition is associated with clinical outcomes in patients with non-dialysis-dependent chronic kidney disease. *Kidney Int.* (2018) 93:733–40. doi: 10.1016/j.kint.2017.08.025
16. Thomas E, Gupta PP, Fonarow GC, Horwich TB. Bioelectrical impedance analysis of body composition and survival in patients with heart failure. *Clin Cardiol.* (2019) 42:129–35. doi: 10.1002/clc.23118
17. Ohori K, Yano T, Katano S, Kouzu H, Honma S, Shimomura K, et al. High percent body fat mass predicts lower risk of cardiac events in patients with heart failure: an explanation of the obesity paradox. *BMC Geriatr.* (2021) 21:16. doi: 10.1186/s12877-020-01950-9
18. Selvaraj S, Kim J, Ansari BA, Zhao L, Cvijic ME, Fronheiser M, et al. Body composition, natriuretic peptides, and adverse outcomes in heart failure with preserved and reduced ejection fraction. *JACC Cardiovasc Imaging.* (2020) 14:203–15. doi: 10.1016/j.jcmg.2020.07.022
19. Konishi M, Akiyama E, Matsuzawa Y, Sato R, Kikuchi S, Nakahashi H, et al. Prognostic impact of muscle and fat mass in patients with heart failure. *J Cachexia Sarcopenia Muscle.* (2021) 12:568–76. doi: 10.1002/jcsm.12702
20. Lee DH, Keum N, Hu FB, Orav EJ, Rimm EB, Willett WC, et al. Predicted lean body mass, fat mass, and all cause and cause specific mortality in men: prospective US cohort study. *BMJ.* (2018) 362:k2575. doi: 10.1136/bmj.k2575
21. Huang X, Yu Y, Li X, Masoudi FA, Spertus JA, Yan X, et al. The China Patient-centred Evaluative Assessment of Cardiac Events (PEACE) prospective heart failure study design. *BMJ Open.* (2019) 9:e025144. doi: 10.1136/bmjopen-2018-025144
22. Zhou BF. Predictive values of body mass index and waist circumference for risk factors of certain related diseases in Chinese adults–study on optimal cut-off points of body mass index and waist circumference in Chinese adults. *Biomed Environ Sci.* (2002) 15:83–96.
23. Lee DH, Keum N, Hu FB, Orav EJ, Rimm EB, Sun Q, et al. Development and validation of anthropometric prediction equations for lean body mass, fat mass and percent fat in adults using the National Health and Nutrition Examination Survey (NHANES) 1999-2006. *Br J Nutr.* (2017) 118:858–66. doi: 10.1017/S0007114517002665
24. Liu X, Sun Q, Sun L, Zong G, Lu L, Liu G, et al. The development and validation of new equations for estimating body fat percentage among Chinese men and women. *Br J Nutr.* (2015) 113:1365–72. doi: 10.1017/S0007114515000616
25. Aimo A, Januzzi JL Jr, Vergaro G, Clerico A, Latini R, Meessen J, et al. Revisiting the obesity paradox in heart failure: per cent body fat as predictor of biomarkers and outcome. *Eur J Prev Cardiol.* (2019) 26:1751–9. doi: 10.1177/2047487319852809
26. Weber D, Long J, Leonard MB, Zemel B, Baker JF. Development of novel methods to define deficits in appendicular lean mass relative to fat mass. *PLoS ONE.* (2016) 11:e0164385. doi: 10.1371/journal.pone.0164385
27. Iizuka K, Machida T, Hirafuji M. Skeletal muscle is an endocrine organ. *J Pharmacol Sci.* (2014) 125:125–31. doi: 10.1254/jphs.14R02CP
28. Severinsen MCK, Pedersen BK. Muscle-organ crosstalk: the emerging roles of myokines. *Endocr Rev.* (2020) 41:594–609. doi: 10.1210/endrev/bnaa016
29. Fülster S, Tacke M, Sandek A, Ebner N, Tschöpe C, Doehner W, et al. Muscle wasting in patients with chronic heart failure: results from the studies investigating co-morbidities aggravating heart failure (SICA-HF). *Eur Heart J.* (2013) 34:512–9. doi: 10.1093/eurheartj/ehs381
30. Orimoloye OA, Kambhampati S, Hicks AJ 3rd, Al Rifai M, Silverman MG, Whelton S, et al. Higher cardiorespiratory fitness predicts long-term survival in patients with heart failure and preserved ejection fraction: the Henry Ford Exercise Testing (FIT) project. *Arch Med Sci.* (2019) 15:350–8. doi: 10.5114/aoms.2019.83290
31. Han M, Qie R, Shi X, Yang Y, Lu J, Hu F, et al. Cardiorespiratory fitness and mortality from all causes, cardiovascular disease and cancer: dose-response meta-analysis of cohort studies. *Br J Sports Med.* (2022). 2022:bjsports-2021-104876. doi: 10.1136/bjsports-2021-104876
32. McGown C, Birerdinc A, Younossi ZM. Adipose tissue as an endocrine organ. *Clin Liver Dis.* (2014) 18:41–58. doi: 10.1016/j.cld.2013.09.012
33. Afshin A, Forouzanfar MH, Reitsma MB, Sur P, Estep K, Lee A, et al. Health effects of overweight and obesity in 195 countries over 25 years. *N Engl J Med.* (2017) 377:13–27. doi: 10.1056/NEJMoa1614362
34. Karampela I, Chrysanthopoulou E, Christodoulatos GS, Dalamaga M. Is there an obesity paradox in critical illness? Epidemiologic and metabolic considerations. *Curr Obes Rep*. (2020) 9:231–44. doi: 10.1007/s13679-020-00394-x
35. Krysztofiak H, Wleklik M, Migaj J, Dudek M, Uchmanowicz I, Lisiak M, et al. Cardiac cachexia: a well-known but challenging complication of heart failure. *Clin Interv Aging.* (2020) 15:2041–51. doi: 10.2147/CIA.S273967
36. Melenovsky V, Kotrc M, Borlaug BA, Marek T, Kovar J, Malek I, et al. Relationships between right ventricular function, body composition, and prognosis in advanced heart failure. *J Am Coll Cardiol.* (2013) 62:1660–70. doi: 10.1016/j.jacc.2013.06.046
37. Streng KW, Voors AA, Hillege HL, Anker SD, Cleland JG, Dickstein K, et al. Waist-to-hip ratio and mortality in heart failure. *Eur J Heart Fail.* (2018) 20:1269–77. doi: 10.1002/ejhf.1244
38. Palmer BF, Clegg DJ. The sexual dimorphism of obesity. *Mol Cell Endocrinol.* (2015) 402:113–9. doi: 10.1016/j.mce.2014.11.029
39. Anker SD, Negassa A, Coats AJ, Afzal R, Poole-Wilson PA, Cohn JN, et al. Prognostic importance of weight loss in chronic heart failure and the effect of treatment with angiotensin-converting-enzyme inhibitors: an observational study. *Lancet.* (2003) 361:1077–83. doi: 10.1016/S0140-6736(03)12892-9
40. Clark AL, Coats AJS, Krum H, Katus HA, Mohacsi P, Salekin D, et al. Effect of beta-adrenergic blockade with carvedilol on cachexia in severe chronic heart failure: results from the COPERNICUS trial. *J Cachexia Sarcopenia Muscle.* (2017) 8:549–56. doi: 10.1002/jcsm.12191
41. Rozentryt P, von Haehling S, Lainscak M, Nowak JU, Kalantar-Zadeh K, Polonski L, et al. The effects of a high-caloric protein-rich oral nutritional supplement in patients with chronic heart failure and cachexia on quality of life, body composition, and inflammation markers: a randomized, double-blind pilot study. *J Cachexia Sarcopenia Muscle.* (2010) 1:35–42. doi: 10.1007/s13539-010-0008-0
42. Passantino A, Dalla Vecchia LA, Corrà U, Scalvini S, Pistono M, Bussotti M, et al. The future of exercise-based cardiac rehabilitation for patients with heart failure. *Front Cardiovasc Med.* (2021) 8:709898. doi: 10.3389/fcvm.2021.709898
43. Nichols S, McGregor G, Al-Mohammad A, Ali AN, Tew G, O'Doherty AF. The effect of protein and essential amino acid supplementation on muscle strength and performance in patients with chronic heart failure: a

systematic review. *Eur J Nutr.* (2020) 59:1785–801. doi: 10.1007/s00394-019-02108-z

Conflict of Interest: The authors declare that the research was conducted in the absence of any commercial or financial relationships that could be construed as a potential conflict of interest.

Publisher's Note: All claims expressed in this article are solely those of the authors and do not necessarily represent those of their affiliated organizations, or those of the publisher, the editors and the reviewers. Any product that may be evaluated in this article, or claim that may be made by its manufacturer, is not guaranteed or endorsed by the publisher.

frontiers in Cardiovascular Medicine

ORIGINAL RESEARCH
published: 30 March 2022
doi: 10.3389/fcvm.2022.839763

Prognosis Implication of N-Terminal Pro-B-Type Natriuretic Peptide in Adult Patients With Acute Myocarditis

Yan Zhao[1], *Naqiang Lyu*[1], *Wei Zhang*[1], *Huiqiong Tan*[2], *Qi Jin*[3,4] *and Aimin Dang*[1]*

[1] State Key Laboratory of Cardiovascular Disease, Department of Special Care Center, National Center for Cardiovascular Diseases, Fuwai Hospital, Chinese Academy of Medical Sciences and Peking Union Medical College, Beijing, China, [2] Emergency and Critical Care Center, National Center for Cardiovascular Diseases, Fuwai Hospital, Chinese Academy of Medical Sciences and Peking Union Medical College, Beijing, China, [3] Center for Pulmonary Vascular Diseases, National Center for Cardiovascular Diseases, Fuwai Hospital, Chinese Academy of Medical Sciences and Peking Union Medical College, Beijing, China, [4] Department of Cardiology, Zhongshan Hospital, Shanghai Institute of Cardiovascular Diseases, Fudan University, Shanghai, China

Background: The aim of this study is to investigate the role of N-terminal pro-B-type natriuretic peptide (NT-proBNP) in assessing the poor outcomes of adult patients with acute myocarditis.

Methods: A total of 170 adult patients with available NT-proBNP information were included in the study. They were grouped according to quartiles of NT-proBNP concentrations at admission. Baseline and follow-up information was collected. Thirty-day major adverse cardiac events (MACE) were death and heart transplantation. Long-term MACE included all-cause death, heart transplantation, re-hospitalization due to heart failure, sustained ventricular arrhythmia, and myocarditis relapse.

Results: During a median follow-up of 3.8 years, patients in the highest NT-proBNP quartile suffered from the highest risk both of 30-day and long-term MACE ($P < 0.001$ by log-rank test). Multivariate analysis showed that apart from left ventricular ejection fraction (LVEF), an increased baseline NT-proBNP > 3,549 pg/mL (hazard ratio 3.535, 95% CI 1.316–9.499, $P = 0.012$) and NT-proBNP > 7,204 pg/mL (hazard ratio 22.261, 95% CI 1.976–250.723, $P = 0.012$) was independent predictor of long-term and 30-day MACE, respectively.

Conclusions: Higher baseline NT-proBNP level was an independent predictor of poor outcomes in adult patients with acute myocarditis. Therefore, NT-proBNP may serve as a useful biomarker for risk stratification in acute myocarditis patients.

Keywords: NT-proBNP, prognosis, biomarker, risk stratification, acute myocarditis

OPEN ACCESS

Edited by:
Gary Tse,
Second Hospital of Tianjin Medical University, China

Reviewed by:
Aleksander Dokollari,
St. Michael's Hospital, Canada
Lars Michel,
Essen University Hospital, Germany

***Correspondence:**
Aimin Dang
gemmadang@163.com

Specialty section:
This article was submitted to Heart Failure and Transplantation, a section of the journal Frontiers in Cardiovascular Medicine

Received: *20 December 2021*
Accepted: *10 March 2022*
Published: *30 March 2022*

Citation:
Zhao Y, Lyu N, Zhang W, Tan H, Jin Q and Dang A (2022) Prognosis Implication of N-Terminal Pro-B-Type Natriuretic Peptide in Adult Patients With Acute Myocarditis. Front. Cardiovasc. Med. 9:839763. doi: 10.3389/fcvm.2022.839763

INTRODUCTION

Acute myocarditis, an inflammatory disease of myocardium, can have various clinical presentations. The prognosis of patients with myocarditis also varies according to distinct etiology. Most of the patients present with mild symptoms and recover completely, however, pathological data show myocarditis in 8.6% of cases of sudden death in young adults (1), while up to 30% of myocarditis proved by biopsy might develop to dilated cardiomyopathy, which is the most common

disease requiring heart transplantation (2). Uncommonly, patients with hemodynamically unstable myocarditis, which is called fulminant myocarditis, face an extremely high risk of death due to sudden onset cardiogenic shock, ventricular arrhythmias, or multiorgan failure and have a dismal prognosis (3).

Therefore, it is crucial to identify high-risk patients as early as possible to provide an optimized treatment strategy in order to improve their outcomes. Although endomyocardial biopsy (EMB) remains to be gold standard for diagnosis and prognosis of myocarditis, it is not performed widely and routinely (4). Previous studies identified prolonged QRS or QTc interval, decreased LVEF, as well as specific location and pattern of late gadolinium enhancement (LGE) in cardiac magnetic resonance (CMR) as predictors for poor prognosis in patients with acute myocarditis (5–10). However, imaging tools such as echocardiography and CMR fail to reflect subtle changes that precede cardiac dysfunction and tissue fibrosis and could hardly be monitored continuously. Hence there is a need to find out a biomarker with prognostic value for adverse outcomes in acute myocarditis patients.

Natriuretic peptides are established biomarkers for the diagnosis and prognosis evaluation of various cardiovascular conditions including acute or chronic heart failure and coronary heart disease (11–13). A series of recent studies reported that N-terminal pro-B-type natriuretic peptide (NT-proBNP) levels may be a useful predictor of mortality in patients with coronavirus disease 2019 (COVID-19) related myocarditis (14–16). In the present study, we hypothesized that NT-proBNP could independently predict poor prognosis of adult patients with acute myocarditis. We tested the hypothesis with complete data of NT-proBNP from a cohort of 170 adult patients with acute myocarditis.

METHODS

Ethics Statement

This study complied with the ethical guidelines of the Declaration of Helsinki and China's regulations and guidelines on good clinical practice and was approved by the ethics committees of Fuwai Hospital (no. 2021-1470).

Study Design and Participants

This single-center, retrospective, observational study was performed at Fuwai Hospital (National Center of Cardiovascular Diseases, Beijing, China). Two hundred and forty eight adult patients were clinically diagnosed with acute myocarditis from August 2006 to March 2020. Among these patients, 170 patients with complete clinical information and NT-proBNP data were selected. The electronic medical records of the patients were reviewed by trained attendings. Clinical data were collected and analyzed, including demographics, medical history, physical examination, laboratory tests, treatment measures, and outcomes. All patients had no history of ischemic or hemorrhagic stroke, renal or liver dysfunction, chronic obstructive pulmonary disease, or thyroid disease. The diagnosis of acute myocarditis was clinically based on Caforio et al. (2), we included patients with presenting symptoms or signs of two or more of the following five criteria: (1) Clinical symptoms (within 3 months): acute chest pain, dyspnea, syncope, heart failure, palpitation, or aborted cardiac death, unexplained cardiogenic shock; (2) electrocardiography (ECG) or Holter features; (3) Elevated myocardium injured markers: troponin I (TnI); (4) Echocardiography findings: functional and structural abnormalities; (5) CMR findings: consistent with myocardial inflammation, if presenting with two or more of the Lake-Louise criteria (17), namely edema, or hyperemia, and/or late gadolinium enhancement. If EMB or pathology of the hearts available after heart transplantation was consistent with the revised Dallas criteria (18), the diagnosis of myocarditis was definite. The exclusion criteria included: (1) evidence of coronary stenosis $\geq$ 50%; (2) other pre-existing cardiovascular disease including valvular heart disease, hypertensive heart disease, congenital heart disease or cardiomyopathy. Participants were divided into four groups according to quartiles of NT-proBNP levels: quartile 1 (<94.37 pg/mL, $n = 42$), quartile 2 group (94.37–425.47 pg/mL, $n = 43$), quartile 3 (425.47–4557.00 pg/mL, $n = 43$), and quartile 4 (>4557.00 pg/mL, $n = 42$). **Figure 1** shows the flow chart of enrollment.

During hospitalization, all patients were treated based on the recommended management for myocarditis (2). Stable patients with injured left ventricular function received recommended heart failure treatment. Patients with severe or cardiogenic shock were treated with inotropes and mechanic circulatory support (MCS). MCS included intra-aortic balloon pump (IABP), venous-arterial extracorporeal membrane oxygenation (va-ECMO), or combination of IABP and va-ECMO.

N-Terminal Pro-B-Type Natriuretic Peptide Tests

Blood samples were obtained from 1 to 3 days after admission. The blood samples were collected into tubes with EDTA-anticoagulant and centrifuged. Serum NT-proBNP was directly measured in the Laboratory of Fuwai Hospital using a commercial electrochemiluminescence assay (Roche Diagnostics GmbH, Mannheim, Germany). The reference range for plasma NT-proBNP in our laboratory was <125 pg/mL.

Follow-Up and Outcomes

Outcome data were obtained by telephone interview, reviewing electronic medical records, or out-patient visit. All events were checked and confirmed by an independent group of trained, clinical physicians. Thirty day major adverse cardiac events (MACE) were defined as death and heart transplantation within 30 days after admission. Long-term MACE included: (1) all-cause death; (2) heart transplantation; (3) heart failure requiring hospitalization; (4) recorded sustained ventricular arrhythmia (>30s); (5) myocarditis relapse.

Abbreviations: LVEF, left ventricular ejection fraction; MACE, major adverse cardiac events; HR, hazard ratio; CI, confidence interval; ROC, receiver operating characteristic; AUC, area under the ROC curve.

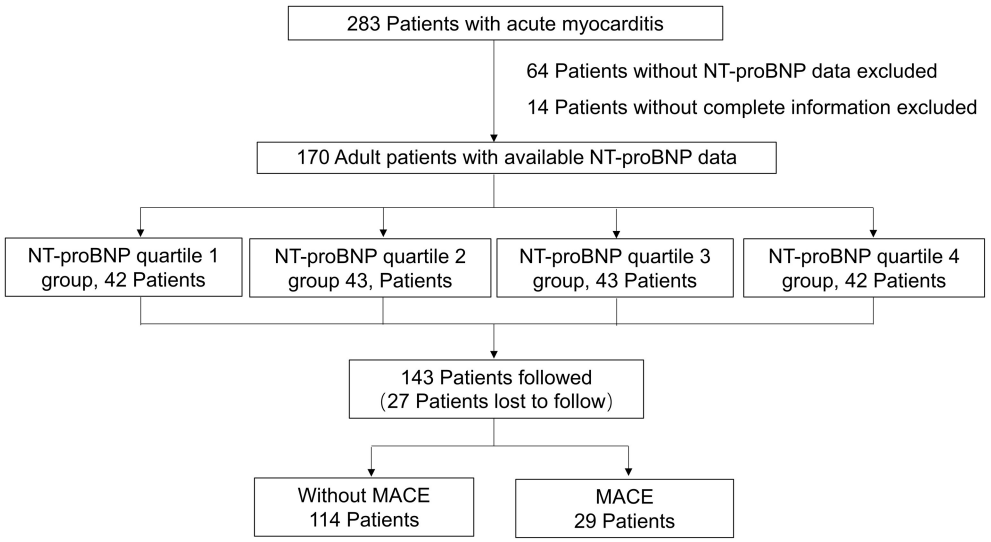

FIGURE 1 | The flow chart of the enrollment of 170 adult patients with acute myocarditis from the overall population with acute myocarditis.

Statistical Analysis

Continuous variables are presented as mean ± SD or as median (Q1-Q3). Differences in baseline participant characteristics were assessed by analysis of variance or Mann-Whitney *U* test for continuous variables and Pearson χ^2 test or Fisher's exact test for categorical variables. The correlation between NT-proBNP and other parameters were assessed by Pearson and Spearman's correlation analysis. Univariate and multivariate Cox proportional hazards analysis was performed to determine the factors predicting MACE. The covariables included in the multivariate Cox analysis was selected according to the following reasons: the variables that were significant in univariate analysis, or the ones were reported to be associated with NT-proBNP levels and MACE (age, BMI, QRS duration > 120 ms, QTc interval > 440 ms, creatinine, LVEF < 50%, etc.). Survival curves were generated by the Kaplan-Meier method and compared with the log-rank test. The ability of NT-proBNP for predicting MACE was evaluated by the receiver operating characteristic (ROC) curve analysis and quantified by the area under the ROC curve (AUC), in which a value of 1.0 indicates perfect ability and a value of 0.5 indicates no ability. All analyses were two tailed, and *P*-values < 0.05 were considered statistically significant. Analyses were performed with IBM SPSS statistics software version 26.0. The Kaplan-Meier curves were made with GraphPad Prism software version 5.0 and the ROC curves were made with MedCalc software version 19.0.

RESULTS

Patients Population and Clinical Presentation

The main baseline characteristics of the study population are reported in **Supplementary Table 1**. One hundred and seventy patients with available NT-proBNP data were included in the analysis. One hundred fourteen patients were diagnosed based on EMB or CMR, while 56 patients without EMB or CMR were diagnosed mainly according to clinical presentations, ECGs, laboratory tests and echocardiography. The baseline characteristics of the patients with or without EMB or CMR are shown in **Supplementary Table 2**, and there was no significant difference in NT-proBNP levels between the two groups. The population was divided according to quartiles of NT-proBNP levels (**Table 1**). Patients in quartile 4 were the oldest and had the highest percentage of female. No significant differences were found in the prevalence of comorbidities among the four groups. Chest pain was less in patients with lower NT-proBNP levels, while dyspnea was more frequent in patients with higher NT-proBNP, and the prevalence of syncope was of no significant difference among the four groups. Patients with higher NT-proBNP had significantly higher heart rate and lower systolic blood pressure. Patients with highest NT-proBNP levels had the most prevalence of arrythmia, including sinus tachycardia, sustained ventricular arrythmias, and bundle-branch block, as well as the longest QRS and QTc intervals. However, the prevalence of complete atrioventricular block and supraventricular tachycardia was not significantly different among the four groups. Patients with higher NT-proBNP levels presented with higher C response protein level, higher troponin I level, and worse renal function. They also had a larger left atrium, lower left ventricular ejection fraction (LVEF), and almost 70% of the patients in the highest quartile group had LVEF <50%. Treatment differed across the four groups with the most invasive life support strategies for patients with the highest NT-proBNP levels. In terms of medication, aldosterone antagonists and corticosteroids were most used in patients in the highest quartile, and no significant difference was found in the use of β-blocker and ACE-I/ARB among the participants.

TABLE 1 | Baseline characteristics of the study population grouped by the quartiles of NT-proBNP.

	Q1 (< 94.37 pg/mL, *n* = 42)	Q2 (94.37–425.47 pg/mL, *n* = 43)	Q3 (425.47–4557.00 pg/mL, *n* = 43)	Q4 (> 4557.00 pg/mL, *n* = 42)	*P*-Value
Demographics					
Age (years, Q1–Q3)	27 (22–36)	26 (22–33)	34 (28–46)	36 (30–53)	<0.001
Male, *n* (%)	30 (71.4)	34 (79.1)	27 (62.8)	21 (50.0)	0.032
BMI (kg/m^2)	23.0 ± 3.6	24.4 ± 3.9	25.3 ± 4.6	23.2 ± 4.1	0.029
Comorbidities and NYHA class					
Hypertension, *n* (%)	1 (2.4)	3 (7.0)	5 (11.6)	4 (9.5)	0.415
Diabetes mellitus, *n* (%)	0 (0)	2 (4.7)	0 (0)	3 (7.1)	0.132
Dyslipidemia, *n* (%)	5 (11.9)	1 (2.3)	3 (7.0)	6 (14.3)	0.213
NYHA III or IV (%)	0 (0)	13 (30.2)	24 (55.8)	36 (85.7)	<0.001
Clinical presentation, *n* (%)					
Chest pain	19 (45.2)	19 (44.2)	15 (34.9)	8 (19.0)	0.044
Dyspnea	8 (19.0)	11 (25.6)	23 (53.5)	28 (66.7)	<0.001
Syncope	5 (11.9)	6 (14.0)	6 (14.0)	7 (16.7)	0.941
Vital signs at admission					
Systolic blood pressure (mmHg)	117 ± 13	115 ± 16	107 ± 17	102 ± 17	<0.001
Diastolic blood pressure (mmHg)	68 ± 10	69 ± 13	68 ± 9	66 ± 12	0.670
Heart rate (beats/minute)	74 ± 13	80 ± 16	89 ± 24	97 ± 24	<0.001
Electrocardiogram at admission					
Normal, *n* (%)	26 (61.9)	10 (23.3)	10 (23.3)	1 (2.4)	<0.001
QRS interval (ms)	94 ± 22	103 ± 32	96 ± 26	115 ± 34	0.003
QTc interval (ms)	428 ± 46	436 ± 48	440 ± 42	463 ± 45	0.003
QRS interval >120 ms, *n* (%)	2 (4.8)	9 (20.9)	6 (14.0)	13 (31.0)	0.014
QTc interval >440 ms, *n* (%)	10 (25.0)	16 (42.1)	21 (51.2)	31 (75.6)	<0.001
Arrhythmia, *n* (%)					
Sinus tachycardia	1 (2.4)	6 (14.0)	15 (34.9)	22 (52.4)	<0.001
Supraventricular tachycardia	1 (2.4)	1 (2.3)	3 (7.0)	6 (14.3)	0.084
Sustained VT/VF	1 (2.4)	2 (4.7)	3 (7.0)	8 (19.0)	0.026
complete AVB	4 (9.5)	7 (16.3)	6 (14.0)	7 (16.7)	0.772
Bundle-branch block	2 (4.8)	10 (23.3)	7 (16.3)	13 (31.0)	0.017
Laboratory tests at admission					
WBC (×10^9/L, Q1–Q3)	6.5 (5.6–8.0)	7.4 (6.5–11.1)	9.0 (6.7–11.8)	10.6 (7.0–14.5)	<0.001
CRP (mg/L, Q1–Q3)	4.4 (2.1–11.6)	13.1 (4.9–56.3)	18.0 (7.0–61.5)	28.7 (15.6–115.3)	<0.001
Creatinine (μmol/L, Q1–Q3)	75.6 (64.3–86.7)	79.0 (66.0–86.1)	82.0 (65.0–102.0)	101.3 (78.8–129.6)	<0.001
Troponin I (ng/mL, Q1–Q3)	0.65 (0.1–3.7)	2.6 (1.0–5.7)	2.7 (0.46–6.46)	2.6 (0.3–12.2)	0.014
NT-proBNP (pg/mL, Q1–Q3)	54.4(34.6–67.1)	249.0 (160.0–326.7)	1417.0 (702.2–2432.6)	9079.8 (6907.8–24143.3)	<0.001
Peak NT-proBNP (pg/mL, Q1–Q3)	57.8 (41.6–83.8)	270.3 (162.0–352.1)	1692.0 (823.0–3395.0)	16902.2(9257.4–35398.0)	<0.001
Echocardiography at admission					
LA (mm)	32 ± 4	33 ± 6	35 ± 6	35 ± 6	0.001
LVEDD (mm)	47 ± 5	50 ± 9	49 ± 6	51 ± 8	0.036
IVS (mm)	9 ± 2	10 ± 2	9 ± 2	10 ± 2	0.046
RV (mm)	21 ± 2	22 ± 6	21 ± 3	23 ± 5	0.094
LVEF (%)	64 ± 4	57 ± 10	48 ± 14	42 ± 13	<0.001
LVEF < 50%, *n* (%)	0 (0)	6 (14.0)	25 (58.1)	29 (69.0)	<0.001
Coronary angiography or CT angiography performed, *n* (%)	34 (81.0)	31 (72.1)	32 (74.4)	29 (69.0)	0.642
No evidence of CAD, *n* (%)	34 (100)	31 (100)	32 (100)	29 (100)	-
MRI performed, *n* (%)	25 (59.5)	23 (53.5)	35 (81.4)	26 (61.9)	0.043

(Continued)

TABLE 1 | Continued

	Q1 (< 94.37 pg/mL, *n* = 42)	Q2 (94.37–425.47 pg/mL, *n* = 43)	Q3 (425.47–4557.00 pg/mL, *n* = 43)	Q4 (> 4557.00 pg/mL, *n* = 42)	*P*-Value
Medications					
β-Blockers, *n* (%)	30 (71.4)	30 (69.8)	34 (79.1)	33 (78.6)	0.669
ACE-I or ARB, *n* (%)	20 (47.6)	19 (44.2)	22 (51.2)	18 (42.9)	0.870
Aldosterone antagonists, n (%)	1 (2.4)	9 (20.9)	16 (37.2)	21 (50.0)	<0.001
Corticosteroids, *n* (%)	5 (7.8)	11 (17.2)	20 (31.3)	28 (43.8)	<0.001
Life support treatment					
MCS, *n* (%)	0 (0)	2 (4.7)	7 (16.3)	15 (35.7)	<0.001
Ventilator, *n* (%)	0 (0)	0 (0)	4 (9.3)	11 (26.2)	<0.001
Temporary pacing, *n* (%)	4 (9.5)	6 (14.0)	5 (11.6)	5 (11.9)	0.940

BMI, Body mass index; VT, ventricular tachycardia; VF, ventricular fibrillation; AVB, atrioventricular block; WBC, white blood cell; CRP, C-reactive protein; NT-proBNP, N-terminal pro-B-type natriuretic peptide; LA, left atrium; LVEDD, left ventricular end-diastolic diameter; IVS, intraventricular septum; RV, right ventricular diameter; LVEF, left ventricular ejection fraction; CAD, coronary atherosclerosis disease; ACE-I, angiotensin-converting enzyme-inhibitor; ARB, angiotensin receptor blocker; MCS, mechanic circulatory support.

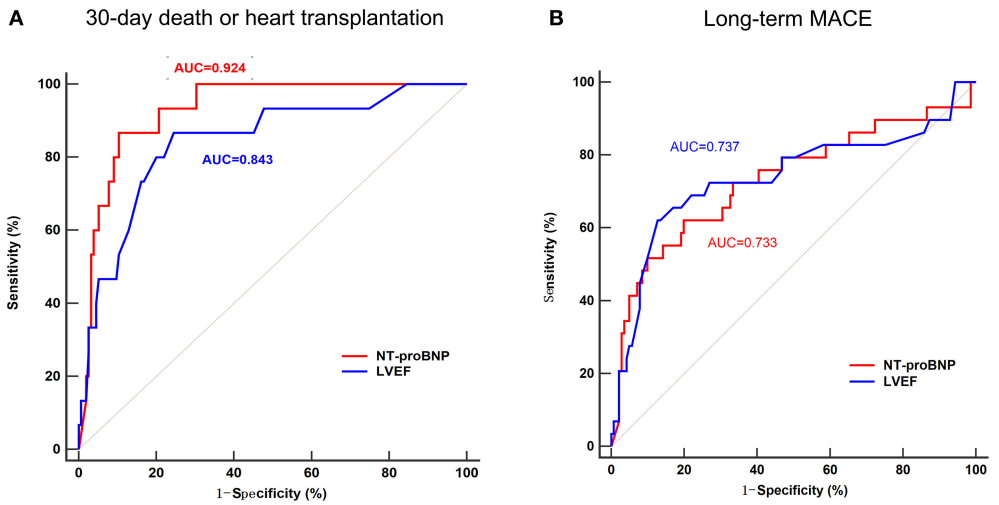

FIGURE 2 | Receiver operating characteristic (ROC) curve of the ability of NT-proBNP and LVEF to predict 30-day death or heart transplantation **(A)** and long-term MACE **(B)** in patients with acute myocarditis. In predicting 30-day death or heart transplantation, the area under the curve (AUC) for NT-proBNP was 0.929, with 86.67% sensitivity and 89.68% specificity, while the AUC for LVEF was 0.843, with 86.67% sensitivity and 75.48% specificity. In predicting long-term MACE, the AUC for NT-proBNP was 0.733, with 62.07% sensitivity and 80.14% specificity, while the AUC for LVEF was 0.737, with 62.07% sensitivity and 87.23% specificity. MACE, major adverse cardiac events; NT-proBNP, N-terminal pro-B-type natriuretic peptide; LVEF, left ventricular ventricle ejection fraction.

Etiology of Acute Myocarditis

Twenty four patients (14.1%) accepted EMB. Histopathology and Immunopathology Findings Showed Lymphocyte Myocarditis in 13 Patients (54.2%), Giant Cell Myocarditis in 3 Patients (12.5%), Eosinophilic Myocarditis in 2 Patients (8.3%), and no Typical Myocarditis Characteristics in the Other 6 Patients (25.0%). No Patient Was Diagnosed With COVID-19 After Clinical Evaluation and Screening of Virus Nucleic Acid by Nasopharyngeal or Oropharyngeal Swabs.

Correlation Analysis of NT-ProBNP Levels With Echocardiographic Parameters and Other Parameters

The serum concentrations of NT-proBNP were mediumly and negatively correlated with LVEF (Rho = −0.616; $P < 0.001$). However, they were only slightly correlated with the left ventricular end-diastolic diameter (Rho = 0.164; $P = 0.033$) and left atrium diameter (Rho = 0.259; $P = 0.001$). Otherwise, NT-proBNP levels were mildly correlated with age (Rho = 0.361; $P < 0.001$), C reactive protein levels (Rho = 0.444; $P < 0.001$), and

creatinine levels (Rho = 0.358; $P < 0.001$). They were slightly correlated with troponin I levels (Rho = 0.195; $P = 0.011$) and were not significantly related with BMI (Rho = 0.004; $P = 0.960$).

ROC Curve Analysis and Predictive Value for MACE

To assess the predictive value of NT-proBNP in patients with acute myocarditis, and to compare with LVEF, the established strong predictor, ROC curves for LVEF and NT-proBNP were compared. In predicting 30-day death or heart transplantation, the sensitivity and specificity of NT-proBNP were 86.67 and 89.68%, respectively (AUC = 0.924, optimal cut-off value: 7,204 pg/mL), while the sensitivity and specificity of LVEF were 86.67 and 75.48%, respectively (AUC = 0.843, optimal cut-off value: 45%) (**Figure 2A**). In predicting long-term MACE, the sensitivity and specificity of NT-proBNP were 62.07 and 80.14%, respectively (AUC = 0.733, optimal cut-off value: 3,549 pg/mL). The sensitivity and specificity of LVEF to predict long-term MACE was 62.07 and 87.23%, respectively (AUC = 0.737, optimal cut-off value: 38%) (**Figure 2B**). ROC curves showed that the predictive values of troponin I were lower than NT-proBNP for both of 30-day (AUC = 0.616, optimal cut-off value: 15.846 ng/mL) and long-term MACE (AUC = 0.509, optimal cut-off value: 0.315 ng/mL) (**Supplementary Figure 2**).

Prognostic Value of the NT-ProBNP Levels in Acute Myocarditis

After a follow-up of 3.8 ± 3.2 years, long-term MACE happened in 29 patients (17.1%) including 11 deaths (6.5%), 4 heart transplantations (2.4%), 8 heart failure hospitalizations (4.7%), 1 sustained ventricular arrhythmia (0.6%), and 5 recurrent myocarditis (2.9%). 30-day MACE occurred in 15 patients (8.8%) including 11 deaths (6.5%) and 4 heart transplantations (2.4%). There were 19 patients (11.2%) lost to follow-up, who had lower baseline NT-proBNP levels and higher LVEF at admission (**Supplementary Table 3**).

Among the four groups, patients in the highest quartile suffered from the highest risk in reaching both 30-day death or heart transplantation and long-term MACE (**Figure 3**; $P < 0.001$ by log-rank test). The MACE-free survival curve of the patients in the highest quartile was evidently different from those in other quartiles, especially in the first month and the first year. Additionally, **Figure 4** shows a negative correlation between NT-proBNP levels and the survival time of the patients who had long-term MACE.

To determine if NT-proBNP was an independent predictor of short-term and long-term adverse outcome, univariate and multivariate Cox analyses were performed (**Tables 2**, **3**). In univariate Cox analysis for long-term MACE, NT-proBNP > 3,549 pg/mL showed a significant predictive value (HR 1.006, 95% CI 1.004–1.008, $P < 0.001$). LVEF (HR 0.936, 95% CI 0.912–0.961, $P < 0.001$), creatinine (HR 1.008, 95% CI 1.005–1.011, $P < 0.001$), age (HR 1.039, 95% CI 1.013–1.066, $P = 0.003$), white blood cell level at admission (HR 1.118, 95% CI 1.030–1.213, $P = 0.008$), right ventricular diameter (HR 1.051, 95% CI 1.008–1.096, $P = 0.020$) and QRS interval (HR 1.011, 95% CI 1.001–1.022, $P = 0.038$) were also predictors of long-term MACE. In multivariate analysis, both of baseline LVEF (HR 0.948, 95% CI 0.919–0.978, $P = 0.001$) and NT-proBNP > 3,549 pg/mL (HR 3.535, 95% CI 1.316–9.499, $P = 0.012$) remained to be strong independent predictors of long-term MACE. For 30-day death or heart transplantation, baseline LVEF (HR 0.919, 95% CI 0.869–0.973, $P = 0.004$), NT-proBNP > 7,204 pg/mL (HR 22.261, 95% CI 1.976–250.723, $P = 0.012$), troponin I level (HR 1.052, 95%CI 1.015–1.090, $P = 0.005$), right ventricular diameter (HR 1.135, 95% CI 1.029–1.252, $P = 0.011$), and age (HR 1.078, 95% CI 1.010–1.151, $P = 0.024$) were independent predictors. Therefore, even after adjustment for other established predictors and confounding factors including LVEF, QRS interval, age, inflammation indicators, and renal function, increased NT-proBNP level was a strong independent predictor for both 30-day and long-term MACE in adult patients with acute myocarditis.

To verify the cut-off value of NT-proBNP abovementioned, Kaplan-Meier survival curves were made and showed that patients with baseline NT-proBNP > 3,549 pg/mL faced higher risk of long-term MACE (**Supplementary Figure 1B**; $P < 0.001$ by log-rank test), especially in the first year. Similarly, 60% of the patients with baseline NT-proBNP > 7,204 pg/mL died or received heart transplantation within 30 days after admission (**Supplementary Figure 1A**; $P < 0.001$ by log-rank test).

DISCUSSION

This study evaluated the predictive value of NT-proBNP in a cohort of adult patients with acute myocarditis. NT-proBNP was a strong predictor for adverse cardiac outcomes both in 30-day and long-term, independently of inflammatory indicators, electrocardiographic and echocardiographic measurements. Among the four quartile groups, patients in the highest quartile of NT-proBNP suffered from not only. In the present cohort, high NT-proBNP level was an independent predictor for adverse cardiac events and provided more information for evaluating the prognosis of adult patients with acute myocarditis. Although NT-proBNP is a well-known marker in predicting poor prognosis in a higher risk of in-hospital death and heart transplantation, but also the poorest long-term outcomes. In the present cohort, high NT-proBNP level was an independent factor associated with MACE and added useful information for assessing the outcomes of acute myocarditis. Although NT-proBNP is a well-known marker in predicting adverse prognosis in different cohorts of cardiac patients, this is the first study evaluating the predictive value of NT-proBNP levels for both of short-term and long-term outcomes of adult patients with acute myocarditis.

NT-proBNP, an inactive N-terminal fragment split from B-Type natriuretic peptide (BNP) prohormone, is released into the circulation by the myocardium due to increased ventricular stress or ischemia (13, 19). Hence it is widely considered a biomarker reflecting the impairment of left ventricular function as well as myocardial ischemia. Previous studies reported that NT-proBNP was a valuable marker of long-term prognostic stratification both in heart failure and coronary heart disease (11–13, 19–21). However, few study assessed its prognostic value in adult

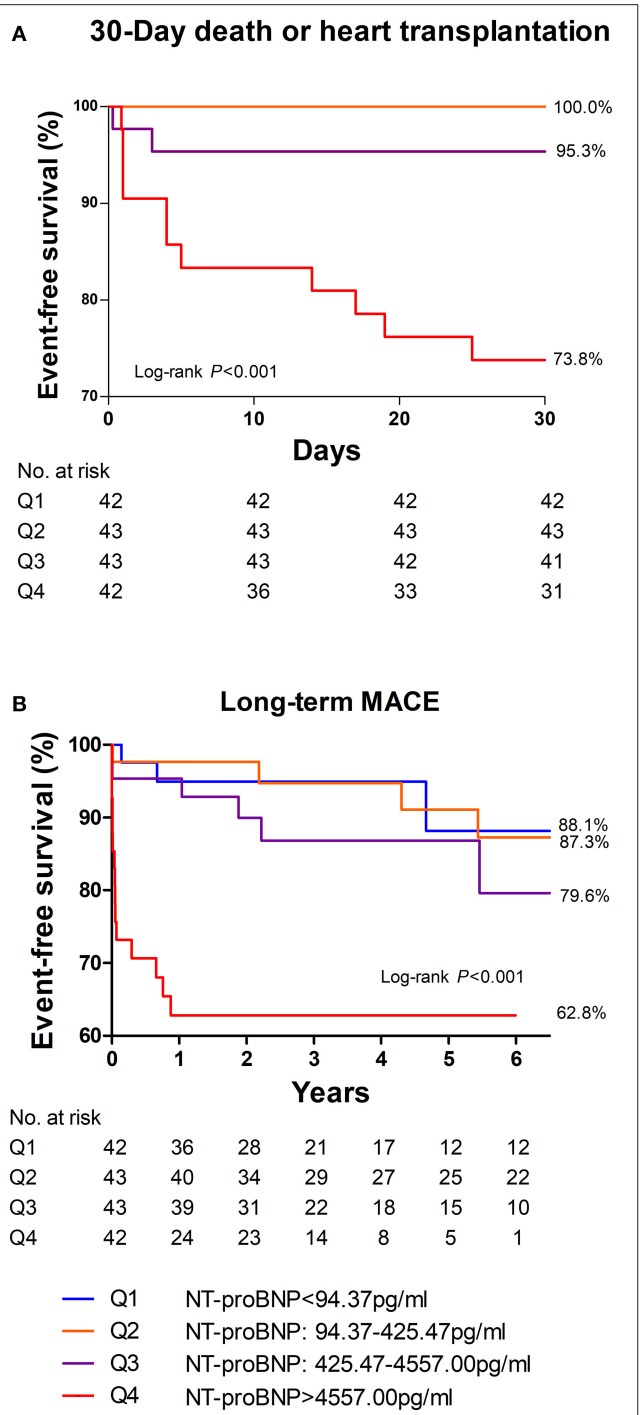

FIGURE 3 | 30-day **(A)** and long-term **(B)** MACE-free survival among different quartiles of NT-proBNP in patients with acute myocarditis. Patients in the highest quartile of NT-proBNP had the most MACE in 30 days as well as in the long-term. Thirty day MACE included deaths and heart transplantation within 30 days after admission. Long-term MACE included deaths, heart transplantations, re-hospitalization for heart failure, and sustained ventricular arrhythmias (>30s).

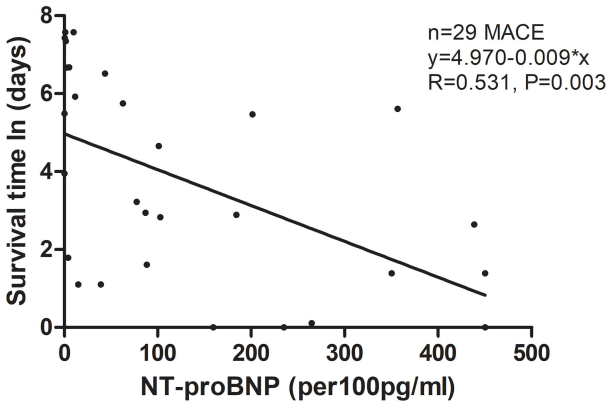

FIGURE 4 | Scatter figure showed a linear correlation between NT-proBNP levels and time of survival (days, Napierian Logarithm scale) in all patients who had long-term MACE ($n = 29$). MACE, major adverse cardiac events; NT-proBNP, N-terminal pro-B-type natriuretic peptide.

patients with acute myocarditis. Previous studies identified that electrocardiographic parameters including pathological Q wave, prolonged QRS duration, and QTc interval were independent predictors for poor outcomes for patients with myocarditis (5–7, 22). Moreover, cardiac dysfunction, LVEF < 50%, and right ventricular dysfunction were robust predictors for poor long-term prognosis (23–27). The present study showed that increased NT-proBNP levels were negatively correlated with decreased LVEF, which was widely accepted to be a strong predictor of poor outcomes of acute myocarditis. Moreover, we demonstrated for the first time that baseline NT-proBNP could provide useful information for prognosis after adjusting established factors such as LVEF and QRS duration, suggesting NT-proBNP as a valuable addition to risk stratification for adult patients with acute myocarditis.

The results of our study are in line with the recently published article by Rodriguez-Gonzalez et al. (28) who reported that baseline NT-proBNP > 5,000 pg/mL could help to identify high-risk pediatric myocarditis patients with poor outcomes. BNP was also related to poor prognosis in two smaller studies of pediatric patients with myocarditis (29, 30). In 218 adult patients with acute severe myocarditis, Zhang et al. (31) recently reported that elevated BNP (>100 pg/mL) was an independent predictor for long-term mortality. However, the best cut-off value of NT-proBNP was still uncertain in predicting poor prognosis in the adult patient with acute myocarditis. In the present study, multivariate Cox analysis showed that NT-proBNP was an independent prognostic predictor for both short-term and long-term MACE for adult patients with acute myocarditis. Moreover, according to ROC analysis and evaluated by Cox analysis, NT-proBNP > 7,204 pg/mL and >3,549 pg/mL might be reasonable cutoff values to predict death or heart transplantation within 30 days and to imply long-term MACE, respectively. The cutoff values of NT-proBNP need to be confirmed by a prospective, multicenter study of larger number of patients in the future.

Apart from age, female sex, renal failure, increased NT-proBNP levels are also associated with inflammation (32–34). Previous studies showed that inflammatory cytokines such

TABLE 2 | Univariate and Multivariate Cox Analysis for Long-term MACE.

	HR	95%CI	*P*-Value
Univariate regression			
Age, y	1.039	1.013–1.066	0.003
Gender, female	1.095	0.508–2.361	0.817
BMI, kg/m^2	0.937	0.853–1.030	0.180
WBC at admission, $\times10^9$/L	1.118	1.030–1.213	0.008
CRP, mg/L	1.002	0.996–1.008	0.593
Creatinine, μmol/L	1.008	1.005–1.011	<0.001
Troponin I, ng/mL	1.014	0.995–1.034	0.147
QRS interval, ms	1.011	1.001–1.022	0.038
QTc interval, ms	1.006	1.000–1.013	0.058
NT–proBNP > 3,549 pg/mL	1.006	1.004–1.008	<0.001
RV, mm	1.051	1.008–1.096	0.020
LVEF at admission (%)	0.936	0.912–0.961	<0.001
Multivariate regression			
Age, y	1.024	0.995–1.053	0.113
Gender	0.754	0.301–1.893	0.548
BMI, kg/m^2	0.926	0.837–1.025	0.138
WBC at admission, $\times10^9$/L	1.032	0.925–1.151	0.576
Creatinine,μmol/L	1.003	0.998–1.007	0.238
QRS interval, ms	0.998	0.985–1.011	0.809
RV, mm	1.041	0.984–1.101	0.163
LVEF at admission, %	0.948	0.919–0.978	0.001
NT-proBNP > 3,549 pg/mL	3.535	1.316–9.499	0.012

Multivariate Cox model selected by a stepwise method with factors that were significant in the univariate analysis. BMI, body mass index; WBC, white blood cell; CRP, C reactive protein; NT-proBNP, N-terminal pro-B-type natriuretic peptide; RV, right ventricular diameter; LVEF, left ventricular ventricle ejection fraction.

TABLE 3 | Univariate and multivariate cox analysis for 30-day death or heart transplantation.

	HR	95%CI	*P*-Value
Univariate regression			
Age, y	1.052	1.014–1.091	0.006
Gender, female	1.084	0.363–3.236	0.884
BMI, kg/m^2	0.929	0.811–1.065	0.291
WBC at admission, $\times10^9$/L	1.218	1.091–1.359	<0.001
CRP, mg/L	1.004	0.996–1.012	0.366
Creatinine,μmol/L	1.008	1.004–1.012	<0.001
Troponin I, ng/mL	1.027	1.007–1.047	0.007
QRS interval, ms	1.020	1.006–1.034	0.006
QTc interval, ms	1.008	0.998–1.017	0.104
RV, mm	1.079	1.028–1.133	0.002
LVEF at admission, %	0.910	0.875–0.947	<0.001
NT–proBNP > 7,204 pg/mL	33.491	7.480–149.945	<0.001
Multivariate regression			
Age, y	1.078	1.010–1.151	0.024
Gender	0.618	0.144–2.661	0.518
BMI, kg/m^2	0.895	0.748–1.070	0.224
WBC at admission, $\times10^9$/L	1.168	0.961–1.419	0.118
Creatinine,μmol/L	1.000	0.993–1.008	0.911
Troponin I, ng/mL	1.052	1.015–1.090	0.005
QRS interval, ms	0.982	0.959–1.006	0.149
RV, mm	1.135	1.029–1.252	0.011
LVEF at admission, %	0.919	0.869–0.973	0.004
NT-proBNP > 7,204 pg/mL	22.261	1.976–250.723	0.012

Multivariate Cox model selected by a stepwise method with factors that were significant in the univariate analysis. BMI, body mass index; WBC, white blood cell; CRP, C reactive protein; NT-proBNP, N-terminal pro-B-type natriuretic peptide; RV, right ventricular diameter; LVEF, left ventricular ventricle ejection fraction.

as interleukin-1β, interleukin-6 (IL-6), and tumor necrosis factor-α could induce natriuretic peptides transcription in cardiomyocytes (35–37). A recently published article by Fish-Trotter also reported that inflammatory conditions were associated with elevated natriuretic peptides release (38). Myocarditis might be caused by various etiology leading to myocardial inflammation and injury. Viral infection, as widely accepted as the most common infectious cause, can harm cardiomyocytes through both direct damage and autoimmune-mediated injury due to systemic inflammatory responses, in which cytokines and antibodies could damage cardiac systolic function and endothelium, leading to systolic dysfunction and ischemia (39). For example, myocarditis is one of the complications in a recent cohort of patients with coronavirus disease 2019 (COVID-19) (40). Guo et al. (14) revealed that NT-pro-BNP elevation was significantly positively linear correlated with myocardial injury in patients with COVID-19. Moreover, Han et al. (16) reported that NT-proBNP was related to the severity and mortality of patients with COVID-19. Thus, in the setting of acute myocarditis, increased NT-proBNP levels might suggest not only cardiac systolic dysfunction, but also acute inflammation and myocardial injury. In this study, we proved that increased NT-proBNP levels were correlated with higher inflammatory factor levels, however, univariate Cox analysis showed no significant association between CRP levels and either 30-day or long-term MACE. But we found that NT-proBNP levels were only slightly correlated with the myocardial injury marker. This might be because of the different extents of myocardial injuries in those patients caused by heterogeneous causes and at different stages of the disease.

Although most patients with acute myocarditis present with mild symptoms and have a good long-term prognosis, a small number of patients with hemodynamically unstable myocarditis, which is called fulminant myocarditis, may have sudden onsets and significant severity with increased in-hospital mortality and poor long-term prognosis (8). The fulminant presentation reflects a more robust immunological and inflammatory response resulting in severe myocyte necrosis and cardiogenic shock (3, 41). Although most of the patients with acute myocarditis have mildly to moderately elevated NT-proBNP levels as a result of inflammation and myocardial injuries, markedly elevated NT-proBNP, which is a marker of severe cardiac dysfunction and extensive myocardial injuries, may help to give useful information for early recognition and prognosis evaluation of patients with fulminant myocarditis. According to the cut-off value by ROC and multivariate Cox analysis, the predictive

cut-off value of NT-proBNP for short-term adverse outcomes might be much higher than that of in the diagnosis of heart failure. Hence the measurement of natriuretic peptides may be considered according to the 2020 AHA scientific statement for the recognition and management of fulminant myocarditis (3). Moreover, it is important that the result of our study identifies that NT-proBNP may play a useful role in risk stratification of adult patients with acute myocarditis, independently of other currently used tools including echocardiography and electrocardiogram, and NT-proBNP more than 7,204 pg/mL might be a reasonable cut-off value in acute stage for risk stratification. Patients with a low and moderate elevated NT-proBNP level might need less frequent monitoring and less aggressive treatments. This might lead to possible cost reduction in public health care. Moreover, patients with a high NT-proBNP should be managed more actively and followed up more closely.

Despite the encouraging results, this study has some limitations. First, as a gold standard for diagnosis, endomyocardial biopsy was performed only in 14.1% of these patients and the diagnosis was mainly based on clinical manifestations. Although CMR was performed in 64.1% of the patients, which could compensate for the weakness to a large extent, the possibility of misdiagnosing still existed. Second, due to the follow-up time span of up to 13 years, some patients dropped out, which might lead to a bias to the evaluation of prognosis. There was no significant difference in clinical presentation, laboratory tests and echocardiography parameters between patients with and without follow-up except those lost to follow-up had better baseline cardiac function, which might be the main reason why they did not come back for reexamination. Third, a small number of patients were so critically ill that died before performing an NT-proBNP test, which might introduce selection bias. Last, due to the single-center data and the retrospective design, large-scale and prospective researches are needed to confirm the findings of this study in the future. Nonetheless, our study has several strengths include the complete information of NT-proBNP data, long-term follow-up, and the multivariate analysis adjusted factors that might affect NT-proBNP levels.

CONCLUSION

In conclusion, we identified baseline NT-proBNP level as an independent prognostic predictor for acute myocarditis. The NT-proBNP concentration at admission can serve as a valuable biomarker for risk evaluation in adult patients with acute myocarditis.

DATA AVAILABILITY STATEMENT

The original contributions presented in the study are included in the article/**Supplementary Materials**, further inquiries can be directed to the corresponding author.

ETHICS STATEMENT

The studies involving human participants were reviewed and approved by Ethics Committees of Fuwai Hospital. The patients/participants provided their written informed consent to participate in this study.

AUTHOR CONTRIBUTIONS

YZ designed the study, collected the data, and prepared the manuscript. YZ, NL, and AD performed the statistics. NL and AD provided professional advice on data explanation and revised the manuscript. WZ, HT, and QJ provided professional advice on data interpretation. All authors contributed to the article and approved the submitted version.

FUNDING

The work was supported by the Chinese Academy of Medical Sciences Initiative for Innovative Medicine (CAMS-I2M) 2017-I2M-2-002 (to AD).

ACKNOWLEDGMENTS

We thank the support from Jinghui Li (MR Center, Fuwai Hospital, National Center for Cardiovascular Disease of China, Beijing, China) with the CMR imaging analysis, and the help from Yang Sun (Department of Pathology, Fuwai Hospital, National Center for Cardiovascular Disease of China, Beijing, China) with myocardial pathological evaluation. We also thank the help from Yang Wang (Medical Research and Biometrics Center, Fuwai Hospital, National Center for Cardiovascular Disease, Beijing, China) with the statistical analyses.

SUPPLEMENTARY MATERIAL

The Supplementary Material for this article can be found online at: https://www.frontiersin.org/articles/10.3389/fcvm.2022.839763/full#supplementary-material

REFERENCES

1. Caforio AL, Calabrese F, Angelini A, Tona F, Vinci A, Bottaro S, et al. A prospective study of biopsy-proven myocarditis: prognostic relevance of clinical and aetiopathogenetic features at diagnosis. *Eur Heart J.* (2007) 28:1326–33. doi: 10.1093/eurheartj/ehm076
2. Caforio AL, Pankuweit S, Arbustini E, Basso C, Gimeno-Blanes J, Felix SB, et al. Current state of knowledge on aetiology, diagnosis, management, and therapy of myocarditis: a position statement of the European society of cardiology working group on myocardial and pericardial diseases. *Eur Heart J.* (2013) 34:2636–48. doi: 10.1093/eurheartj/eht210
3. Kociol RD, Cooper LT, Fang JC, Moslehi JJ, Pang PS, Sabe MA, et al. Recognition and initial management of fulminant myocarditis: a scientific statement from the American heart association. *Circulation.* (2020) 141:e69–92. doi: 10.1161/CIR.0000000000000745

4. Ammirati E, Cipriani M, Moro C, Raineri C, Pini D, Sormani P, et al. Clinical presentation and outcome in a contemporary cohort of patients with acute myocarditis: multicenter lombardy registry. *Circulation.* (2018) 138:1088–99. doi: 10.1161/CIRCULATIONAHA.118.035319
5. Ukena C, Mahfoud F, Kindermann I, Kandolf R, Kindermann M, Böhm M. Prognostic electrocardiographic parameters in patients with suspected myocarditis. *Eur J Heart Fail.* (2011) 13:398–405. doi: 10.1093/eurjhf/hfq229
6. Butta C, Zappia L, Laterra G, Roberto M. Diagnostic and prognostic role of electrocardiogram in acute myocarditis: a comprehensive review. *Ann Noninvasive Electrocardiol.* (2020) 25:e12726. doi: 10.1111/anec.12726
7. Hung Y, Lin WH, Lin CS, Cheng SM, Tsai TN, Yang SP, et al. The prognostic role of QTc interval in acute myocarditis. *Acta Cardiol Sin.* (2016) 32:223–30. doi: 10.6515/acs20150226a
8. Ammirati E, Cipriani M, Lilliu M, Sormani P, Varrenti M, Raineri C, et al. Survival and left ventricular function changes in fulminant versus nonfulminant acute myocarditis. *Circulation.* (2017) 136:529–45. doi: 10.1161/CIRCULATIONAHA.117.026386
9. Aquaro GD, Perfetti M, Camastra G, Monti L, Dellegrottaglie S, Moro C, et al. Cardiac MR with late gadolinium enhancement in acute myocarditis with preserved systolic function: ITAMY study. *J Am Coll Cardiol.* (2017) 70:1977–87. doi: 10.1016/j.jacc.2017.08.044
10. Grani C, Eichhorn C, Biere L, Murthy VL, Agarwal V, Kaneko K, et al. Prognostic value of cardiac magnetic resonance tissue characterization in risk stratifying patients with suspected myocarditis. *J Am Coll Cardiol.* (2017) 70:1964–76. doi: 10.1016/j.jacc.2017.08.050
11. Ponikowski P, Voors AA, Anker SD, Bueno H, Cleland JGF, Coats AJS, et al. 2016 ESC guidelines for the diagnosis and treatment of acute and chronic heart failure: the task force for the diagnosis and treatment of acute and chronic heart failure of the European society of cardiology (ESC) developed with the special contribution of the heart failure association (HFA) of the ESC. *Eur Heart J.* (2016) 37:2129–200. doi: 10.1093/eurheartj/ehw128
12. Zhang C, Jiang L, Xu L, Tian J, Liu J, Zhao X, et al. Implications of N-terminal pro-B-type natriuretic peptide in patients with three-vessel disease. *Eur Heart J.* (2019) 40:3397–405. doi: 10.1093/eurheartj/ehz394
13. Kragelund C, Grønning B, Køber L, Hildebrandt P, Steffensen R. N-terminal pro-B-type natriuretic peptide and long-term mortality in stable coronary heart disease. *N Engl J Med.* (2005) 352:666–75. doi: 10.1056/NEJMoa042330
14. Guo T, Fan Y, Chen M, Wu X, Zhang L, He T, et al. Cardiovascular implications of fatal outcomes of patients with coronavirus disease 2019 (COVID-19). *JAMA Cardiol.* (2020) 5:811–8. doi: 10.1001/jamacardio.2020.1017
15. Gao L, Jiang D, Wen XS, Cheng XC, Sun M, He B, et al. Prognostic value of NT-proBNP in patients with severe COVID-19. *Respir Res.* (2020) 21:83. doi: 10.1186/s12931-020-01352-w
16. Han H, Xie L, Liu R, Yang J, Liu F, Wu K, et al. Analysis of heart injury laboratory parameters in 273 COVID-19 patients in one hospital in Wuhan, China. *J Med Virol.* (2020) 92:819–23. doi: 10.1002/jmv.25809
17. Friedrich MG, Sechtem U, Schulz-Menger J, Holmvang G, Alakija P, Cooper LT, et al. Cardiovascular magnetic resonance in myocarditis: a JACC white paper. *J Am Coll Cardiol.* (2009) 53:1475–87. doi: 10.1016/j.jacc.2009.02.007
18. Leone O, Veinot JP, Angelini A, Baandrup UT, Basso C, Berry G, et al. 2011 consensus statement on endomyocardial biopsy from the association for European cardiovascular pathology and the society for cardiovascular pathology. *Cardiovasc Pathol.* (2012) 21:245–74. doi: 10.1016/j.carpath.2011.10.001
19. Chow SL, Maisel AS, Anand I, Bozkurt B, de Boer RA, Felker GM, et al. Role of biomarkers for the prevention, assessment, and management of heart failure: a scientific statement from the American heart association. *Circulation.* (2017) 135:e1054–e91. doi: 10.1161/CIR.0000000000000490
20. Volpe M, Rubattu S, Burnett J. Natriuretic peptides in cardiovascular diseases: current use and perspectives. *Eur Heart J.* (2014) 35:419–25. doi: 10.1093/eurheartj/eht466
21. Squire IB, O'Brien RJ, Demme B, Davies JE, Ng LL. N-terminal pro-atrial natriuretic peptide (N-ANP) and N-terminal pro-B-type natriuretic peptide (N-BNP) in the prediction of death and heart failure in unselected patients following acute myocardial infarction. *Clin sci.* (2004) 107:309–16. doi: 10.1042/CS20040087
22. Ammirati E, Veronese G, Brambatti M, Merlo M, Cipriani M, Potena L, et al. Fulminant versus acute nonfulminant myocarditis in patients with left ventricular systolic dysfunction. *J Am Coll Cardiol.* (2019) 74:299–311. doi: 10.1016/j.jacc.2019.04.063
23. Anzini M, Merlo M, Sabbadini G, Barbati G, Finocchiaro G, Pinamonti B, et al. Long-term evolution and prognostic stratification of biopsy-proven active myocarditis. *Circulation.* (2013) 128:2384–94. doi: 10.1161/CIRCULATIONAHA.113.003092
24. Kindermann I, Kindermann M, Kandolf R, Klingel K, Bultmann B, Muller T, et al. Predictors of outcome in patients with suspected myocarditis. *Circulation.* (2008) 118:639–48. doi: 10.1161/CIRCULATIONAHA.108.769489
25. Ammirati E, Veronese G, Bottiroli M, Wang DW, Cipriani M, Garascia A, et al. Update on acute myocarditis. *Trends Cardiovasc Med.* (2020) 31:370-9. doi: 10.1016/j.tcm.2020.05.008
26. Sagar S, Liu PP, Cooper LT. Myocarditis. *Lancet.* (2012) 379:738–47. doi: 10.1016/S0140-6736(11)60648-X
27. Mendes LA, Dec GW, Picard MH, Palacios IF, Newell J, Davidoff R. Right ventricular dysfunction: an independent predictor of adverse outcome in patients with myocarditis. *Am Heart J.* (1994) 128:301–7. doi: 10.1016/0002-8703(94)90483-9
28. Rodriguez-Gonzalez M, Sanchez-Codez MI, Lubian-Gutierrez M, Castellano-Martinez A. Clinical presentation and early predictors for poor outcomes in pediatric myocarditis: a retrospective study. *World J Clin Cases.* (2019) 7:548–61. doi: 10.12998/wjcc.v7.i5.548
29. Sachdeva S, Song X, Dham N, Heath DM, DeBiasi RL. Analysis of clinical parameters and cardiac magnetic resonance imaging as predictors of outcome in pediatric myocarditis. *Am J Cardiol.* (2015) 115:499–504. doi: 10.1016/j.amjcard.2014.11.029
30. Abrar S, Ansari MJ, Mittal M, Kushwaha KP. Predictors of mortality in paediatric myocarditis. *J Clin Diagn Res.* (2016) 10:SC12–6. doi: 10.7860/JCDR/2016/19856.7967
31. Zhang Q, Zhao R. Risk factors analysis of prognosis of adult acute severe myocarditis. *World J Clin Cases.* (2020) 8:5547–54. doi: 10.12998/wjcc.v8.i22.5547
32. Suthahar N, Meems LMG, Ho JE, de Boer RA. Sex-related differences in contemporary biomarkers for heart failure: a review. *Eur J Heart Fail.* (2020) 22:775–88. doi: 10.1002/ejhf.1771
33. Jensen J, Ma LP, Fu ML, Svaninger D, Lundberg PA, Hammarsten O. Inflammation increases NT-proBNP and the NT-proBNP/BNP ratio. *Clin Res Cardiol.* (2010) 99:445–52. doi: 10.1007/s00392-010-0140-z
34. Bar SL, Swiggum E, Straatman L, Ignaszewski A. Nonheart failure-associated elevation of amino terminal pro-brain natriuretic peptide in the setting of sepsis. *Can J Cardiol.* (2006) 22:263–6. doi: 10.1016/S0828-282X(06)70908-4
35. Szabo-Fresnais N, Lefebvre F, Germain A, Fischmeister R, Pomerance M. A new regulation of IL-6 production in adult cardiomyocytes by beta-adrenergic and IL-1 beta receptors and induction of cellular hypertrophy by IL-6 trans-signalling. *Cell Signal.* (2010) 22:1143–52. doi: 10.1016/j.cellsig.2010.03.009
36. Fredj S, Bescond J, Louault C, Delwail A, Lecron JC, Potreau D. Role of interleukin-6 in cardiomyocyte/cardiac fibroblast interactions during myocyte hypertrophy and fibroblast proliferation. *J Cell Physiol.* (2005) 204:428–36. doi: 10.1002/jcp.20307

37. Tanaka T, Kanda T, Takahashi T, Saegusa S, Moriya J, Kurabayashi M. Interleukin-6-induced reciprocal expression of SERCA and natriuretic peptides mRNA in cultured rat ventricular myocytes. *J Int Med Res.* (2004) 32:57–61. doi: 10.1177/147323000403200109
38. Fish-Trotter H, Ferguson JF, Patel N, Arora P, Allen NB, Bachmann KN, et al. Inflammation and circulating natriuretic peptide levels. *Circ Heart Fail.* (2020) 13:e006570. doi: 10.1161/CIRCHEARTFAILURE.119.006570
39. Pollack A, Kontorovich AR, Fuster V, Dec GW. Viral myocarditis–diagnosis, treatment options, and current controversies. *Nat Rev Cardiol.* (2015) 12:670–80. doi: 10.1038/nrcardio.2015.108
40. Inciardi RM, Lupi L, Zaccone G, Italia L, Raffo M, Tomasoni D, et al. Cardiac involvement in a patient with coronavirus disease 2019 (COVID-19). *JAMA Cardiol.* (2020) 5:819–24. doi: 10.1001/jamacardio.2020.1096
41. Hang W, Chen C, Seubert JM, Wang DW. Fulminant myocarditis: a comprehensive review from etiology to treatments and outcomes. *Signal Transduct Target Ther.* (2020) 5:287. doi: 10.1038/s41392-020-00360-y

Conflict of Interest: The authors declare that the research was conducted in the absence of any commercial or financial relationships that could be construed as a potential conflict of interest.

frontiers in Cardiovascular Medicine

ORIGINAL RESEARCH
published: 05 April 2022
doi: 10.3389/fcvm.2022.847205

Diastolic Plateau – Invasive Hemodynamic Marker of Adverse Outcome Among Left Ventricular Assist Device Patients

Avishay Grupper[1,2], Afek Kodesh[2], Jacob Lavee[1,2], Paul Fefer[1,2], Israel M. Barbash[1,2], Dan Elian[1,2], Alexander Kogan[1,2], Avi Morgan[1,2], Amit Segev[1,2] and Elad Maor[1,2]*

[1] Division of Cardiology, Leviev Center of Cardiovascular Medicine, Sheba Medical Center in Tel HaShomer, Ramat Gan, Israel, [2] The Sackler School of Medicine, Tel Aviv University, Tel Aviv, Israel

OPEN ACCESS

Edited by:
Gary Tse,
Second Hospital of Tianjin Medical University, China

Reviewed by:
Fabrizio D'Ascenzo,
San Giovanni Battista Molinette, Italy
Selim Bozkurt,
Ulster University, United Kingdom
Andrew Rosenbaum,
Mayo Clinic, United States
Minoru Ono,
The University of Tokyo Hospital, Japan

***Correspondence:**
Avishay Grupper
avishay.grupper@sheba.health.gov.il

Specialty section:
This article was submitted to Heart Failure and Transplantation, a section of the journal Frontiers in Cardiovascular Medicine

Received: 01 January 2022
Accepted: 03 March 2022
Published: 05 April 2022

Citation:
Grupper A, Kodesh A, Lavee J, Fefer P, Barbash IM, Elian D, Kogan A, Morgan A, Segev A and Maor E (2022) Diastolic Plateau – Invasive Hemodynamic Marker of Adverse Outcome Among Left Ventricular Assist Device Patients. Front. Cardiovasc. Med. 9:847205. doi: 10.3389/fcvm.2022.847205

Background: Diastolic plateau is an invasive hemodynamic marker of impaired right ventricular (RV) diastolic filling. The purpose of the current analysis was to evaluate the prognostic importance of this sign in left ventricular assist device (LVAD) patients.

Methods: The analysis included all LVAD patients who received continuous-flow LVAD (HeartMate 3) at the Sheba medical center and underwent right heart catheterization (RHC) during follow up post-LVAD surgery. Patients were dichotomized into 2 mutually exclusive groups based on a plateau duration cutoff of 55% of diastole. The primary end point of the current analysis was the composite of death, heart transplantation, or increase in diuretic dosage in a 12-month follow-up period post-RHC.

Results: Study cohort included 59 LVAD patients with a mean age of 57 (IQR 54–66) of whom 48 (81%) were males. RHC was performed at 303 ± 36 days after LVAD surgery. Patients with and without diastolic plateau had similar clinical, echocardiographic, and hemodynamic parameters. Kaplan–Meier survival analysis showed that the cumulative probability of event at 1 year was 65 ± 49% vs. 21 ± 42% for primary outcomes among patients with and without diastolic plateau (p Log rank < 0.05 for both). A multivariate model with adjustment for age, INTERMACS score and ischemic cardiomyopathy consistently showed that patients with diastolic plateau were 4 times more likely to meet the study composite end point (HR = 4.35, 95% CI 1.75–10.83, $p = 0.002$).

Conclusion: Diastolic plateau during RHC is a marker of adverse outcome among LVAD patients.

Keywords: hemodynamic, diastolic plateau, LVAD, right ventricular, outcome

INTRODUCTION

Right ventricular failure (RVF) following left ventricular assist device (LVAD) implantation remains a major complication which may significantly impair patient outcomes. It is associated with prolonged length of intensive care unit and hospital stay, as well as high long-term morbidity and mortality (1–4). Since many LVAD patients have clinical or subclinical right ventricular (RV)

dysfunction, accurate RV function assessment is essential in diagnosing RVF, guiding therapies, and determining prognoses. As the RV is embryologically and morphologically distinct, non-invasive imaging tests traditionally used for the left ventricle (LV) may not be ideal in measuring RV function (5). In addition, there are no clear invasive hemodynamic criteria that can be used to define or diagnose RVF post-LVAD. The pathophysiology of RVF post-LVAD is multifactorial; however, one of the major factors affecting RV function is LVAD speed, leading to alterations of RV preload and afterload as well as positional distortions of the interventricular septum. These changes limit the flexibility and mobility of the RV myocardium and can create a restrictive-like physiology.

Dip and plateau ("square root sign") is a classic hemodynamic parameter used to describe a typical RV pressure pattern in patients with constrictive or restrictive physiology (6, 7). An early rapid filling of the RV in early diastole due to high atrial pressure, followed by a limitation in filling from the stiff myocardium results in a prominent "y" descent on the atrial pressure curves. The pressure in late diastole elevates and plateaus in accordance with the impaired RV relaxation or pericardial compression, resulting in the "square root" sign on RV pressure curves.

While classic teaching associates the square root sign with constrictive pericarditis, cardiac tamponade, and restrictive cardiomyopathy, we hypothesized that this sign could be used to assist in identifying LVAD patients with failing RVs. Therefore, the purpose of the current study was to evaluate the role of the invasive hemodynamic dip and plateau pattern as a marker of adverse outcomes among LVAD patients.

MATERIALS AND METHODS

The study included 59 consecutive patients who had undergone LVAD—HeartMate3 implantations at the Sheba medical center in Ramat Gan, Israel and underwent invasive right heart catheterization (RHC) as part of their follow up at the LVAD clinic. All patient data was taken from the computerized medical records. For patients who had more than one RHC study, the first RHC post-LVAD implantation was used to calculate the dip and plateau of the RV waveform. All measurements were based on end-expiration phase. All RV waveforms were reviewed, and the measurement was based on the best waveform (the one with the minimum number of artifacts). Plateau was calculated by dividing the length of the plateau by the length of the entire RV diastole; for dip calculations, catheterization pressure readings were used (**Figure 1**). Since there is no acceptable cutoff for diastolic plateau, positive plateau was defined as the plateau $\geq$ 55% of diastole, and the study population was dichotomized into 2 groups according to the diastolic plateau pattern (positive vs. negative plateau). This cutoff was used as it is statistically significant in multiple models (Kaplan–Meier, univariate Cox regression and multivariate Cox regression).

All reported echocardiographs were carried out based on the American Society of Echocardiography guidelines. Right atrial pressure was estimated by visualizing the inferior vena cava (IVC) and its response to respiration. Right atrial pressure was estimated as 5 mm Hg if the IVC was $<$ 2.0 cm in diameter at the junction of the right atrium, 15 mm Hg if the IVC was dilated and collapsed with respiration, and 20 mm Hg if the IVC was dilated and did not collapse with respiration.

Outcome events used in this study included all-cause mortality, heart transplantation, and furosemide dosage increases throughout a 12-month period post index RHC (as a parameter associated with worsening RV failure signs). The primary composite outcome of the study included death, heart transplantation, or increase in diuretic dosage in a 12-month follow-up period post-RHC. Secondary composite outcome included only death and diuretic dose increase post-RHC. Mortality data was available for all patients from the national registry. Heart transplantation and furosemide dosage increases were available for all patients from the electronic medical record. The Institutional Review Board of the Sheba Medical Center approved this retrospective analysis based on strict maintenance of participants' anonymity during database analyses. No individual consent was obtained.

Statistical Analysis

Patient characteristics were presented as means for continuous variables and a binary system was used for categorical variables. Student *t*-test was used for comparison of continuous variables between the study groups. Pearson's R and Spearman correlations were used for the same purpose for categorical variables. The probability of meeting the composite endpoint according to the study groups was graphically displayed according to the method of Kaplan–Meier, with a comparison of cumulative survival across strata by the log-rank test. Univariate and multivariable Cox proportional hazards regression modeling were used to determine the Hazard Ratio (HR) for the composite study endpoint. In addition to diastolic plateau groups, the multivariable model included age, INTERMACS score and ischemic cardiomyopathy. Hazards Ratio is presented with a 95% confidence interval and statistical significance was accepted for a 2-sided $P < 0.05$. All statistical analyses were performed using IBM SPSS version 23.

RESULTS

Final study cohort included 59 LVAD patients with a mean age of 57 years (IQR 54-66), and 48 patients (81%) were male. Baseline patients' characteristics at the time of RHC are shown in **Table 1**. A histogram depicting the distribution of diastolic plateau length measured at the time of RHC is shown in **Figure 2**. Overall, 26 (44%) patients exhibited a positive diastolic plateau and were more likely to have chronic kidney disease, defined as a GFR $<$ 40 ml/min/1.73 m^2, as well as lack of mineralocorticoid treatment compared to LVAD patients without diastolic plateau ($p \leq 0.05$). Other baseline characteristics did not differ between the 2 groups (**Table 1**). None of the study cohort patients experienced in-hospital postoperative RVF after LVAD implantation according to the Interagency Registry for Mechanically Assisted Circulatory Support (INTERMACS) definition (8).

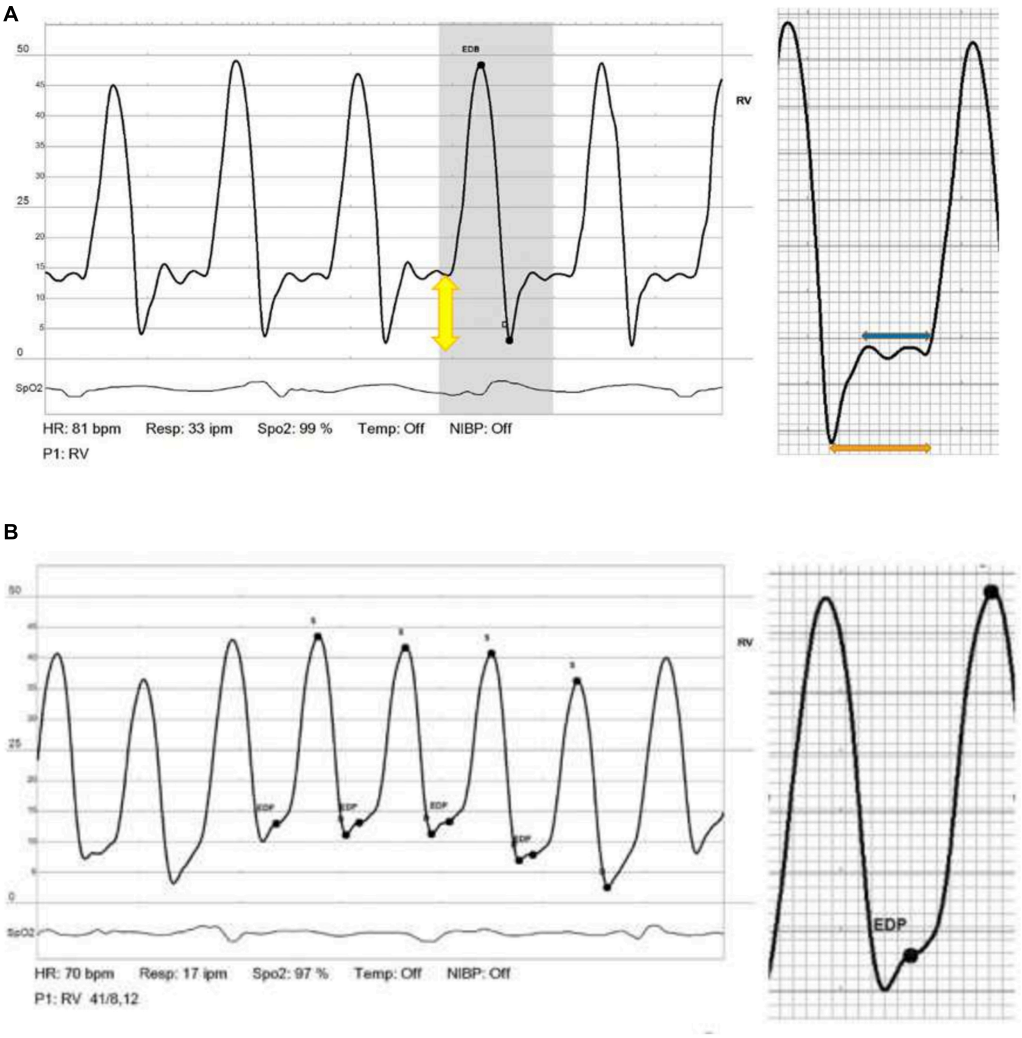

FIGURE 1 | (A) Positive diastolic plateau. **(B)** Normal right heart tracing with no diastolic plateau.

Echocardiography characteristics are shown in **Table 2**. Echo exams were performed at 7 ± 16 days from RHC without significant difference between the groups (21 ± 15 days for patients with negative plateau and 12 ± 19 days for patients with a positive plateau, $p = 0.40$). There were no statistically significant differences between patients with and without diastolic plateau in most echocardiographic parameters including RV functional assessment and pulmonary systolic pressure estimations. The inter-ventricular septum was in neutral position in all patients and no pump parameters adjustment was required during echo exams. Patients with a positive diastolic plateau were more likely to have more significant aortic regurgitation compared to patients without diastolic plateau ($p = 0.02$).

RHC was performed at 303 ± 36 days after LVAD implantation surgery. There was no significant difference at the mean time from LVAD surgery to RHC between the groups (291 ± 33 days for patients with negative plateau vs. 318 ± 38 days for patients with positive plateau, $p = 0.647$). RHC data are shown in **Table 3** with no statistically significant differences in all hemodynamic parameters between study groups. Hence, there was no need for LVAD parameters adjustment during RHC.

Kaplan–Meier survival analysis demonstrated that the cumulative probability of meeting the primary composite endpoint at 12 months was 65 49% among LVAD patients with a positive diastolic plateau vs. 21 42% among those without a diastolic plateau (p log rank < 0.001) (**Figure 3A**). The cumulative probability of meeting the secondary composite endpoint at 12 months for patients with positive plateau was 42 50% compared to 18 39% for those with negative plateau (p log rank = 0.043) (**Figure 3B**).

The distribution of outcome events during follow up was as follow: 7/33 patients without diastolic plateau presented with positive end points: (4 diuretic dose increase, 2 heart transplant, 1 death); 17/26 patients with diastolic plateau presented with positive end points: (7 diuretic dose increase, 7 heart transplant,

TABLE 1 | Baseline patient characteristics.

	All (*N* = 59)	Diastolic Plateau (+) (*N* = 26)	Diastolic Plateau (–) (*N* = 33)	*P* value
Age, y	57	59	56	0.25
Gender (M)	48	21 (81%)	27 (82%)	0.92
INTERMACS (1)	2	1 (4%)	1 (3%)	0.75
INTERMACS (2)	14	7 (27%)	7 (21%)	0.75
INTERMACS (3)	18	7 (27%)	11 (33%)	0.75
INTERMACS (4)	25	11 (42%)	14 (42%)	0.75
Ischemic cause	31	15 (58%)	16 (48%)	0.49
Diabetes	30	15 (58%)	15 (45%)	0.36
Hypertension	18	9 (35%)	9 (27%)	0.55
Body mass index	27	27 ± 4	28 ± 4	0.26
AICD	49	21 (81%)	28 (85%)	0.69
Atrial fibrillation	26	12 (46%)	14 (42%)	0.78
History of VT	26	10 (38%)	16 (48%)	0.45
GFR, ml/min·1.73 m^2	74	76	73	0.61
GFR < 40	3	3 (12%)	0 (0%)	0.05
Hgb, g/dl	12.6	12.3	12.8	0.39
Serum sodium, mEq/L	138.9	138.8	138.9	0.88
Total bilirubin, mg/dl	0.76	0.83	0.71	0.37
AST, U/L	27	25	28	0.54
ALT, U/L	24	20	26	0.1
Beta blockers	55	26 (100%)	29 (88%)	0.07
ACEI/ARBs	26	13 (50%)	13 (39%)	0.42
MRA	44	16 (62%)	28 (85%)	0.04
Furosemide	34	15 (58%)	19 (58%)	0.99

AICD, Automatic Implantable Cardioverter Defibrillator; VT, ventricular tachycardia; GFR, glomerular filtration rate; Hgb, hemoglobin; AST, aspartate aminotransferase; ALT, Alanine transaminase; ACEI, Angiotensin converting enzyme inhibitor; ARB, angiotensin receptor blocker; MRA, Mineralocorticoid receptor antagonist.

3 death). Overall, 11 outcome events due to increase diuretic dose vs. 13 outcome events due to heart transplant or mortality.

Cox regression survival analysis with adjustment for age, INTERMACS score and ischemic cardiomyopathy showed an independent association of the diastolic plateau with primary study outcomes such that patients with positive diastolic plateau were 4 times more likely to reach the study end points (HR = 4.35, 95% CI 1.75–10.83, $p = 0.002$). The significant association was consistent for secondary composite outcomes as well, such that patient with positive diastolic plateau were 3 times more likely to suffer study endpoint (HR = 2.96, 95% CI 1.04–8.41, $p = 0.041$).

In contrast to the diastolic plateau, hemodynamic "dip" pattern was not significantly associated with event outcomes in the study population. On average, patients that did not suffer an event had dips of 7.5 mmHg according to their RHC while patients who did suffer an event had an average dip of 8.1 mmHg ($p = 0.37$).

DISCUSSION

The main finding of the current analysis is that diastolic plateau, a classic hemodynamic sign of impaired right heart filling, is associated with adverse outcomes among LVAD patients. Our data demonstrated a significant association between positive diastolic plateau, measured during an ambulatory RHC of LVAD patients, and increased risk for the combination of mortality, heart transplantation, and the need for diuretic therapy augmentation. Furthermore, adjusted survival analysis showed that LVAD patients with positive diastolic plateau were 4 times more likely to reach the study end points after adjustment for age, INTERMACS score and ischemic HF etiology.

Despite technological applications and evolving surgical experience with LVAD, the incidence of RHF is ranging from 10 to 40% after LVAD therapy, and approximately 6–10% of patients require right ventricular assist device support (1–4, 9, 10). Post-LVAD RHF remains a significant reason for morbidity and mortality and is associated with more than a 20% reduction in perioperative survival (1–4). The mechanisms underlying RVF post-LVAD are often multifactorial. Alterations in RV geometry with septal distortion due to high LVAD speed, exacerbations of pre-existing RV failure due to sudden increases in venous return and RV preload induced by the improvement in cardiac output, additional intra-operative RV injury, and increased RV sensitivity to afterload over time can all lead to RVF (11, 12). However, while RVF was initially felt to be an early post-operative complication, development of late RVF has been more frequently described (13). Late-onset RVF can manifest several months to years after device implantation and has significant adverse prognostic implications for patient outcomes (13). Hence, diagnosing RVF post-LVAD is paramount in patient management, which is established by adjusting LVAD speed, tailoring diuretic therapy, and determining a patient's status for heart transplant candidacy.

Although Transthoracic echocardiography (TTE) is routinely utilized for assessment of RV size and function, post-LVAD evaluation of RV dimensions and function by TTE may be technically difficult. This is not only because of the intrinsic complex RV geometry, but also because post-operative changes and device-related artifacts limit visualization and accuracy of ultrasound-based measurements (5). RHC, however, remains an important tool in post-LVAD follow up, providing direct hemodynamic measurements that can be used to determine cardiac chambers filling pressures, cardiac output, and vascular resistance. Hemodynamic testing has been shown to be effective in guiding patient management and reducing adverse events, even in apparently stable and well-compensated LVAD patients (14, 15).

To date, the role of hemodynamic dip and plateau measurements have not been investigated in LVAD patients. Various studies have implicated changes in the RV during LVAD implantation process with prolonged mechanical circulatory support. These include damage to the RV during surgery, disadvantageous changes in ventricular interdependence mediated by reduced LV contractility, changes in septal architecture, and alterations in RV shape, which may create a restrictive-like RV physiology (11, 16). The primary hemodynamic consequence of restriction is the limitation of the total volume of blood that can be accommodated by the heart during diastole. Accentuated early rapid ventricular filling occurs due to increase preload and improved cardiac

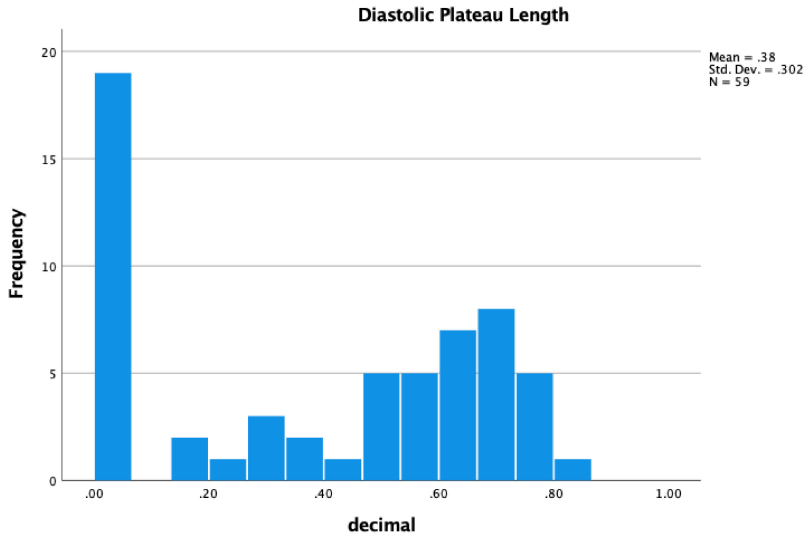

FIGURE 2 | Diastolic plateau distribution.

output with LVAD support, followed by a sudden rapid rise in pressure from the RV. These filling pressures are confined by the interventricular septum and by the geometric changes post-LVAD that limit myocardial stretching during diastole. These changes may account for the "square root" sign on ventricular pressures.

Imamura et al. reported an association between deep y-descent on RHC waveform at 6 months post-LVAD implantation and LVAD related complications (gastrointestinal bleeding, stroke, or pump thrombosis) (17). Our study, however, evaluated both components of the diastolic pressure curves (dip and plateau) and demonstrated a significant association between positive diastolic plateau and, more specifically, RVF related outcomes (mortality and diuretic therapy augmentation). Although our findings did not demonstrate a significant association between hemodynamic

TABLE 2 | Echocardiography characteristics.

	All (*N* = 59)	Diastolic plateau (+) (*N* = 26)	Diastolic plateau (–) (*N* = 33)	*P* value
Baseline Pre-LVAD				
Estimated RVSP (mmHg)	52.2	53.2	51.3	0.59
RV Size	0.44	0.40	0.47	0.61
RV dysfunction	1.19	1.11	1.24	0.63
TR degree	1.25	1.21	1.27	0.79
Post LVAD				
LVESD (mm)	43	43	44	0.82
LVEDD (mm)	53	53	54	0.78
Left atrium size (cm)	4.7	4.7	4.6	0.64
IVS (mm)	10.3	9.6	10.8	0.07
LV mass (gr)	205	191	217	0.27
LV mass index (gr/m^2)	104	98	110	0.25
MR > mild	9	5 (19%)	4 (12%)	0.48
AI > mild	16	11 (42%)	5 (15%)	0.02
RV dysfunction	35	15 (58%)	20 (61%)	0.85
RV dilatation > mild	30	13 (50%)	17 (52%)	0.86
TR > mild	24	10 (38%)	14 (42%)	0.7
Estimated RA pressure (mmHg)	12	11	12	0.45
Estimated RVSP (mmHg)	31	30	33	0.19
Pump Speed (RPM)	5602	5635	5576	0.40

RVSP, right ventricular systolic pressure; RV, right ventricle; TR, tricuspid regurgitation; LVESD, left ventricular end systolic diameter; LVEDD, left ventricular end diastolic diameter; IVS, inter-ventricular septum; LV, left ventricle; MR, mitral regurgitation; AI, aortic insufficiency; RA, right atrium.
RV Size: 0 = normal, 1 = dilated; RV Function: 0 = normal, 1 = mildly reduced, 2 = moderately reduced, 3 = severely reduced; TV Function: 0 = trivial; 1 = mild; 2 = moderate; 3 = severe.

TABLE 3 | Right heart catheterization data.

	All (*N* = 59)	Diastolic Plateau (+) (*N* = 26)	Diastolic Plateau (–) (*N* = 33)	*P* value
RA mean (mmHg)	14	14	13	0.9
RVEDP (mmHg)	7.4	7	7.7	0.66
PA mean (mmHg)	23	23	24	0.55
PA systolic (mmHg)	35	35	35	0.98
PA diastolic (mmHg)	17	16	18	0.1
PCWP (mmHg)	14	13	15	0.18
TPG	10	10	9	0.13
Diastolic TPG	3.3	3.3	3.2	0.93
PVR (WU)	2.3	2.2	2.4	0.68
Cardiac output, l/min	4.2	4.2	4.3	0.74
Cardiac index, L/min/m^2	2.2	2.2	2.1	0.7
Pump Speed (RPM)	5602	5635	5576	0.40
Heart rate (BPM)	78	79	76	0.32

RA, right atrium; RVEDP, right ventricular end diastolic pressure; PA, pulmonary artery; PCWP, pulmonary capillary wedge pressure; TPG, trans-pulmonary gradient; PVR, pulmonary vascular resistance.

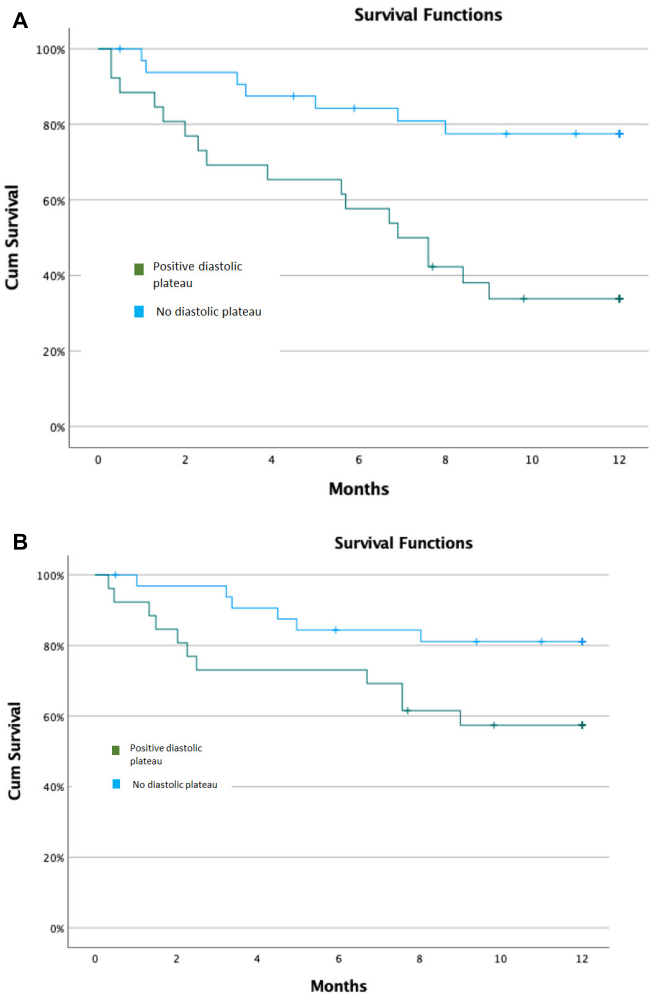

FIGURE 3 | Kaplan–Meier Survival Models. **(A)** Kaplan–Meier Survival Model for primary composite outcomes. **(B)** Kaplan–Meier Survival Model for secondary composite outcomes.

dip and event outcomes, all our study population had a y descent deeper than 3 mmHg (which was the value used for analysis in the study by Imamura et al.). In addition, the prominent y descent on the pressure curves represents early rapid filling of the ventricles in early diastole due to high atrial pressures of increased preload, while positive diastolic plateau pattern is often seen in ventricular restrictive physiology (6, 7). Our results showing similar right atrial pressure in both groups may explain the lack of association between hemodynamic dip and patients' outcome and highlight the role of diastolic plateau as a more specific marker for RV diastolic dysfunction.

Importantly, there were no significant differences in most clinical, laboratory, echocardiographic, or hemodynamic parameters among patients with or without diastolic plateau in our study population, which may suggest this hemodynamic parameter is an earlier sign for RVF and clinical deterioration among LVAD patients. The decreased kidney function among LVAD patients with positive diastolic plateau may suggest a cardio-renal effect as another early sign of RVF post-LVAD (18). Furthermore, the present study suggests that even a hemodynamic snapshot can be used as a clinical marker to identify possible RV dysfunction. This can serve to guide LVAD patient management and can be an improvement to the standard TTE examination.

Study Limitations

This analysis has all the inherent limitations of a small-size, single-center, retrospective study. Due to the single-center nature of this study and the small number of patients included, generalization of the results should be applied with caution before confirmation is available from larger population analyses. Our cohort has a potential patient selection bias, as our study included LVAD patients who were able to perform RHC during follow up post LVAD surgery. All RHC studies did not include volume challenge or any other provocation test. Our study design included a relative short follow up of 12 months post RHC and although the data were collected prospectively, our study is limited by its retrospective design.

Conclusion and Clinical Implications

The current study is the first to report the association between invasively measured diastolic plateau and adverse outcomes among LVAD patients. Our findings identify diastolic plateau as a parameter associate with increased risk for future RV failure before diagnosed by echocardiographic or hemodynamic studies. Due to the challenges in evaluating RV function in LVAD patients, our findings encourage clinicians to carefully evaluate diastolic plateau during RHC in LVAD patients in the real-life scenario, and once identify, to consider closer surveillance with more frequent studies for early diagnosis of clinical RV failure, and to adjust medical therapy as needed. Larger studies are warranted to validate our findings.

DATA AVAILABILITY STATEMENT

The raw data supporting the conclusions of this article will be made available by the authors, without undue reservation.

ETHICS STATEMENT

The studies involving human participants were reviewed and approved by the Institutional Review Board of the Sheba Medical Center. Written informed consent for participation was not required for this study in accordance with the national legislation and the institutional requirements.

AUTHOR CONTRIBUTIONS

AG and EM contributed to conception and design of the study, analysis and interpretation of the data, drafting of the manuscript, revising it critically before submission, and responsible for the overall content as guarantor. AfK contributed to analysis and interpretation of data, critically revising the manuscript, and final approval of the manuscript submitted. JL, PF, IB, DE, AlK, AM, and AS critically revised the manuscript and approved the final version of the manuscript submitted. All authors contributed to the article and approved the submitted version.

REFERENCES

1. Lampert BC, Teuteberg JJ. Right ventricular failure after left ventricular assist devices. *J Heart Lung Transplant.* (2015) 34:1123–30. doi: 10.1016/j.healun.2015.06.015
2. Dang NC, Topkara VK, Mercando M, Kay J, Kruger KH, Aboodi MS, et al. Right heart failure after left ventricular assist device implantation in patients with chronic congestive heart failure. *J Heart Lung Transplant.* (2006) 25:1–6. doi: 10.1016/j.healun.2005.07.008
3. LaRue SJ, Raymer DS, Pierce BR, Nassif ME, Sparrow CT, Vader JM. Clinical outcomes associated with INTERMACS-defined right heart failure after left ventricular assist device implantation. *J Heart Lung Transplant.* (2017) 36:475–7. doi: 10.1016/j.healun.2016.12.017
4. Shad R, Fong R, Quach N, Bowles C, Kasinpila P, Li M, et al. Long-term survival in patients with post-LVAD right ventricular failure: multi-state modelling with competing outcomes of heart transplant. *J Heart Lung Transplant.* (2021) 40:778–85. doi: 10.1016/j.healun.2021.05.002
5. Dandel M, Javier MFDM, Javier Delmo EMD, Hetzer R. Accurate assessment of right heart function before and after long-term left ventricular assist device implantation. *Expert Rev Cardiovasc Ther.* (2020) 18:289–308. doi: 10.1080/14779072.2020.1761790
6. Geske JB, Anavekar NS, Nishimura RA, Oh JK, Gersh BJ. Differentiation of constriction and restriction: complex cardiovascular hemodynamics. *J Am Coll Cardiol.* (2016) 68:2329–47. doi: 10.1016/j.jacc.2016.08.050
7. Talreja DR, Nishimura RA, Oh JK, Holmes DR. Constrictive pericarditis in the modern era novel criteria for diagnosis in the cardiac catheterization laboratory. *J Am Coll Cardiol.* (2008) 51:315–9. doi: 10.1016/j.jacc.2007.09.039
8. Argiriou M, Kolokotron SM, Sakellaridis T, Argiriou O, Charitos C, Zarogoulidis P, et al. Right heart failure post left ventricular assist device implantation. *J Thorac Dis.* (2014) 6:S52–9.
9. Drakos SG, Janicki L, Horne BD, Kfoury AG, Reid BB, Clayson S, et al. Risk factors predictive of right ventricular failure after left ventricular assist device implantation. *Am J Cardiol.* (2010) 105:1030–5. doi: 10.1016/j.amjcard.2009.11.026
10. Kukucka M, Stepanenko A, Potapov E, Krabatsch T, Redlin M, Mladenow A, et al. Right-to-left ventricular end-diastolic diameter ratio and prediction of right ventricular failure with continuous-flow left ventricular assist devices. *J Heart Lung Transplant.* (2011) 30:64–9. doi: 10.1016/j.healun.2010.09.006
11. Houston BA, Shah KB, Mehra MR, Tedford RJ. A new "twist" on right heart failure with left ventricular assist systems. *J Heart Lung Transplant.* (2017) 36:701–7. doi: 10.1016/j.healun.2017.03.014
12. Romano MA, Cowger J, Aaronson KD, Pagani FD. Diagnosis and management of right-sided heart failure in subjects supported with left ventricular assist devices. *Curr Treat Options Cardiovasc Med.* (2010) 12:420–30. doi: 10.1007/s11936-010-0091-8
13. Kapelios CJ, Charitos C, Kaldara E, Malliaras K, Nana E, Pantsios C, et al. Late-onset right ventricular dysfunction after mechanical support by a continuous-flow left ventricular assist device. *J Heart Lung Transplant.* (2015) 34:1604–10. doi: 10.1016/j.healun.2015.05.024
14. Uriel N, Sayer G, Addetia K, Fedson S, Kim GH, Rodgers D, et al. Hemodynamic ramp tests in patients with left ventricular assist devices. *JACC Heart Fail.* (2016) 4:208–17. doi: 10.1016/j.jchf.2015.10.001
15. Imamura T, Jeevanandam V, Kim G, Raikhelkar J, Sarswat N, Kalantari S, et al. Optimal hemodynamics during left ventricular assist device support are associated with reduced readmission rates. *Circ Heart Fail.* (2019) 12:e005094. doi: 10.1161/CIRCHEARTFAILURE.118.005094
16. Mandarino WA, Morita S, Kormos RL, Kawai A, Deneault LG, Gasior TA, et al. Quantification of right ventricular shape changes after left ventricular assist device implantation. *ASAIO J.* (1992) 38:228–31. doi: 10.1097/00002480-199207000-00026
17. Imamura T, Nitta D, Fujino T, Smith B, Kalantari S, Nguyen A, et al. Deep Y-descent in right atrial waveforms following left ventricular assist device implantation. *J Card Fail.* (2020) 26:360–7. doi: 10.1016/j.cardfail.2020.01.004
18. Ross DW, Stevens GR, Wanchoo R, Majure DT, Jauhar S, Fernandez HA, et al. Left ventricular assist devices and the kidney. *Clin J Am Soc Nephrol.* (2018) 13:348–55.

Conflict of Interest: The authors declare that the research was conducted in the absence of any commercial or financial relationships that could be construed as a potential conflict of interest.

frontiers | Frontiers in Cardiovascular Medicine

ORIGINAL RESEARCH
published: 12 April 2022
doi: 10.3389/fcvm.2022.859608

Value of FT3/FT4 Ratio in Prognosis of Patients With Heart Failure: A Propensity-Matched Study

*Chuanhe Wang, Su Han, Ying Li, Fei Tong, Zhichao Li and Zhijun Sun**

Department of Cardiology, Shengjing Hospital of China Medical University, Shenyang, China

Aims: Abnormal thyroid hormone secretions can alter the manifestation and prognosis of cardiovascular disease. To assess the effect of the free triiodothyronine (FT3)/free thyroxine (FT4) ratio on the prognosis of patients with heart failure (HF), we performed a propensity-matched study on patients with well-balanced baseline characteristics.

Methods: Overall, 8,887 patients with HF were divided into two groups according to the FT3/FT4 ratio. Propensity scores were calculated from each patient. A cohort comprising 2,164 pairs with high or low ratios and with 34 well-balanced baseline characteristics was then assembled. The endpoints were Cardiovascular (CV) mortality and all-cause mortality. The correlation between FT3/FT4 ratio and prognosis was assessed using matched Cox regression analyses. The mean follow-up was 3.3 years.

Results: In the full pre-match cohort, 3,710 (41.7%) patients died, with 2,581 (29.0%) cases of CV mortality. In the matched-pair cohort, all-cause mortality occurred in 923 (1,238/10,000 person-years of follow-up) patients with a high ratio and 1,036 (1,484/10,000 person-years) patients with a low ratio, resulting in a matched HR of 0.841 (95% CI: 0.769–0.919; $P < 0.001$). For CV mortality, the result was 638 (856/10,000 person-years) and 714 (1,023/10,000 person-years) patients, respectively, resulting in a matched HR of 0.844 (95% CI: 0.759–0.940; $P < 0.001$). Subgroup analysis revealed that a low FT3/FT4 ratio had a greater predictive value for all-cause and CV mortality in elderly or male patients and in patients with coronary artery disease (CAD), hypertension, diabetes mellitus, HFmrEF, or HFpEF.

Conclusions: A low FT3/FT4 ratio is valuable for predicting CV mortality and all-cause mortality in patients with HF.

Keywords: heart failure, long-term, mortality, prognosis, FT3/FT4 ratio, propensity-matched

OPEN ACCESS

Edited by:
Tong Liu,
Tianjin Medical University, China

Reviewed by:
Qing Zhang,
Sichuan University, China
Kuo Zhang,
Chinese Academy of Medical Sciences and Peking Union Medical College, China
Ling Sun,
Nanjing Medical University, China

****Correspondence:***
Zhijun Sun
sunzj@sj-hospital.org

Specialty section:
This article was submitted to Heart Failure and Transplantation, a section of the journal Frontiers in Cardiovascular Medicine

Received: *21 January 2022*
Accepted: *21 March 2022*
Published: *12 April 2022*

Citation:
Wang C, Han S, Li Y, Tong F, Li Z and Sun Z (2022) Value of FT3/FT4 Ratio in Prognosis of Patients With Heart Failure: A Propensity-Matched Study. Front. Cardiovasc. Med. 9:859608. doi: 10.3389/fcvm.2022.859608

INTRODUCTION

Heart failure (HF) is a serious or advanced stage of any heart disease that has remained a major public health threat despite advances in medical therapy (1, 2). The prevalence of HF in developed countries ranges from 1.5 to 2.0% and increases significantly with age, with a reported prevalence of ≥10% in patients older than 70 years (3). Moreover, patients with HF have consistently been associated with a poor quality of life, reporting an in-hospital and 5-year mortality of up to 4.1% (4) and 50% (1, 2), respectively. Therefore, it is important to establish an individualized approach to improve the symptoms and prognosis of patients with HF. In particular, biomarkers can mirror the

physical functions and affect patient outcomes, in addition to predicting the prognosis (5). Previous studies have even shown that biomarkers and relative mechanisms-guided management would be helpful in the prognostication, diagnosis, and treatment of patients with HF (6, 7).

Free triiodothyronine (FT3) and free thyroxine (FT4) are two major thyroid hormones that affect the physiological and pathological processes of the cardiovascular system (8–10). Studies show that low T3 syndrome has been associated with poor prognosis in patients with HF (11, 12). FT3/FT4 ratio has also been significantly correlated with adverse outcomes in patients with acute coronary syndrome (8, 9). Despite these findings, no recent literature on the effect of FT3/FT4 ratio on the prognosis of patients with HF has been found.

Traditional multivariable risk adjustment models based on regression are limited by model assumptions, which may not always be appropriate and can become a concern for residual bias and procedural transparency (13). However, propensity-matched cohort can be used to assemble two groups of patients with balanced baseline covariates (14, 15). Thus, in our present large-scale retrospective cohort study, we deduced that the FT3/FT4 ratio would be a significant biomarker for the prediction of long-term outcome in a propensity-matched cohort of patients with HF.

MATERIALS AND METHODS

Study Population

Retrospective clinical data were collected from patients with HF hospitalized in the Department of Cardiology, Shengjing Hospital of China Medical University, Shenyang, China between 2013 and 2018. HF was diagnosed based on symptoms and signs, elevated levels of natriuretic peptides and at least one additional criterion of relevant structural heart disease (left atrial enlargement or left ventricular hypertrophy) or diastolic dysfunction (16). In accordance with the cardiac function classification published by the New York Heart Association (NYHA), heart function was divided into four levels (II–IV). Furthermore, HF with reduced ejection fraction (HFrEF) was defined as having a left ventricular ejection fraction (LVEF) of $<$40%, HF with mid-range LVEF (HFmrEF) was defined as having an LVEF of $\geq$40% but $<$50%, and HF with preserved LVEF (HFpEF) was defined as having an LVEF $\geq$50%. Patients displaying evidence of acute myocardial infarction, severe hepatic or renal failure, severe anemia, severe infection, thyroid disease (hyperthyroidism or hypothyroidism), or malignancy were excluded. This study was approved by the Shengjing Hospital of China Medical University Ethics Committee and was carried out in accordance with the principles of the Declaration of Helsinki. The ethics approval number is 2019PS594K.

Patients

Our cohort retrospectively included 8,887 patients with HF hospitalized from January 2013 to December 2018. The investigators extracted their corresponding comprehensive clinical data from the electronic medical records. Obtained variables included patient demographics, past cardiac and non-cardiac history, physical examination results, laboratory test results, and echocardiography. All laboratory tests of the fasting peripheral venous blood samples were also taken on the day of admission or the morning after admission. LVEF was determined by echocardiography using the biplane Simpson method within 3 days of admission. In December 2020, efforts were made to determine the nature of death in each case, patients' survival status were also investigated using the population death information registration management system of the Disease Control and Prevention Center of Liaoning Province, wherein cardiac and non-cardiac death was determined in accordance with the International Classification of Diseases (ICD) code of death diagnosis. When information was not available in the system, data were obtained from the medical records, patients' physicians, or patients' relatives via telephone.

Statistical Analysis

To avoid potential confounders and selection biases, we utilized propensity score matching. For the unmatched and matched populations, differences in the baseline characteristics were tested with chi-square and *t*-tests for categorical and continuous variables, respectively. The optimal cutoff value for the FT3/FT4 ratio was determined with the receiver operating characteristic (ROC) curve. The propensity score (PS) for FT3/FT4 category was separately calculated by a logistic regression model to reduce the selection bias. The clinically relevant variables, which had significant difference between high FT3/FT4 ratio and low FT3/FT4 ratio groups at baseline were included as covariates (**Table 1**). High FT3/FT4 ratio and low FT3/FT4 ratio were then matched 1:1 using the nearest neighbor method with a caliper of $<$0.01 without any replacement. The ability of the matching to balance baseline characteristics in high vs. low ratios was assessed using absolute standard differences and a quartile, reporting a non-significant value of $<$10%. The absolute standardized differences before and after matching were shown as Love plots. Primary outcomes of this study included 8-year all-cause mortality and 8-year CV mortality. Cox proportional hazards models were also used in overall cohort adjustment and matched population to estimate the association between the FT3/FT4 ratio and outcomes. Results were presented with their hazard ratio (HR) and corresponding 95% confidence interval (CI), and survival estimates were visualized using the Kaplan–Meier method. Interaction analyses were further conducted with consideration to the age, gender, CAD, hypertension, diabetes mellitus, stroke, atrial fibrillation, previous myocardial infarction, and LVEF in the matching population. All statistical analyses were performed using the R software version 3.6.1, and a two-tailed *P*-value of $<$0.05 was considered to be statistically significant.

RESULTS

Baseline Characteristics

A total of 8,887 patients met the inclusion criteria. Patients in the cohort had a mean age of 69 ($\pm$ 13) years, and 53.8% were male. The median follow-up time was 3.3 years (2–8 years).The optimal cutoff value for FT3/FT4 is 0.233, which was determined with

TABLE 1 | Baseline characteristics of patients in the high and low FT3/FT4 ratio groups before and after propensity matching.

	Unmatched			Propensity-Matched		
	High FT3/FT4	**Low FT3/FT4**	***P*-value**	**High FT3/FT4**	**Low FT3/FT4**	***P*-value**
N	5,245	3,642		2,164	2,164	
Age (years)	67.38 ± 13.27	71.05 ± 13.33	<0.001	70.40 ± 12.73	70.22 ± 13.41	0.637
Male sex, *n* (%)	2,979 (56.8%)	1,801 (49.5%)	<0.001	1,107 (51.2%)	1,110 (51.3%)	0.927
NYHA Fc			<0.001			0.426
NYHA class II, *n* (%)	1,583 (30.2%)	405 (11.1%)		339 (15.7%)	350 (16.2%)	
NYHA class III, *n* (%)	2,300 (43.9%)	1,477 (40.6%)		953 (44.0%)	984 (45.5%)	
NYHA class IV, *n* (%)	1,362 (26.0%)	1,760 (48.3%)		872 (40.3%)	830 (38.4%)	
CAD, *n* (%)	3,498 (66.7%)	2,413 (66.3%)	0.668	1,474 (68.1%)	1,457 (67.3%)	0.580
Hypertension, *n* (%)	3,317 (63.2%)	2,180 (59.9%)	0.001	1,373 (63.4%)	1,356 (62.7%)	0.592
Diabetes mellitus, *n* (%)	1,664 (31.7%)	1,301 (35.7%)	<0.001	770 (35.6%)	757 (35.0%)	0.679
Stroke, *n* (%)	914 (17.4%)	741 (20.3%)	0.001	419 (19.4%)	424 (19.6%)	0.848
Atrial fibrillation, *n* (%)	1,818 (34.7%)	1,092 (30.0%)	<0.001	678 (31.3%)	690 (31.9%)	0.695
Previous MI, *n* (%)	967 (18.4%)	704 (19.3%)	0.289	435 (20.1%)	416 (19.2%)	0.467
Current smoker, *n* (%)	1,529 (29.2%)	936 (25.7%)	<0.001	584 (27.0%)	576 (26.6%)	0.784
Alcohol-related, *n* (%)	1,014 (19.3%)	529 (14.5%)	<0.001	334 (15.4%)	355 (16.4%)	0.383
SBP (mmHg)	137.12 ± 23.64	133.37 ± 25.46	<0.001	135.74 ± 22.85	135.62 ± 23.38	0.869
DBP (mmHg)	81.97 ± 14.50	78.95 ± 14.81	<0.001	80.44 ± 13.59	80.26 ± 13.95	0.682
Heart rate (bpm)	84.98 ± 22.21	89.76 ± 25.01	<0.001	88.05 ± 21.38	87.64 ± 23.05	0.548
NT-proBNP (ng/L)	2008.00 (785.30–4300.75)	5317.00 (2374.32–10724.50)	<0.001	3414.00 (1559.00–6917.00)	3569.50 (1697.00–7296.00)	0.113
Troponin I (ug/L)	0.02 (0.01–0.06)	0.05 (0.02–0.23)	<0.001	0.03 (0.01–0.11)	0.04 (0.01–0.14)	0.057
Hemoglobin (g/L)	131.93 ± 20.72	122.04 ± 24.37	<0.001	125.96 ± 21.74	126.03 ± 22.04	0.898
BUN (mmol/L)	7.57 ± 4.02	10.30 ± 6.25	<0.001	8.67 ± 4.97	8.79 ± 4.71	0.413
Creatinine (μmol/L)	78.60 (65.00–98.00)	91.60 (72.00–121.28)	<0.001	83.00 (67.20–102.90)	84.60 (70.00–110.20)	0.064
Uric acid (μmol/L)	433.10 (336.00–468.00)	441.36 (359.98–557.50)	<0.001	441.36 (356.00–501.40)	441.36 (346.00–506.43)	0.398
Prealbumin (g/L)	0.21 ± 0.06	0.17 ± 0.06	<0.001	0.19 ± 0.05	0.19 ± 0.06	0.484
Platelets (10^9L)	192.19 ± 62.94	193.70 ± 77.99	0.346	191.95 ± 70.29	189.92 ± 66.72	0.328
Albumin (g/L)	38.43 ± 4.09	35.55 ± 4.35	<0.001	36.87 ± 3.88	36.85 ± 3.92	0.842
TC (mmol/L)	4.23 ± 1.09	3.91 ± 1.14	<0.001	4.06 ± 0.70	4.06 ± 0.80	0.948
Triglycerides (mmol/L)	1.45 ± 1.04	1.16 ± 0.86	<0.001	1.26 ± 0.74	1.24 ± 0.95	0.544
HDL (mmol/L)	1.01 ± 0.30	0.93 ± 0.32	<0.001	0.96 ± 0.29	0.97 ± 0.31	0.267
LDL-C (mmol/L)	2.66 ± 0.94	2.47 ± 0.96	<0.001	2.56 ± 0.91	2.55 ± 0.96	0.828
HbA1c%	6.45 ± 1.30	6.59 ± 1.47	<0.001	6.58 ± 1.30	6.55 ± 1.37	0.441
Potassium (mmol/L)	4.06 ± 0.49	4.11 ± 0.61	<0.001	4.09 ± 0.54	4.08 ± 0.56	0.472
Sodium (mmol/L)	139.60 ± 3.20	137.89 ± 4.42	<0.001	138.92 ± 3.64	138.89 ± 3.64	0.833
Chloride ion (mmol/L)	105.73 ± 3.87	103.58 ± 5.10	<0.001	104.78 ± 4.30	104.83 ± 4.25	0.753
LVEDV (ml)	157.69 ± 62.40	159.66 ± 61.03	0.138	158.56 ± 64.27	157.38 ± 60.91	0.524
LVESV (ml)	82.71 ± 50.55	89.18 ± 49.56	<0.001	86.52 ± 50.06	85.40 ± 48.89	0.455
LVEF (%)	50.37 ± 12.12	46.70 ± 12.13	<0.001	47.99 ± 12.05	48.29 ± 11.86	0.403

NYHA, New York Heart Association (NYHA); CAD, Coronary artery disease; Previous MI, Previous myocardial infarction; SBP, Systolic blood pressure; DBP, Diastolic blood pressure; NT-proBNP, N-terminal pro-B-type natriuretic peptide; BUN: Blood urea nitrogen; TC, Total cholesterol; HDL, High density lipoprotein; LDL-C, Low density lipoprotein cholesterol; LVEDV, Left ventricular end-diastolic volume; LVESV, Left ventricular end-systolic volume; LVEF, Left ventricular ejection fraction.

the receiver operating characteristic (ROC) curve, with a area under the ROC curve (AUC) of 0.668. According to this cutoff value, FT3/FT4 is divided into two groups: the high FT3/FT4 (0.233∼0.563) and low FT3/FT4 ratio group (0.085∼0.233). The propensity score for the FT3/FT4 category was separately calculated using a logistic regression model, and the clinically relevant variables listed in **Table 1** were used as covariates. Prior to matching, patients in the high FT3/FT4 ratio group were found to be younger, more likely to be male, had a more severe NYHA heart function, and had lower NT-proBNP levels than those in the low FT3/FT4 ratio group (**Table 1**, **Figure 1**). Other significant imbalances in baseline characteristics before matching and the balances after matching are displayed in **Table 1**, **Figure 1**. After matching, absolute standardized differences for all measured covariates were <10% (usually 5%), indicating significant covariate balance between the two groups (**Figure 1**).

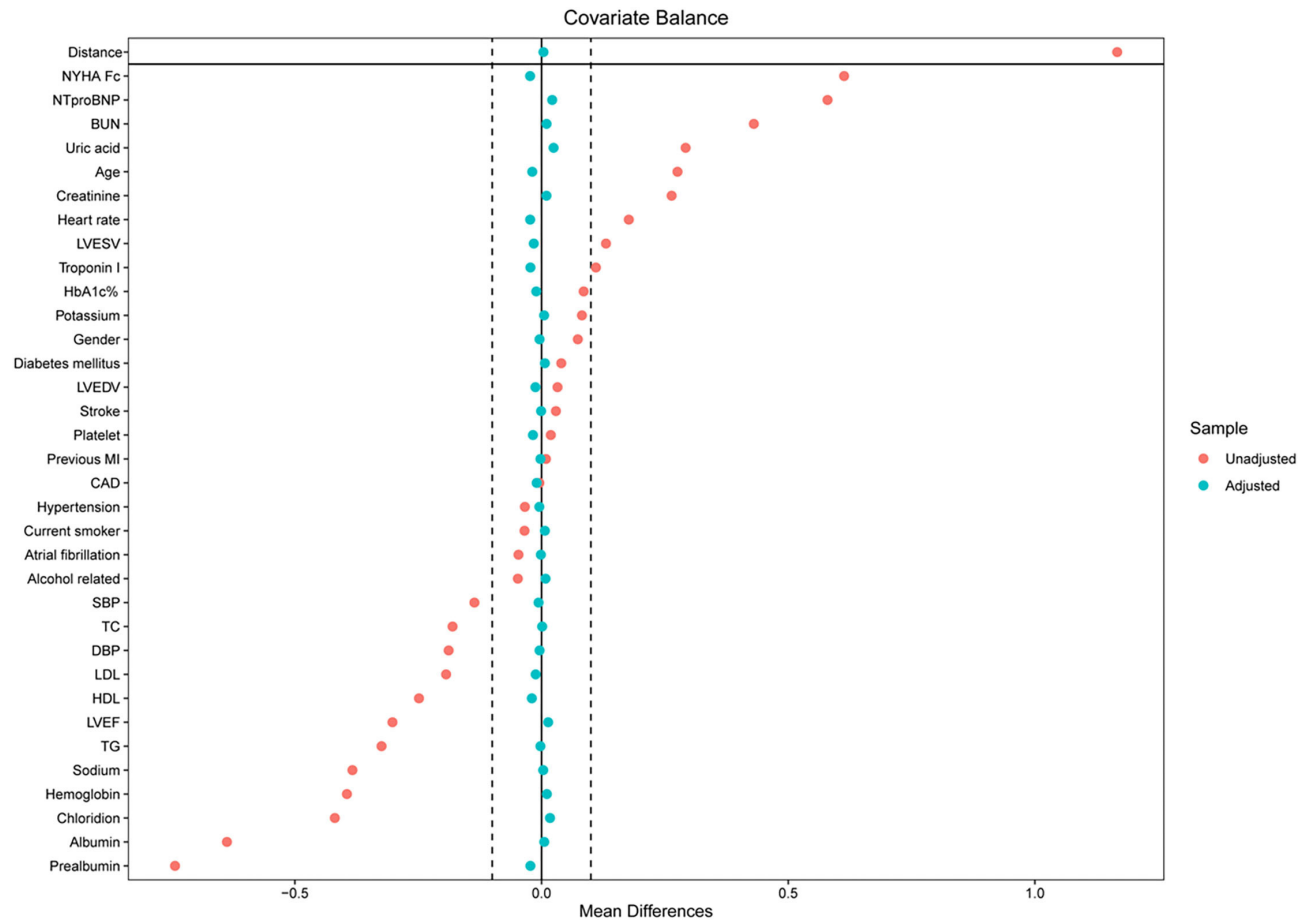

FIGURE 1 | Love plots for absolute standardized differences for baseline covariates of patients between high and low FT3/FT4 ratio group, before and after propensity score matching.

FT3/FT4 Ratio and Mortality

Overall, in the full pre-match cohort of 8,887 patients, 3,710 (41.7%) patients died, with 2,581 (29.0%) cases of CV mortality, during a median follow-up of 3.2 years. All-cause mortality occurred in 1,655 (rate, 850/10,000 person-years of follow-up) patients with a high FT3/FT4 ratio and 2,055 (rate, 1,981/10,000 person-years) patients with a low ratio, resulting in an unadjusted HR of 0.442 (95% CI: 0.414–0.471; $P < 0.001$) and an adjusted HR of 0.810 (95% CI: 0.752–0.872; $P < 0.001$) (**Table 2**). Meanwhile, CV mortality occurred in 1,117 (rate, 573/10,000 person-years) patients with a high FT3/FT4 ratio and 1,464 (rate, 1,412/10,000 person-years) patients with a low ratio, resulting in an unadjusted HR of 0.422 (95% CI:0.391–0.457; $P < 0.001$) and an adjusted HR of 0.795 (95% CI: 0.727–0.870; $P < 0.001$) (**Table 2**).

In the matched-pair cohort of 2,164 patients, all-cause mortality occurred in 923 (rate, 1,238/10,000 person-years) patients with a high FT3/FT4 ratio and 1,036 (rate, 1,484/10,000 person-years) patients with a low ratio, resulting in a matched HR of 0.841 (95% CI: 0.769–0.919; $P < 0.001$) (**Figure 2A**, **Table 2**). For CV mortality, this was observed in 638 (rate, 856/10,000 person-years) patients with a high FT3/FT4 ratio and 714 (rate, 1,023/10,000 person-years) patients with a low ratio, resulting in a matched HR of 0.844 (95% CI: 0.759–0.940; $P < 0.001$) (**Figure 2B**, **Table 2**).

Findings from our sensitivity analysis indicate that the covariate (FT3/FT4), which is a predictor of mortality in patients with HF, may potentially explain the association between HF and mortality.

Correlations between the FT3/FT4 ratio and all-cause/CV mortality among various subgroups are displayed in **Figure 3**. Generally, a low FT3/FT4 ratio had a greater predictive value for all-cause mortality and CV mortality in elderly or male patients and in patients with CAD, hypertension, diabetes mellitus, HFmrEF, or HFpEF.

DISCUSSION

In our retrospective cohort of 8,887 patients, 3,710 (41.7%) patients died, with 2,581 (29.0%) cases of CV mortality, during a median follow-up of 3.2 years. In the matched-pair cohort of 2,164 pairs of patients with high and low FT3/FT4 ratios and with 34 balanced baseline characteristics, we found that

TABLE 2 | Hazard ratio for FT3/FT4 ratio and all-cause/CV mortality.

	Rate per 10,000 person-years (events/total follow-up years)		Absolute rate difference (per 10,000 person-years)	Hazard ratio (95% CI)	*P*-value
	High FT3/FT4	Low FT3/FT4			
Before matching	*n* = 5,245	*n* = 3,642			
All-cause mortality					
Unadjusted	850 (1,655/19,481)	1,981 (2,055/10,371)	−1,131	0.442 (0.414–0.471)	<0.001
Adjusted				0.810 (0.752–0.872)	<0.001
CV mortality					
Unadjusted	573 (1,117/19,481)	1,412 (1,464/10,371)	−839	0.422 (0.391–0.457)	<0.001
Adjusted				0.795 (0.727–0.870)	<0.001
After matching	*n* = 2,164	*n* = 2,164			
All-cause mortality	1,238 (923/7,453)	1,484 (1,036/6,980)	−246	0.841 (0.769–0.919)	<0.001
CV mortality	856 (638/7,453)	1,023 (714/6,980)	−167	0.844 (0.759–0.940)	0.002

CV, cardiovascular disease.

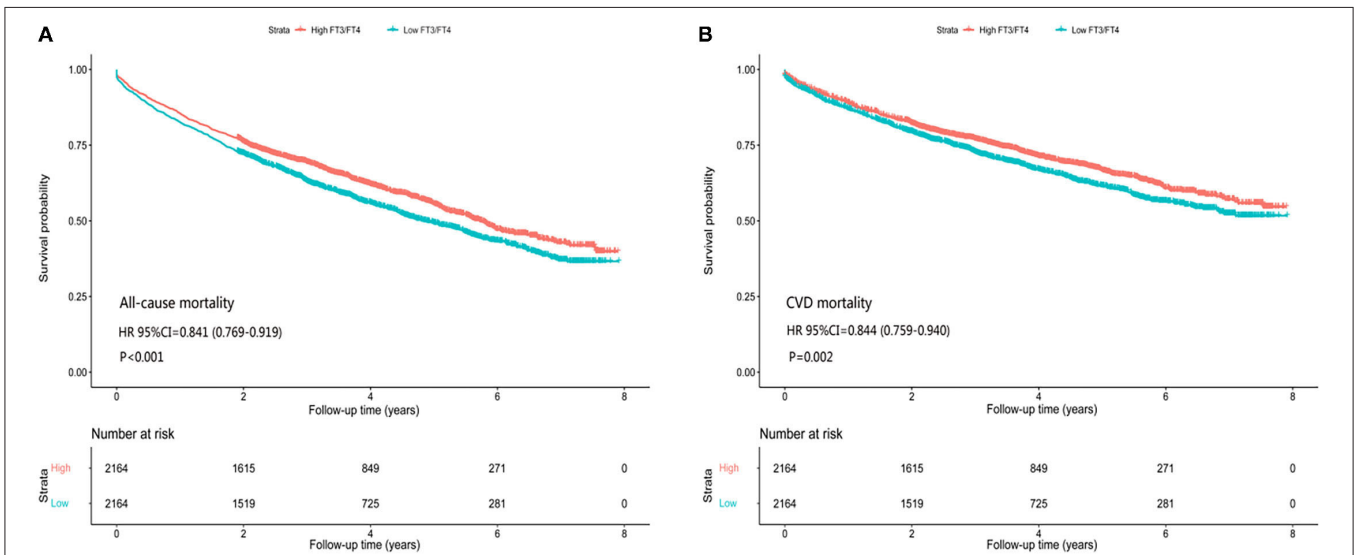

FIGURE 2 | Association of high and low FT3/FT4 ratio with all-cause/CV mortality in subgroups of propensity score-matched patients, **(A)** all-cause mortality, **(B)** CV mortality.

all-cause and CV mortality in patients with HF could be predicted independently using a low FT3/FT4 ratio. Specifically, the hazard ratio of long-term all-cause mortality for patients with a high FT3/FT4 ratio was 0.841 times less than that in patients with a low FT3/FT4 ratio. This was similarly seen in CV mortality, with a value of 0.844.

Baseline analysis showed that a lower FT3/FT4 ratio was associated with worse heart function and clinical characteristics, including advanced age; higher rates of diabetes and stroke; increased troponin I and NT-probNP; and decreased hemoglobin, albumin, and sodium; all of which may be related to poor prognosis in HF. Numerous studies have also shown that reduced FT3 was associated with increased cardiovascular morbidity and mortality (including HF) (10, 12), and high FT4 level within normal thyroid function has been correlated with HF and sudden cardiac death (17, 18). In particular, Kannan et al. demonstrated that higher FT4 and lower total triiodothyronine were associated with an increased risk of the composite end point for left ventricular assist device implantation, heart transplantation, or all-cause mortality (19). Furthermore, previous studies have indicated that a decreased FT3/FT4 ratio is associated with an increased risk of long-term all-cause mortality, cardiovascular mortality, and major adverse cardiovascular events in patients with CAD (9, 20).

The cardiovascular system is an important target organ of thyroid hormones, as their main effect on this system increases the heart rate, enhances myocardial contractility, reduces circulation resistance, and relieves cardiac afterload (21, 22). Thyroid hormone abnormalities, such as thyroid function hyperfunction, hypothyroidism, and low T3 syndrome,

A All-cause mortality

	High FT3/FT4(n=2164) Number of events/ number at risk (%)	Low FT3/FT4(n=2164) Number of events/ number at risk (%)	Hazard Ratio(95% CI)	P-value Effect	P-value Interaction
Age (years)					
<60 (n=778)	120/380 (31.6%)	131/398 (32.9%)	0.927 (0.723–1.187)	0.547	0.925
60–75 (n=1700)	314/860 (36.5%)	372/840 (44.3%)	0.773 (0.666–0.899)	0.001	
>75 (n=1850)	489/924 (52.9%)	533/926 (57.6%)	0.860 (0.760–0.972)	0.016	
Gender					
Male(n=2217)	465/1107 (42.0%)	541/1110 (48.7%)	0.798 (0.705–0.903)	<0.001	0.234
Female (n=2111)	458/1057 (43.3%)	495/1054 (47.0%)	0.888 (0.782–1.008)	0.066	
Coronary artery disease					
Yes (n=2931)	651/1474 (44.2%)	725/1457 (49.8%)	0.835 (0.751–0.928)	0.001	0.859
No (n=1397)	272/690 (39.4%)	311/707 (44.0%)	0.850 (0.722–1.000)	0.051	
Hypertension					
Yes (n=2729)	576/1373 (42.0%)	659/1356 (48.6%)	0.795 (0.711–0.889)	<0.001	0.124
No (n=1599)	347/791 (43.9%)	377/808 (46.7%)	0.916 (0.792–1.060)	0.240	
Diabetes mellitus					
Yes (n=1527)	339/770 (44.0%)	396/757 (52.3%)	0.771 (0.667–0.892)	<0.001	0.144
No (n=2801)	584/1394 (41.9%)	640/1407 (45.5%)	0.882 (0.788–0.987)	0.028	
Stroke					
Yes (n=843)	195/419 (46.5%)	242/424 (57.1%)	0.701 (0.580–0.847)	<0.001	0.030
No (n=3485)	728/1745 (41.7%)	794/1740 (45.6%)	0.882 (0.797–0.975)	0.014	
Atrial fibrillation					
Yes (n=1368)	266/678 (39.2%)	273/690 (39.6%)	0.950 (0.802–1.125)	0.560	0.081
No (n=2960)	657/1486 (44.2%)	763/1474 (51.8%)	0.801 (0.721–0.889)	<0.001	
Previous myocardial infarction					
Yes (n=851)	203/435 (46.7%)	248/416 (59.6%)	0.708 (0.588–0.853)	<0.001	0.048
No (n=3477)	720/1729 (41.6%)	788/1748 (45.1%)	0.879 (0.794–0.972)	0.012	
Left ventricular ejection fraction					
HFrEF (n=1080)	276/561 (49.2%)	282/519 (54.3%)	0.878 (0.744–1.037)	0.125	0.966
HFmrEF (n=1216)	246/597 (41.2%)	312/619 (50.4%)	0.759 (0.642–0.898)	0.001	
HFpEF (n=2032)	401/1006 (39.9%)	442/1026 (43.1%)	0.866 (0.756–0.991)	0.036	

B CVD mortality

	High FT3/FT4(n=2164) Number of events/ number at risk (%)	Low FT3/FT4(n=2164) Number of events/ number at risk (%)	Hazard Ratio(95% CI)	P-value Effect	P-value Interaction
Age (years)					
<60 (n=778)	97/380 (25.5%)	103/398 (25.9%)	0.951 (0.720–1.255)	0.721	0.538
60–75 (n=1700)	228/860 (26.5%)	256/840 (30.5%)	0.818 (0.685–0.978)	0.028	
>75 (n=1850)	313/924 (33.9%)	355/926 (38.3%)	0.828 (0.712–0.965)	0.015	
Gender					
Male(n=2217)	322/1107 (29.1%)	377/1110 (34.0%)	0.795 (0.685–0.922)	0.002	0.244
Female (n=2111)	316/1057 (29.9%)	337/1054 (32.0%)	0.900 (0.772–1.049)	0.178	
Coronary artery disease					
Yes (n=2931)	443/1474 (30.1%)	508/1457 (34.9%)	0.811 (0.714–0.921)	0.001	0.281
No (n=1397)	195/690 (28.3%)	206/707 (29.1%)	0.922 (0.758–1.122)	0.416	
Hypertension					
Yes (n=2729)	384/1373 (28.0%)	439/1356 (32.4%)	0.801 (0.699–0.919)	0.002	0.869
No (n=1599)	254/791 (32.1%)	275/808 (34.0%)	0.918 (0.774–1.089)	0.329	
Diabetes mellitus					
Yes (n=1527)	228/770 (29.6%)	277/757 (36.6%)	0.745 (0.625–0.887)	0.001	0.075
No (n=2801)	410/1394 (29.4%)	437/1407 (31.1%)	0.907 (0.792–1.037)	0.154	
Stroke					
Yes (n=843)	128/419 (30.5%)	148/424 (34.9%)	0.759 (0.599–0.962)	0.023	0.296
No (n=3485)	510/1745 (29.2%)	566/1740 (32.5%)	0.867 (0.769–0.977)	0.019	
Atrial fibrillation					
Yes (n=1368)	171/678 (25.2%)	173/690 (25.1%)	0.964 (0.780–1.191)	0.734	0.134
No (n=2960)	467/1486 (31.4%)	541/1474 (36.7%)	0.803 (0.710–0.909)	0.001	
Previous myocardial infarction					
Yes (n=851)	152/435 (34.9%)	179/416 (43.0%)	0.736 (0.593–0.913)	0.005	0.185
No (n=3477)	486/1729 (28.1%)	535/1748 (30.6%)	0.875 (0.774–0.989)	0.033	
Left ventricular ejection fraction					
HFrEF (n=1080)	216/561 (38.5%)	227/519 (43.7%)	0.854 (0.709–1.029)	0.097	0.884
HFmrEF (n=1216)	171/597 (28.6%)	209/619 (33.8%)	0.788 (0.644–0.965)	0.021	
HFpEF (n=2032)	251/1006 (25.0%)	278/1026 (27.1%)	0.865 (0.729–1.026)	0.095	

FIGURE 3 | Association of high and low FT3/FT4 ratio with all-cause/CV mortality in subgroups of propensity score-matched patients, **(A)** all-cause mortality, **(B)** CV mortality.

can influence the clinical manifestations and outcomes of cardiovascular disease (11). Subclinical hyperthyroidism, subclinical hypothyroidism, and low T3 syndrome are associated with high risk of atrial fibrillation and increased mortality of patients with cardiac disease (23, 24). Even a minor alteration in thyroid hormone concentration will affect the pathological and physiological process of the cardiovascular system (25, 26). Among these thyroid hormones, FT3 and FT4 are usually more sensitive and clinically relevant than T3 and T4, given that former are the physiologically active forms of the latter (27).

Previous studies have demonstrated that the FT3/FT4 ratio could reflect deiodinase activity (28), so the decline of this ratio may reflect the reduced transformation from T4 to T3 in the peripheral blood (27, 29). Therefore, the possible mechanisms of the influence of FT3/FT4 ratio on HF prognosis can be as follows. First, insufficient FT3 transformation leads to more obvious oxidative stress damage of the endoplasmic reticulum and impaired utilization of ATP by cardiomyocytes, resulting in an impaired systolic function and development of HF (30). Second, there are specific T3 receptors in the myocardium, and the decrease of FT3 may lower myocardial contractility and increase susceptibility to arrhythmia, possibly resulting in death in patients with HF (12). Third, low levels of FT3 are related to the increase of right atrial pressure, pulmonary artery pressure, and pulmonary capillary wedge pressure, as well as the decrease of ejection fraction and cardiac index, which results in myocardial fibrosis, ventricular remodeling, and myocardial perfusion and metabolism abnormalities (30). Furthermore, the FT3/FT4 ratio may be an important predictor of metabolic disease (31) and acute myocardial infarction (20).

Given the effect of thyroid hormones on the prognosis of heart failure, some scholars believe that replacement therapy, regulation of deiodinase activity, and heart-specific thyroid receptor agonists are potential treatments for HF (32). However, the potential benefits of thyroid hormone supplementation for these patients should be weighed against the risks of overtreatment. Moreover, the tolerability and safety of the aforementioned treatment regimens need further studies to confirm their viability.

Despite the large sample of the present study, a few limitations were noted. First, although we eliminated the influence of confounding factors and selection bias using propensity-matched scoring, we consequently missed a large portion of real-world data. Second, FT3 and FT4 were measured at baseline without dynamic monitoring, which may have limited the accuracy of the results. Lastly, we failed to mention and analyze the drug use of the included patients. This is important since iodized contrast agents, including amiodarone and glucocorticoids, might have affected thyroid function.

In conclusion, this propensity-matched study revealed that a low FT3/FT4 ratio had a greater predictive value for all-cause mortality and CV mortality, especially in elderly and male patients and in patients with CAD, hypertension, diabetes mellitus, HFmrEF, or HFpEF.

DATA AVAILABILITY STATEMENT

The original contributions presented in the study are included in the article/supplementary material, further inquiries can be directed to the corresponding author/s.

ETHICS STATEMENT

The studies involving human participants were reviewed and approved by Shengjing Hospital of China Medical University Ethics Committee and was carried out in accordance with the principles of the Declaration of Helsinki. The ethics approval number is 2019PS594K. Written informed consent for participation was not required for this study in accordance with the national legislation and the institutional requirements.

AUTHOR CONTRIBUTIONS

CW and ZS conceived and designed the study and wrote the paper. CW, SH, and YL extracted and sorted clinical data. ZL and FT analyzed the data. All authors contributed to the article and approved the submitted version.

FUNDING

The present study was financially supported by a grant from the Science and Technology Program of Liaoning Province (No. 2018225003).

ACKNOWLEDGMENTS

The statistical analysis contributions of Hao Sun at the 1st Hospital of China Medical University is gratefully acknowledged.

REFERENCES

1. Yancy CW, Jessup M, Bozkurt B, Jessup M, Bozkurt B, Butler J, et al. ACC/AHA/HFSA focused update of the 2013 ACCF/AHA guideline for the management of heart failure: a report of the American College of Cardiology/American Heart Association task force on clinical practice guidelines and the heart failure society of America. *J Am Coll Cardiol.* (2017) 70:776–803. doi: 10.1161/CIR.0000000000000509
2. Taylor CJ, Ordóñez-Mena JM, Roalfe AK, Lay-Flurrie S, Jones NR, Marshall, et al. Trends in survival after a diagnosis of heart failure in the United Kingdom 2000-2017: population based cohort study. *BMJ.* (2019) 364:l223. doi: 10.1136/bmj.l223
3. Mosterd A, Hoes AW. Clinical epidemiology of heart failure. *Heart.* (2007) 93:1137–46. doi: 10.1136/hrt.2003.025270
4. Zhang Y, Zhang J, Butler J, Yang XM, Xie PY, Guo DS, et al. Contemporary epidemiology, management, and outcomes of patients hospitalized for heart failure in China: results from the China heart failure (China-HF) registry. *J Card Fail.* (2017) 23:868–75. doi: 10.1016/j.cardfail.2017.09.014
5. Wang CH, Han S, Tong F, Li Y, Li ZC, Sun ZJ. Predictive value of the serum cystatin C/Prealbumin ratio in combination with NT-proBNP levels for long-term prognosis in chronic heart failure patients: a retrospective cohort study. *Front Cardiovasc Med.* (2021) 8:684919. doi: 10.3389/fcvm.2021.684919

6. Sarhene M, Wang Y, Wei J, Huang Y, Li M, Li L, et al. Biomarkers in heart failure: the past, current and future. *Heart Fail Rev.* (2019) 24:867–903. doi: 10.1007/s10741-019-09807-z
7. Dungen HD, Petroni R, Correale M, Coiro S, Monitillo F, Triggiani M, et al. A new educational program in heart failure drug development: the Brescia international master program. *J Cardiovasc Med.* (2018) 19:411–21. doi: 10.2459/JCM.0000000000000669
8. Smith SJ, Bos G, Gerbrandy J, Docter R, Visser TJ, Hennemann G, et al. Lowering of serum 3,3′,5-triiodothyronine thyroxine ratio in patients with myocardial infarction; relationship with extent of tissue injury. *Eur J Clin Investig.* (1978) 8:99–102. doi: 10.1111/j.1365-2362.1978.tb00819.x
9. Yuan DH, Zhang C, Jia SD, Liu Y, Jiang, Xu LJ, et al. Predictive value of free triiodothyronine (FT3) to free thyroxine (FT4) ratio in long-term outcomes of euthyroid patients with three-vessel coronary artery disease. *Nutr Metab Cardiovasc Dis.* (2021) 31:579–86. doi: 10.1016/j.numecd.2020.10.011
10. Razvi S, Jabbar A, Pingitore A, Danzi S, Biondi B, Klein I, et al. Thyroid hormones and cardiovascular function and diseases. *J Am Coll Cardiol.* (2018) 71:1781–96. doi: 10.1016/j.jacc.2018.02.045
11. Sato Y, Yoshihisa A, Kimishima Y, Kiko T, Kanno Y, Yokokawa T, et al. Low T3 syndrome is associated with high mortality in hospitalized patients with Heart failure. *J Card Fail.* (2019) 25:195–203. doi: 10.1016/j.cardfail.2019.01.007
12. Okayama D, Minami Y, Kataoka S, Shiga T, Hagiwara N. Thyroid function on admission and outcome in patients hospitalized for acute decompensated heart failure. *J Cardiol.* (2015) 66:205–11. doi: 10.1016/j.jjcc.2015.04.006
13. Fitzmaurice G. Confounding: regression adjustment. *Nutrition.* (2006) 22:581–3. doi: 10.1016/j.nut.2006.02.004
14. Ahmed A, Rich MW, Sanders PW, Perry GJ, Bakris GL, Zile MR, et al. Chronic kidney disease associated mortality in diastolic versus systolic heart failure: a propensity matched study. *Am J Cardiol.* (2007) 99:393–8. doi: 10.1016/j.amjcard.2006.08.042
15. Ahmed A, Zannad F, Love TE, Tallaj J, Gheorghiade M, Ekundayo OJ, et al. A propensity-matched study of the association of low serum potassium levels and mortality in chronic heart failure. *Eur Heart J.* (2007) 28:1334–43. doi: 10.1093/eurheartj/ehm091
16. Ponikowski P, Voors AA, Anker SD, Bueno H, Cleland JG, Coats AJ, et al. 2016 ESC guidelines for the diagnosis treatment of acute chronic heart failure: the Task Force for the diagnosis treatment of acute chronic heart failure of the European Society of Cardiology (ESC). developed with the special contribution of the Heart Failure Association (HFA) of the ESC. *Eur J Heart Fail.* (2016) 18:891–975. doi: 10.1002/ejhf.592
17. Cappola AR, Arnold AM, Wulczyn K, Carlson M, Robbins J, Psaty BM. Thyroid function in the euthyroid range and adverse outcomes in older adults. *J Clin Endocrinol Metab.* (2015) 100:1088–96. doi: 10.1210/jc.2014-3586
18. Chaker L, van den Berg ME, Niemeijer MN, Franco OH, Dehghan A, Hofman A, et al. Thyroid function and sudden cardiac death: a prospective population-based cohort study. *Circulation.* (2016) 134:713–22. doi: 10.1161/CIRCULATIONAHA.115.020789
19. Kannan L, Shaw PA, Morley MP, Brandimarto J, Fang JC, Sweitzer NK, et al. Thyroid dysfunction in heart failure and cardiovascular outcomes. *Circ Heart Fail.* (2018) 11:e005266. doi: 10.1161/CIRCHEARTFAILURE.118.005266
20. Yu TT, Tian CY, Song J, He DX, Wu JK, Wen ZY, et al. Value of the fT3/fT4 ratio and its combination with the GRACE risk score in predicting the prognosis in euthyroid patients with acute myocardial infarction undergoing percutaneous coronary intervention: a prospective cohort study. *BMC Cardiovasc Disord.* (2018) 18:181. doi: 10.1186/s12872-018-0916-z
21. Grais IM, Sowers JR. Thyroid and the heart. *Am J Med.* (2014) 127:691–8. doi: 10.1016/j.amjmed.2014.03.009
22. Bruere H, Fauchier L, Bernard Brunet A, Pierre B, Simeon E, Babuty D, et al. History of thyroid disorders in relation to clinical outcomes in atrial fibrillation: a cohort study. *Am J Med.* (2015) 128:30–7. doi: 10.1016/j.amjmed.2014.07.014
23. Cappola AR, Fried LP, Arnold AM, Danese MD, Kuller LH, Burke GL, et al. Thyroid status, cardiovascular risk, and mortality in older adults. *JAMA.* (2006) 295:1033–41. doi: 10.1001/jama.295.9.1033
24. Iervasi G, Pingitore A, Landi P, Raciti M, Ripoli A, Scarlattini M, et al. Low-T3 syndrome: a strong prognostic predictor of death in patients with heart disease. *Circulation.* (2003) 107:708–13. doi: 10.1161/01.CIR.0000048124.64204.3F
25. Iervasi G, Molinaro S, Landi P, Taddei MC, Galli E, Mariani F, et al. Association between increased mortality and mild thyroid dysfunction in cardiac patients. *Arch Intern Med.* (2007) 167:1526–32. doi: 10.1001/archinte.167.14.1526
26. Zhang M, Sara JD, Matsuzawa Y, Gharib H, Bell MR, Gulati R, et al. Clinical outcomes of patients with hypothyroidism undergoing percutaneous coronary intervention. *Eur Heart J.* (2016) 37:2055–65. doi: 10.1093/eurheartj/ehv737
27. Maia AL, Goemann IM, Meyer ELS, Wajner SM. Deiodinases: the balance of thyroid hormone: type 1 iodothyronine deiodi-nase in human physiology and disease. *J Endocrinol.* (2011) 209:283–97. doi: 10.1530/JOE-10-0481
28. Maia AL, Kim BW, Huang SA, Harney JW, Larsen PR. Type 2 iodothyronine deiodinase is the major source of plasma T3 in euthyroid humans. *J Clin Invest.* (2005) 115:2524–33. doi: 10.1172/JCI25083
29. Itoh S, Yamaba Y, Oda T, Kawagoe K. Serum thyroid hormone, triiodothyronine, thyroxine, and triiodothyronine/thyroxine ratio in patients with fulminant, acute, and chronic hepatitis. *Am J Gastroenterol.* (1986) 81:444–9.
30. van der Molen AJ, Thomsen HS, Morcos SK. Effect of iodinated contrast media on thyroid function in adults. *Eur Radiol.* (2004) 14:902–7. doi: 10.1007/s00330-004-2238-z
31. Park SY, Park SE, Jung SW, Jin HS, Park IB, Ahn SV et al. Free triiodothyronine/free thyroxine ratio rather than TSH is more associated with metabolic parameters in healthy euthyroid adult subjects. *Clin Endocrinol.* (2017) 87:87–96. doi: 10.1111/cen.13345
32. Neves JS, Vale C, von Hafe M, Borges-Canha M, Leite AR, Almeida-Coelho J, et al. Thyroid hormones and modulation of diastolic function: a promising target for heart failure with preserved ejection fraction. *Ther Adv Endocrinol Metab.* (2020) 11:2042018820958331. doi: 10.1177/2042018820958331

Conflict of Interest: The authors declare that the research was conducted in the absence of any commercial or financial relationships that could be construed as a potential conflict of interest.

frontiers | Frontiers in Cardiovascular Medicine

MINI REVIEW
published: 16 June 2022
doi: 10.3389/fcvm.2022.928244

RBM20, a Therapeutic Target to Alleviate Myocardial Stiffness *via* Titin Isoforms Switching in HFpEF

*Na Li, Weijian Hang, Hongyang Shu and Ning Zhou**

Hubei Key Laboratory of Genetics and Molecular Mechanisms of Cardiological Disorders, Division of Cardiology, Department of Internal Medicine, Tongji Hospital, Tongji Medical College, Huazhong University of Science and Technology, Wuhan, China

Increased myocardial stiffness is critically involved in heart diseases with impaired cardiac compliance, especially heart failure with preserved ejection fraction (HFpEF). Myocardial stiffness mainly derives from cardiomyocyte- and extracellular matrix (ECM)-derived passive stiffness. Titin, a major component of sarcomeres, participates in myocardial passive stiffness and stress-sensitive signaling. The ratio of two titin isoforms, N2BA to N2B, was validated to influence diastolic dysfunction *via* several pathways. RNA binding motif protein 20 (RBM20) is a well-studied splicing factor of titin, functional deficiency of RBM20 in mice profile improved cardiac compliance and function, which indicated that RBM20 functions as a potential therapeutic target for mitigating myocardial stiffness by modulating titin isoforms. This minor review summarized how RBM20 and other splicing factors modify the titin isoforms ratio, therefore providing a promising target for improving the myocardial compliance of HFpEF.

Keywords: RNA binding motif protein 20, titin, myocardial stiffness, heart failure with preserved ejection fraction, splicing factors

OPEN ACCESS

Edited by:
Tong Liu,
Tianjin Medical University, China

Reviewed by:
Chen Liu,
The First Affiliated Hospital of Sun Yat-sen University, China

***Correspondence:**
Ning Zhou
zhouning@tjh.tjmu.edu.cn

Specialty section:
This article was submitted to Heart Failure and Transplantation, a section of the journal Frontiers in Cardiovascular Medicine

Received: *25 April 2022*
Accepted: *30 May 2022*
Published: *16 June 2022*

Citation:
Li N, Hang W, Shu H and Zhou N (2022) RBM20, a Therapeutic Target to Alleviate Myocardial Stiffness via Titin Isoforms Switching in HFpEF. Front. Cardiovasc. Med. 9:928244. doi: 10.3389/fcvm.2022.928244

INTRODUCTION

Heart failure (HF) with preserved ejection fraction (HFpEF) is prevalent in an aging society and effective therapy is still unavailable for this public health issue. Augmented cardiac stiffness is an unfavorable state characterized by diastolic dysfunction and impaired cardiac compliance that is mainly involved in HFpEF (1). Increased cardiovascular stiffness plays a substantial role in the development of multiple diseases, including hypertension and heart failure (2). Echocardiography (3) and cardiac magnetic resonance imaging (CMRI) (4) have been applied to evaluate the compliance of the heart in clinical work. However, little attention has been attracted to cardiomyocyte or myofibril passive stiffness although atomic force microscopy (AFM) has been applied in laboratory experiments (5). Cardiac stiffness is dependent on cardiomyocyte-dependent and independent factors. Cardiomyocyte-dependent factors mainly derive from the elasticity of titin protein, while cardiomyocyte-independent factors are composed of cardiac fibroblasts and extracellular matrix (ECM). Both increased titin-based and collagen-dependent stiffness contribute to myocardial stiffness and excavate HFpEF (6, 7).

The largest monomer protein among identified proteins (8), titin spans across the sarcomere of striated muscle, providing mechanical support as well as passive tension to the sarcomere during the systole (9, 10). Genotypic or phenotypic mutations of titin are involved in cardiac remodeling and cardiomyopathy (11–13). However, the underlying mechanisms remain largely unclear.

Both alternative splicing and posttranslational modifications (PTMs) of titin play a pivotal role in its function (9). Apart from PTMs of titin that has been well summarized in previous reviews (14, 15), titin's pre-mRNA is mainly modulated by RNA binding motif 20 (RBM20)

(16). RBM20 is one of the splicing factors that regulate titin isoforms switching (17, 18). Two dominant titin isoforms, N2BA and NAB, differ in extensibility due to the composition of the structural domains (15). The elasticity of N2BA is higher than N2B owing to more proportion of proline-glutamate-valine-lysine (PEVK) and Ig motifs, which are the extensible elements in I-band titin (15). Myocardial compliance is modulated by different ratios of N2BA and N2B. In other words, improving the ratio of N2BA and N2B contributes to improving myocardial compliance. Previous studies showed a promising role in regulating RBM20 expression or interfering with its structure to alleviate myocardial stiffness *via* interfering with the ratio of N2BA and N2B (19, 20).

In this review, we summarized and analyzed the role of RBM20 and its co-operators in alternative splicing to regulate titin isoforms ratio, revealing a potential therapeutic target of attenuating myocardial stiffness presented in HFpEF.

MYOCARDIAL STIFFNESS

Cardiac diastolic performance mainly depends on ventricular compliance, which presents a negative relationship with myocardial stiffness and accompanies by increased viscoelastic forces that resist diastolic filling (21). Increased cardiovascular stiffness impairs myocardial and vascular elasticity, and leads to insufficient organic perfusion and clinical symptoms (22). Echocardiography (3, 23) and CMRI have been used to evaluate cardiac stiffness (4). The E', E/A ratio, left ventricle end-diastolic diameter (LVED; d), LV end-diastolic pressure (LVEDP) and pressure-volume loop evaluated by echocardiography were regarded as markers to reflect the cardiac compliance (24). LV pressure-volume (P-V) relationship, an indirect marker for ventricle compliance, was determined by LV volume and aortic pressure acquired in CMRI (4). Despite these tests, currently there is still no effective treatment for cardiac stiffness to improve cardiac compliance and flexibility. Basic research is in an urgent need to find out potential targets for improving cardiac stiffness.

The mechanism of cardiac stiffness has not been fully understood. Various pathological changes are involved in myocardial stiffness, including cardiac fibrosis (25), increased collagen in ECM (26), and most importantly, increased intrinsic cardiomyocyte stiffness which results from impairment of the cytoskeleton. Increased ECM, especially fibrillar collagen, contributes to the development of cardiac fibrosis (7, 27), which limits the systolic and diastolic function of the heart and ultimately leads to a decline in cardiac function (7). However, treatments for cardiac fibrosis have limited contribution to improving cardiac stiffness. More importantly, multiple studies over decades have revealed the substantial role of myocyte-derived compliance, which is closely related to titin (10, 28, 29). Apart from structural alterations, metabolic disorders were involved in myocardial stiffness. For instance, serum circulating proteins such as secreted frizzled-related protein 1 (sFRP1) promoted pathological changes in gene expression and cellular stiffness (30). Furthermore, coronary microvascular dysfunction, increased inflammation, oxidative stress and myocardial sodium glucose cotransporter-2 (SGLT-2)-mediated effects were significantly involved in myocardial stiffness induced by diabetic cardiomyopathy (31). Such pathological changes may lead to a decrease in energetic efficiency and suggest possible value to developing potential drugs targeting these listed mechanisms.

THE RELATIONSHIP BETWEEN TITIN AND CARDIAC STIFFNESS

The giant filament protein titin plays an essential role in facilitating the contraction of the myocardium. Titin is the largest protein in the human body encoded by 364 exons of the *TTN* gene (8, 32). Composed of four main structural domains, titin crosses sarcomeres to connect the Z-disk and the M-line and Serves as a physiological spring (**Figure 1A**) (29). The main extensible region of titin is composed of three domains: N2Bus, the spring-like PEVK domain and the immunoglobulin (Ig)-like domains. The PEVK and N2B regions hold a spring-like function (33), while a shortened Ig domain resulted in titin-based cardiac diastolic dysfunction (34), besides, Unfolding and refolding of the Ig domain exert different impacts on myocardial elasticity (35–37).

Studies demonstrated that Ig-like domains affect titin elasticity through redox modification (38) and S-glutathionylated (35) in the unfolded state. In detail, S-glutathionylation of cryptic cysteines enhances titin elasticity by blocking protein folding in human cardiomyocytes (35).

Titin provides structural support and elastic forces to heart tissue while being stretched. Length and viscoelasticity are predominant components of the passive tension during the heart systaltic process and the major contributors to the Frank-Starling mechanism (28, 29). The alternative splicing process produce different isoforms of titin, including adult N2BA, adult N2B and fetal cardiac titin (FCT) that are composed of different proportion of domains (Ig, PEVK, N2Bus and N2A), which differ in length and elasticity. The long, soft N2BA isoform (3,200–3,500 kDa) and the short, rigid N2B isoform (3,000 kDa) are expressed in adult human hearts (**Figure 1A**). Distensibility of different isoforms mainly depends on the length of spring N2B and PEVK regions (39). The longer PEVK and N2Bus expressed in N2BA isoform determined its softer property than N2A. The N2BA: N2B ratio has a pronounced impact on myocardial stiffness (40). Different titin isoforms ratio was shown to affect cardiac phenotypes and heart diseases (13, 41). The titin-isoform shift may be beneficial for myocardial diastolic function but could impair the contractile performance in systole (42). A larger proportion of N2BA is expressed in the dilated cardiomyopathy (DCM) patients' hearts than the normal ones, accompanying by impaired cardiac systolic function (42). However, some studies demonstrated that upregulating compliant titin isoforms in a murine model with HFpEF-like symptoms improved diastolic function resulting in greater tolerance to exercise (13). Further studies need to make the mechanism clear and explore the potential therapeutics modulating the titin isoform ratio to alleviate myocardial stiffness.

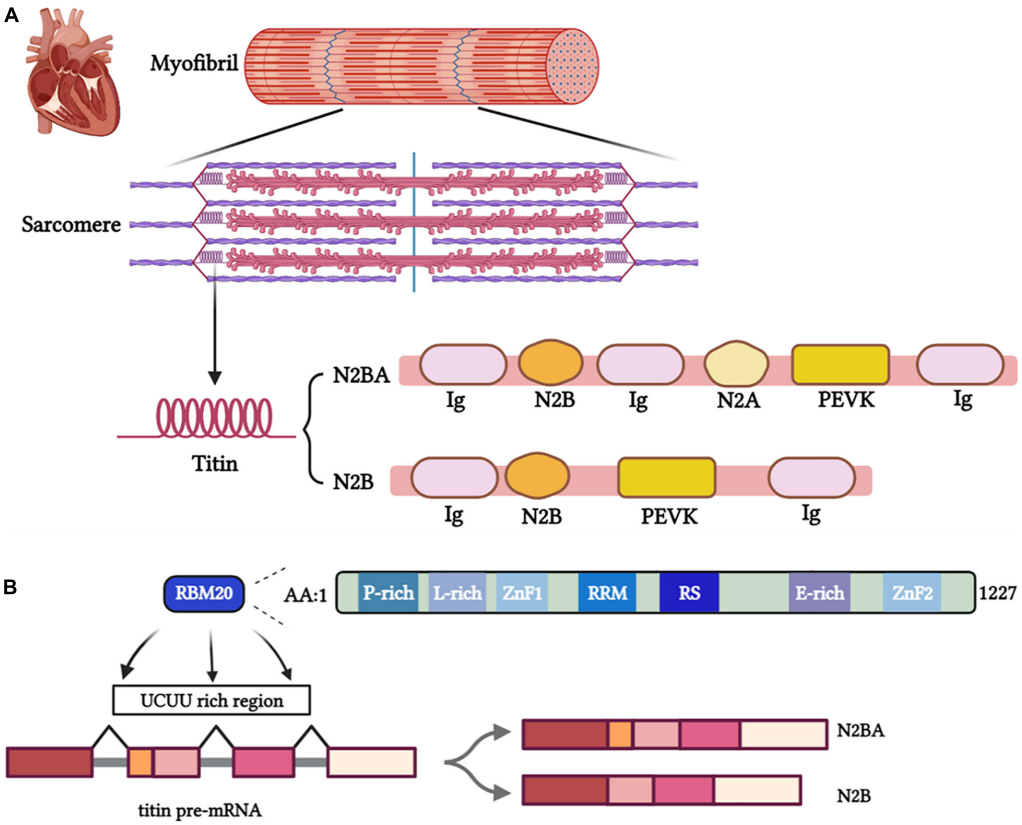

FIGURE 1 | (A) Titin isoforms serve essential functional roles as part of the sarcomere, myofibril, and cardiac tissue. **(B)** The binding site of RBM20 on pre-mRNA and the structural and functional domains of RBM20.

PTMs are well-studied to modulate titin stiffness *via* phosphorylation and dephosphorylation (10, 15). Elasticity of titin was regulated by activating PKG or PKCα at the N2B element with its extensible unique sequence (N2Bus) or PEVK region (9, 43). Myocardial stiffness was, respectively, decreased and increased by phosphorylating the N2Bus and PEVK region of titin (44, 45). Phosphoserines within N2Bus, including P-S4010, P-S4099 and P-S4062, are independently activated by ERK1/2 (46), cAMP-dependent PKA (47), cGMP-dependent PKG and CaMKII (14, 47, 48). In contrast, phosphorylating the PEVK region of titin by PKC exacerbated myocardial stiffness (49). Accordingly, regulating the phosphorylation of N2Bus and PEVK domains may attenuate cardiac stiffness induced by chronic heart diseases (CHD).

SPLICING FACTORS PLAY AN ESSENTIAL ROLE IN MODULATING TITIN ISOFORMS

RBM20, a Silver Lining for Patients With Cardiac Diastolic Dysfunction

Mis-splicing of titin mitigated by RBM20 was markedly involved in heart diseases (50, 51). As a striated muscle-specific gene located on chromosome 10, the RBM20 gene contains 14 exons and encodes a protein of 1,227 amino acids mostly expressed in the myocardium (52, 53). RBM20 contains two zinc finger domains, an RNA recognition motif (RRM), a serine- and arginine-rich region (RS region), a leucine-rich region, and a glutamate-rich region (**Figure 1B**) (54). Two pivotal functional regions, RRM and RS region play a dominant role in the nuclear localization of RBM20. Meanwhile, the most frequent pathogenic RBM20 mutations occur in the RS region.[55] RBM20 binds with introns near splice sites and adjacent to U1 and U2 small nuclear ribonucleoprotein (snRNP) binding sites to regulate splicing (53). Haploinsufficiency of RBM20 led to altered alternative splicing of *TTN* and a dramatic shift to highly compliant titin isoforms and impaired Frank-Starling mechanism (55). Moreover, the serine and arginine residues in the RS region (RSRSP stretch) can be phosphorylated, which is necessary for the nuclear localization of RBM20. Loss of phosphorylation of these mutated residues promoted the translocation of RBM20 from the nucleus and negated the function of RBM20 (56). Given a better understanding of regions of RBM20 (57), it is intriguingly to elucidate how mutation of RBM20 affect cardiac function *via* regulating splicing of pre-mRNA of titin. RBM20 represses splicing to orchestrate cardiac pre-mRNA processing. In failing human hearts, reduced expression of RBM20 affects alternative splicing of several direct

targets, indicating that differences in RBM20 expression may affect cardiac function (53).

RBM20 plays an essential role in titin isoform switching (16). Genotype mutations or functional site alterations in RBM20 lead to different outcomes (57, 58). For instance, genetic mutations (59) and mutations in RS domain (60) of RBM20 were observed to closely associated with familial DCM cases. In addition, a mutation in the glutamate-rich region of RBM20 causes DCM through missplicing of titin and impaired Frank–Starling mechanism (55). More descriptions of the relationship between RBM20 variation and corresponding exons and pathogenicity were summarized in previous reviews (61). Subendocardial fibrosis accompanied by electrical abnormalities has been observed in RBM20-null heterozygous or homozygous rats (58). RBM20 deficiency in rats leads to many phenotypic features that are observed in individuals with cardiomyopathy related to mutant RBM20, suggesting conserved RBM20 function. Researchers found that RBM20 was a global regulator of cardiac alternative splicing and document considerable overlap of post-transcriptionally regulated genes that depend on RBM20. They offer mechanistic insights and functional annotation of RBM20 substrates that contribute to cardiomyopathy and heart failure (58).

Among the cardiac genes regulated by RBM20, *TTN* is a major human disease-causing one (50, 58). DCM was closely related to mutations in RBM20 (59). A previous study demonstrated that RBM20-mutated (a missense mutation in the RSRSP stretch) mice caused the development of DCM (62). However, researchers experimentally promoted the compliance of titin by RBM20 inhibition with a mouse model termed cRbm20ΔRRM, referred to as one of the RRM of the RBM20 alleles was floxed and which expressed the MerCreMer transgene under control of the αMHC promoter (63). Inhibiting the RBM20-based titin splicing system contributed to upregulating compliant titin and improving diastolic function in an HFpEF model (63). In addition, increased ventricular stiffness and diastolic dysfunction in N2B-KO mice were reversed by a 50% reduction of functional RBM20 expression (64), which relied on mechanical properties of titin and broadened the therapeutics of cardiac stiffness mediated by RBM20 (64).

The latest study revealed that inhibition of RBM20 with antisense oligonucleotides (ASOs) in HFpEF mouse and engineered human heart tissue improved diastolic function (20), which indicated a marked translational value of RBM20 in attenuating myocardial wall stiffness. Myocardial stiffness was estimated by pressure-volume catheter and or AFM and also reflected by increased radial and circumferential strains (65). Myocardial compliance was reflected by the velocity of LV pressure varying with LV volume in the P-V curve, while AFM assesses the elastic and adhesive behavior of cardiomyocytes through topography detection to the exploiting advanced nanomechanical mapping (66). AFM increasingly provides a thorough insight into cardiac physiological and pathological conditions, as well as the effects of therapeutic approaches at the cardiomyocytes scale.

RBM20 is crucial for the formation of a subset of circRNAs that originate from the I-band of the titin gene (67). CircRNAs affect splicing (68) and regulate gene expression (69). Khan et al. identified 80 different circRNAs within the *TTN* gene and determined RBM20-sensitive exons served as a substrate for circRNA formation when they were spliced out of the linear titin transcript (67).

RBM20 Coordinates With RBM24 to Regulate Cardiac Hypertrophy

RNA Binding Motif 24 (RBM24), a member of the RNA binding protein (RBP) family, is also an important splicing factor involved in titin splicing. The RBM24 full and conditional knockout mice were embryonic lethal and exhibited DCM or heart failure, respectively (70). RBM24 deletion in mouse model resulted in misconnection of genes encoding structural proteins of sarcomere, such as *Tpm2*, *TTN*, *Neb1*, *Fhod3*, *Enah*, and *Ablim1* (71). As a major regulator of muscle-specific alternative splicing, RBM24 is necessary for sarcomere assembly and cardiac contraction (72). Latest study showed that RBM24 modulates the temporal dynamics of core myofibrillogenesis genes and thereby orchestrates sarcomere organization *via* facilitating inclusion of exon 6 of *ACTN2* (73). In addition, RBM24 promoted the inclusion of exons 11 and 13 of *TTN*, which located on the Z-disk and participate in the assembly, stabilization, and maintenance of myofibrils (70, 74). More research are called for indicating mechanisms involved in RBM24 regulating *TTN* and myocardial fibrils assembly in the future.

Intriguingly, RBM20 and RBM24 were shown to co-regulate the splicing of scaffold proteins expressed by the *ENH* genes in rat cardiomyocytes (75). In healthy conditions, RBM20 and RBM24 cooperate to promote the expression of short *ENH* isoforms (*ENH3*), which prevents hypertrophic growth. However, RBM20 or RBM24 alone had no significant effect on the alteration of scaffold protein subtypes. In addition, promoting RBM20 and RBM24 increased the expression of *ENH* subtypes lacking LIM domains (such as *ENH3* and *ENH4*), thus prevented myocardial hypertrophy in mice (75). It is reasonable to speculate that the cooperatively regulating RBM20 and RBM24 may affect myocardial stiffness, because cardiac hypertrophy is closely related to wall stiffness and compliance, but the mechanisms remain unknown.

Therefore, future studies are needed to determine whether exist potential mechanism that RBM20 and RBM24 cooperate to regulate myocardial stiffness by muscle-specific alternative splicing.

The Mechanism of the Regulation of the Titin Isoforms Conversion by RBM20 and PTB4

RBM20 splicing upon the post-transcriptional precursor mRNA of the *TTN* gene effectively regulated cardiomyocyte stiffness (28). The specific mechanism may be related to the phosphorylation of the RS domain, the deletion of the glutamate-rich domain, and the change in plasma hormone levels. Determining the *TTN* pre-mRNA binding sites is the key to regulating the proportion of titin subtypes by RBM20.

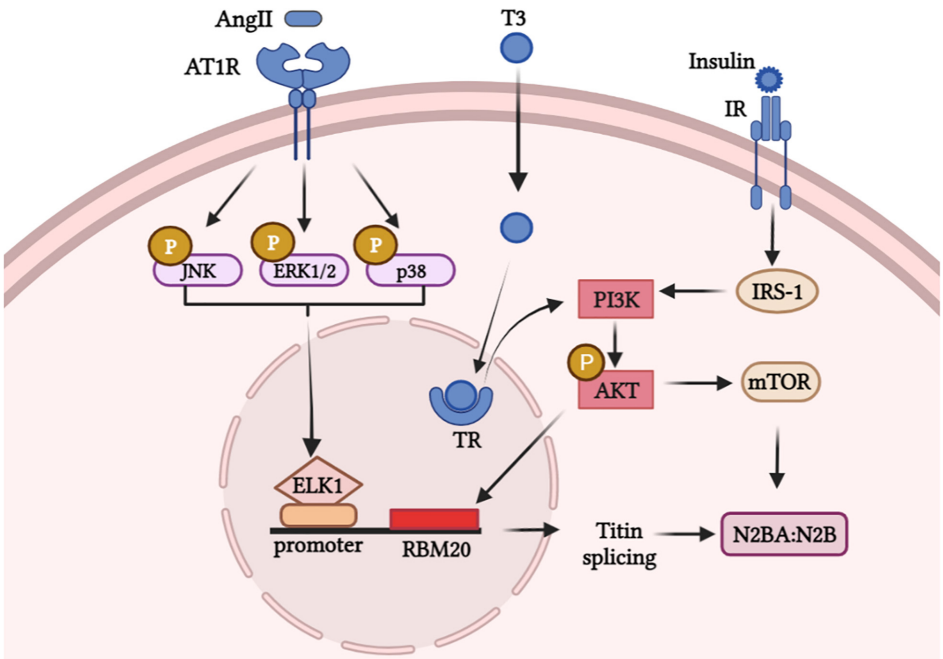

FIGURE 2 | Hormone stimuli promote signaling pathways in modulating the expression of titin isoforms *via* RBM20.

As a splicing inhibitor near exons, RBM20 Predominantly binds to intron sequences containing UCUU motifs (**Figure 1B**) (52, 58). Recent studies have confirmed RBM20 uses a coupled folding binding mechanism by the C-terminal helix to specifically recognize the UCUU RNA motif (76).

The novel titin splicing factor PTB4 (alias PTBP1) is a member of the heterogeneous nuclear ribonucleoprotein (hnRNP) family that expressed in the heart, skeletal muscle, and brain (77). PTB4 binds to UC-rich regions in introns on both sides of regulatory exons (78). PTB4 and RBM20 jointly regulated the splicing of cardiac precursor mRNA (17). Interestingly, PTB4 acts as a novel regulator of titin splicing in exon exclusion through counteracting the RBM20 repressor activity (79). PTB4/RNA complexes are formed only with RNAs containing UCUU motifs. Dauksaite et al. showed that PTB4 and RBM20 bind to the transcriptional sequence with the same motif on the 5′SS downstream of the alternative exon (79). This provided a possible mechanism of regulating titin isoform expression through additive binding of PTB4 and RBM20 to the downstream intron (79). It is of great significance to figure out RBM20 and PTBP4 as the potential therapeutic targets for attenuating myocardial stiffness and diastolic dysfunction.

As one of the main inhibitors of splicing events, PTB4 inhibited specific exons in alternative splicing isomers (80). The expression of RBM20 and PTB4 increased and decreased during cardiac development, respectively. This contrary trend of PTB4 and RBM20 during heart development showed an inhibition effect of PTBP1 on the splicing effect of RBM20 on titin (17, 81).

In addition, both PTB4 and RBM20 are involved in regulating the alternative splicing of formin homologous 2 domains containing 3 (FHOD3) proteins, the sarcomere proteins regulating the dynamics of actin, thus participating in actin assembly and sarcomeric organization of cardiomyocyte (81). Further study of alternative splicing of FHOD3 by RBM20 and PTB4 may contribute to exploring mechanisms and therapeutic targets of cardiomyopathy.

TITIN ISOFORMS SWITCHING IS MODULATED BY HORMONE STIMULI *VIA* MODULATING RBM20 EXPRESSION

RBM20 was demonstrated to be involved in the process of multiple external stimuli regulating titin isoforms transition, thus modulating the myocardial wall stiffness. Here, we summarized signaling pathways that linking factors and RBM20 to regulate titin isoforms switching (**Figure 2**). For instance, titin isoform transition triggered by the thyroid hormone-triiodothyronine (T3) is linked to RBM20 *via* the PI3K/Akt/mTOR signaling pathway, phosphorylating RBM20 and/or increasing gene expression of RBM20 (18). No N2B isoform was expressed in RBM20$^{-/-}$ rat hearts under T3 treatment relative to control groups implanted with placebo, while propylthiouracil (PTU) treatment attenuated N2BA:N2B ratio in RBM20$^{+/+}$ rats (18). Furthermore, researchers revealed that mechanism linking titin isoforms and T3 mainly due to the PTMs (specifically phosphorylation) of RBM20 (18).

Besides, insulin controls titin-based cardiac stiffness *via* activating PI3K/Akt/mTOR pathway and increasing titin phosphorylation (82). Researchers showed the mean proportion of the stiffer N2B-titin isoform significantly increased in insulin-treated primary neonatal rat cardiomyocytes (NRCMs) and

diastolic function was improved in diabetic cardiomyopathy (82). Likewise, the central position of RBM20 in PI3K/Akt/mTOR pathway for insulin-induced titin alternative splicing was validated in another study (83). However, whether Akt directly act on the SR rich region or phosphorylate RBM20 to regulate splicing of titin remains unclear and worth further exploration.

AngII has been demonstrated to activate MAPK-ELK axis and to upregulate the expression of RBM20 (84). This study revealed that Ang II can trigger ELK1 through activation of MAPK signaling by enhancing RBM20 expression which regulates pre-mRNA splicing. After AngII binds to AngII receptor 1 (AT1R), intracellular molecules including JNK/ERK1/p38 are phosphorylated and the downstream transcription factor ELK1 translocated into the nucleus. ELK1 was activated and combined with titin pre-mRNA, which triggered the expression of RBM20 and regulated the titin isoforms ratio (84).

Furthermore, RBM20 methylation was decreased and the RBM20 mRNA level increased upon doxorubicin treatment (85). Accordingly, further studies need to reveal signaling pathways involved in RBM20 and unravel the potential therapeutic targets of augmented cardiac stiffness.

Better understanding the mechanisms involved in titin isoforms transition shows a silver lining for treating heart failure with myocardial wall stiffness.

CONCLUSION

HFpEF characterized by diastolic dysfunction remains a serious public health problem with high morbidity and mortality. Novel therapeutics or prevention strategies are urgent for solving this problem. Titin, the spring protein of sarcomere in myocardium, plays an essential role in controlling compliance and elasticity during contractile relaxation. Modification of titin isoforms ratio *via* splicing factor RBM20 represents a potential target to attenuate myocardial stiffness. As effective regulators of cardiac stiffness based on titin, RBM20 provides novel strategies to treat heart diseases with impaired cardiac compliance, especially HFpEF. RBM24 and PTB4 broadened the splicing scope of titin, which provided new therapeutics and is worthy of further exploration.

Both RBM20 heterozygous mouse model (86) and reducing RBM20 activity in N2B-KO mouse (64) inhibited titin-based stiffness and diastolic dysfunction and improved cardiac function. However, patients that carry a pathogenic RBM20 mutation have more ventricular arrhythmias comparing to patients with a *TTN* mutation (87). Haploinsufficiency of RBM20 disturbed alternative splicing of *TTN* and resulted in a dramatic shift to highly compliant titin isoforms and an impaired Frank-Starling Mechanism (55). Titin isoform analysis revealed a dramatic shift from the less compliant N2B toward the highly compliant N2BA isoforms in RBM20$^{E913K/+}$ heart that carrying a mutation in a glutamate-rich region of RBM20. These effects may contribute to the early onset, and malignant course of DCM caused by RBM20 mutations (55). As those side effects exist, more research are urgently needed to translate the clinical therapy value of RBM20.

Besides, multiple small molecules modulate titin isoforms switching, *via* RBM20-dependent or independent way. C-type natriuretic peptide (CNP) modulated titin-based ventricular compliance (88) and Digoxin attenuated RBM20 protein level (89), respectively. Cardenolides affect RBM20-dependent titin isoforms expression *via* decreasing RBM20 protein levels and altering transcription of select splicing factors that interact with RBM20 (90). It is promising that taking small molecules to inhibit the splicing activity of RBM20 (90).

In summary, our mini review has illustrated a promising way to attenuate myocardial stiffness characterized in heart failure, which mainly depends on the role of splicing factor RBM20 on titin pre-mRNA to modulate titin isoforms ratio.

AUTHOR CONTRIBUTIONS

NL wrote the original draft. NZ, WH, and HS revised the manuscript. All authors agreed to be accountable for the content of the work.

FUNDING

This work was supported by grants from the National Natural Science Foundation of China (Nos. 81570261 and 82070316) and Chinese Cardiovascular Association-Access Fund (2020-CCA-ACCESS-059). The funding source(s) had no involvement in study design; in the collection, analysis and interpretation of data; in the writing of the report; and in the decision to submit the article for publication.

REFERENCES

1. Hieda M, Sarma S, Hearon CM Jr., Dias KA, Martinez J, Samels M, et al. Increased myocardial stiffness in patients with high-risk left ventricular hypertrophy: the hallmark of stage-B heart failure with preserved ejection fraction. *Circulation.* (2020) 141:115–23.
2. Westermann D, Kasner M, Steendijk P, Spillmann F, Riad A, Weitmann K, et al. Role of left ventricular stiffness in heart failure with normal ejection fraction. *Circulation.* (2008) 117:2051–60.
3. Pernot M, Villemain O. In the heart of stiffness: are natural heart vibrations reliable enough to assess myocardial stiffness, the new holy grail in echocardiography? *JACC Cardiovasc Imaging.* (2019) 12:2399–401. doi: 10.1016/j.jcmg.2019.01.012
4. Namasivayam M, Adji A, Lin L, Hayward CS, Feneley MP, O'Rourke MF, et al. Non-invasive quantification of ventricular contractility, arterial elastic function and ventriculo-arterial coupling from a single diagnostic encounter using simultaneous arterial tonometry and magnetic resonance imaging. *Cardiovasc Eng Technol.* (2020) 11:283–94. doi: 10.1007/s13239-020-00462-2
5. An Y, Manuguri SS, Malmstrom J. Atomic force microscopy of proteins. *Methods Mol Biol.* (2020) 2073:247–85.
6. Chung CS, Granzier HL. Contribution of titin and extracellular matrix to passive pressure and measurement of sarcomere length in the mouse left ventricle. *J Mol Cell Cardiol.* (2011) 50:731–9. doi: 10.1016/j.yjmcc.2011.01.005
7. Zile MR, Baicu CF, Ikonomidis JS, Stroud RE, Nietert PJ, Bradshaw AD, et al. Myocardial stiffness in patients with heart failure and a preserved

ejection fraction: contributions of collagen and titin. *Circulation.* (2015) 131:1247–59.
8. Freiburg A, Trombitas K, Hell W, Cazorla O, Fougerousse F, Centner T, et al. Series of exon-skipping events in the elastic spring region of titin as the structural basis for myofibrillar elastic diversity. *Circ Res.* (2000) 86:1114–21. doi: 10.1161/01.res.86.11.1114
9. LeWinter MM, Granzier H. Cardiac titin: a multifunctional giant. *Circulation.* (2010) 121:2137–45. doi: 10.1161/CIRCULATIONAHA.109.860171
10. Tharp CA, Haywood ME, Sbaizero O, Taylor MRG, Mestroni L. The giant protein titin's role in cardiomyopathy: genetic, transcriptional, and post-translational modifications of TTN and their contribution to cardiac disease. *Front Physiol.* (2019) 10:1436. doi: 10.3389/fphys.2019.01436
11. Taylor M, Graw S, Sinagra G, Barnes C, Slavov D, Brun F, et al. Genetic variation in titin in arrhythmogenic right ventricular cardiomyopathy-overlap syndromes. *Circulation.* (2011) 124:876–85. doi: 10.1161/CIRCULATIONAHA.110.005405
12. Herman DS, Lam L, Taylor MR, Wang L, Teekakirikul P, Christodoulou D, et al. Truncations of titin causing dilated cardiomyopathy. *N Engl J Med.* (2012) 366:619–28. doi: 10.1056/NEJMoa1110186
13. Bull M, Methawasin M, Strom J, Nair P, Hutchinson K, Granzier H. Alternative splicing of titin restores diastolic function in an HFpEF-like genetic murine model (TtnDeltaIAjxn). *Circ Res.* (2016) 119:764–72. doi: 10.1161/CIRCRESAHA.116.308904
14. Kruger M, Kotter S, Grutzner A, Lang P, Andresen C, Redfield MM, et al. Protein kinase G modulates human myocardial passive stiffness by phosphorylation of the titin springs. *Circ Res.* (2009) 104:87–94. doi: 10.1161/CIRCRESAHA.108.184408
15. Koser F, Loescher C, Linke WA. Posttranslational modifications of titin from cardiac muscle: how, where, and what for? *FEBS J.* (2019) 286:2240–60. doi: 10.1111/febs.14854
16. Guo W, Sun M. RBM20, a potential target for treatment of cardiomyopathy via titin isoform switching. *Biophys Rev.* (2018) 10:15–25. doi: 10.1007/s12551-017-0267-5
17. Fochi S, Lorenzi P, Galasso M, Stefani C, Trabetti E, Zipeto D, et al. The emerging role of the RBM20 and PTBP1 ribonucleoproteins in heart development and cardiovascular diseases. *Genes.* (2020) 11:402. doi: 10.3390/genes11040402
18. Zhu C, Yin Z, Ren J, McCormick RJ, Ford SP, Guo W. RBM20 is an essential factor for thyroid hormone-regulated titin isoform transition. *J Mol Cell Biol.* (2015) 7:88–90. doi: 10.1093/jmcb/mjv002
19. Methawasin M, Hutchinson KR, Lee EJ, Smith JE III, Saripalli C, Hidalgo CG, et al. Experimentally increasing titin compliance in a novel mouse model attenuates the Frank-Starling mechanism but has a beneficial effect on diastole. *Circulation.* (2014) 129:1924–36. doi: 10.1161/CIRCULATIONAHA.113.005610
20. Radke MH, Badillo-Lisakowski V, Britto-Borges T, Kubli DA, Juttner R, Parakkat P, et al. Therapeutic inhibition of RBM20 improves diastolic function in a murine heart failure model and human engineered heart tissue. *Sci Transl Med.* (2021) 13:eabe8952. doi: 10.1126/scitranslmed.abe8952
21. Caporizzo MA, Chen CY, Bedi K, Margulies KB, Prosser BL. Microtubules increase diastolic stiffness in failing human cardiomyocytes and myocardium. *Circulation.* (2020) 141:902–15. doi: 10.1161/CIRCULATIONAHA.119.043930
22. Jia G, Aroor AR, Hill MA, Sowers JR. Role of renin-angiotensin-aldosterone system activation in promoting cardiovascular fibrosis and stiffness. *Hypertension.* (2018) 72:537–48. doi: 10.1161/HYPERTENSIONAHA.118.11065
23. Shah AM, Shah SJ, Anand IS, Sweitzer NK, O'Meara E, Heitner JF, et al. Cardiac structure and function in heart failure with preserved ejection fraction: baseline findings from the echocardiographic study of the Treatment of Preserved Cardiac Function Heart Failure with an Aldosterone Antagonist trial. *Circ Heart Fail.* (2014) 7:104–15. doi: 10.1161/CIRCHEARTFAILURE.113.000887
24. Iwanaga Y, Nishi I, Furuichi S, Noguchi T, Sase K, Kihara Y, et al. B-type natriuretic peptide strongly reflects diastolic wall stress in patients with chronic heart failure: comparison between systolic and diastolic heart failure. *J Am Coll Cardiol.* (2006) 47:742–8. doi: 10.1016/j.jacc.2005.11.030
25. Paulus WJ, Zile MR. From systemic inflammation to myocardial fibrosis: the heart failure with preserved ejection fraction paradigm revisited. *Circ Res.* (2021) 128:1451–67. doi: 10.1161/CIRCRESAHA.121.318159
26. Nielsen SH, Mouton AJ, DeLeon-Pennell KY, Genovese F, Karsdal M, Lindsey ML. Understanding cardiac extracellular matrix remodeling to develop biomarkers of myocardial infarction outcomes. *Matrix Biol.* (2019) 75-76:43–57. doi: 10.1016/j.matbio.2017.12.001
27. Franssen C, Gonzalez Miqueo A. The role of titin and extracellular matrix remodelling in heart failure with preserved ejection fraction. *Neth Heart J.* (2016) 24:259–67. doi: 10.1007/s12471-016-0812-z
28. Linke WA. Titin gene and protein functions in passive and active muscle. *Annu Rev Physiol.* (2018) 80:389–411. doi: 10.1146/annurev-physiol-021317-121234
29. Tharp C, Mestroni L, Taylor M. Modifications of titin contribute to the progression of cardiomyopathy and represent a therapeutic target for treatment of heart failure. *J Clin Med.* (2020) 9:2770. doi: 10.3390/jcm9092770
30. Jeffrey DA, Pires Da Silva J, Garcia AM, Jiang X, Karimpour-Fard A, Toni LS, et al. Serum circulating proteins from pediatric patients with dilated cardiomyopathy cause pathologic remodeling and cardiomyocyte stiffness. *JCI Insight.* (2021) 6:e148637. doi: 10.1172/jci.insight.148637
31. Nikolajevic Starcevic J, Janic M, Sabovic M. Molecular mechanisms responsible for diastolic dysfunction in diabetes mellitus patients. *Int J Mol Sci.* (2019) 20:1197. doi: 10.3390/ijms20051197
32. Fukuda N, Granzier HL. Titin/connectin-based modulation of the Frank-Starling mechanism of the heart. *J Muscle Res Cell Motil.* (2005) 26:319–23. doi: 10.1007/s10974-005-9038-1
33. LeWinter MM, Granzier HL. Cardiac titin and heart disease. *J Cardiovasc Pharmacol.* (2014) 63:207–12. doi: 10.1097/FJC.0000000000000007
34. Chung CS, Hutchinson KR, Methawasin M, Saripalli C, Smith JE III, Hidalgo CG, et al. Shortening of the elastic tandem immunoglobulin segment of titin leads to diastolic dysfunction. *Circulation.* (2013) 128:19–28. doi: 10.1161/CIRCULATIONAHA.112.001268
35. Alegre-Cebollada J, Kosuri P, Giganti D, Eckels E, Rivas-Pardo JA, Hamdani N, et al. S-glutathionylation of cryptic cysteines enhances titin elasticity by blocking protein folding. *Cell.* (2014) 156:1235–46. doi: 10.1016/j.cell.2014.01.056
36. Martonfalvi Z, Bianco P, Linari M, Caremani M, Nagy A, Lombardi V, et al. Low-force transitions in single titin molecules reflect a memory of contractile history. *J Cell Sci.* (2014) 127:858–70. doi: 10.1242/jcs.138461
37. Rivas-Pardo JA, Eckels EC, Popa I, Kosuri P, Linke WA, Fernandez JM. Work done by titin protein folding assists muscle contraction. *Cell Rep.* (2016) 14:1339–47. doi: 10.1016/j.celrep.2016.01.025
38. Loescher CM, Breitkreuz M, Li Y, Nickel A, Unger A, Dietl A, et al. Regulation of titin-based cardiac stiffness by unfolded domain oxidation (UnDOx). *Proc Natl Acad Sci USA.* (2020) 117:24545–56. doi: 10.1073/pnas.2004900117
39. Weeland CJ, van den Hoogenhof MM, Beqqali A, Creemers EE. Insights into alternative splicing of sarcomeric genes in the heart. *J Mol Cell Cardiol.* (2015) 81:107–13. doi: 10.1016/j.yjmcc.2015.02.008
40. Nagueh SF, Shah G, Wu Y, Torre-Amione G, King NM, Lahmers S, et al. Altered titin expression, myocardial stiffness, and left ventricular function in patients with dilated cardiomyopathy. *Circulation.* (2004) 110:155–62. doi: 10.1161/01.CIR.0000135591.37759.AF
41. Yin Z, Ren J, Guo W. Sarcomeric protein isoform transitions in cardiac muscle: a journey to heart failure. *Biochim Biophys Acta.* (2015) 1852:47–52. doi: 10.1016/j.bbadis.2014.11.003
42. Makarenko I, Opitz CA, Leake MC, Neagoe C, Kulke M, Gwathmey JK, et al. Passive stiffness changes caused by upregulation of compliant titin isoforms in human dilated cardiomyopathy hearts. *Circ Res.* (2004) 95:708–16. doi: 10.1161/01.RES.0000143901.37063.2f
43. Labeit S, Kolmerer B. Titins: giant proteins in charge of muscle ultrastructure and elasticity. *Science.* (1995) 270:293–6. doi: 10.1126/science.270.5234.293
44. Kotter S, Andresen C, Kruger M. Titin: central player of hypertrophic signaling and sarcomeric protein quality control. *Biol Chem.* (2014) 395:1341–52. doi: 10.1515/hsz-2014-0178
45. Linke WA, Hamdani N. Gigantic business: titin properties and function through thick and thin. *Circ Res.* (2014) 114:1052–68. doi: 10.1161/CIRCRESAHA.114.301286

46. Raskin A, Lange S, Banares K, Lyon RC, Zieseniss A, Lee LK, et al. A novel mechanism involving four-and-a-half LIM domain protein-1 and extracellular signal-regulated kinase-2 regulates titin phosphorylation and mechanics. *J Biol Chem.* (2012) 287:29273–84. doi: 10.1074/jbc.M112.372839
47. Kotter S, Gout L, Von Frieling-Salewsky M, Muller AE, Helling S, Marcus K, et al. Differential changes in titin domain phosphorylation increase myofilament stiffness in failing human hearts. *Cardiovasc Res.* (2013) 99:648–56. doi: 10.1093/cvr/cvt144
48. Hamdani N, Krysiak J, Kreusser MM, Neef S, Dos Remedios CG, Maier LS, et al. Crucial role for Ca2(+)/calmodulin-dependent protein kinase-II in regulating diastolic stress of normal and failing hearts via titin phosphorylation. *Circ Res.* (2013) 112:664–74. doi: 10.1161/CIRCRESAHA.111.300105
49. Hidalgo C, Hudson B, Bogomolovas J, Zhu Y, Anderson B, Greaser M, et al. PKC phosphorylation of titin's PEVK element: a novel and conserved pathway for modulating myocardial stiffness. *Circ Res.* (2009) 105:631–8,17following638. doi: 10.1161/CIRCRESAHA.109.198465
50. Rexiati M, Sun M, Guo W. Muscle-specific Mis-splicing and heart disease exemplified by RBM20. *Genes.* (2018) 9:18. doi: 10.3390/genes9010018
51. van den Hoogenhof MM, Pinto YM, Creemers EE. RNA splicing: regulation and dysregulation in the heart. *Circ Res.* (2016) 118:454–68. doi: 10.1161/CIRCRESAHA.115.307872
52. Li S, Guo W, Dewey CN, Greaser ML. Rbm20 regulates titin alternative splicing as a splicing repressor. *Nucleic Acids Res.* (2013) 41:2659–72. doi: 10.1093/nar/gks1362
53. Maatz H, Jens M, Liss M, Schafer S, Heinig M, Kirchner M, et al. RNA-binding protein RBM20 represses splicing to orchestrate cardiac pre-mRNA processing. *J Clin Invest.* (2014) 124:3419–30. doi: 10.1172/JCI74523
54. Watanabe T, Kimura A, Kuroyanagi H. Alternative Splicing Regulator RBM20 and Cardiomyopathy. *Front Mol Biosci.* (2018) 5:105. doi: 10.3389/fmolb.2018.00105
55. Beqqali A, Bollen IA, Rasmussen TB, van den Hoogenhof MM, van Deutekom HW, Schafer S, et al. A mutation in the glutamate-rich region of RNA-binding motif protein 20 causes dilated cardiomyopathy through missplicing of titin and impaired Frank-Starling mechanism. *Cardiovasc Res.* (2016) 112:452–63. doi: 10.1093/cvr/cvw192
56. Murayama R, Kimura-Asami M, Togo-Ohno M, Yamasaki-Kato Y, Naruse TK, Yamamoto T, et al. Phosphorylation of the RSRSP stretch is critical for splicing regulation by RNA-Binding Motif Protein 20 (RBM20) through nuclear localization. *Sci Rep.* (2018) 8:8970. doi: 10.1038/s41598-018-26624-w
57. Lennermann D, Backs J, van den Hoogenhof MMG. New Insights in RBM20 Cardiomyopathy. *Curr Heart Fail Rep.* (2020) 17:234–46. doi: 10.1007/s11897-020-00475-x
58. Guo W, Schafer S, Greaser ML, Radke MH, Liss M, Govindarajan T, et al. RBM20, a gene for hereditary cardiomyopathy, regulates titin splicing. *Nat Med.* (2012) 18:766–73. doi: 10.1038/nm.2693
59. Refaat MM, Lubitz SA, Makino S, Islam Z, Frangiskakis JM, Mehdi H, et al. Genetic variation in the alternative splicing regulator RBM20 is associated with dilated cardiomyopathy. *Heart Rhythm.* (2012) 9:390–6. doi: 10.1016/j.hrthm.2011.10.016
60. Li D, Morales A, Gonzalez-Quintana J, Norton N, Siegfried JD, Hofmeyer M, et al. Identification of novel mutations in RBM20 in patients with dilated cardiomyopathy. *Clin Transl Sci.* (2010) 3:90–7. doi: 10.1111/j.1752-8062.2010.00198.x
61. Koelemen J, Gotthardt M, Steinmetz LM, Meder B. RBM20-Related Cardiomyopathy: current Understanding and Future Options. *J Clin Med.* (2021) 10:4101. doi: 10.3390/jcm10184101
62. Ihara K, Sasano T, Hiraoka Y, Togo-Ohno M, Soejima Y, Sawabe M, et al. A missense mutation in the RSRSP stretch of Rbm20 causes dilated cardiomyopathy and atrial fibrillation in mice. *Sci Rep.* (2020) 10:17894. doi: 10.1038/s41598-020-74800-8
63. Methawasin M, Strom JG, Slater RE, Fernandez V, Saripalli C, Granzier H. Experimentally increasing the compliance of titin through RNA binding motif-20 (RBM20) inhibition improves diastolic function in a mouse model of heart failure with preserved ejection fraction. *Circulation.* (2016) 134:1085–99.
64. Hinze F, Dieterich C, Radke MH, Granzier H, Gotthardt M. Reducing RBM20 activity improves diastolic dysfunction and cardiac atrophy. *J Mol Med.* (2016) 94:1349–58. doi: 10.1007/s00109-016-1483-3
65. Morishita T, Takeishi N, Ii S, Wada S. Effects of left ventricular hypertrophy and myocardial stiffness on myocardial strain under preserved ejection fraction. *Ann Biomed Eng.* (2021) 49:1670–87. doi: 10.1007/s10439-020-02706-7
66. Borin D, Pecorari I, Pena B, Sbaizero O. Novel insights into cardiomyocytes provided by atomic force microscopy. *Semin Cell Dev Biol.* (2018) 73:4–12. doi: 10.1016/j.semcdb.2017.07.003
67. Khan MA, Reckman YJ, Aufiero S, van den Hoogenhof MM, van der Made I, Beqqali A, et al. RBM20 regulates circular RNA production from the titin gene. *Circ Res.* (2016) 119:996–1003. doi: 10.1161/CIRCRESAHA.116.309568
68. Kelly S, Greenman C, Cook PR, Papantonis A. Exon skipping is correlated with exon circularization. *J Mol Biol.* (2015) 427:2414–7. doi: 10.1016/j.jmb.2015.02.018
69. Hansen TB, Jensen TI, Clausen BH, Bramsen JB, Finsen B, Damgaard CK, et al. Natural RNA circles function as efficient microRNA sponges. *Nature.* (2013) 495:384–8. doi: 10.1038/nature11993
70. Liu J, Kong X, Zhang M, Yang X, Xu X. RNA binding protein 24 deletion disrupts global alternative splicing and causes dilated cardiomyopathy. *Protein Cell.* (2019) 10:405–16. doi: 10.1007/s13238-018-0578-8
71. Tayal U, Prasad S, Cook SA. Genetics and genomics of dilated cardiomyopathy and systolic heart failure. *Genome Med.* (2017) 9:20. doi: 10.1186/s13073-017-0410-8
72. Liu J, Kong X, Lee YM, Zhang MK, Guo LY, Lin Y, et al. Stk38 modulates Rbm24 protein stability to regulate sarcomere assembly in cardiomyocytes. *Sci Rep.* (2017) 7:44870.
73. Lu SH, Lee KZ, Hsu PW, Su LY, Yeh YC, Pan CY, et al. Alternative splicing mediated by RNA-binding protein RBM24 facilitates cardiac myofibrillogenesis in a differentiation stage-specific manner. *Circ Res.* (2022) 130:112–29. doi: 10.1161/CIRCRESAHA.121.320080
74. van den Hoogenhof MMG, van der Made I, de Groot NE, Damanafshan A, van Amersfoorth SCM, Zentilin L, et al. AAV9-mediated Rbm24 overexpression induces fibrosis in the mouse heart. *Sci Rep.* (2018) 8:11696. doi: 10.1038/s41598-018-29552-x
75. Ito J, Iijima M, Yoshimoto N, Niimi T, Kuroda S, Maturana AD. RBM20 and RBM24 cooperatively promote the expression of short enh splice variants. *FEBS Lett.* (2016) 590:2262–74. doi: 10.1002/1873-3468.12251
76. Upadhyay SK, Mackereth CD. Structural basis of UCUU RNA motif recognition by splicing factor RBM20. *Nucleic Acids Res.* (2020) 48:4538–50. doi: 10.1093/nar/gkaa168
77. Wollerton MC, Gooding C, Robinson F, Brown EC, Jackson RJ, Smith CW. Differential alternative splicing activity of isoforms of polypyrimidine tract binding protein (PTB). *RNA.* (2001) 7:819–32. doi: 10.1017/s1355838201010214
78. Zhang X, Chen MH, Wu X, Kodani A, Fan J, Doan R, et al. Cell-type-specific alternative splicing governs cell fate in the developing cerebral cortex. *Cell.* (2016) 166:1147–1162e1115. doi: 10.1016/j.cell.2016.07.025
79. Dauksaite V, Gotthardt M. Molecular basis of titin exon exclusion by RBM20 and the novel titin splice regulator PTB4. *Nucleic Acids Res.* (2018) 46:5227–38. doi: 10.1093/nar/gky165
80. Blech-Hermoni Y, Ladd AN. RNA binding proteins in the regulation of heart development. *Int J Biochem Cell Biol.* (2013) 45:2467–78.
81. Lorenzi P, Sangalli A, Fochi S, Dal Molin A, Malerba G, Zipeto D, et al. RNA-binding proteins RBM20 and PTBP1 regulate the alternative splicing of FHOD3. *Int J Biochem Cell Biol.* (2019) 106:74–83. doi: 10.1016/j.biocel.2018.11.009
82. Kruger M, Babicz K, von Frieling-Salewsky M, Linke WA. Insulin signaling regulates cardiac titin properties in heart development and diabetic cardiomyopathy. *J Mol Cell Cardiol.* (2010) 48:910–6. doi: 10.1016/j.yjmcc.2010.02.012
83. Zhu C, Yin Z, Tan B, Guo W. Insulin regulates titin pre-mRNA splicing through the PI3K-Akt-mTOR kinase axis in a RBM20-dependent manner. *Biochim Biophys Acta Mol Basis Dis.* (2017) 1863:2363–71. doi: 10.1016/j.bbadis.2017.06.023
84. Cai H, Zhu C, Chen Z, Maimaiti R, Sun M, McCormick RJ, et al. Angiotensin II influences Pre-mRNA splicing regulation by enhancing RBM20 transcription through activation of the MAPK/ELK1 signaling pathway. *Int J Mol Sci.* (2019) 20:5059. doi: 10.3390/ijms20205059

85. Nordgren KKS, Hampton M, Wallace KB. Editor's highlight: the altered DNA methylome of chronic doxorubicin exposure in sprague dawley rats. *Toxicol Sci.* (2017) 159:470–9. doi: 10.1093/toxsci/kfx150
86. Hutchinson KR, Saripalli C, Chung CS, Granzier H. Increased myocardial stiffness due to cardiac titin isoform switching in a mouse model of volume overload limits eccentric remodeling. *J Mol Cell Cardiol.* (2015) 79:104–14. doi: 10.1016/j.yjmcc.2014.10.020
87. van den Hoogenhof MMG, Beqqali A, Amin AS, van der Made I, Aufiero S, Khan MAF, et al. RBM20 mutations induce an arrhythmogenic dilated cardiomyopathy related to disturbed calcium handling. *Circulation.* (2018) 138:1330–42. doi: 10.1161/CIRCULATIONAHA.117.031947
88. Michel K, Herwig M, Werner F, Spiranec Spes K, Abesser M, Schuh K, et al. C-type natriuretic peptide moderates titin-based cardiomyocyte stiffness. *JCI Insight.* (2020) 5:e139910. doi: 10.1172/jci.insight.139910
89. Liss M, Radke MH, Eckhard J, Neuenschwander M, Dauksaite V, von Kries JP, et al. Drug discovery with an RBM20 dependent titin splice reporter identifies cardenolides as lead structures to improve cardiac filling. *PLoS One.* (2018) 13:e0198492. doi: 10.1371/journal.pone.0198492
90. Pawallek A, McElroy S, Samatov T, Mitchell L, Woodland A, Ryder U, et al. Identification of small molecule inhibitors of pre-mRNA splicing. *J Biol Chem.* (2015) 290:6005.

Conflict of Interest: The authors declare that the research was conducted in the absence of any commercial or financial relationships that could be construed as a potential conflict of interest.

Publisher's Note: All claims expressed in this article are solely those of the authors and do not necessarily represent those of their affiliated organizations, or those of the publisher, the editors and the reviewers. Any product that may be evaluated in this article, or claim that may be made by its manufacturer, is not guaranteed or endorsed by the publisher.

frontiers | Frontiers in Cardiovascular Medicine

ORIGINAL RESEARCH
published: 27 June 2022
doi: 10.3389/fcvm.2022.900313

Clinical Profile and Prognosis of Hereditary Transthyretin Amyloid Cardiomyopathy: A Single-Center Study in South China

Shuai Wang, Wenke Peng, Min Pang, Ling Mao, Daoquan Peng, Bilian Yu, Sha Wu, Die Hu, Yang Yang, Jia He and Mingqi Ouyang*

Department of Cardiovascular Medicine, Second Xiangya Hospital, Central South University, Changsha, China

Background: Hereditary transthyretin amyloid cardiomyopathy (ATTR-CM) is a genotypically heterogeneous disorder with a poor prognosis. There is limited literature describing the variants responsible for ATTRv in areas outside the United State, the United Kingdom and Europe. This study was performed to describe the clinical characteristics and genotypic profiles of this disease in South China.

Methods: This was a single-center retrospective study that evaluated 29 patients with a confirmed diagnosis of hereditary transthyretin amyloid cardiomyopathy enrolled from January 2016 to November 2021.

Results: 93.1% patients were male and the median age of symptom onset was 53 (46, 62.5) years old. The initial manifestations of ATTR-CM were cardiovascular symptoms (55.2%), neuropathy (41.4%) and vitreous opacity (3.4%). Phenotypes at diagnosis were mixed (82.8%), predominant cardiac (6.9%), neurological (6.9%) and ophthalmic (3.4%). Poor R-wave progression (41%), pseudo-infarct (31%) and low-voltage (31%) patterns were common findings on electrocardiogram. Unexplained increased wall thickness was observed in all 29 patients, with mean septal and posterior wall thicknesses of 14.25 ± 6.26 mm and 15.34 ± 2.84 mm, respectively. Diastolic dysfunction was also seen in all 29 patients, and 17 (58%) had a restrictive fill pattern at diagnosis. Nine different missense mutations of the TTR gene were found in 29 patients from 23 families, with c.349G>T (p.Ala117Ser) the most common mutation. The median survival time after diagnosis was 47.6 (95% CI 37.9-57.4) months, with 1, 3 and 5-year survival rates of 91.2%, 74% and 38% respectively. Patients with advanced heart failure (National Amyloidosis Staging stage II/III) had worse survival than stage I [Breslow (Generalized Wilcoxon), $\chi 2 = 4.693$, $P = 0.03$)].

Conclusions: ATTR amyloidosis genotypes and phenotypes are highly heterogeneous. Advanced heart failure predicts a poor prognosis. Understanding the different clinical profiles of ATTR cardiac amyloidosis with different genotype is important to its early recognition.

Keywords: hereditary, transthyretin amyloidosis, cardiomyopathy, prognosis, China

OPEN ACCESS

Edited by:
Jeffrey Shi Kai Chan, Cardiovascular Analytics Group, Hong Kong SAR, China

Reviewed by:
Concetta Zito, University of Messina, Italy
Marcus V. Pinto, Mayo Clinic, United States

****Correspondence:***
Daoquan Peng
pengdq@csu.edu.cn

Specialty section:
This article was submitted to Heart Failure and Transplantation, a section of the journal Frontiers in Cardiovascular Medicine

Received: *20 March 2022*
Accepted: *07 June 2022*
Published: *27 June 2022*

Citation:
Wang S, Peng W, Pang M, Mao L, Peng D, Yu B, Wu S, Hu D, Yang Y, He J and Ouyang M (2022) Clinical Profile and Prognosis of Hereditary Transthyretin Amyloid Cardiomyopathy: A Single-Center Study in South China. Front. Cardiovasc. Med. 9:900313. doi: 10.3389/fcvm.2022.900313

INTRODUCTION

Hereditary transthyretin amyloidosis (ATTRv) represents a group of severe diseases with a broad spectrum of genotypes and phenotypes caused by transthyretin (TTR) gene mutations. ATTR is the result of dissociation of the transthyretin tetramer into monomers that mis-fold, forming amyloid deposits in the extracellular space (1). The most common manifestations of ATTR are polyneuropathy and cardiomyopathy (2). As our understanding of the molecular mechanisms behind ATTR amyloidosis improves, disease-modifying treatments including stabilizing molecular (tafamidis) and genetic silencers (partisiran and inotersen) have been made available. As pharmacotherapy is more effective in the early stages of the disease, the early diagnosis of ATTR by understanding its genotype-phenotype correlations is important (3–5).

More than 120 mutations of the TTR gene have been described, and as of December 2021 there are 68 pathogenic/likely pathogenic variants of the TTR gene listed in the National Center for Biotechnology Information ClinVar database (6–8). Some genotype-phenotype variability has been reported. Although the THAOS registry collected ATTR phenotypes and genotypes from continental Western Europe and the United States, few studies have been performed in China. Two recent retrospective cohort studies revealed that the mutation of TTR in Chinese patients may be quite different from that seen in the United States and Europe (9, 10). Further, those two studies mainly discussed ATTRv patients from northern China and one study focused on ATTRv patients with neuropathy as main symptom. Here, we report the phenotype and genotype of 29 patients with ATTRv cardiomyopathy (ATTRv-CM) from 23 unrelated South Chinese families.

METHODS

Study Design and Population

This was a descriptive, observational, and retrospective study that included patients diagnosed with hereditary ATTRv-CM at our institution from January 2016 to November 2021. The study was undertaken in accordance with the Declaration of Helsinki and was approved by the ethics committee of Second Xiangya Hospital. Due to the retrospective nature of this study, informed consent was waived for patients who had died. Otherwise, all patients provided written informed consent.

Diagnosis of Hereditary ATTR Cardiac Amyloidosis

The diagnosis of hereditary ATTRv-CM was established by clinical presentation, family history, echocardiography, tissue biopsy and DNA sequencing for the presence of a mutation in the TTR gene. Cardiac magnetic resonance (CMR) and ^{99m}technetium (^{99m}Tc)-pyrophosphate (PYP) scintigraphy were performed in select cases. All included patients had a positive tissue biopsy (endocardium or extracardiac, e.g., abdominal adipose tissue or vitreous body) for amyloidosis and a pathogenic/likely pathogenic TTR variant. Light chain amyloidosis was ruled out by confirming a normal free light chain ratio and the absence of detectable serum and/or urine monoclonal protein. Patients without a related gene mutation on TTR gene sequencing were excluded.

The date of symptom onset was reported by the patient as the date on which symptoms related to amyloidosis first were noted. The date of diagnosis was the date on which the diagnosis of amyloidosis was confirmed histologically.

Phenotype categories based on clinical presentation at the time of diagnosis were: 1) predominantly cardiac. 2) predominantly neurological. 3) mixed (cardiac and neurological); and 4) ophthalmic. Patients with a predominantly cardiac phenotype were those (1) with heart failure, dyspnea and/or abnormal electrocardiogram findings caused by rhythm disturbance and (2) who did not have more than mild neurological or gastrointestinal symptoms (excluding erectile dysfunction, constipation and carpal tunnel syndrome). Patients with a predominantly neurologic phenotype were those with (1) walking disability of any severity, other neurologic symptoms of any severity or gastrointestinal symptoms (early satiety, nausea, vomiting, unintentional weight loss, diarrhea, constipation or fecal incontinence) of any severity and (2) who did not have heart failure, dyspnea, or an abnormal ECG due to a rhythm disturbance. Patients with a (3) mixed phenotype were patients who had at least 1 cardiac and neurological symptom as described above. Patients with (4) an ophthalmic phenotype had vitreous opacity with none of the cardiac or neurological symptoms described above.

Cardiomyopathy was defined as an end-diastolic thickness of the left ventricular wall $>$ 1.2 cm (in the absence of any other plausible causes of LV hypertrophy). Other clues suggestive of cardiac amyloidosis included granular sparkling appearance of the ventricular myocardium, increased thickness of the atrioventricular valves or the interatrial septum and reduced tissue doppler e' velocities. CMR and ^{99m}Tc-PYP were performed in select cases. Characteristic CMR findings of (1) the inability to suppress or "null" the myocardial signal or (2) the presence of diffuse subendocardial or transmural enhancement patterns on late gadolinium enhancement CMR were recorded. Grade 2 or 3 cardiac uptake on ^{99m}Tc-PYP scintigraphy was also recorded.

N-terminal pro-B type natriuretic peptide (NT-proBNP), estimated glomerular filtration rate (eGFR), cardiac troponin (cTnT), modified poly neuropathy disability (PND) score and the U.K. National Amyloidosis Staging (NAC) and New York Heart Association (NYHA) stages were recorded. NAC Stage I is defined as NT-proBNP $\leq$ 3000 ng/L and eGFR $\geq$ 45 mL/min, and NAC stage III was defined as NT-proBNP>3000 ng/L and eGFR<45 mL/min. The remainder of the patients were assigned to NAC stage II.

Neurological Work-Up

Neurological examination included an assessment of motor, cerebellar and reflex function as well as screening for sensory function. Muscle strength was documented according to the Medical Research Council (MRC) scale (5/5 normal strength, 0/5 no contractions). Motor and sensory nerve conduction studies were performed on patients with reported neurologic symptoms. The PND score was used to stage patients with ATTRv

and polyneuropathy at baseline. PND I was defined as sensory disturbances in the extremities but preserved walking capacity; PND II was defined as difficulty walking but without the need for a walking stick; PND III was defined as sticks or crutches required for walking; and PND IV was defined as confined to a wheelchair or bed.

Genetic Testing of the TTR Gene

Genomic DNA was isolated from whole peripheral blood using standard techniques. Exon 1–4 of the *TTR* gene were amplified with polymerase chain reaction. Sequences of the *TTR* gene (NM_000371.3; NG_009490.1) were analyzed using the Applied BioSystems SeqScape software v4.0 (Carlsbad, USA) and the DNA Dynamo Sequence Analysis Software (North Wales, UK). The datasets presented in this study can be found in an online repository. The name of the repository and its accession numbers can be found in the supplementary material (**Supplementary Table 1**). Genetic testing and clinical penetrance assessments were performed on family members for probands if available.

Follow-Up

Patient follow-ups at 6 to 12-month intervals included an ECG, NT-proBNP and yearly echocardiogram. Mutation carriers were surveilled via regular (yearly) telephone contact.

Statistical Analyses

Continuous variables are reported as mean ± SD or median and interquartile range (IQR) (for non-normal distributions). Categorical variables are reported as percentages. Kaplan-Meier survival was calculated from the date of the original diagnosis to the date of death or the most recent contact. Gehan-Breslow-Wilcoxon method was used to compare survival curves. All tests were 2-tailed and a P-value < 0.05 was considered statistically significant. Statistical analyses were performed using SPSS Statistics (version 26. IBM Corp., Chicago, IL, USA).

RESULTS

Clinical Characteristics of Patients With ATTR Cardiac Amyloidosis

The clinical characteristics at diagnosis of the 29 patients are summarized in **Tables 1**, **2**. Twenty-seven (93.1%) patients were male. The median age at symptom onset was 53 (46, 62.5) years and the median age at diagnosis was 56 (47.75–66.25) years. The median time from symptom onset to diagnosis was 24 (12−24) months and the median course from diagnosis to the last visit was 15 (6.5–37.5) months.

Dyspnea on exertion and limited physical capacity were the initial complaints that prompted a comprehensive cardiological examination in 16 cases (55.2%). Another 12 (41.4%) patients presented with distal sensory disturbances and/or weakness predominantly of the lower limbs. One patient reported vitreous opacity as their initial manifestation and had asymptomatic cardiac hypertrophy at diagnosis.

Twenty-four (82.8%) patients presented with a mixed phenotype that included both cardiomyopathy and neuropathy, while 2 (6.9%) had a predominantly cardiac phenotype and 2 (6.9%) had a predominantly neurological phenotype. One patient (3.4%) presented with vitreous opacity with asymptomatic myocardial hypertrophy. Peripheral and autonomic nerve dysfunction were found in 25 (86.2%) and 14 (48.3%) subjects at diagnosis, respectively. Six patients (20.7%) had a history of uni- or bilateral carpal tunnel syndrome. Lumber spinal stenosis was reported in one patient. The PND score was used to describe the severity of the peripheral neuropathy (**Table 1**). At diagnosis, 72.4% (21) had severe heart failure (NYHA III/IV), 3.4% (1) had mild heart failure (NYHA II) and 24.1% (7) had asymptomatic myocardial hypertrophy (**Table 1**). Elevated NT-proBNP and cTnT were found in 29 (100%) and 28 (97%) patients, respectively. The median NT-proBNP and cTnT levels were 2789 (1206–5024) pg/ml and 61.5 (42.8–88.9) pg/ml at diagnosis. Only one patient had an eGFR < 45 and the median eGFR was 81.7 (66.4–93.6) ml/min/1.73 m^2 (**Table 2**). Of the 29 patients, 19 (65.6%) were NAC stage I, 9 (31%) stage II and 1 (3.4%) stage III.

Electrocardiogram abnormalities were evident in 15 (51.7%) patients at diagnosis. Two (6.9%) had atrial fibrillation, 5 (17.2%) presented with an atrial-ventricular block and 2 went on to require a permanent pacemaker. The classic low-voltage pattern of ATTR-CM was found in 9 (31%) patients, while a low-voltage pattern according to the Sokolow criteria was found in 8 (27.5%). A pseudo-infarct pattern was found in 9 (31%) patients and poor R wave progression was found in 12 (41%, **Table 2**).

Unexplained increased wall thickness (>12 mm) and diastolic dysfunction were observed in 29 (100%) patients. Two (6.9%) had systolic dysfunction with an ejection fraction <50%. Restrictive filling (e'<5 cm/s) was present in 17 (58%) patients at diagnosis. Pericardial effusions were present in 9 patients (31%). The mean septal and posterior wall thicknesses of the cohort were 16.39±3.04 mm and 15.34±2.84 mm, respectively, and the mean systolic left atrial diameter was 39.47±5.54 mm. The mean LVEF was 52.65±10.6%. CMR was performed on 16 (55.2%) patients to diagnose ATTR cardiac amyloidosis, all of which showed diffuse subendocardial or transmural LGE and abnormal gadolinium kinetics. ^{99m}TC-PYP scintigraphy was performed on 9 patients (31%). Seven had grade 3 cardiac uptake and 2 patients had grade 2 uptake. Biopsies were performed on all patients, and originated from the abdominal fat (28), endomyocardium (1) or vitreous body (1) (**Table 2**). All samples were positive on Congo red staining and TTR immunochemistry. Four patients (9.5%) in this cohort were on tafamidis post-enrollment, and no patient received a liver transplant.

Genetic Spectrum of TTR Mutations

Genetic testing of the probands and their family members identified 9 different missense *TTR* mutations [Asp18Asn(p.Asp38Asn), Ser23Asn(p.Ser43Asn), Glu42Gly (p.Glu62Gly), Gly47Glu(p.Gly67Glu), Leu55Arg(p.Leu75Arg), Thr59Lys(p.Thr79Lys), Glu61Lys(p.Glu81Lys), His108Arg (p.His108Arg), Ala97Ser(p.Ala117Ser)] and 1 small deletion mutation (3'UTR c.624_632 del GACTTCTCC) in 29 patients from 23 families. Pedigree analysis found another 11 asymptomatic mutation carriers without electrocardiographic and echocardiographic abnormalities. The predominant genotypes identified in ATTR-CA were the Ala97Ser

TABLE 1 | Clinical Manifestations of ATTRv-CM and the *TTR* variant Ala97Ser.

	All ($n = 29$)	Ala97Ser ($n = 11$)	Non Ala97Ser ($n = 18$)	*p*-value
General characteristics				
Male, *n* (%)	27 (93.1)	10 (91)	17 (89.5)	0.702
Age of symptom onset, y	53 (46–62.5)	65 (62–66)	50 (45–58.5)	<0.001
Age at diagnosis, y	56 (47.8–66.3)	68 (64–72.5)	50.5 (46.8–59.3)	<0.001
Time from symptom onset to diagnosis, m	24 (12–48)	48 (24–102)	24 (13–45)	0.084
Course from diagnosis to last visit, m	15 (6.5–37.5)	13 (8–30)	19 (5.75–45.75)	0.65
Initial presentation				
Neuropathy as initial presentation, *n* (%)	12 (41.4)	11 (100)	15 (83.3)	0.27
Cardiovascular symptom as initial presentation, *n* (%)	16 (55.2)	0 (0)	16 (88.9)	<0.001
Vitreous opacity, *n* (%)	1 (3.4)	0 (0)	1 (5.6)	1.0
Clinical presentation at diagnosis				
HF, *n* (%)	23 (79.3)	8 (72.7)	15 (88.2)	0.35
NYHA stage, *n* (%)				
I	7 (24.1)	3 (27)	4 (36.4)	0.65
II	1 (3.4)	1 (9.1)	0 (0)	0.38
III	14 (48.3)	5 (45.5)	9 (52.9)	1.0
IV	7 (24.1)	2 (18.2)	5 (29.4)	0.68
Typical echocardiography at diagnosis, *n* (%)	29 (100)	11 (100)	19 (100)	1.0
Abnormal ECG, *n* (%)	15 (51.7)	5 (45.5)	10 (55.6)	0.71
NAC staging score, *n* (%)				
Stage I	21 (67.7)	8 (72.7)	12 (70.6)	1.0
Stage II	6 (19.4)	3 (27.3)	3 (17.6)	0.65
Stage III	4 (12.9)	0 (0)	2 (11.8)	0.51
Somatic neuropathy, *n* (%)				
(Diarrhea, Constipation, Orthostatic hypotension, Upper gastrointestinal tract symptoms, eg. early satiety, dyspepsia, dysphagia, vomiting)	14 (48.3)	6 (54.5)	8 (47.1)	0.70
Peripheral neuropathy, *n* (%)	25 (86.2)	11 (100)	14 (82.4)	0.26
History of Carpal tunnel syndrome, *n* (%)	6 (20.7)	2 (18.2)	4 (23.5)	0.73
Lumber Spinal stenosis, *n* (%)	1 (3.4)	1 (9.1)	0 (0)	0.38
PND score at diagnosis				
0	4 (12.9)	0 (0)	4 (22.2)	0.27
I	8 (25.8)	1 (9.1)	7 (38.9)	0.11
II	9 (29)	3 (27.3)	6 (35.3)	0.001
III	7 (22.6)	6 (54.5)	1 (5.9)	0.006
IV	3 (9.7)	1 (9.1)	2 (11.8)	0.14
Phenotype				
Predominantly cardiac, *n* (%)	2 (6.9)	0 (0)	2 (11.1)	0.51
Predominantly neurological, *n* (%)	2 (6.9)	1 (9)	1 (5.6)	1.0
Mixed, *n* (%)	24 (82.8)	10 (91)	14 (77.8)	0.62
Ocular, *n* (%)	1 (3.4)	0 (0)	1 (5.6)	1.0
Patients receiving tafamidis, *n* (%)	4 (9.5)	3 (25%)	1 (5.6)	0.14

Values are mean ± SD, n (%), or median (25th to 75th percentile). HF, heart failure; NYHA, New York Heart Association; NAC, National Amyloidosis Staging; PND, polyneuropathy disability.

(p.Ala117Ser) mutation (11/29, 37.9%) followed by Thr59Lys (p.Thr79Lys) (5, 17.2%) (**Figure 1**). Of these variants, Asp18Asn, Ser23Asn, Glu42Gly, Gly47Glu, Thr59Lys, Glu61Lys, His88Arg and Ala97Ser were associated with the mixed phenotype while Leu55Arg was associated with the ophthalmic phenotype. The deletion mutation was found in a patient with a cardiac phenotype (**Table 3**).

Ala97Ser was the most common mutation in this cohort. 72.7% (8/11 cases) of patients carrying the Ala97Ser presented with evidence of heart failure at confirmed diagnosis of ATTRv cardiac amyloidosis, with 63.7% (7/11) having NYHAIII/IV (**Table 1**). All patients with Ala97Ser mutations initially presented with neurological dysfunction, but cardiac symptoms followed 2–9 years later. The median age of onset of neurological

TABLE 2 | Complementary baseline tests for ATTRv–CM and the *TTR* variant Aal97Ser.

	All (*n* = 29)	**Aal97Ser (*n* = 11)**	**Non–Ala97Ser (*n* = 18)**	***p*–value**
Biomarkers				
NT–proBNP, pg/ml	2789 (1206–5024)	2081 (973–3706.3)	2722 (1425–5245)	0.30
cTnT, pg/ml	61.5 (42.8–88.9)	45.5 (42.1–73.7)	85.3 (27.7–125.5)	0.41
eGFR, ml/min/1.73 m^2	81.7 (66.4–93.6)	90 (83.7–95.4)	79.3 (64.5–94.6)	0.16
Electrocardiogram				
Atrial fibrillation/flutter, *n* (%)	2 (7)	0 (0)	2 (25)	0.51
AV block, *n* (%)	5 (17)	0 (0)	5 (27.8)	0.13
RBBB/LBBB, *n* (%)	3 (10)	1 (9.1)	2 (25)	1.0
Pacemaker, *n* (%)	2 (7)	0 (0)	2 (25)	0.51
LV hypertrophy (Sokolow), *n* (%)	0 (0)	0 (0)	0 (0)	1.0
Low voltage				
Classic criteria[a], *n* (%)	9 (31)	5 (45.5)	4 (22)	0.24
Sokolow[b], *n* (%)	8 (58)	3 (27.3)	5 (27.8)	1.0
Pseudo–infarct pattern, *n* (%)	9 (31)	3 (27.3)	6 (33.3))	1.0
Poor Precordial R wave progression, *n* (%)	12 (41)	5 (45.5)	7 (38.9)	1.0
Echocardiography				
LVH, *n* (%)	29 (100)	11 (100)	18 (100)	1.0
LVEF<50%, *n* (%)	2 (6.8)	1 (9.1)	1 (5.6)	1.0
LV diastolic dysfunction, *n* (%)	29 (100)	11 (100)	18 (100)	1.0
Restrictive filling (e' <5 cm/s)	17 (58)	6 (54.5)	11 (61.1)	1.0
Pericardial effusion, *n* (%)	9 (31)	3 (27.3)	6 (33.3)	
LVIDd, mm	47.74 ± 5.37	43.16 ± 3.18	43.33±4.50	0.99
IVS thickness, mm	16.39±3.04	15.83±4.26	17.00±2.60	0.59
PWT, mm	15.34 ± 2.84	14.50 ± 2.26	17.00±2.61	0.08
Left atrial size, mm	39.47 ± 5.54	38.83 ± 5.51	43.50±4.46	0.68
LVEF, %	52.65 ± 10.65	55.17 ± 13.87	49.83±5.12	0.70
PA systolic pressure, mm Hg	33.36(26.16–35.18)	32.00 (26.16–34.59)	28.00 (24.36–30.00)	0.37
e' average, cm/s	4.64 ± 1.11	5.33 ± 1.25	4.07±0.62	0.05
Cardiac magnetic resonance at diagnosis	***n* = 17**	***n* = 5**	***n* = 12**	
Inability to suppress or "null" the myocardial signal, *n* (%)	17 (100)	5 (100)	12 (100)	1.0
Diffuse subendocardial/transmural enhancement pattern, *n* (%)	17 (100)	5 (100)	12 (100)	1.0
Cardiac uptake grading in ^{99m}Tc–PYP scintigraphy at diagnosis	***n* = 9**	***n* = 5**	***n* = 4**	
Grade 0	0 (0)	0 (0)	0 (0)	
Grade 1	0 (0)	0 (0)	0 (0)	
Grade 2	2 (22.2)	1 (20)	1 (25)	1.0
Grade 3	7 (77.8)	4 (80)	3 (75)	1.0

Values are mean ± SD, n (%), or median (25th to 75th percentile). NT–proBNP, N–terminal pro–B type natriuretic peptide; cTnT, cardiac troponin; eGFR, estimated glomerular filtration rate; AV, atrioventricular; RBBB, right bundle branch block; LBBB: left bundle branch block; LV, left ventricular; LVH, left ventricular hypertrophy; LVEF, left ventricular ejection fraction; LVIDd, left ventricular internal diameter at end–diastole; IVS, interventricular septum; PWT, posterior wall thickness; PA, pulmonary artery.

[a] *<0.5 mV in all limb leads or < 1.0 mV in all precordial leads.*

[b] *sum of S in V1 and R in V5/V6 < 25mm.*

symptom related to ATTR amyloidosis in patients carrying the Ala97Ser variant was 65 (62–67) years old and the median time from neurological symptom onset to diagnosis of ATTRv-CM was 48 (24–102) months.

Survival

During January 2016 to November 2021, 29 patients were diagnosed with hereditary ATTRv-CM and followed up at our institution. The date when symptoms related to ATTRv began, (which was 30 (12, 54) months before diagnosis of ATTR-CM), was recorded according to the patient's report. The mortality rate of the cohort over a median follow-up of 14 (5.75, 32.25) months was 7/29 (24%). The estimated median survival times after initial symptom onset related to ATTRv and at confirmed diagnosis of ATTRv-CM by Kaplan-Meier survival curve analysis were 131 (95%CI 88.6–173.7) and 47.6 (95%CI 37.9–57.4) months, respectively. According to Kaplan-Meier survival curve analysis, the estimated 3-, 5- and 10-year survival rates after symptom

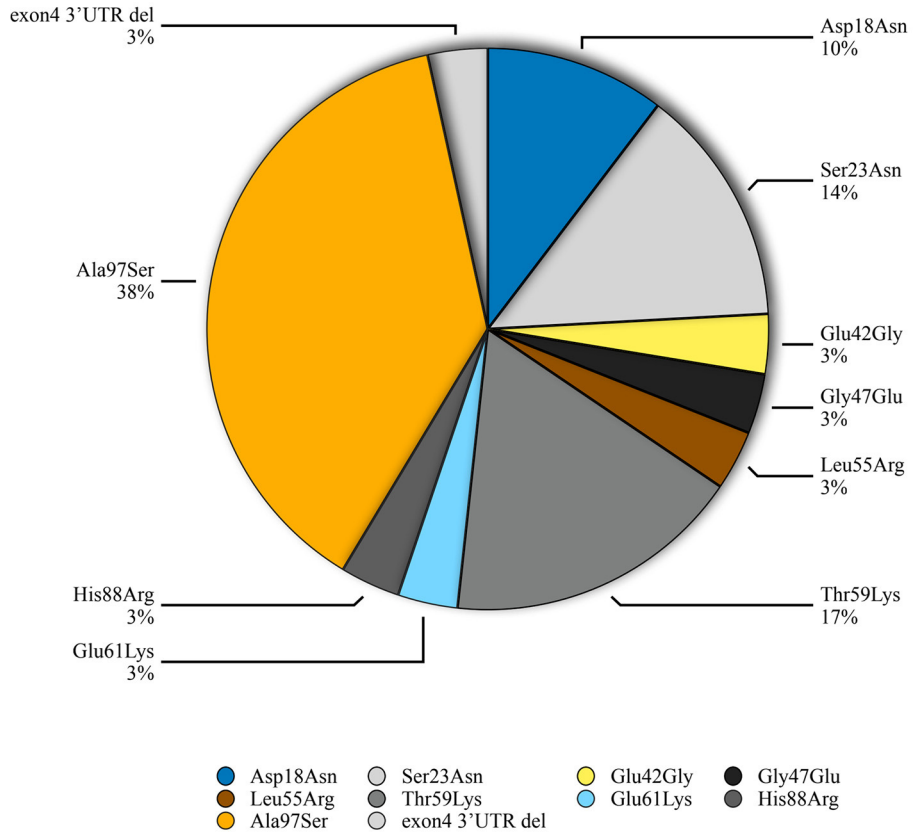

FIGURE 1 | Distribution of *TTR* mutations in a cohort of ATTR-CA patients from South China.

onset were 90%, 70% and 52.6%, respectively (**Figure 2A**). The overall 1-year survival rate after diagnosis was 91.2%, and the 3- and 5-year survival rates were 74% and 38%, respectively (**Figure 2B**).

For patient carrying Ala97Ser variant, survival curve analysis revealed the estimated mean survival time after symptom onset and at diagnosis were 181(95%CI 120.2, 241.8) months and 38.5 (95%CI 30.9, 46.1) months. Patient with other variants had estimated mean survival time of 102 (95%CI 73.1, 132.1) months after symptom onset and 43.9 (95%CI 31.3, 56.4) months at diagnosis. Cumulative survival rate at 150 months after symptom onset was 66.7% in Ala97Ser and 0% in other variants. The difference in survival curve for Ala97Ser and other variants at symptom onset was not significant [Breslow (Generalized Wilcoxon), $\chi 2 = 2.92$, $p = 0.087$] (**Figure 3A**). No significant difference was found in survival curve between patient carrying Ala97Ser and other variants at confirmed diagnosis. [Breslow (Generalized Wilcoxon), $\chi 2 = 0.859$, $p = 0.35$] (**Figure 3B**).

Patient at an early disease stage (NAC stage I) tended to have a lower mortality rate, with a median survival time of 48 months (95%CI 39–63 month) and a cumulative survival rate at 60 months of 46.7% [Breslow (Generalized Wilcoxon), $\chi 2 = 4.693$, $p = 0.03$]. In contrast, the median survival time of patients at a later disease stage (NAC II, III) was 33 months (95%CI 13.7–55.3), with a cumulative survival rate at 60 months of 0% (**Figure 3C**) All deaths were observed in patients with NYHA III-IV heart failure.

DISCUSSION

Male predominance (93%) was observed in this cohort, which was higher than previous reports on ATTRv-CM whose samples were approximately 70% (11–13). This may be due to the small sample size of this study. The underlying mechanism for male predominance is unclear. The small sample size of women did not permit summarization of the sex-related clinical characteristics of ATTRv-CM. However, a recent systematic literature review on sex-related differences in transthyretin amyloid cardiomyopathy revealed that women tended to have lower interventricular septal and posterior wall thicknesses, smaller left ventricular end diastolic diameters and a higher LV ejection fraction. It was postulated that the disparity in the incidence of ATTRv-CM between sexes may be due to either the cardioprotective effects of estrogen or sex-related differences in clinical presentation or disease characteristics (11).

A mixed phenotype was most common presentation in this cohort (82.8%), while a predominantly cardiac phenotype and neurological phenotype was seen in 6.9% of patients each. ATTRv phenotype is associated with *TTR* mutations.

While some mutations are associated with a predominantly cardiac phenotype, others are primarily related to a neurological phenotype. Previously reported common cardiac mutations (Val122Ile, leu111Met, Thr60Alr, Ile68Leu) in ATTRv were not identified in our cohort (14). However, we found that non-cardiac mutations such as Asp18Asn, Ser23Asn, Glu42Gly, Gly47Glu, Thr59Lys, Glu61Lys, His88Arg and Ala97Ser were associated with a cardiac phenotype with or without neurologic symptoms. These differences in genotype-phenotype relationship may be the result of their diagnosis at different disease stages.

Ten different *TTR* gene mutations, including 9 missense variants and 1 small deletion mutation, were identified. All of the missense variants have been listed as pathogenic or likely pathogenic in the TTR mutation and ClinVar databases (**Table 4**) (15–23). The missense mutations were related to the mixed phenotype. Glu61Lys, which was previously found to cause ATTR neuropathy, had never been reported in ATTR-CM. The cardiac mutations Asp18Asn and His68Arg also caused neuropathy in our study. The small deletion *TTR* mutation (c.624_632delGACTTCTCC) was located outside the coding region in exon 3 of the *TTR* gene. As the patient's family history could not be collected due to the limited medical records of the deceased parents, it could not be excluded that this variant of unknown significance occurred by chance in a patient with wild-type ATTR.

TABLE 3 | Genotype distribution in probands and family members.

TTR mutation	Overall *N = 40, n (%)*	Symptomatic patients *N = 29, n (%)*	Associated phenotype in the cohort
A97S	16 (40)	11 (37.9)	N, H
D18N	4 (10)	3 (10.3)	N, H
E42G	1 (2.5)	1 (3.4)	N, H
E61K	1 (2.5)	1 (3.4)	N, H
G47E	1 (2.5)	1 (3.4)	N, H
H88R	1 (2.5)	1 (3.4)	N, H
L55R	1 (2.5)	1 (3.4)	E, H
S23N	4 (10)	1 (3.4)	N, H
T59K	8 (20)	5 (17.2)	N, H
Exon3 3'UTR c.624_632delGACTTCTCC	1 (2.5)	1 (3.4)	H

N, neurological; H, Heart; E, eye.

In this study, 10 different mutations ($n = 40$) have been identified in probands and family members, with the most common being Ala97Ser ($n = 16$; 40%). In addition, Ala97Ser is the most common mutation in symptomatic patient ($n = 11$;37.9%). This was different in the United States, where Val1122Ile (p.Val142Ile) and Thr60Ala (p.T80A) were the most common mutations (14). In European countries, Val30Met was the most frequent mutation in subjects with ATTR in the THAOS registry, followed by Ile68Leu (12). This discrepancy may reflect the heterogeneity of ATTR genotypes between different countries. Ala97Ser has been previously found to be a common ATTR mutation in cohorts of Chinese patients with predominant neurologic phenotypes, including patients from north China and Taiwan. It has also been reported in Chinese Malaysians (10, 24–27). (**Supplementary Table 2**) Similar with previous studies, male predominance was observed in Ala97Ser. Consistant with other studies, our study found that all patients with Ala97Ser initially presented with a predominantly neurologic phenotype in the early stages of disease. However, the proportion of

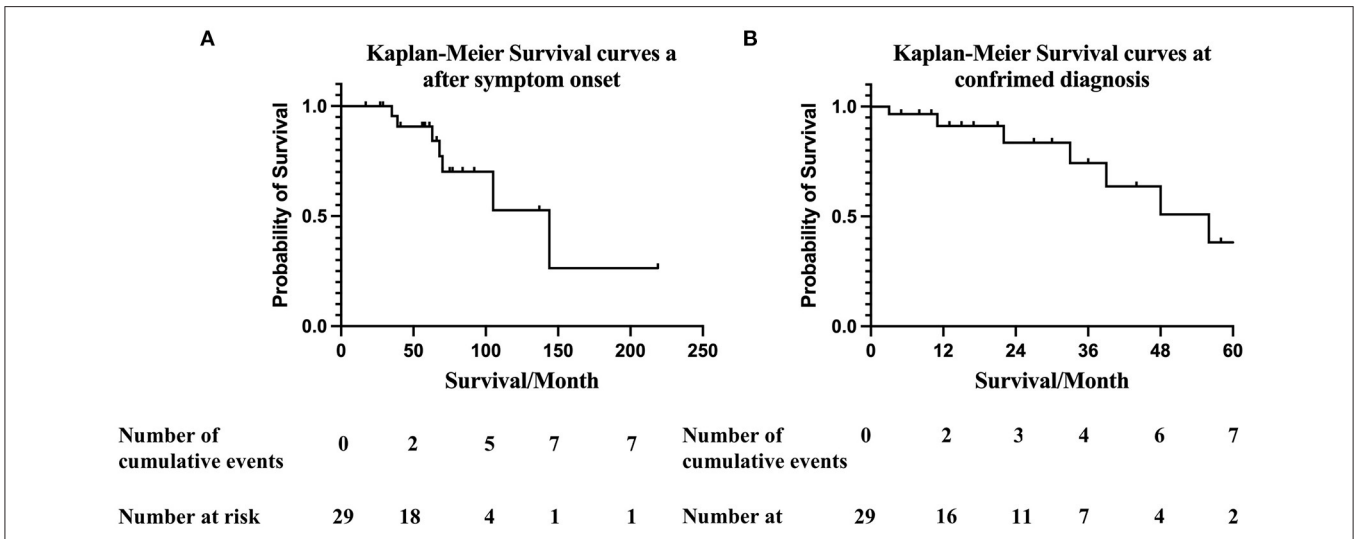

FIGURE 2 | (A) Kaplan-Meier survival curves of data obtained from ATTR-CA symptom onset. Overall survival at 12-, 36-, 60-, and 120- months after symptom onset were 100%, 90%, 70% and 52.6%, respectively. Numbers below the plot represent the number of subjects at risk at each time point. Cumulative events refer to all-cause death. The median survival time after symptom onset was 131 (95%CI 88.6–173.7) months. **(B)** Kaplan-Meier survival curves at confirmed diagnosis. Overall survival at 12-, 36-, and 60- months was 91.2%, 74%, and 38% respectively. Numbers below the plot represent the number of subjects at risk at each time point. Cumulative events refer to all-cause death. The estimated median survival time after confirmed diagnosis of ATTRv-CM was 47.6 (95%CI 37.9–57.4) months.

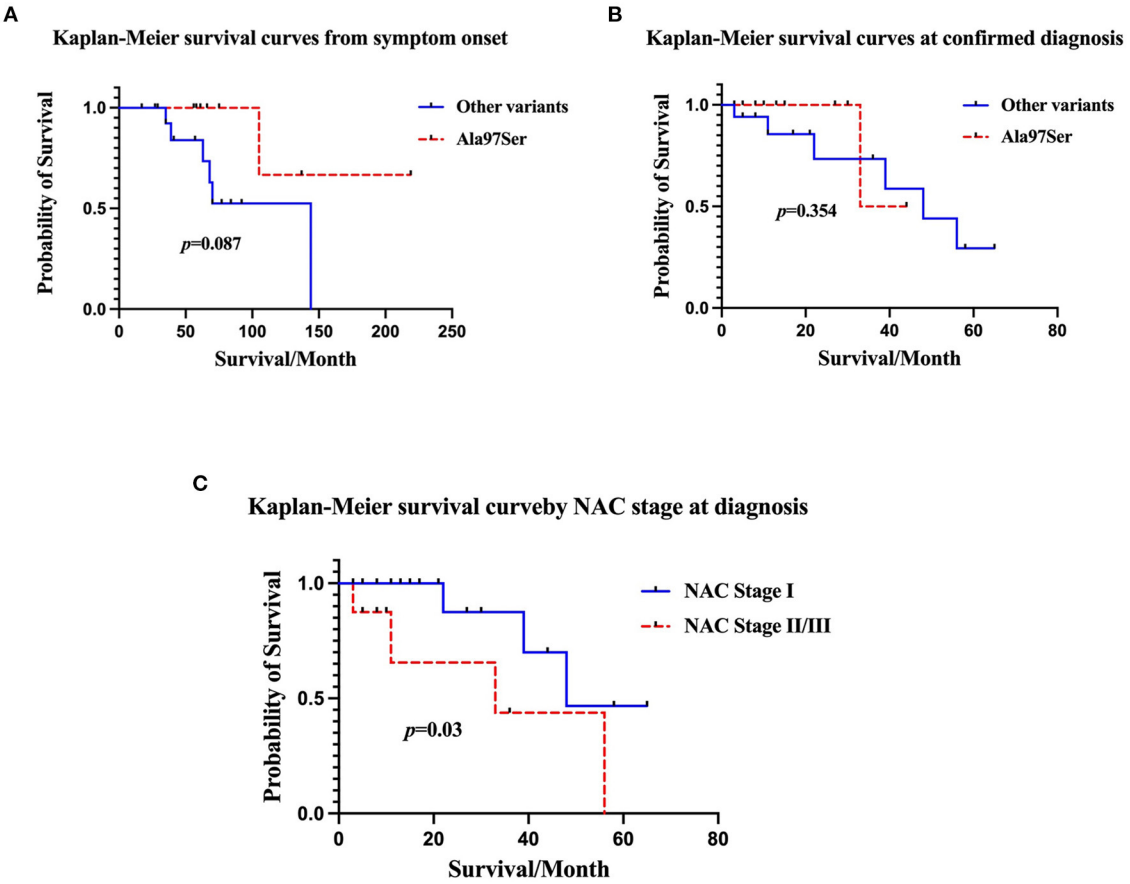

FIGURE 3 | (A) Comparison of Kaplan-Meier survival curves of data obtained from ATTR-CA symptom onset between patients with Ala97Ser and other variants. There was no significant difference in survival in patients with Ala97Ser and other variants [Breslow (Generalized Wilcoxon), $\chi 2 = 2.92$, $p = 0.087$]. **(B)** Comparison of Kaplan-Meier survival curves at confirmed diagnosis between patients with Ala97Ser and other variants. Survival after diagnosis was not significantly different in patients with Ala97Ser and other variants [Breslow (Generalized Wilcoxon), $\chi 2 = 0.859$, $p = 0.35$]. **(C)** Kaplan-Meier survival curve for patients grouped by NAC stage at diagnosis. Patients with NAC stage II/III disease had worse survival than those with NAC stage I disease [Breslow (Generalized Wilcoxon), $\chi 2 = 4.693$, $p = 0.03$)]. The median survival time of patients in NAT stage I was 48 months (95%CI 39–63) and the cumulative survival at 60 months was 46.7%. The median survival time of patients in NAC stage II/III was 33 months (95%CI 13.7–55.3) and the cumulative survival at 60 months was 0%.

patients developing cardiomyopathy as the disease progressed was higher (72.7%) than previous reports. Most Ala97Ser patients exhibited a mixed phenotype at their time of diagnosis in our study, which suggests that diagnosis was delayed until a late disease stage. This may be attributed to the difficulty with diagnosing ATTR in patients with isolated peripheral neuropathy symptoms, especially when reg flag symptoms such as carpal tunnel syndrome and lumber stenosis were rarely presented in this cohort. In this situation, family history and genetic examination were important to the early diagnosis of an ATTR patient with a neurological phenotype. On the other hand, CMR and ^{99m}Tc-PYP scintigraphy may help to identify myocardial involvement in patients who does not report symptom of heart failure due to limited physical activity caused by neuropathy.

Survival is poor in patients with ATTR cardiac amyloidosis. Although survival varies by genotype, phenotype, and disease stage, most series have reported a median survival of 2.5–3.5 years for patients with heart failure (8). There was a poorer prognosis in the present work for subjects with more severe heart failure, with a 5 year survival rate of <20% for those with NYHA III-IV disease. Several studies have noted the prognostic role of NT-proBNP (28). The NAC staging system includes NT-proBNP and eGFR and has a good prognostic accuracy (29). Patients with advanced NAC stage (stage 2, 3) had a poor prognosis (median survival: 34.5 months, 3-year survival rate: 43%). More advanced NYHA classification at diagnosis also tended to predict a poor prognosis, although there was no statistical significance due to the limited sample size of our study. Phenotype, genotype, initial manifestation and severity of peripheral neuropathy as shown by PND score were not predictive in our study.

The natural average life expectancy is 9 to 13 years after the symptom onset and death usually results from cardiac involvement and cachexia (30). As disease modifying therapy, liver transplantation has been demonstrated to prolong survival.

TABLE 4 | Bioinformatic results of the identified missense *TTR* mutations.

Sequence variant (mRNA)	Mutation (protein variant incl.20–aa signal peptide)	Location	ClinVar	Reported phenotype	Reported ethnic group	References
c.112G>A	p.Asp38Asn (Asp18Asn)	Exon 2	Likely pathogenic	H	American	Connors et al. (15) Amyloid 10, 160
c.128G>A	p.Ser43Asn (Ser23Asn)	Exon 2	Likely pathogenic	E, H, PN	Portuguese, American	Connors et al. (16) Amyloid 6, 114
c.185A>G	p.Glu62Gly (Glu42Gly)	Exon 2	pathogenic	SN, H, PN	Japanese, Russian, American	Ueno et al. (17) Biochem Biophys Res Commun 169, 1117
c.200G>A	p.GLy67Glu (Gly47Glu)	Exon 2	pathogenic	H, K, PN	German, Italian	Pelo et al. (18) Amyloid 9, 35
c.224T>G	p.Leu75Arg (Leu55Arg)	Exon 3	pathogenic	LM, PN, E	Chinese, German	Long et al. (19) Ophthalmic Genet 33(1):28–33 Connors (2003) Amyloid 10, 160
c.236C>A	p.Thr79Lys (Thr59Lys)	Exon 3	Likely pathogenic	SN, H, PN	Italian, American (Asian)	Saraiva et al. (20) Hum Mutat 5, 191
c.241G>A	p.Glu81Lys (Glu61Lys)	Exon 3	Pathogenic	PN	Japanese	Shiomi et al. (21) Biochem Biophys Res Commun 194, 1090
c.323A>G	p.His108Arg (His88Arg)	Exon 3	Pathogenic	H	Swedish	Holmgren et al. (22) Amyloid 12, 184
c.349G>T	p.Ala117Ser (Ala97Ser)	Exon 4	Pathogenic	PN, H, E, SN	Chinese, Taiwanese	Tachibana et al. (23) Amyloid 6, 282

H, heart; PN, peripheral neuropathy; SN, Somatic neuropathy; E, eye; K, kidney; LM, lumber stenosis.

However, the statistics are mostly related to patients with ATTR V30M (31), which was not identified in our study cohort. Different from previous two cohort studies in China, no patient received liver transplantation in our cohort because the following reasons 1) For patients with advanced heart failure, liver transplantation does not provide a complete cure for the disease due to the newly formed amyloid around the preexisting amyloid seeds (32). Combining liver and heart transplantation may be a better strategy. 2) Liver transplantation is restricted by the availability of transplant organs as well as the advanced age and comorbidities of ATTR-CM patients. 3) The need for life-long immunosuppression therapy.

Tafamidis, a small molecule that inhibits the dissociation of transthyretin tetramers, was granted marketing authorization by China Food and Drug Administration for the treatment of inherited or wild type cardiac transthyretin amyloidosis in adult patients in 2020. However, only a few patients could afford this disease modifying therapy because the price of tafamidis was expensive (64,100￥/month in 2020, then reduced to 24,650￥/month in 2021). Up to November 2021, only 9.5% (4) patients received tafamidis in our cohort. Fortunately, more patients will have chance to receive this disease modifying therapy since National Health Insurance Administration has issued a national coverage decision to incorporate Tafamidis into medical insurance payouts in 2022.

There are several limitations to our study. First, this was a retrospective study that included a limited sample size. Second, all probands were admitted to our cardiology department first, which results in selection bias that may not permit the description of the actual phenotype-genotype relationship. Third, nuclear scintigraphy was only used in 9 (31%) patients. Expanding the sample size and long-term follow-up of the proband patients and their genotype positive phenotype negative pedigree is needed to understand the relationship between ATTRv genotype and disease course.

CONCLUSION

Hereditary ATTRv-CM has heterogeneous phenotypes and genotypes. Most patients had a mixed phenotype that included both cardiomyopathy and neuropathy. Ala97Ser, the most common mutation in South China, initially presented as peripheral and automatic neuropathy and progressed to heart failure at a later disease stage. The prognosis of ATTR was poor, and patients with NYHA III-IV and NAC stage 3 had the worst prognosis.

DATA AVAILABILITY STATEMENT

The original contributions presented in the study are included in the article/**Supplementary Materials**, further inquiries can be directed to the corresponding author.

ETHICS STATEMENT

The studies involving human participants were reviewed and approved by the Ethics Committee of Second Xiangya Hospital. The patients/participants provided their written informed consent to participate in this study.

AUTHOR CONTRIBUTIONS

SW wrote the protocol, evaluated cardiac involvement, analyzed the results and wrote the manuscript. WP and MP collected the data. LM did the TTR sequencing and analyzed the gene

data. DP conceived of the study. BY revised the manuscript and provided guidance for the study. SW, BY, DP, SW, DH, YY, and JH evaluated the patients and made the clinical diagnosis for each patient. All authors contributed to the article and approved the submitted version.

FUNDING

This work was supported by grants from the National Nature Science Foundation Youth Project (81600359) and the National Nature Science Foundation General Project (81870336).

ACKNOWLEDGMENTS

We would like to thank all of the participating families and investigators for their important contributions to this study. Additional investigators contributing to analysis Na Liu.

SUPPLEMENTARY MATERIAL

The Supplementary Material for this article can be found online at: https://www.frontiersin.org/articles/10.3389/fcvm.2022.900313/full#supplementary-material

REFERENCES

1. Wechalekar AD, Gillmore JD, Hawkins PN. Systemic amyloidosis. *Lancet.* (2016) 387:2641–54. doi: 10.1016/S0140-6736(15)01274-X
2. Koike H, Okumura T, Murohara T, Katsuno M. Multidisciplinary approaches for transthyretin amyloidosis. *Cardiol Ther.* (2021) 10:289–311. doi: 10.1007/s40119-021-00222-w
3. Maurer MS, Schwartz JH, Gundapaneni B, Elliott PM, Merlini G, Waddington-Cruz M, et al. Tafamidis treatment for patients with transthyretin amyloid cardiomyopathy. *N Engl J Med.* (2018) 379:1007–16. doi: 10.1056/NEJMoa1805689
4. Benson MD, Waddington-Cruz M, Berk JL, Polydefkis M, Dyck PJ, Wang AK, et al. Inotersen treatment for patients with hereditary transthyretin amyloidosis. *N Engl J Med.* (2018) 379:22–31. doi: 10.1056/NEJMoa1716793
5. Adams D, Gonzalez-Duarte A, O'Riordan WD, Yang CC, Ueda M, Kristen AV, et al. Patisiran, an RNAi therapeutic, for hereditary transthyretin amyloidosis. *N Engl J Med.* (2018) 379:11–21. doi: 10.1056/NEJMoa1716153
6. Landrum MJ, Lee JM, Benson M, Brown GR, Chao C, Chitipiralla S, et al. ClinVar: improving access to variant interpretations and supporting evidence. *Nucleic Acids Res.* (2018) 46:D1062–D7. doi: 10.1093/nar/gkx1153
7. Carry BJ, Young K, Fielden S, Kelly MA, Sturm AC, Avila JD, et al. Genomic screening for pathogenic transthyretin variants finds evidence of underdiagnosed amyloid cardiomyopathy from health records. *JACC CardioOncol.* (2021) 3:550–61. doi: 10.1016/j.jaccao.2021.07.002
8. Ruberg FL, Berk JL. Transthyretin (TTR) cardiac amyloidosis. *Circulation.* (2012) 126:1286–300. doi: 10.1161/CIRCULATIONAHA.111.078915
9. He S, Tian Z, Guan H, Li J, Fang Q, Zhang S. Clinical characteristics and prognosis of Chinese patients with hereditary transthyretin amyloid cardiomyopathy. *Orphanet J Rare Dis.* (2019) 14:251. doi: 10.1186/s13023-019-1235-x
10. Du K, Li F, Wang H, Miao Y, Lv H, Zhang W, et al. Hereditary transthyretin amyloidosis in mainland China: a unicentric retrospective study. *Ann Clin Transl Neurol.* (2021) 8:831–41. doi: 10.1002/acn3.51328
11. Bruno M, Castano A, Burton A, Grodin JL. Transthyretin amyloid cardiomyopathy in women: frequency, characteristics, and diagnostic challenges. *Heart Fail Rev.* (2021) 26:35–45. doi: 10.1007/s10741-020-10010-8
12. Damy T, Kristen AV, Suhr OB, Maurer MS, Plante-Bordeneuve V, Yu CR, et al. Transthyretin cardiac amyloidosis in continental western Europe: an insight through the Transthyretin Amyloidosis Outcomes Survey (THAOS). *Eur Heart J.* (2019). doi: 10.1093/eurheartj/ehz173
13. Batra J, Rosenblum H, Defilippis EM, Griffin JM, Saith SE, Gamino D, et al. Sex differences in the phenotype of transthyretin cardiac amyloidosis due to val122ile mutation: insights from noninvasive pressure-volume analysis. *J Card Fail.* (2021) 27:67–74. doi: 10.1016/j.cardfail.2020.08.007
14. Ruberg FL, Grogan M, Hanna M, Kelly JW, Maurer MS. Transthyretin amyloid cardiomyopathy: JACC state-of-the-art review. *J Am Coll Cardiol.* (2019) 73:2872–91. doi: 10.1016/j.jacc.2019.04.003
15. Connors LH, Lim A, Prokaeva T, Roskens VA, Costello CE. Tabulation of human transthyretin (TTR) variants, 2003. *Amyloid.* (2003) 10:160–84. doi: 10.3109/13506120308998998
16. Connors LH, Theberge R, Skare J, Costello CE, Falk RH, Skinner M, et al. New transthyretin variant (Ser23Asn) associated with familial amyloidosis in a Portuguese patient. *Amyloid.* (1999) 6:114–8. doi: 10.3109/13506129909007311
17. Ueno S, Uemichi T, Takahashi N, Soga F, Yorifuji S, Tarui S. Two novel variants of transthyretin identified in Japanese cases with familial amyloidotic polyneuropathy: transthyretin (Glu42 to Gly) and transthyretin (Ser50 to Arg). *Biochem Biophys Res Commun.* (1990) 169:1117–21. doi: 10.1016/0006-291X(90)92011-N
18. Pelo E, Da Prato L, Ciaccheri M, Castelli G, Gori F, Pizzi A, et al. Familial amyloid polyneuropathy with genetic anticipation associated to a gly47glu transthyretin variant in an Italian kindred. *Amyloid.* (2002) 9:35–41. doi: 10.3109/13506120209072443
19. Long D, Zeng J, Wu LQ, Tang LS, Wang HL, Wang H. Vitreous amyloidosis in two large mainland Chinese kindreds resulting from transthyretin variant Lys35Thr and Leu55Arg. *Ophthalmic Genet.* (2012) 33:28–33. doi: 10.3109/13816810.2011.599356
20. Saraiva MJ. Transthyretin mutations in health and disease. *Hum Mutat.* (1995) 5:191–6.
21. Shiomi K, Nakazato M, Matsukura S, Ohnishi A, Hatanaka H, Tsuji S, et al. A basic transthyretin variant (Glu61–>Lys) causes familial amyloidotic polyneuropathy: protein and DNA sequencing and PCR-induced mutation restriction analysis. *Biochem Biophys Res Commun.* (1993) 194:1090–6. doi: 10.1006/bbrc.1993.1933
22. Holmgren G, Hellman U, Anan I, Lundgren HE, Jonasson J, Stafberg C, et al. Cardiomyopathy in Swedish patients with the Gly53Glu and His88Arg transthyretin variants. *Amyloid.* (2005) 12:184–8. doi: 10.1080/13506120500223126
23. Tachibana N, Tokuda T, Yoshida K, Taketomi T, Nakazato M, Li YF, et al. Usefulness of MALDI/TOF mass spectrometry of immunoprecipitated serum variant transthyretin in the diagnosis of familial amyloid polyneuropathy. *Amyloid.* (1999) 6:282–8. doi: 10.3109/13506129909007341
24. Hsu HC, Liao MF, Hsu JL, Lo AL, Kuo HC Lyu RK, et al. Phenotypic expressions of hereditary Transthyretin Ala97Ser related Amyloidosis (ATTR) in Taiwanese. *BMC Neurol.* (2017) 17:178. doi: 10.1186/s12883-017-0957-4
25. Low SC, Tan CY, Md Sari NA, Ahmad-Annuar A, Wong KT, Lin KP, et al. Ala97Ser mutation is common among ethnic Chinese Malaysians with transthyretin familial amyloid polyneuropathy. *Amyloid.* (2019) 26:7–8. doi: 10.1080/13506129.2019.1582479
26. Liu YT, Lee YC, Yang CC, Chen ML, Lin KP. Transthyretin Ala97Ser in Chinese-Taiwanese patients with familial amyloid polyneuropathy: genetic studies and phenotype expression. *J Neurol Sci.* (2008) 267:91–9. doi: 10.1016/j.jns.2007.10.011
27. Chao CC, Huang CM, Chiang HH, Luo KR, Kan HW, Yang NC, et al. Sudomotor innervation in transthyretin amyloid neuropathy: Pathology and functional correlates. *Ann Neurol.* (2015) 78:272–83. doi: 10.1002/ana.24438
28. Castiglione V, Franzini M, Aimo A, Carecci A, Lombardi CM, Passino C, et al. Use of biomarkers to diagnose and manage cardiac amyloidosis. *Eur J Heart Fail.* (2021) 23:217–30. doi: 10.1002/ejhf.2113
29. Garcia-Pavia P, Rapezzi C, Adler Y, Arad M, Basso C, Brucato A, et al. Diagnosis and treatment of cardiac amyloidosis. a position statement of the European Society of cardiology working group on myocardial and pericardial diseases. *Eur J Heart Fail.* (2021) 23:512–26. doi: 10.1002/ejhf.2140

30. Suhr OB, Herlenius G, Friman S, Ericzon BG. Liver transplantation for hereditary transthyretin amyloidosis. *Liver Transpl.* (2000) 6:263–76. doi: 10.1053/lv.2000.6145
31. Carvalho A, Rocha A, Lobato L. Liver transplantation in transthyretin amyloidosis: issues and challenges. *Liver Transpl.* (2015) 21:282–92. doi: 10.1002/lt.24058
32. Liepnieks JJ, Zhang LQ, Benson MD. Progression of transthyretin amyloid neuropathy after liver transplantation. *Neurology.* (2010) 75:324–7. doi: 10.1212/WNL.0b013e3181ea15d4

Conflict of Interest: The authors declare that the research was conducted in the absence of any commercial or financial relationships that could be construed as a potential conflict of interest.

Publisher's Note: All claims expressed in this article are solely those of the authors and do not necessarily represent those of their affiliated organizations, or those of the publisher, the editors and the reviewers. Any product that may be evaluated in this article, or claim that may be made by its manufacturer, is not guaranteed or endorsed by the publisher.

frontiers | Frontiers in Cardiovascular Medicine

ORIGINAL RESEARCH
published: 01 July 2022
doi: 10.3389/fcvm.2022.932044

Atrial Cardiomyopathy Predicts Worse Outcome in Patients With Lung Cancer

Mengdi Ren[1†], Yuyan Ma[1†], Meng Wei[2], Yuye Ning[3], Hui Liu[4], Xue Shi[4], Yu Yao[1] and Fengwei Guo[5*]*

[1] Department of Oncology, The First Affiliated Hospital of Xi'an Jiaotong University, Xi'an, China, [2] Department of Neurology, The First Affiliated Hospital of Xi'an Jiaotong University, Xi'an, China, [3] The Second Department of Neurology, Shaanxi Provincial People's Hospital, Xi'an, China, [4] Biobank, The First Affiliated Hospital of Xi'an Jiaotong University, Xi'an, China, [5] Department of Cardiovascular Surgery, The First Affiliated Hospital of Xi'an Jiaotong University, Xi'an, China

OPEN ACCESS

Edited by:
Tong Liu,
Tianjin Medical University, China

Reviewed by:
Feng Hu,
Shanghai Jiao Tong University, China
Datun Qi,
Fuwai Central China Cardiovascular Hospital, China

***Correspondence:**
Yu Yao
13572101611@163.com
Fengwei Guo
guofengwei@xjtu.edu.cn

[†] These authors have contributed equally to this work and share first authorship

Specialty section:
This article was submitted to Heart Failure and Transplantation, a section of the journal Frontiers in Cardiovascular Medicine

Received: 29 April 2022
Accepted: 30 May 2022
Published: 01 July 2022

Citation:
Ren M, Ma Y, Wei M, Ning Y, Liu H, Shi X, Yao Y and Guo F (2022) Atrial Cardiomyopathy Predicts Worse Outcome in Patients With Lung Cancer.
Front. Cardiovasc. Med. 9:932044.
doi: 10.3389/fcvm.2022.932044

Background: Reports of the clinical outcomes associated with the co-occurrence of atrial cardiomyopathy (ACM) and lung cancer (LC) are limited.

Objectives: This study aims to investigate the influence of ACM on the prognosis of LC patients and related clinical determinants.

Methods: Newly diagnosed LC patients from January 1st, 2015, to December 31st, 2020, were retrospectively enrolled at the First Affiliated Hospital of Xi'an Jiaotong University. The demographics and overall survival (OS) of the patients with or without ACM were compared. The survival rate was analyzed using the Kaplan–Meier method and multivariate Cox regression analysis. Binary logistic regression analysis was used to determine the risk factors for ACM.

Results: A total of 306 patients (65.04 ± 10.30 years of age, 72.88% male) were analyzed. The prevalence of ACM in the non-small cell lung cancer (241, 78.76%) and small cell lung cancer (65, 21.24%) population was not statistically different. Overall, 53 (17.32%) LC patients had coexisting ACM. ACM patients were older (69 vs. 64, $p = 0.0013$) and had higher D-dimer levels (1.0 vs. 0.6, $p = 0.001$), lower serum calcium levels (2.23 vs. 2.31, $p = 0.001$), lower left ventricular ejection fraction (LVEF) values (67% vs. 69%, $p = 0.036$) and had more frequent coronary comorbidity disease (16.98% vs. 8.82%, $p = 0.031$). The median OS for patients with or without ACM was 15 months and 25 months, respectively ($p = 0.018$). Coexisting ACM compared to non-ACM was associated with worse OS in patients with LC (HR = 1.543, 95% CI: 1.042–2.283, $p = 0.030$).

Conclusion: Coexisting ACM is associated with undesirable survival outcomes in patients with LC. These findings could help us to better understand the cardiac burden in these patients and provide additional risk stratification for them.

Keywords: lung cancer, atrial cardiomyopathy, atrial fibrillation, oncocardiology, ischemic stroke

INTRODUCTION

Lung cancer (LC) and cardiovascular disease (CVD) are two leading reasons of morbidity and mortality worldwide (1, 2). With the survival of LC patients greatly improved due to multiple revolutionary oncological treatments, such as immunotherapy and targeted-based therapy, several concomitant conditions that significantly impact survival, including CVD, and ischemic stroke (IS) (3, 4), have increased markedly (5, 6). LC and CVD share many risk factors that affect cancer-related survival (7, 8). A study showed that cancer patients are 2–6 times more likely to die of CVD or stroke than the general population (9).

Atrial cardiomyopathy (ACM), initially proposed more than a decade ago, is a pathophysiological concept describing covert atrial structural lesions and functions that involve architectural or physiological changes in the atria (10, 11). Previous research has considered ACM as one of the important etiologies of embolic stroke of undetermined source (ESUS), a subset of cryptogenic ischemic IS (12). The mechanisms of cryptogenic IS include occult structural cardiac lesion, hyper viscosity syndrome or undiagnosed cancer (13). Although it is widely acknowledged that there is a close association between IS and cancer (especially LC) (14), the mechanisms underlying the heightened risks of IS in cancer patients are still uncertain. Moreover, many ACM-related risk factors, such as advanced age, hypertension, diabetes, coronary heart disease, and chronic obstructive pulmonary disease (COPD) (15), are very common in LC patients (16, 17). In addition, cancer and anticancer therapy may cause pathological changes and directly affect atrial substrates (18). Therefore, it can be reasonably inferred that LC patients are also at high risk of ACM, which may confer a higher IS risk.

The influence of ACM on the prognosis of LC patients has never been studied. In this context, we hypothesized that coexisting ACM would be associated with an increased risk of IS and poor prognosis among general LC patients. We investigated the association of ACM with LC outcomes and further examined the related clinical parameters of ACM.

MATERIALS AND METHODS

Study Population

A total of 306 patients with newly diagnosed LC at the First Affiliated Hospital of Xi'an Jiaotong University between January 2015 and December 2020 were retrospectively enrolled in this study. The design of study is described in **Figure 1**. The protocol was carried out on the basis of the Declaration of Helsinki and approved by the Ethics Committee of the First Affiliated Hospital of Xi'an Jiaotong University (Approval No. XJTU1AF2021LSK-117). These patients were divided into two groups: LC patients with or without ACM. All clinical covariates were abstracted from electronic medical records.

Diagnostic and Eligibility Criteria

ACM was defined as having at least one of the following biomarkers according to published literature: (1) *p*-wave terminal force in V1 (PTFV1) > 5,000 μV* ms; (2) N-terminal pro–B-type natriuretic peptide (NT-proBNP) > 250 pg/mL; and (3) severe left atrial enlargement (LAE: female > 38 mm; male > 40 mm) (19–21).

The inclusion criteria were as follows: (1) newly histologically or cytologically confirmed LC patients and (2) complete medical data for defining ACM and assessing cancer, namely, electrocardiogram (ECG), echocardiography, and NT-proBNP data.

Patients with any of the following conditions were excluded from this cohort: (1) cardiac and valvular history (congenital heart disease, other cardiomyopathies), myocardial infarction within 4 weeks, severe heart failure (left ventricular ejection fraction (LVEF) < 30%), intra-atrial thrombus, or infective endocarditis; (2) pericardial disease (pericardial metastasis, pericardial effusion); (3) heart arrhythmia disorder (atrial flutter, atrial fibrillation); and 4. renal insufficiency (serum creatinine ≥ 186 μmol/L or eGFR < 60 mL/min or chronic kidney disease (CKD) grade 3 and above).

Statistical Analysis

Descriptive statistics are held up as the mean ± standard deviation (*SD*) for continuous normally distributed variables and as the median (25th percentile, 75th percentile) [*M* (QL, QU)] for non-normally distributed data. Categorical variables are presented as frequencies and percentages.

For continuous variables, the independent sample *t*-test is used to compare normally distributed data, and the Wilcoxon rank sum test was used to compare non-normal variables. Count data were statistically analyzed using the chi-square or Fisher exact test. Binary logistic regression was used to determine the risk factors for ACM. Overall survival (OS) was estimated by the Kaplan–Meier method, and significance was evaluated using the log-rank (Mantel–Cox) test. Mortality hazard ratios (HRs) were generated by multivariate Cox regression analysis using univariate Cox predictors. Statistical significance was defined as a $p < 0.05$.

RESULTS

Patient Demographics

Our study included 306 patients; their median age was 65 years (range 29–94), and 72.88% were male. In all, 53 (17.32%) patients met the ACM diagnostic criteria. In **Table 1**, we present the baseline clinical characteristics of the LC patients with or without ACM. The distributions of sex, smoking history, pathological subtype, clinical stage, extrapulmonary/brain metastasis, hypertension, prior stroke, diabetes, and COPD were similar between the groups ($p > 0.05$), while those of age and coronary disease were different across the groups ($p < 0.05$). The ACM group had a slightly higher age (69.42 vs. 63.87) and more frequent coronary comorbidity disease (16.98% vs. 8.82%). We then analyzed the gene mutations and PD-L1 characteristics of the non-small-cell lung cancer (NSCLC) subgroup. The distributions of EGFR mutations/ALK fusions and PD-L1 expression levels were not related to ACM in the NSCLC patients (**Table 2**).

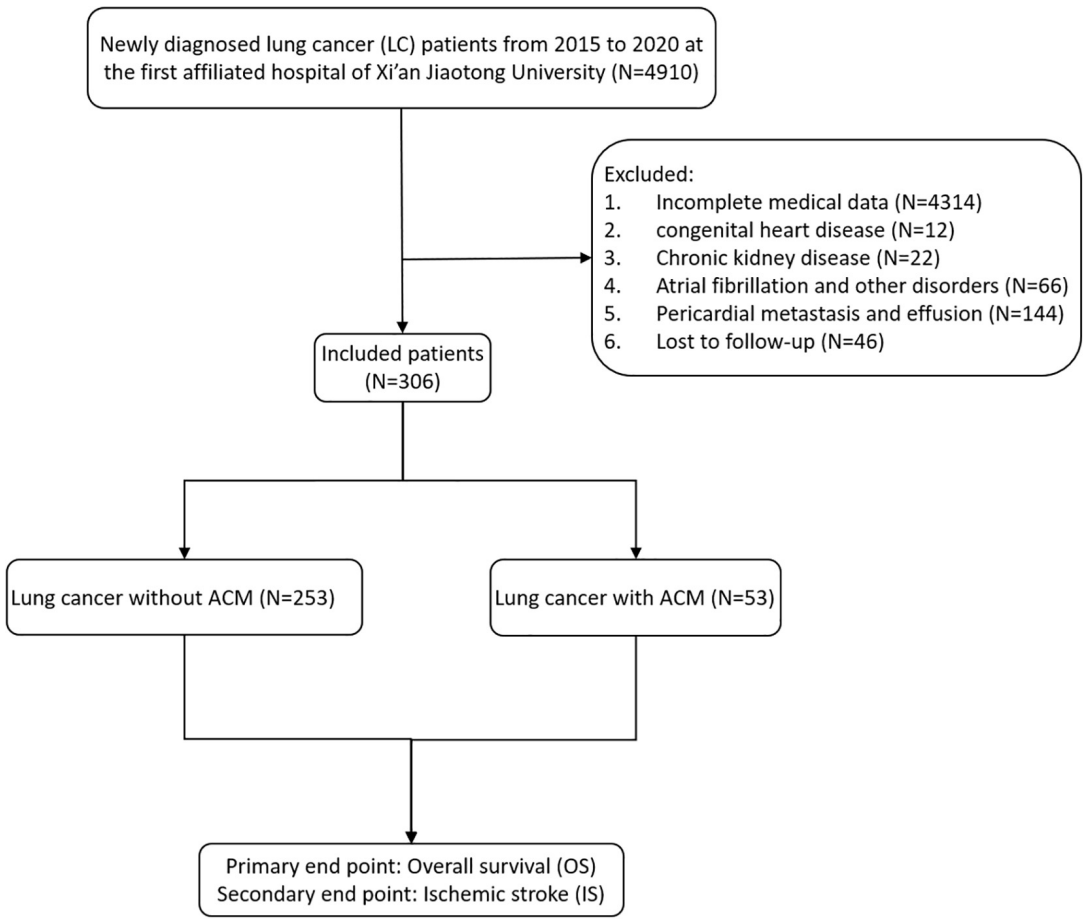

FIGURE 1 | Flowchart detailing patient enrollment.

Atrial Cardiomyopathy in Non-small-Cell Lung Cancer vs. Small-Cell Lung Cancer Patients

Overall, the prevalence of ACM in the LC patients was 17.32% (**Table 3**). The prevalence of ACM in the NSCLC (241, 78.76%) and small-cell lung cancer (SCLC) (65, 21.24%) populations was not significantly different. The prevalence of ACM in the NSCLC and SCLC populations was not significantly different. In all the LC patients, the frequency of ACM was mostly due to the presence of NT-proBNP (94.34%) and a PTFV1 value > 5,000 μV·ms (9.43%). The prevalence of severe LAE was 7.55% in the ACM patients (**Table 3**).

Atrial Cardiomyopathy and Overall Survival

Half of the LC patients (153 of 306) died. To avoid deviation caused by different distributions of treatment methods, all the treatments that patients received after diagnosis were recorded (**Table 1**). The therapeutic mode was similar for patients with ACM compared to those without ACM, which implies that ACM is a risk factor for survival regardless of the subsequent treatment.

To verify this, univariate analysis showed that sex, pathological subtype, clinical stage, smoking history, and ACM positivity had a significant association with survival (**Table 4**). Notably, Kaplan–Meier curves and log-rank tests showed that ACM was significantly associated with worse survival in LC patients (**Figure 2**). The median overall survival (mOS) for this LC patients was 23 months. The mOS for patients with or without ACM was 15 months and 25 months, respectively (p = 0.018) (**Table 1**).

In the multi-variable analysis of the Cox regression models, ACM was significantly associated with worse OS [hazard ratio (HR) = 1.556; 95% CI, 1.069–2.264; p = 0.021]. In the multivariate Cox proportional hazard model adjusting for clinicopathologic variables, the HR of the patients with ACM was 1.543 (95% CI, 1.042–2.283; p = 0.030) compared with that for the patients without ACM (**Table 5**), suggesting that ACM was an independent risk factor for LC patient prognosis.

Risk Parameters Associated With Atrial Cardiomyopathy

Given that 18.5% of the LC patients had ACM and exhibited worse survival, we examined the risk factors in this group. The

TABLE 1 | Demographic characteristics of patients with LC.

Characteristic	All patients (*N* = 306)	LC with ACM (*N* = 53)	LC without AC (*N* = 253)	*P*
Age at diagnosis, year	65.04 ± 10.30	69.06 ± 8.50	64.20 ± 10.46	0.001
Sex, female	83 (27.12)	13 (24.53)	70 (27.67)	0.640
Smoking, previous or current	207 (67.65)	37 (69.81)	170 (67.19)	0.711
Pathological subtype				
NSCLC	241 (78.76)	41 (77.36)	200 (79.05)	0.784
Adenocarcinoma	125 (40.85)	20 (37.74)	105 (41.50)	
Squamous cell	110 (35.95)	21 (39.62)	89 (35.18)	
Others	4 (1.31)		4 (1.58)	
Mixed	2 (0.65)		2 (0.79)	
SCLC	65 (21.24)	12 (22.64)	53 (20.95)	
Clinical stage[a]				0.165
Unknown	32 (10.46)	30 (11.86)	2 (3.77)	
Early	47 (15.36)	40 (15.81)	7 (13.21)	
Late	227 (74.18)	183 (72.33)	44 (83.02)	
Extra pulmonary metastasis				0.383
0	188 (61.44)	37 (69.81)	151 (59.68)	
1	76 (24.84)	10 (18.87)	66 (26.09)	
≥2	42 (13.73)	6 (11.32)	36 (14.23)	
Brain metastasis	27 (8.82)	4 (7.55)	23 (9.09)	0.482
Comorbidity disease history				
Hypertension	64 (20.92)	13 (24.53)	51 (20.16)	0.477
Coronary disease	27 (8.82)	9 (16.98)	18 (7.11)	0.031
Prior ischemic stroke	5 (1.63)	2 (3.77)	3 (1.19)	0.208
Diabetes	32 (10.46)	5 (9.43)	27 (10.67)	0.789
COPD	29 (9.48)	7 (13.21)	22 (8.70)	0.306
Treatment				
Chemotherapy	168 (54.90)	29 (54.72)	139 (54.94)	0.976
Radiation therapy	39 (12.75)	5 (9.43)	34 (13.44)	0.427
Surgery	33 (10.78)	9 (16.98)	24 (9.49)	0.110
Antiangiogenic treatment	26 (8.50)	5 (9.43)	21 (8.30)	0.787
Target therapy	47 (15.36)	8 (15.09)	39 (15.42)	0.953
Immunotherapy	57 (18.63)	6 (11.32)	51 (20.16)	0.133
Outcomes				
Ischemic stroke	12 (3.92)	1 (1.89)	11 (4.35)	0.699
Death	153 (50.00)	36 (67.92)	117 (46.25)	0.004
mOS; mo	24	15	25	0.018[b]

Data are presented as the mean ± SD or No. (%).
ACM, atrial cardiomyopathy; NSCLC, non-small-cell lung cancer; SCLC, small-cell lung cancer; COPD, chronic obstructive pulmonary disease; mOs, median overall survival.
[a]*Clinical stage: early stage, NSCLC stage I, II (TNM), SCLC limited stage; late stage, NSCLC stage III, IV (TNM), SCLC extensive stage; unknown: missing or not evaluated.*
[b]*Log-rank test.*

ECG, echocardiography, complete blood count (CBC) and blood biochemical examination tests performed closest to the date of diagnosis were used for the analysis. Our results showed that ACM patients had higher PTFV1 values (2,350 vs. 1,530, $p < 0.000$), higher NT-proBNP levels (460.1 vs. 68.54, $p < 0.000$), lower oxygen saturation values (95 vs. 96, $p = 0.0299$), higher pH (1.43 vs. 1.42, $p = 0.0111$), higher D-dimer levels (1.0 vs. 0.6, $p = 0.0006$) and prothrombin time (PT) (12.9 vs. 12.2, $p = 0.0065$), lower lymphocyte (1.17 vs. 1.28, $p = 0.0469$) and hemoglobin levels (123 vs. 133, $p = 0.0049$), higher CRP levels (mean CRP: 28.35 vs. 18.86, $p = 0.00373$), lower serum calcium levels (2.23 vs. 2.31, $p = 0.001$), and lower phosphate levels (0.96 vs. 1.03, $p = 0.0046$) (**Table 6** and **Supplementary Table 1**).

In addition, admission transthoracic echocardiograms were reviewed for all the patients. Those with ACM had lower LVEF values (67% vs. 69%, $p = 0.0357$). Univariate logistic analysis showed that patients with lower LVEF values were likely to be complicated with ACM (OR = 0.938, $p = 0.007$, 95% CI, 0.895–0.938). Hematological examinations and echocardiography indexes were included in the multivariate logistic regression analysis. As shown in **Table 7**, we found that higher D-dimer levels ($p = 0.016$, OR = 1.246) and lower serum calcium levels ($p = 0.019$, OR =

TABLE 2 | Gene mutations and PD-L1 characteristics in the NSCLC subgroup.

	All patients (*N* = 241)	LC with ACM (*N* = 62)	LC without ACM (*N* = 195)	*P*
Gene mutations, +	49 (20.33)	5 (11.63)	44 (22.22)	0.118
EGFR, +	39 (18.84)	5 (11.64)	34 (17.17)	
ALK, +	3 (1.45)	–	3 (1.52)	
Others, +	7 (3.38)	–	7 (3.54)	
PD-L1, +	25 (10.37)	3 (6.98)	22 (11.11)	0.584

Data are presented as No. (%).
EGFR, epidermal growth factor receptor; ALK, anaplastic lymphoma kinase. Gene mutations were recorded using fluorescent in situ hybridization (FISH) and immunohistochemistry in tissue microarray sections; PD-L1 IHC assays: SP263.

TABLE 3 | Prevalence of ACM in NSCLC vs. SCLC patients.

	All patients (*N* = 53)	NSCLC (*N* = 241)	SCLC (*N* = 65)	*P*
NT-proBNP > 250 pg/mL	50 (94.34)	40 (93.02)	12 (18.46)	0.712
PTFV1 ≥ 5,000	5 (9.43)	3 (6.98)	2 (16.67)	0.288
Severe large artery enlargement	4 (7.55)	4 (9.30)	0	0.582
ACM	53 (17.32)	43 (17.84)	12 (18.46)	0.854

Data are presented as No. (%).
ACM, atrial cardiomyopathy; NSCLC, non-small-cell lung cancer; SCLC, small-cell lung cancer; NT-proBNP, N-terminal pronc-type natriuretic peptide; PTFV1, p-wave terminal force in V1.

TABLE 4 | Univariate analyses of overall survival.

Characteristic	Chi-square	Log-rank *P*
Age (> 60 vs. ≤ 60)	1.94	0.164
Sex (male vs. female)	10.98	0.001
Pathological subtype (SCLC vs. NSCLC)	4.4	0.036
Clinical stage (late vs. early)	7.92	0.019
Smoking history (previous or current vs. never)	3.85	0.050
ACM (with vs. without)	4.8	0.018
Stroke (yes vs. no)	0.77	0.381
Extra-pulmonary metastasis (with vs. without)	2.15	0.341
Brain metastasis (with vs. without)	1.91	0.168

ACM, atrial cardiomyopathy.

0.001) were significant risk factors for ACM. In the multivariate analysis, transthoracic echocardiogram indexes failed to show any meaningful value (**Supplementary Table 2**).

DISCUSSION

In this observational, retrospective cohort study, 585 patients with LC were followed for a median of 20 months. In our study, the prevalence of LC patients with ACM was 17.32%, and these patients had a higher age (69 vs. 65) and more frequent coronary comorbidity disease (16.98% vs. 8.82%). However, the prevalence of ACM in LC patients was not significantly different in different pathological subtypes. In addition, we found that coexisting ACM was associated with worse OS (15 vs. 25) in patients with LC, who had higher D-dimer levels, lower serum calcium levels and lower LVEF values than the non-ACM patients. Together, these findings support that the comorbidity of ACM is associated with poorer survival in LC patients. However, we did not find that cancer-related IS was associated with ACM. These data highlight the need for further studies to better investigate the underlying mechanisms of stroke and cancer.

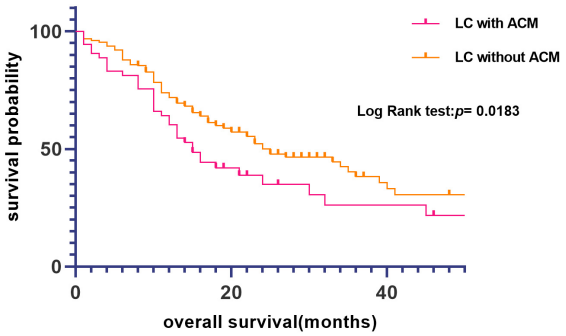

FIGURE 2 | Kaplan–Meier curve of overall survival (OS) based on atrial cardiomyopathy (ACM).

Atrial Cardiomyopathy Is Prevalent in Lung Cancer Patients

Any abnormalities of the atria of structural, architectural, contractile, or electrophysiological changes have been used to define a new entity known as ACM (22). In EHRAS (European Heart Rhythm Association; EHRA/Heart Rhythm Society; HRS/Asian Pacific Heart Rhythm Association; APHRS/Latin American Society of Electrophysiology and Cardiac Stimulation; SOLAECE) classification, ACM were defined into four types: principal cardiomyocyte changes; fibrotic changes; combined cardiomyocyte-pathology/fibrosis and non-collagen infiltration (23). However, most patients would not receive myocardial biopsy, making histological and pathopysiological classification hard to evaluate. At present, there is no absolute diagnostic criteria for ACM, but most of the studies are defined by the relevant markers of ACM. For example, it is reported that PTFV 1 abnormality is related to the increase of left atrial volume and the decrease of left atrial emptying fraction and reservoir function (24). Any pathological state that causes atrial dysfunction can lead to the increase of PTFV1, implying this ECG biomarkers may be the signs of ACM. Numerous randomized studies have adopted the combined biomarkers to define ACM (25). Other biomarkers includes LAE, paroxysmal supraventricular tachycardia, bayes syndrome, and serum biomarkers associated with atrial dysfunction, etc. In recent years, more emerging imaging techniques (such as cardiac computed tomography or magnetic resonance imaging and so on) have been used for accurate assessment of atrial structure and function, which may provide more supports of detecting ACM (26, 27).

TABLE 5 | Multivariate Cox proportional hazard analyses of overall survival.

	Haz. ratio	*P*	[95% CI]
Sex (male vs. female)	2.684	0.004	1.369–5.264
Pathological subtype (SCLC vs. NSCLC)	1.588	0.015	1.092–2.308
Clinical stage (late vs. early)	2.336	0.003	1.337–4.081
Smoking history (previous or current vs. never)	0.755	0.340	0.424–1.345
ACM (with vs. without)	1.543	0.030	1.042–2.283

ACM, atrial cardiomyopathy.

TABLE 6 | Comparison of baseline LC patients with/without ACM.

Parameter	LC with ACM (*n* = 53)	LC without ACM (*N* = 253)	*P*
PTVF1, μV*ms	2,350 (1,800–3,460)	1,530 (1,050–2,080)	0.000
NT-proBNP, pg/mL	460.1 (301.9–650.9)	68.54 (30.82–127.1)	0.000
SaO2,%	95 (93–96)	96 (95–97)	0.030
pH	7.43 (7.42–7.5)	7.42 (7.4–7.44)	0.011
D-D, mg/L	1 (0.5–2.5)	0.6 (0.3–1.1)	0.001
PT, s	12.9 (12–13.5)	12.2 (11.1–13.2)	0.007
ALC,10^9/L	1.17 (0.95–1.42)	1.28 (1.03–1.66)	0.047
HGB, g/L	123 (109–140)	133 (122–144)	0.005
CRP, mg/L	10 (10–41.7)	10 (10–14)	0.037
CK, U/L	54 (36–75.5)	63 (47–87)	0.048
ALB, g/L	35.2 (31.3–39)	39.65 (36.9–42.05)	0.000
Ca, mmol/L	2.23 (2.14–2.35)	2.31 (2.22–2.39)	0.001
P, mmol/L	0.96 (0.83–1.06)	1.03 (0.91–1.15)	0.005
LVEF,%	67 (63–71)	69 (65–73)	0.036
LVEDD, mm	49 (46–52)	47 (45–49)	0.005
LVESD, mm	30 (28–34)	28 (26–31)	0.002

SaO_2, oxygen saturation; D-D, D-dimer; PT, prothrombin time; ALC, absolute lymphocyte count; HGB, hemoglobin; CRP, C-reactive protein; CK, creatine kinase; ALB, albumin; LVEF, left ventricular systolic function; LVEDD, left ventricular end diastolic dimension; LVESD, left ventricular end systolic dimension.

A study use late gadolinium enhancement MRI (LGE-MRI) to evaluate atrial fibrosis and it is associated with appendage thrombus (28).

A previous study reported that the prevalence of ACM (26.6%) is increased in patients with ESUS compared to patients with other established etiologies for IS (21). In this study, we found that 17.32% of the LC patients had ACM. The key clinical determinants of ACM are unclear, but it is reported to be related to many disease or conditions, such as aging, smoking, hypertension, diabetes, coronary heart disease, and heart failure (15, 29). These high-risk factors overlap in most LC patients (30). This is also shown in this study. In addition, ACM-related biomarkers play an important role in the development of malignancies (18), suggesting that some physiological changes are shared by LC and ACM. For example, various studies have confirmed that NT-proBNP, a biomarker of ACM, and other biomarkers of CVD have prognostic significance in cancer (31, 32). A study showed that coexisting CVD precancerous polyps lead to tumor progression and secretion of cardiac excreted factors, mechanically supporting the above hypothesis (33).

TABLE 7 | Multivariate logistic regression analysis of clinical parameters.

Parameter	OR	*P*	95% conf. interval
D-D, mg/L	1.245	0.016	1.041–1.49
PT, s	1.477	0.149	0.869–2.509
ALC,10^9/L	1.068	0.916	0.312–3.661
HGB, g/L	0.967	0.056	0.934–1.001
CRP, mg/L	0.99	0.444	0.966–1.015
CK, U/L	0.999	0.953	0.988–1.011
ALB, g/L	1.02	0.774	0.89–1.168
Ca, mmol/L	0.001	0.019	0.000–0.316
P, mmol/L	0.099	0.174	0.004–2.776

SaO_2, oxygen saturation; D-D, D-dimer; PT, prothrombin time; ALC, absolute lymphocyte count; HGB, hemoglobin; CRP, C-reactive protein; CK, creatine kinase; ALB, albumin.

On the other hand, recognition of the interaction between cancer and atrial fibrillation (AF) has shed new light on the relationship with ACM. The basic pathology characteristic of AF and ACM is myocardial fibrosis. Fibrosis can be caused by inflammation and its mediators (34), such as systemic infection and autoimmune diseases, and may also occur in chronic inflammation (such as cancer) (35). Atrial fibrosis can precede AF or even exist without AF, which implies that ACM is the substrate for AF (18). This means that cancer or other coexisting subclinical inflammatory diseases (such as hypertension and coronary artery disease) and conditions (like aging and endocrine abnormalities) can produce inflammatory mediators, which change atrial electrophysiology and structural substrates (36). Many studies have reported that patients with malignancy have increased susceptibility to AF (37, 38), which also supports this theory.

Atrial Cardiomyopathy Predicts Worse Survival

We explored the relationship between ACM and LC and its influence on the survival of LC patients. The coexisting ACM was significantly associated with worse survival in patients with LC.

The biological mechanisms by which ACM may influence prognosis are unclear, but several lines of evidence suggest that this result is biologically reasonable. First, cancer is a systemic inflammatory condition originated from a combination of genetic, habitual and environmental factors (39). ACM has been associated with several clinical comorbidities and inflammatory conditions, such as systemic infections (15, 34). This means that the various comorbidities or conditions that may adversely affect the occurrence and outcomes of LC could also lead to ACM. Second, the factors that cause abnormalities in atrial tissue substrates can also be systemic manifestations of tumor progression. Cancer can promote the development of atrial fibrosis, leading to metabolic and electrolyte abnormalities, fluid imbalance, and infections. These inflammatory states then contribute to atrial remodeling (40), making ACM a prognostic marker. In other words, there is a bidirectional and progressive relationship between ACM and

LC. The abnormality of many ACM-related markers has been shown to be associated with the prognosis of cancer patients. For example, NT-proBNP levels are related to the severity of malignancy without cardiac disease or cardiotoxicity in anticancer therapy (41, 42). In addition, atrial lesions have substantial related adverse outcomes including arrhythmogenic changes, atrial fibroblast proliferation, hyperinnervation, and thrombogenic changes (23, 43), all of which can lead to worse prognosis in lung cancer patients. For instance, arterial thrombosis is a marker of occult cancer (especially lung cancer) and an unfavorable prognostic factor (44, 45). Taken together, with the effect of cancer and other risk factors, pathological changes of atrial cells (like myocardial hypertrophy, fibrosis, and fatty infiltration and so on) results in mechanical dysfunction or abnormal electrical conduction, which eventually converts to atrial dilatation and the congestive heart failure. These factors all contributes to the worse survival of LC. Our study showed that patients with lower LVEF values were likely to be complicated with ACM, which buttressed that view.

Atrial Cardiomyopathy Is Not Related to Ischemic Stroke Among Lung Cancer Patients

A new perspective of the relationship between AF and stroke has emerged in the past decade.

Although AF has been proved to be related to IS, the causal relationship between them is still indirect. A study found that there was no consistent time correlation between AF and IS (46).

A study reported that variants of chromosome associated with increased risk of cardioembolic IS, even in those not detected to have AF (47). A study reported nearly 65% of patients with cryptogenic stroke have ACM (20). These evidences verify that ACM may be the basis of IS.

Taken together, ACM is an important marker of increased risk of thromboembolism, particularly IS. Atrial abnormality forms the substrate for thrombus formation and AF may be a sign of potential risk of ACM. ACM itself, even without AF, is a risk factor for stroke (48). The mechanism of elevated risk of thrombus formation is likely related to the interaction between a generalized and local pro-thrombotic and inflammatory state (22). Moreover, atrial fibrosis, enlargement, and dysfunction may further lead to atrial congestion, pre-thrombotic state and subsequent IS (49).

Clinical trials have shown that treatment with ACM may reduce the risk of IS (50). Cryptogenic stroke (40–51%) is more common in cancer patients than in the general population (51). Compared with cancer-free controls, survivors of LC show a higher risk of stroke (52). Previous studies have reported that 45–65% of cryptogenic stroke patients have comorbidities of ACM (19, 20). Therefore, there are good reasons to hypothesize that ACM has a strong association with cancer-related stroke.

Unfortunately, we have not demonstrated this relevance in this set of data. The univariate analysis showed that there was no significant correlation between stroke and survival (**Table 4**). There are several possible reasons. The main reason is that the number of stroke events was too small in this cohort to verify the conclusion. Some patients received treatments at other centers, leading to some lost-to-follow-up and thus unknown ending events. Moreover, in order to evaluate the comorbidity of ACM, many patients with incomplete information occurring ending events were excluded from analysis. However, given that ACM is associated with a second era in understanding the relationship of disorders of the atria to stroke risk and anticoagulant therapy is still open to debate, we look forward to more research in this field in the future to reveal the etiology of stroke in cancer patients.

Study Limitations

Our study has limitations due to its single-center design, small sample size, and incomplete matching or exclusion of many patients from the analysis. Second, data were extract retrospectively, and much clinical information related to tumor assessment was not complete and lacked elaboration. Third, this study failed to analyze the impact of completing treatment for some patients who received treatments at other centers. More studies are needed in the future, such as prospective studies to determine reliable biomarkers to predict cancer-related stroke and clinical trials to determine the treatment and prevention of ACM.

CONCLUSION

Our study provides the first evidence that the comorbidity of ACM predicts worse prognosis in patients with LC. In addition, we found that higher D-dimer levels, lower serum calcium levels, and lower LVEF values were significant risk factors for ACM. NT-proBNP and PTFV1 are not routine clinical assessments for cancer patients. Our results imply that patients with those abnormal indexes may have coexisting ACM and a worse prognosis. Given that patients with ACM have a higher risk of poor survival, more frequent follow-up and detection in these patients should be considered.

DATA AVAILABILITY STATEMENT

The raw data supporting the conclusions of this article will be made available by the authors, without undue reservation.

ETHICS STATEMENT

The studies involving human participants were reviewed and approved by the Ethics Committee of the First Affiliated Hospital of Xi'an Jiaotong University. The patients/participants provided their written informed consent to participate in this study.

AUTHOR CONTRIBUTIONS

MR and YM contributed to clinical data collection and analysis. HL and XS provided support and assistance in data extraction. All authors contributed to the article and approved the submitted version.

FUNDING

This study was supported by the Shaanxi Provincial Key R&D Program General Project (2022SF-058).

ACKNOWLEDGMENTS

We thank the Biobank of First Affiliated Hospital of Xi'an Jiaotong University for providing clinical data.

SUPPLEMENTARY MATERIAL

The Supplementary Material for this article can be found online at: https://www.frontiersin.org/articles/10.3389/fcvm.2022.932044/full#supplementary-material

REFERENCES

1. Duarte CW, Lindner V, Francis SA, Schoormans D. Visualization of cancer and cardiovascular disease co-occurrence with network methods. *JCO Clin Cancer Inform.* (2017) 1:1–12. doi: 10.1200/CCI.16.00071
2. Zhou M, Wang H, Zeng X, Yin P, Zhu J, Chen W, et al. Mortality, morbidity, and risk factors in China and its provinces, 1990-2017: a systematic analysis for the global burden of disease study 2017. *Lancet.* (2019) 394:1145–58. doi: 10.1016/S0140-6736(19)30427-1
3. Navi BB, Iadecola C. Ischemic stroke in cancer patients: a review of an underappreciated pathology. *Ann Neurol.* (2018) 83:873–83. doi: 10.1002/ana.25227
4. Armenian SH, Xu L, Ky B, Sun C, Farol LT, Pal SK, et al. Cardiovascular disease among survivors of adult-onset cancer: a community-based retrospective cohort study. *J Clin Oncol.* (2016) 34:1122–30. doi: 10.1200/JCO.2015.64.0409
5. Stoltzfus KC, Zhang Y, Sturgeon K, Sinoway LI, Trifiletti DM, Chinchilli VM, et al. Fatal heart disease among cancer patients. *Nat Commun.* (2020) 11:2011.
6. Sung H, Ferlay J, Siegel RL, Laversanne M, Soerjomataram I, Jemal A, et al. Global cancer statistics 2020: globocan estimates of incidence and mortality worldwide for 36 cancers in 185 countries. *CA Cancer J Clin.* (2021) 71:209–49. doi: 10.3322/caac.21660
7. Lyon AR, Dent S, Stanway S, Earl H, Brezden-Masley C, Cohen-Solal A, et al. Baseline cardiovascular risk assessment in cancer patients scheduled to receive cardiotoxic cancer therapies: a position statement and new risk assessment tools from the cardio-oncology study group of the heart failure association of the European society of cardiology in collaboration with the international cardio-oncology society. *Eur J Heart Fail.* (2020) 22:1945–60. doi: 10.1002/ejhf.1920
8. Alvarez-Cardona JA, Ray J, Carver J, Zaha V, Cheng R, Yang E, et al. Cardio-oncology education and training: JACC council perspectives. *J Am Coll Cardiol.* (2020) 76:2267–81. doi: 10.1016/j.jacc.2020.08.079
9. Sturgeon KM, Deng L, Bluethmann SM, Zhou S, Trifiletti DM, Jiang C, et al. A population-based study of cardiovascular disease mortality risk in US cancer patients. *Eur Heart J.* (2019) 40:3889–97. doi: 10.1093/eurheartj/ehz766
10. Hammwöhner M, Bukowska A, Mahardika W, Goette A. Clinical importance of atrial cardiomyopathy. *Int J Cardiol.* (2019) 287:174–80.
11. Dong M, Liu T, Li G. Atrial cardiomyopathy–a not yet classified cardiomyopathy? *Int J Cardiol.* (2011) 151:394–6. doi: 10.1016/j.ijcard.2011.07.003
12. Leifer D, Rundek T. Atrial cardiopathy: a new cause for stroke? *Neurology.* (2019) 92:155–6. doi: 10.1212/WNL.0000000000006749
13. Mac Grory B, Flood SP, Apostolidou E, Yaghi S. Cryptogenic stroke: diagnostic workup and management. *Curr Treat Options Cardiovasc Med.* (2019) 21:77. doi: 10.1007/s11936-019-0786-4
14. Navi BB, Reiner AS, Kamel H, Iadecola C, Okin PM, Elkind MSV, et al. Risk of arterial thromboembolism in patients with cancer. *J Am Coll Cardiol.* (2017) 70:926–38.
15. Guichard JB, Nattel S. Atrial cardiomyopathy: a useful notion in cardiac disease management or a passing fad? *J Am Coll Cardiol.* (2017) 70:756–65. doi: 10.1016/j.jacc.2017.06.033
16. Zhai R, Yu X, Shafer A, Wain JC, Christiani DC. The impact of coexisting COPD on survival of patients with early-stage non-small cell lung cancer undergoing surgical resection. *Chest.* (2014) 145:346–53. doi: 10.1378/chest.13-1176
17. Mao Y, Yang D, He J, Krasna MJ. Epidemiology of lung cancer. *Surg Oncol Clin N Am.* (2016) 25:439–45. doi: 10.1016/j.jtho.2015.09.015
18. Ren M, Yao Y, Yue X, Ning Y, Yang Y. Atrial cardiomyopathy and atrial fibrillation in cancer. *Cardiol Res Pract.* (2021) 2021:6685953. doi: 10.1155/2021/6685953
19. Ntaios G, Perlepe K, Lambrou D, Sirimarco G, Strambo D, Eskandari A, et al. Prevalence and overlap of potential embolic sources in patients with embolic stroke of undetermined source. *J Am Heart Assoc.* (2019) 8:e012858. doi: 10.1161/JAHA.119.012858
20. Yaghi S, Boehme AK, Hazan R, Hod EA, Canaan A, Andrews HF, et al. Atrial cardiopathy and cryptogenic stroke: a cross-sectional pilot study. *J Stroke Cerebrovasc Dis.* (2016) 25:110–4. doi: 10.1016/j.jstrokecerebrovasdis.2015.09.001
21. Jalini S, Rajalingam R, Nisenbaum R, Javier AD, Woo A, Pikula A. Atrial cardiopathy in patients with embolic strokes of unknown source and other stroke etiologies. *Neurology.* (2019) 92:e288–94.
22. Yaghi S, Kamel H, Elkind MSV. Atrial cardiopathy: a mechanism of cryptogenic stroke. *Expert Rev Cardiovasc Ther.* (2017) 15:591–9. doi: 10.1080/14779072.2017.1355238
23. Goette A, Kalman JM, Aguinaga L, Akar J, Cabrera JA, Chen SA, et al. EHRA/HRS/APHRS/SOLAECE expert consensus on atrial cardiomyopathies: definition, characterization, and clinical implication. *Europace.* (2016) 18:1455–90.
24. Tiffany Win T, Ambale Venkatesh B, Volpe GJ, Mewton N, Rizzi P, Sharma RK, et al. Associations of electrocardiographic P-wave characteristics with left atrial function, and diffuse left ventricular fibrosis defined by cardiac magnetic resonance: the PRIMERI Study. *Heart Rhythm.* (2015) 12:155–62. doi: 10.1016/j.hrthm.2014.09.044
25. Kamel H, Longstreth WT Jr., Tirschwell DL, Kronmal RA, Broderick JP, Palesch YY, et al. The AtRial cardiopathy and antithrombotic drugs in prevention after cryptogenic stroke randomized trial: rationale and methods. *Int J Stroke.* (2019) 14:207–14. doi: 10.1177/1747493018799981
26. Oakes RS, Badger TJ, Kholmovski EG, Akoum N, Burgon NS, Fish EN, et al. Detection and quantification of left atrial structural remodeling with delayed-enhancement magnetic resonance imaging in patients with atrial fibrillation. *Circulation.* (2009) 119:1758–67. doi: 10.1161/CIRCULATIONAHA.108.811877
27. Kurotobi T, Iwakura K, Inoue K, Kimura R, Toyoshima Y, Ito N, et al. The significance of the shape of the left atrial roof as a novel index for determining the electrophysiological and structural characteristics in patients with atrial fibrillation. *Europace.* (2011) 13:803–8. doi: 10.1093/europace/eur039
28. Akoum N, Fernandez G, Wilson B, McGann C, Kholmovski E, Marrouche N. Association of atrial fibrosis quantified using LGE-MRI with atrial appendage thrombus and spontaneous contrast on transesophageal echocardiography in patients with atrial fibrillation. *J Cardiovasc Electrophysiol.* (2013) 24:1104–9. doi: 10.1111/jce.12199
29. Patnaik JL, Byers T, DiGuiseppi C, Dabelea D, Denberg TD. Cardiovascular disease competes with breast cancer as the leading cause of death for older females diagnosed with breast cancer: a retrospective cohort study. *Breast Cancer Res.* (2011) 13:R64. doi: 10.1186/bcr2901

30. Esposito K, Chiodini P, Colao A, Lenzi A, Giugliano D. Metabolic syndrome and risk of cancer: a systematic review and meta-analysis. *Diabetes Care.* (2012) 35:2402–11.
31. Tuñón J, Higueras J, Tarín N, Cristóbal C, Lorenzo Ó, Blanco-Colio L, et al. N-Terminal pro-brain natriuretic peptide is associated with a future diagnosis of cancer in patients with coronary artery disease. *PLoS One.* (2015) 10:e0126741. doi: 10.1371/journal.pone.0126741
32. Narayan V, Thompson EW, Demissei B, Ho JE, Januzzi JL Jr., Ky B. Mechanistic biomarkers informative of both cancer and cardiovascular disease: JACC state-of-the-art review. *J Am Coll Cardiol.* (2020) 75:2726–37. doi: 10.1016/j.jacc.2020.03.067
33. Meijers WC, Maglione M, Bakker SJL, Oberhuber R, Kieneker LM, de Jong S, et al. Heart failure stimulates tumor growth by circulating factors. *Circulation.* (2018) 138:678–91.
34. Hu YF, Chen YJ, Lin YJ, Chen SA. Inflammation and the pathogenesis of atrial fibrillation. *Nat Rev Cardiol.* (2015) 12:230–43.
35. Zhao H, Wu L, Yan G, Chen Y, Zhou M, Wu Y, et al. Inflammation and tumor progression: signaling pathways and targeted intervention. *Signal Transduction Targeted Ther.* (2021) 6:263. doi: 10.1038/s41392-021-00658-5
36. Leiva O, AbdelHameid D, Connors JM, Cannon CP, Bhatt DL. Common pathophysiology in cancer, atrial fibrillation, atherosclerosis, and thrombosis: JACC: cardiooncology state-of-the-art review. *JACC CardioOncol.* (2021) 3:619–34. doi: 10.1016/j.jaccao.2021.08.011
37. Jakobsen CB, Lamberts M, Carlson N, Lock-Hansen M, Torp-Pedersen C, Gislason GH, et al. Incidence of atrial fibrillation in different major cancer subtypes: a nationwide population-based 12 year follow up study. *BMC Cancer.* (2019) 19:1105. doi: 10.1186/s12885-019-6314-9
38. D'Souza M, Smedegaard L, Madelaire C, Nielsen D, Torp-Pedersen C, Gislason G, et al. Incidence of atrial fibrillation in conjunction with breast cancer. *Heart Rhythm.* (2019) 16:343–8. doi: 10.1016/j.hrthm.2018.10.017
39. Cao X, Wang X, Wang H, Xu G, Yu H. Systemic inflammation status relates to anti-inflammatory drug benefit and survival in rectal cancer. *J Surg Res.* (2022) 269:249–59. doi: 10.1016/j.jss.2021.08.028
40. Chu G, Versteeg HH, Verschoor AJ, Trines SA, Hemels MEW, Ay C, et al. Atrial fibrillation and cancer – an unexplored field in cardiovascular oncology. *Blood Rev.* (2019) 35:59–67. doi: 10.1016/j.blre.2019.03.005
41. Pavo N, Cho A, Wurm R, Strunk G, Krauth M, Agis H, et al. N-terminal B-type natriuretic peptide (NT-proBNP) is associated with disease severity in multiple myeloma. *Eur J Clin Invest.* (2018) 48:e12905. doi: 10.1111/eci.12905
42. Patel SR, Herrmann J, Vierkant RA, Olson JE, Couch FJ, Hazim A, et al. N-Terminal pro brain natriuretic peptide, sST2, and galectin-3 levels in breast cancer survivors. *J Clin Med.* (2021) 10:3313. doi: 10.3390/jcm10153313
43. Hoit BD. Left atrial size and function: role in prognosis. *J Am Coll Cardiol.* (2014) 63:493–505. doi: 10.1016/j.jacc.2013.10.055
44. Sundbøll J, Veres K, Horváth-Puhó E, Adelborg K, Sørensen HT. Risk and prognosis of cancer after lower limb arterial thrombosis. *Circulation.* (2018) 138:669–77. doi: 10.1161/CIRCULATIONAHA.117.032617
45. Mulder FI, Horváth-Puhó E, van Es N, Pedersen L, Büller HR, Bøtker HE, et al. Arterial thromboembolism in cancer patients: a Danish population-based cohort study. *JACC CardioOncol.* (2021) 3:205–18. doi: 10.1016/j.jaccao.2021.02.007
46. Brambatti M, Connolly SJ, Gold MR, Morillo CA, Capucci A, Muto C, et al. Temporal relationship between subclinical atrial fibrillation and embolic events. *Circulation.* (2014) 129:2094–9.
47. Gretarsdottir S, Thorleifsson G, Manolescu A, Styrkarsdottir U, Helgadottir A, Gschwendtner A, et al. Risk variants for atrial fibrillation on chromosome 4q25 associate with ischemic stroke. *Ann Neurol.* (2008) 64:402–9. doi: 10.1002/ana.21480
48. Kamel H, Okin PM, Elkind MS, Iadecola C. Atrial fibrillation and mechanisms of stroke: time for a new model. *Stroke.* (2016) 47:895–900. doi: 10.1161/STROKEAHA.115.012004
49. Goldberger JJ, Arora R, Green D, Greenland P, Lee DC, Lloyd-Jones DM, et al. Evaluating the atrial myopathy underlying atrial fibrillation: identifying the arrhythmogenic and thrombogenic substrate. *Circulation.* (2015) 132:278–91.
50. Healey JS, Gladstone DJ, Swaminathan B, Eckstein J, Mundl H, Epstein AE, et al. Recurrent stroke with rivaroxaban compared with aspirin according to predictors of atrial fibrillation: secondary analysis of the NAVIGATE ESUS randomized clinical trial. *JAMA Neurol.* (2019) 76:764–73. doi: 10.1001/jamaneurol.2019.0617
51. Salazar-Camelo RA, Moreno-Vargas EA, Cardona AF, Bayona-Ortiz HF. Ischemic stroke: a paradoxical manifestation of cancer. *Crit Rev Oncol Hematol.* (2021) 157:103181. doi: 10.1016/j.critrevonc.2020.103181
52. Zhang F, Wang K, Du P, Yang W, He Y, Li T, et al. Risk of stroke in cancer survivors: a meta-analysis of population-based cohort studies. *Neurology.* (2021) 96:e513–26. doi: 10.1212/WNL.0000000000011264

Conflict of Interest: The authors declare that the research was conducted in the absence of any commercial or financial relationships that could be construed as a potential conflict of interest.

frontiers | Frontiers in Cardiovascular Medicine

TYPE Review
PUBLISHED 18 July 2022
DOI 10.3389/fcvm.2022.922398

OPEN ACCESS

EDITED BY
Ana Ciobanu,
Carol Davila University of Medicine and Pharmacy, Romania

REVIEWED BY
Bernhard L. Gerber,
Cliniques Universitaires Saint-Luc, Belgium
Moritz Montenbruck,
Katholisches Marienkrankenhaus GmbH, Germany

*CORRESPONDENCE
Clement Lau
clement.lau@nhs.net

SPECIALTY SECTION
This article was submitted to Heart Failure and Transplantation, a section of the journal Frontiers in Cardiovascular Medicine

RECEIVED 17 April 2022
ACCEPTED 28 June 2022
PUBLISHED 18 July 2022

CITATION
Lau C, Elshibly MMM, Kanagala P, Khoo JP, Arnold JR and Hothi SS (2022) The role of cardiac magnetic resonance imaging in the assessment of heart failure with preserved ejection fraction.
Front. Cardiovasc. Med. 9:922398.
doi: 10.3389/fcvm.2022.922398

The role of cardiac magnetic resonance imaging in the assessment of heart failure with preserved ejection fraction

Clement Lau[1]*, Mohamed M. M. Elshibly[2], Prathap Kanagala[3], Jeffrey P. Khoo[2], Jayanth Ranjit Arnold[2] and Sandeep Singh Hothi[1,4]

[1]Department of Cardiology, New Cross Hospital, Royal Wolverhampton NHS Trust, Wolverhampton, United Kingdom, [2]Department of Cardiovascular Sciences, University of Leicester, Leicester, United Kingdom, [3]Department of Cardiology, Liverpool University Hospitals NHS Foundation Trust and Liverpool Centre for Cardiovascular Science, Liverpool, United Kingdom, [4]Institute of Cardiovascular Sciences, College of Medical and Dental Sciences, University of Birmingham, Birmingham, United Kingdom

Heart failure (HF) is a major cause of morbidity and mortality worldwide. Current classifications of HF categorize patients with a left ventricular ejection fraction of 50% or greater as HF with preserved ejection fraction or HFpEF. Echocardiography is the first line imaging modality in assessing diastolic function given its practicality, low cost and the utilization of Doppler imaging. However, the last decade has seen cardiac magnetic resonance (CMR) emerge as a valuable test for the sometimes challenging diagnosis of HFpEF. The unique ability of CMR for myocardial tissue characterization coupled with high resolution imaging provides additional information to echocardiography that may help in phenotyping HFpEF and provide prognostication for patients with HF. The precision and accuracy of CMR underlies its use in clinical trials for the assessment of novel and repurposed drugs in HFpEF. Importantly, CMR has powerful diagnostic utility in differentiating acquired and inherited heart muscle diseases presenting as HFpEF such as Fabry disease and amyloidosis with specific treatment options to reverse or halt disease progression. This state of the art review will outline established CMR techniques such as transmitral velocities and strain imaging of the left ventricle and left atrium in assessing diastolic function and their clinical application to HFpEF. Furthermore, it will include a discussion on novel methods and future developments such as stress CMR and MR spectroscopy to assess myocardial energetics, which show promise in unraveling the mechanisms behind HFpEF that may provide targets for much needed therapeutic interventions.

KEYWORDS

HFpEF, CMR in HFpEF, diastolic function, diastolic dysfunction, diastolic heart failure

Introduction

Heart failure (HF) is a clinical syndrome caused by abnormalities in cardiac structure and function resulting in increased intracardiac pressures and/or reduced cardiac output (1). Patients with HF frequently present with dyspnea, fatigue and fluid retention, organ dysfunction due to hypoperfusion and have a higher risk of sudden cardiac death due to ventricular arrhythmia or pump failure. Although the range of pathologies resulting in impaired cardiac function is broad, current clinical guidance on the classification and management of HF places great emphasis upon left ventricular ejection fraction (LVEF). Thus, patients with HF and LVEF of 50% or greater are commonly categorized as having HF with preserved ejection fraction (HFpEF). The prevalence of HF is estimated at 64.3 million globally (2) with more than half of these people having HFpEF (3). In this review, we discuss the utility of cardiovascular magnetic resonance imaging (CMR) for the assessment of HFpEF.

In patients presenting with HFpEF, the pathological hallmarks are abnormal left ventricular (LV) filling and increased LV end diastolic pressures (LVEDP), collectively termed diastolic dysfunction. HFpEF has diverse causes associated with a multitude of co-morbidities. Established risk factors implicated in the development of HFpEF include hypertension, type 2 diabetes (T2D), chronic kidney disease and obesity. HFpEF also appears to be more prevalent in females and presents at an older age than heart failure with reduced ejection fraction (HFrEF). Importantly, atrial fibrillation (AF) has a complex association with HFpEF (4) and AF commonly coexists with HFpEF with a reported prevalence of up to 65% in older patients (5). The underlying pathological changes are thought to be related to chronic inflammation, neurohormonal activation, changes in intracellular signaling pathways, endothelial and microvascular dysfunction and myocardial fibrosis (6).

To date, a number of diagnostic algorithms have been proposed since accurate identification of HFpEF can be problematic (7). Importantly, a wide range of HFpEF clinical phenocopies also exist, each with underlying pathophysiologically distinct etiologies including hypertrophic cardiomyopathy (HCM), ATTR cardiac amyloidosis, Fabry disease iron overload cardiomyopathy and cardiac sarcoidosis. Moreover, unique disease-targeted therapies in these conditions might reverse, halt or slow disease progression.

Diagnosing HFpEF with CMR

Cardiac imaging plays a pivotal role in the diagnosis of HFpEF. Echocardiography is the initial modality of choice to assess LV diastolic function particularly because of its availability, cost-effectiveness and technical capabilities through Doppler imaging. However, CMR is increasingly being utilized for the further evaluation of patients with HFpEF (Figure 1). CMR is currently second line to echocardiography in the imaging assessment of diastolic function as it remains a limited resource, is less economical and is challenging in patients with claustrophobia. Practical limitations in HFpEF patients include difficulties in breath holding in older patients and in obese patients. Image quality may be impacted in patients with AF and in those with cardiac devices and post valvular intervention. In addition, there remains a larger clinical and research evidence base for echocardiographic assessment of HFpEF. Despite these drawbacks, the strengths of CMR include its higher spatial resolution and ability to quantify structural changes in the heart with greater precision and reproducibility compared to other imaging modalities, and its unique tissue characterization capability (8). The diagnostic utility of CMR is highlighted by a study comparing CMR and echocardiography. Kanagala et al. (9) found that CMR diagnosed new, significant clinical cardiac pathologies such as myocardial infarction, HCM and constrictive pericarditis in 27% of 154 patients with HFpEF and these patients were at higher risk of death and HF hospitalization at 6 months. Recent data further suggests integration of different CMR measures of diastolic function into a novel diagnostic algorithm (10) in a similar vein to echocardiography but further validation and consensus agreement is required before putting such algorithms into routine clinical practice.

LV functional assessment

CMR is the current gold standard imaging technique to assess LV volumes and therefore LVEF, and LV mass, as it avoids the geometric assumptions made by echocardiography and provides superior reproducibility (11, 12). Advances in CMR machine learning further serve to increase repeatability for measuring LV volumes and mass (13). To provide the highest spatial and temporal resolution, ECG-gated bright-blood balanced steady state free precession (SSFP) sequences of contiguous short-axis slices from the LV base to apex are acquired (14, 15). In patients with HF, cardiac remodeling and left ventricular hypertrophy (LVH) are associated with impairment of myocardial contractility and diastolic dysfunction even with preserved LV ejection fraction (16). LVH is an established risk factor for adverse cardiovascular events (17–19) and is associated with incident HF events (20).

Phase contrast CMR is routinely used to determine flow for valvular assessment using through-plane velocity encoding. These sequences can also be utilized to measure transmitral inflow, generating E (passive diastolic inflow) and A (active diastolic inflow) waves and pulmonary vein inflow, which correlate well with echocardiographic Doppler indices (21–23). However, CMR-derived values tend to be lower and may underestimate velocities compared to echocardiography, which

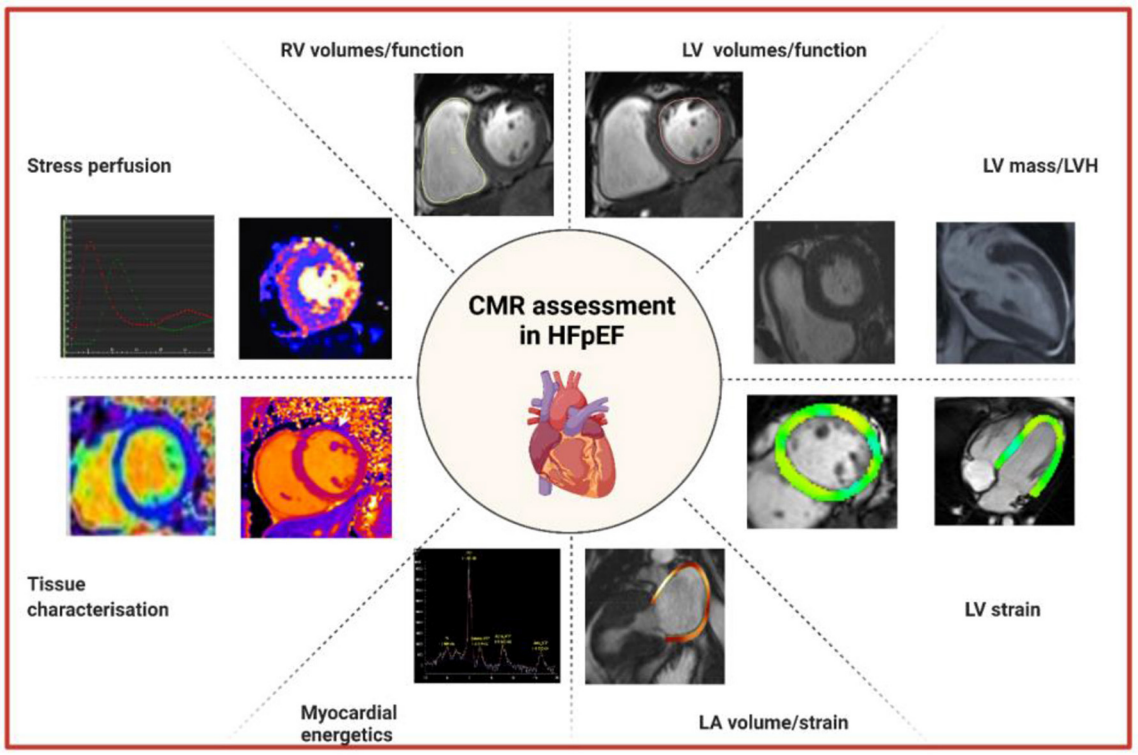

FIGURE 1
Approaches to the assessment of HFpEF by CMR. CMR, cardiovascular magnetic resonance; HFpEF, heart failure with preserved ejection fraction; LA, left atrial; LV, left ventricular; LVH, left ventricular hypertrophy; RV, right ventricular.

may relate to the lower temporal resolution with CMR (30–40 ms) vs. echocardiography (<5 ms) (24, 25). Additional pitfalls of CMR include time consuming data acquisition and analysis in addition to positive or negative phase offset errors with through-plane flow imaging due to local non-compensated eddy currents (26).The recently developed CMR golden-angle method permits acquisition of 150 to 250 frames per cardiac cycle to match that of echocardiography (27). This novel method involves k-space lines acquired continuously determined by the golden-angle of each sector, together with alternating velocity-encoding signs (27). Advances in CMR sequences have led to the development of 3D and 4D flow sequences which may prove to be useful for a more advanced assessment of diastolic filling than measurement of mitral inflow and pulmonary vein inflow by phase contrast CMR alone. For example, a 3D velocity-encoded MRI with retrospective mitral valve annular plane tracking sequence had better agreement with Doppler echocardiography for LV diastolic filling patterns compared to a 2D one-directional velocity-encoded sequence (28). Furthermore, in 53 healthy volunteers, a comparison of 4D flow CMR kinetic energy to mitral inflow E/A ratio showed a stronger independent association with age than standard 2D metrics (29).

Tissue Doppler imaging (TDI) for the quantification of myocardial velocities is a fundamental, clinically validated method for the assessment of diastolic function by echocardiography (30, 31). Similarly, phase contrast CMR can be used to determine myocardial e' velocities (peak modal velocity in early diastole by pulsed TDI waveform at the mitral valve annulus). CMR-derived mean e' and E/e' have consistently shown excellent correlation with echocardiographic values in patients with diastolic dysfunction (23, 32). In a small observational study of patients with hypertensive heart disease ($n = 18$), CMR E/e' strongly correlated with invasively measured mean pulmonary capillary wedge pressure (PCWP) ($r = 0.8$, $p < 0.0001$) and had a 100% positive predictive value for $E/e' < 8$ and PCWP $\leq$ 15 mmHg, and similarly so for $E/e' > 15$ and PCWP >15 mmHg (32). Measurement of CMR LV fractional area change during the first 30% of diastole (termed diastolic-index) in the short axis view correlated well with e' on echocardiography (33).

LV strain

Although the use of LVEF is clinically the dominant imaging method for defining severity, subtype and progression of HF, it has limitations (34). Other imaging parameters, particularly LV strain may detect changes in myocardial architecture and

function before changes in LVEF occur (35). Strain is a measure of myocardial mechanics that describes the deformation of LV myocardial fibers which are orientated in the longitudinal, circumferential and radial directions. Changes in longitudinal function occur early on in HF (36). Accordingly, global longitudinal strain (GLS) has been identified as an important marker of early myocardial dysfunction (37). Indeed, GLS has proven to have powerful prognostic value superior to LVEF (38). In a systematic review involving 5,721 patients with cardiovascular disease (CVD), there was stronger independent association with mortality with each SD change in the absolute value of baseline GLS (HR 0.50, 95% CI 0.36–0.69; $p < 0.002$) compared to LVEF (HR 0.81, 95% CI 0.72–0.92; $p = 0.572$) (38). Different methods to measure strain by CMR have evolved from myocardial tagging and phase contrast velocity-encoding to feature tracking, the latter now being the more commonly employed sequence.

Strain measurement by myocardial tagging using Spatial Modulation of Magnetization (SPAMM) involves tagging orthogonally intersecting sets of lines marking rectangular grids in a 2D image (39). In 1,500 participants from the MESA (Multi-Ethnic Study of Atherosclerosis) cohort, diastolic function from circumferential strain curves independently predicted incident HF and atrial fibrillation over an 8-year follow-up period (40). However, the requirement to acquire dedicated images and time-consuming post-processing has meant that myocardial tagging has not gained routine clinical use for the assessment of LV diastolic function. Strain-encoded (SENC) imaging uses tags parallel to the image plane rather than as a series of orthogonal lines (41). In systole, the tagged planes compress together leading to a shift in the peak spectrum location in k space (42). The rate of shift is then used to determine strain. Compared to conventional tagging, SENC can be acquired in half the time (43) and provides higher temporal resolution of strain measurements through the entire cardiac cycle (41). Fast-SENC techniques can shorten the image acquisition duration down to a single heartbeat (44).

An alternative method to assess myocardial deformation is by phase contrast velocity-encoding which offers better spatial resolution but lower temporal resolution than myocardial tagging (45). This allows measures of instantaneous velocity over a short time period. Displacement encoding with stimulated echoes (DENSE) is a free-breathing, phase-velocity based method which permits measurement of displacement during most but not all of the cardiac cycle (46). Unfortunately, this limits the assessment of diastolic tissue displacement and acquired images have low signal to noise ratio.

Feature tracking (FT) CMR analysis (FT-CMR) tracks points or features in the myocardium across successive imaging frames over the whole cardiac cycle, generating strain values and curves (Figure 2). FT-CMR is increasingly favored for the assessment of strain due its close correlation with echocardiographic speckle tracking (47) and myocardial tagging (48, 49). Moreover, the ability to utilize routine SSFP-based cine images simplifies clinical workflows. In a small study of 18 HFpEF patients compared to 18 age and sex-matched controls, GLS independently predicted abnormal relaxation index, Tau, by invasively measured pressure-volume loops (50). GLS measured by FT-CMR proved to be a powerful independent predictor of all-cause mortality in a multi-center study of 1,012 patients with HFrEF and a median follow-up of 4.4 years (51). In a study of 131 patients with HFpEF, GLS $\geq -8\%$ by FT-CMR independently predicted HF hospitalization and cardiovascular death at 2.5 years follow up (52). Novel applications of FT-CMR include the assessment of LV torsion, rotation and diastolic recoil (53). Interestingly, different rotational mechanics are found in patients with amyloidosis and HCM, conditions which often masquerade as HFpEF (54).

Left atrial size

Changes in left atrial size (LA) are a hallmark of elevated LV filling pressures in patients with HFpEF (55). Maximal LA volume measured at end-systole in sinus rhythm and indexed to body surface area (BSA) has strong predictive value for adverse cardiovascular events (56). CMR provides a more accurate measurement of LA size compared to echocardiography, owing to inherently superior spatial resolution. LA size can be measured by contouring the LA in the short axis stack or, more commonly, by the area-length method or Simpson's biplane in the 4-chamber and 2-chamber views. Although Simpson's biplane is the reference standard to assess LA size by echocardiography, there is limited consensus on the preferred method by CMR (57, 58). Nevertheless, in a multicenter study of nearly 11,000 subjects with a median follow up of 4 years, increased BSA-indexed LA size measured by CMR was independently associated with all-cause mortality (59).

Left atrial function

LA function can be subdivided into its reservoir (LA filling during LV systole), conduit (passive LV filling in early to mid-diastole) and pumping (LA contraction to augment LV filling in late diastole) phases. LA conduit-filling capacity is calculated by maximum LA volume minus pre-atrial contraction volume whilst LA active filling capacity is calculated by pre-atrial contraction volume minus the minimum LA volume (60). LA stroke volume is defined as maximum minus minimum LA volume. Furthermore, LA ejection fraction (LAEF) can be derived from these measured volumes with both biplane and short axis methods showing good agreement in sinus rhythm (61). Left atrial ejection fraction is closely associated with LVEDP on cardiac catheterization (62).

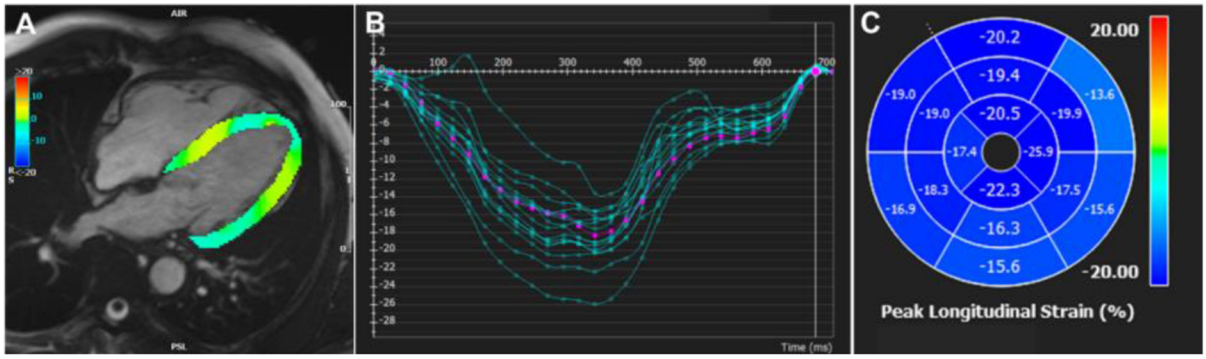

FIGURE 2
Feature tracking CMR strain analysis. **(A)** Feature tracking CMR in the 4-chamber view generating **(B)** longitudinal strain curves, **(C)** displayed as a polar map for each AHA segment. AHA, American Heart Association.

Increased LA volumes, reduced LAEF, reduced LA reservoir and booster pump strains are all associated with diastolic dysfunction as well as its severity (63). In the multi-ethnic population-based Dallas Heart Study of 1,802 patients, lower LAEF was independently associated with increased mortality [hazard ratio per 1 SD (8.0%): 1.56 (1.32–1.87)] with superior and incremental predictive value over maximum LA volume index (64). These findings were further supported by the MESA study of 536 patients with T2D, in whom incident cardiovascular disease was strongly and independently associated with lower passive, active and total LAEF (65). Kanagala et al. demonstrated that LAEF is reduced in HFpEF ($n = 140$) compared to controls ($n = 48$) and that a lower LAEF was associated with an increased risk of all-cause mortality or first HF hospitalization (log-rank, all $p = 0.028$; sinus $p = 0.036$) (61, 66). Furthermore, the strong association with adverse outcomes was similar for LAEF derived by either the biplane or short axis methods during CMR (61).

Left atrial strain

Application of CMR-FT to the LA generates strain data that have been evaluated as measures of LA function (67). Chirinos et al. (68) compared patients with HFpEF ($n = 101$), HFrEF ($n = 120$) and without HF ($n = 640$) demonstrating that conduit and reservoir LA strain measured using CMR-FT independently predicted risk of incident HF admission or mortality. In the MESA cohort, incident HF was predicted by lower longitudinal atrial strain (25 ± 11% vs. 38 ± 16%; $p < 0.001$) and lower LA emptying fraction (40 ± 11 vs. 48 ± 9%; $p < 0.001$) at baseline (69). In a small study of 22 HFpEF patients compared to heathy controls, LA conduit strain was significantly reduced in HFpEF and was associated with impaired oxygen uptake (VO_2 max) during cardiopulmonary exercise testing and invasive measurements of impaired early LV filling (70).

Right ventricle

CMR is also the gold standard non-invasive method to assess right ventricular (RV) size and function. In a prospective, observational study the prevalence of RV dysfunction (RVEF < 47%) as determined by CMR was present in 19% of individuals with HFpEF ($n = 135$) (71). Furthermore, RV dysfunction was independently associated with death and HF hospitalization (adjusted HR 3.946, 95% CI 1.878–8.290, $p = 0.0001$). (71). HFpEF is a recognized cause of elevated pulmonary artery pressures (PAP) and pulmonary hypertension. Resultant changes in the right heart readily assessed by CMR include increased right atrial size, RV hypertrophy and septal bowing. Assessment of diastolic dysfunction must take into account an estimation of PAP which is typically elevated in patients with HFpEF. Echocardiography can estimate systolic PAP by measurement of the peak tricuspid regurgitant (TR) velocity using the formula $PAP = 4^*(TRV_{max})^2$. While measurement of the tricuspid regurgitant jet peak velocity is readily assessed by echocardiography, this is less readily performed by CMR. However, systolic PAP can be indirectly estimated by identifying the peak TR velocity using phase contrast CMR flow analysis at the level of the tricuspid valve (72).

Myocardial tissue characterization

In HFpEF, alterations in the extracellular matrix with increased collagen deposition are thought to be a result of inflammation and increased oxidative stress (73). This process leads to myocardial fibrosis, which may contribute to the impaired relaxation that is observed in HFpEF. CMR has the unique capability to detect both focal replacement myocardial fibrosis using late gadolinium enhancement (LGE) and diffuse interstitial fibrosis through parametric mapping sequences (native T1 and extra cellular volume (ECV) quantification).

The presence of replacement fibrosis by LGE in patients at risk of HFpEF including in AF (74) and diabetes (75) has been shown to increase the risk of mortality. Furthermore, identifying LGE can provide additional risk stratification for patients at risk for hospitalization for HF regardless of etiology or LV systolic dysfunction (76). In an observational cohort study of 1,096 patients with AF, LA fibrosis by LGE was associated with an overall incidence of developing HF at 3.1% per year (77). Moreover, 80% of patients developed HFpEF ($n = 63$) rather than HFrEF ($n = 20$) after a median 2.7 years follow-up and that the incidence of HF increased with increasing LA fibrosis.

T1 measures the time taken for longitudinal relaxation of excited protons to return to equilibrium following application of a radiofrequency pulse. Colored maps can be generated so that pixel values represent the T1 in each voxel. T1 values in the myocardium and blood pool acquired pre- and post-contrast, and by accounting for hematocrit, can be used to calculate ECV. ECV quantifies the relative expansion of the extracellular matrix acting as a validated surrogate imaging biomarker for myocardial fibrosis (78, 79).

Both native T1 mapping and ECV are helpful in detecting inherited and acquired cardiomyopathies, particularly Fabry disease and cardiac amyloidosis (Figure 3). Diffuse myocardial fibrosis by native T1 mapping and ECV appears to be associated with diastolic dysfunction and LV stiffness in HFpEF ($n = 62$) but not in HFrEF ($n = 40$) or healthy controls ($n = 22$) (80). ECV has been demonstrated to correlate with invasive measures of load-independent passive LV stiffness (81, 82). In a study comparing patients with HFpEF, hypertension and healthy controls, ECV was significantly increased in HFpEF (35.9 ± 5.0%) compared to both hypertensive patients (31.9 ± 5.2%) and healthy controls (27.0 ± 4.3%) (83). Moreover, ECV was superior to GLS in differentiating between HFpEF and hypertension.

ECV may have a unique role to play in identifying HFpEF phenotypes at higher risk of cardiovascular events and death (84). In a cohort of 410 patients at risk for or diagnosed with HFpEF, ECV correlated with BNP levels and outcomes of heart failure hospitalization or death (85). This may indicate that the degree of myocardial fibrosis occurs in a continuum of severity and may precede overt clinical features of HFpEF. These findings are corroborated by other studies demonstrating that a lower post-contrast T1 time (median <388 ms) is a strong predictor of adverse events (86). Furthermore, both focal and diffuse myocardial fibrosis was noted to be more prevalent in HFpEF ($n = 140$), compared to age and sex matched control subjects. ECV indexed to body surface area correlated with LV mass:volume ratio, RV end-diastolic volume index and maximum LA volume index and independently predicted adverse outcomes (87). Interestingly, a recent study demonstrated that anterior RV insertion point fibrosis measured by increased native T1 times significantly correlated with markers of increased LV end-diastolic pressures and filling (88).

Stress perfusion and exercise stress CMR

Patients with HFpEF may only develop dyspnea on exertion and have limited indices of diastolic dysfunction at rest. The gold standard for diagnosing the effects of HFpEF during exertion is invasive right heart catheterization during exercise (89), although it is more often assessed indirectly by exercise stress echocardiography (90). Recent studies have shown a role for stress perfusion or CMR combined with exercise to increase the diagnostic yield for HFpEF (91–93). In particular, there appears to be significant coronary microvascular dysfunction in HFpEF patients as revealed by myocardial perfusion reserve following stress perfusion imaging (94). Stress perfusion CMR identifies patients at higher risk of major cardiovascular events in HFpEF without known coronary artery disease (95, 96).

In a feasibility study, exercise stress combined with real-time CMR was able to detect HFpEF, confirmed by right heart catheterization, with high accuracy (93). The authors also demonstrated that LA longitudinal shortening was the most accurate parameter to detect HFpEF. In future, exercise stress CMR may play a prominent role alongside exercise echocardiography in the workup of HFpEF patients, without the need for invasive tests.

Myocardial energetics

The high energy requirement of the heart and minimal capacity to store energy suggests that an imbalance of energy supply and demand may predispose to the development of myocardial dysfunction. MR spectroscopy has the capability to assess myocardial energetics by measuring phosphocreatine to adenosine-triphosphate (PCr/ATP) ratio, and cardiac steatosis by measuring myocardial triglyceride content (MTG). In a small study of 12 patients with T2D and diastolic dysfunction, there were reductions in PCr/ATP ratio when compared to controls (97). Burrage et al. (98) investigated patients with a spectrum of diastolic dysfunction including T2D ($n = 9$), HFpEF ($n = 14$) and cardiac amyloidosis ($n = 9$) and controls ($n = 11$). Across the spectrum of HFpEF, there was a decrease in PCr/ATP ratio in parallel to increases in E/e', NT-proBNP and lower LV diastolic filling rates with low workload exercise. Moreover, patients with HFpEF and cardiac amyloidosis had transient pulmonary congestion with exercise as revealed by pulmonary proton density mapping. In HFpEF, significantly greater MTG and therefore myocardial steatosis correlates with reductions in CMR measured diastolic strain and VO_2max (99).

Recent clinical trials have identified beneficial effects of therapeutics on cardiac metabolism. Evidence has been growing for the sodium–glucose cotransporter 2 (SGLT2) inhibitor, empagliflozin, for the treatment of HFpEF (100). The mechanism of these benefits have not been fully elucidated

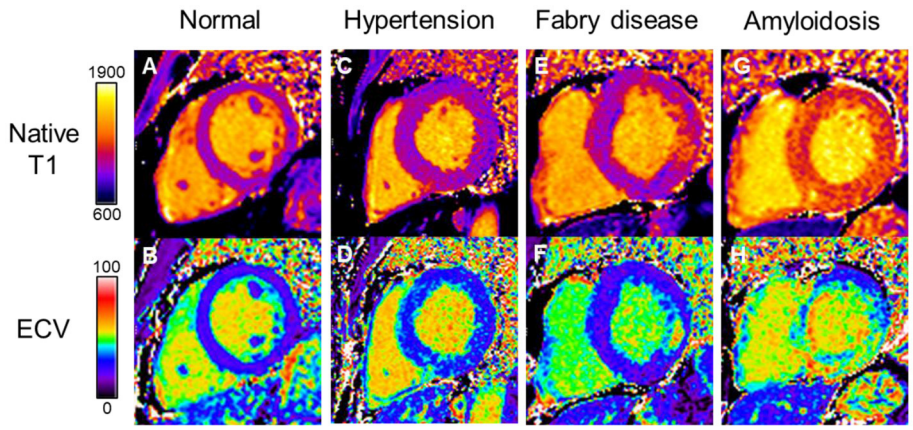

FIGURE 3
Myocardial tissue characterization by native T1 and ECV differentiating disease processes in HFpEF. **(A)** Normal native T1 and **(B)** normal ECV maps. Hypertensive heart disease with LVH showing diffuse myocardial fibrosis on **(C)** native T1 map and **(D)** increased ECV. Fabry disease showing **(E)** globally reduced native T1 values and **(F)** replacement fibrosis in the basal inferolateral wall on ECV map; Cardiac amyloidosis showing globally elevated **(G)** native T1 and **(H)** ECV values. Color scales are represented for native T1 in milliseconds and ECV in percentage. ECV, extracellular volume; HFpEF, heart failure with preserved ejection fraction; LVH, left ventricular hypertrophy.

but an improvement in cardiac metabolism has been shown following in a significant increase in PCr/ATP in a small study of 18 patients with T2D compared to 10 healthy volunteers (101). The authors also found an increase in mean LVEF of 7% and a 3% increase in GLS.

Epicardial adipose tissue (EAT) surrounding myocardium and within the pericardium is metabolically active providing energy to myocardium through the breakdown of triglycerides and also generates pro-inflammatory mediators (102). Furthermore, EAT may affect mechanical properties of ventricular function. In obese HFpEF ($n = 99$) compared to non-obese HFpEF ($n = 97$) and healthy controls ($n = 71$), there was significantly higher total epicardial heart volume [945 ml (831–1,105 ml) vs. 797 ml (643–979 ml) and 632 ml (517–768 ml); $p < 0.0001$] and EAT thickness (10 ± 2 vs. 7 ± 2 and 6 ± 2 mm; $p < 0.0001$) measured by CMR (103). Furthermore, the larger epicardial heart volume in obese HFpEF was associated with increased pericardial restraint and ventricular interdependence.

Novel methods in assessing HFpEF by CMR

Recent advances in CMR have generated novel sequences and measures to assess HFpEF. Diastolic dysfunction results from altered LV compliance leading to changes in LV filling patterns. LV time-volume and peak filling rate curves generated using CMR acquired LV volumetric datasets associate with the severity of echocardiographic-derived diastolic dysfunction (104). Patients with HFpEF have a lower peak filling rate adjusted for end diastolic volume (105), prolonged peak filling rates (106) and greater diastolic volume recovery (proportion of diastole required for recovery of 80% of stroke volume) by CMR (107).

A fundamental aspect of HFpEF assessment is to determine PAP. Vortices of blood, measured by 3D or 4D phase-contrast CMR, appear in the main pulmonary artery in pulmonary hypertension (108, 109). Measurement of the duration of blood vortices allows estimation of pulmonary artery pressures (110). A vortex duration ≥15% corresponds to an invasive mean PAP ≥25 mmHg. Using 4D flow analysis there is good correlation to Doppler echocardiographic estimates with potentially higher diagnostic yields in the detection of raised pulmonary artery pressures (111).

Central transit times have long been to known to be increased in HF (112). Using first pass perfusion, Cao and colleagues (113) demonstrated that global central transit times from the right atrium to aorta were significantly prolonged in HFpEF, which correlated with increased PCWP. Measurement of central transit time may therefore act as an additional marker of HFpEF for patients undergoing CMR though data on its use remains limited.

Experimental CMR sequences in the pipeline may further serve to characterize the myocardium and alterations in diastolic function potentially adding to the diagnostic role of CMR in the assessment of HFpEF. Examples include diffusion tensor imaging (114), MR elastography (115), artificial intelligence and radiomics (116), which are beyond the scope of this review article.

Conclusion

Assessment by CMR enables refinement of a clinical HFpEF diagnosis into underlying cardiac conditions such as

HCM and cardiac amyloidosis. Furthermore, the strengths of CMR over other imaging modalities include the capability for sub-categorization into pathophysiological sub-types such as increased myocardial fibrosis, left atrial dysfunction or microvascular dysfunction. The comprehensive evaluation of HFpEF by CMR may enable risk profiling of patients with HFpEF and perhaps allow focused, targeted therapies in the future. Advances in CMR sequences and postprocessing are generating novel indices of diastolic dysfunction which not only aid diagnosis but may hold prognostic risk prediction. The role of CMR in assessment of diastolic dysfunction continues to evolve at a rapid rate but large-scale studies are still required to permit technical reproducibility as well as clinical validation across different populations and subcategories of HFpEF. Moreover, future research could focus on the challenge of identifying which established and novel indices should be routinely incorporated into clinical workflows. It remains to be determined how such advances compare to a predominant echocardiographic based approach to clinical diagnosis and management of HFpEF, especially whether the use of CMR can lead to improved prognostication and outcomes.

Author contributions

CL drafted the manuscript, performed literature review, and created figures. ME created a figure and reviewed the manuscript. PK and JK critically appraised the manuscript and made constructive modifications and suggestions. JA codevised the topic for the manuscript, critically appraised the manuscript, and made constructive modifications and suggestions. SH devised the idea for the manuscript, led the whole project, critically appraised the manuscript from inception, and co-wrote the manuscript from the outset. All authors contributed to the article and approved the submitted version.

Conflict of interest

The authors declare that the research was conducted in the absence of any commercial or financial relationships that could be construed as a potential conflict of interest.

Publisher's note

References

1. McDonagh TA, Metra M, Adamo M, Gardner RS, Baumbach A, Böhm M, et al. 2021 ESC Guidelines for the diagnosis and treatment of acute and chronic heart failure. *Eur Heart J.* (2021) 42:3599–726. doi: 10.1093/eurheartj/ehab368

2. James SL, Abate D, Abate KH, Abay SM, Abbafati C, Abbasi N, et al. Global, regional, and national incidence, prevalence, and years lived with disability for 354 diseases and injuries for 195 countries and territories, 1990–2017: a systematic analysis for the Global Burden of Disease Study 2017. *Lancet.* (2018) 392:1789–858. doi: 10.1016/S0140-6736(18)32279-7

3. Lam CSP, Donal E, Kraigher-Krainer E, Vasan RS. Epidemiology and clinical course of heart failure with preserved ejection fraction. *Eur J Heart Fail.* (2011) 13:18–28. doi: 10.1093/EURJHF/HFQ121

4. Kotecha D, Lam CSP, Van Veldhuisen DJ, Van Gelder IC, Voors AA, Rienstra M. Heart failure with preserved ejection fraction and atrial fibrillation: vicious twins. *J Am Coll Cardiol.* (2016) 68:2217–28. doi: 10.1016/J.JACC.2016.08.048

5. Sartipy U, Dahlström U, Fu M, Lund LH. Atrial fibrillation in heart failure with preserved, mid-range, and reduced ejection fraction. *JACC Heart Fail.* (2017) 5:565–74. doi: 10.1016/J.JCHF.2017.05.001

6. Shah SJ, Kitzman DW, Borlaug BA, van Heerebeek L, Zile MR, Kass DA, et al. Phenotype-specific treatment of heart failure with preserved ejection fraction. *Circulation.* (2016) 134:73–90. doi: 10.1161/CIRCULATIONAHA.116.021884

7. Ho JE, Zern EK, Wooster L, Bailey CS, Cunningham T, Eisman AS, et al. Differential clinical profiles, exercise responses, and outcomes associated with existing HFpEF definitions. *Circulation.* (2019) 140:353–65. doi: 10.1161/CIRCULATIONAHA.118.039136

8. Arnold JR, McCann GP. Cardiovascular magnetic resonance: applications and practical considerations for the general cardiologist. *Heart.* (2020) 106:174–81. doi: 10.1136/HEARTJNL-2019-314856

9. Kanagala P, Cheng ASH, Singh A, McAdam J, Marsh AM, Arnold JR, et al. Diagnostic and prognostic utility of cardiovascular magnetic resonance imaging in heart failure with preserved ejection fraction - implications for clinical trials. *J Cardiovasc Magn Reson.* (2018) 20:1–12. doi: 10.1186/S12968-017-0424-9

10. Ramos JG, Fyrdahl A, Wieslander B, Thalén S, Reiter G, Reiter U, et al. Comprehensive cardiovascular magnetic resonance diastolic dysfunction grading shows very good agreement compared with echocardiography. *JACC Cardiovasc Imaging.* (2020) 13:2530–42. doi: 10.1016/j.jcmg.2020.06.027

11. Bottini PB, Carr AA, Prisant LM, Flickinger FW, Allison JD, Gottdiener JS. Magnetic resonance imaging compared to echocardiography to assess left ventricular mass in the hypertensive patient. *Am J Hypertens.* (1995) 8:221–8. doi: 10.1016/0895-7061(94)00178-E

12. Myerson SG, Bellenger NG, Pennell DJ. Assessment of left ventricular mass by cardiovascular magnetic resonance. *Hypertension.* (2002) 39:750–5. doi: 10.1161/hy0302.104674

13. Bhuva A, Bai W, Lau C, Davies R, Ye Y, Bulluck H, et al. A multicenter, scan-rescan, human and machine learning cmr study to test generalizability and precision in imaging biomarker analysis. *Circ Cardiovasc Imaging.* (2019) 12:e009214. doi: 10.1161/CIRCIMAGING.119.009214

14. Barkhausen J, Ruehm SG, Goyen M, Buck T, Laub G, Debatin JF. MR evaluation of ventricular function: true fast imaging with steady-state precession versus fast low-angle shot cine MR imaging: feasibility study. *Radiology.* (2001) 219:264–9. doi: 10.1148/radiology.219.1.r01ap12264

15. Childs H, Ma L, Ma M, Clarke J, Cocker M, Green J, et al. Comparison of long and short axis quantification of left ventricular volume parameters by cardiovascular magnetic resonance, with ex-vivo validation. *J Cardiovasc Magn Reson.* (2011) 13:1–9. doi: 10.1186/1532-429X-13-40

16. Palmieri V, Bella JN, Dequattro V, Roman MJ, Hahn RT, Dahlof B, et al. Relations of diastolic left ventricular filling to systolic chamber and myocardial contractility in hypertensive patients with left ventricular hypertrophy (the PRESERVE study). *Am J Cardiol.* (1999) 84:558–62.

17. Kannel WB. Factors of risk in the development of coronary heart disease—six-year follow-up experience. *Ann Intern Med.* (1961) 55:33. doi: 10.7326/0003-4819-55-1-33

18. Levy D, Garrison R, Savage D, Kannel W, Castelli W. Prognostic implications of echocardiographically determined left ventricular mass in the Framingham Heart Study. *N Engl J Med.* (1990) 322:1561–6. doi: 10.1056/nejm199005313222203

19. Tsao CW, Gona PN, Salton CJ, Chuang ML, Levy D, Manning WJ, et al. Left ventricular structure and risk of cardiovascular events: a framingham heart study cardiac magnetic resonance study. *J Am Heart Assoc.* (2015) 4:e002188. doi: 10.1161/JAHA.115.002188

20. Bluemke DA, Kronmal RA, Lima JAC, Liu K, Olson J, Burke GL, et al. The relationship of left ventricular mass and geometry to incident cardiovascular events. The MESA (Multi-Ethnic Study of Atherosclerosis) Study. *J Am Coll Cardiol.* (2008) 52:2148–55. doi: 10.1016/j.jacc.2008.09.014

21. Rathi VK, Doyle M, Yamrozik J, Williams RB, Caruppannan K, Truman C, et al. Routine evaluation of left ventricular diastolic function by cardiovascular magnetic resonance: a practical approach. *J Cardiovasc Magn Reson.* (2008) 10:36. doi: 10.1186/1532-429X-10-36

22. Bollache E, Redheuil A, Clément-Guinaudeau S, Defrance C, Perdrix L, Ladouceur M, et al. Automated left ventricular diastolic function evaluation from phase-contrast cardiovascular magnetic resonance and comparison with Doppler echocardiography. *J Cardiovasc Magn Reson.* (2010) 12:1–11. doi: 10.1186/1532-429X-12-63

23. Buss SJ, Krautz B, Schnackenburg B, Abdel-Aty H, Santos MFB, Andre F, et al. Classification of diastolic function with phase-contrast cardiac magnetic resonance imaging: validation with echocardiography and age-related reference values. *Clin Res Cardiol.* (2014) 103:441–50. doi: 10.1007/s00392-014-0669-3

24. Lin E, Alessio A. What are the basic concepts of temporal, contrast, and spatial resolution in cardiac CT? *J Cardiovasc Comput Tomogr.* (2009) 3:403. doi: 10.1016/J.JCCT.2009.07.003

25. Chamsi-Pasha MA, Zhan Y, Debs D, Shah DJ. CMR in the evaluation of diastolic dysfunction and phenotyping of HFpEF: current role and future perspectives. *JACC Cardiovasc Imaging.* (2020) 13:283–96. doi: 10.1016/j.jcmg.2019.02.031

26. Gulsin GS, Singh A, McCann GP. Cardiovascular magnetic resonance in the evaluation of heart valve disease. *BMC Med Imaging.* (2017) 17:1–14. doi: 10.1186/S12880-017-0238-0/FIGURES/16

27. Fyrdahl A, Ramos JG, Eriksson MJ, Caidahl K, Ugander M, Sigfridsson A. Sector-wise golden-angle phase contrast with high temporal resolution for evaluation of left ventricular diastolic dysfunction. *Magn Reson Med.* (2020) 83:1310–21. doi: 10.1002/MRM.28018

28. Brandts A, Bertini M, Van Dijk EJ, Delgado V, Marsan NA, Van Der Geest RJ, et al. Left ventricular diastolic function assessment from three-dimensional three-directional velocity-encoded MRI with retrospective valve tracking. *J Magn Reson Imaging.* (2011) 33:312–9. doi: 10.1002/jmri.22424

29. Crandon S, Westenberg JJM, Swoboda PP, Fent GJ, Foley JRJ, Chew PG, et al. Impact of age and diastolic function on novel, 4D flow CMR biomarkers of left ventricular blood flow kinetic energy. *Sci Rep.* (2018) 8:1–11. doi: 10.1038/s41598-018-32707-5

30. Ho CY, Solomon SD. A clinician's guide to tissue doppler imaging. *Circulation* (2006) 113:579268. doi: 10.1161/CIRCULATIONAHA.105.579268

31. Nagueh SF, Smiseth OA, Appleton CP, Byrd BF, Dokainish H, Edvardsen T, et al. Recommendations for the evaluation of left ventricular diastolic function by echocardiography: an update from the american society of echocardiography and the European Association of Cardiovascular Imaging. *Eur Hear J Cardiovasc Imaging.* (2016) 17:1321–60. doi: 10.1093/ehjci/jew082

32. Paelinck BP, De Roos A, Bax JJ, Bosmans JM, Van Der Geest RJ, Dhondt D, et al. Feasibility of tissue magnetic resonance imaging: a pilot study in comparison with tissue Doppler imaging and invasive measurement. *J Am Coll Cardiol.* (2005) 45:1109–16. doi: 10.1016/j.jacc.2004.12.051

33. Okayama S, Nakano T, Uemura S, Fujimoto S, Somekawa S, Watanabe M, et al. Evaluation of left ventricular diastolic function by fractional area change using cine cardiovascular magnetic resonance: a feasibility study. *J Cardiovasc Magn Reson.* (2013) 15:2–7. doi: 10.1186/1532-429X-15-87

34. Marwick TH. Ejection fraction pros and cons: JACC state-of-the-art review. *J Am Coll Cardiol.* (2018) 72:2360–79. doi: 10.1016/J.JACC.2018.08.2162

35. Potter E, Marwick TH. Assessment of left ventricular function by echocardiography: the case for routinely adding global longitudinal strain to ejection fraction. *JACC Cardiovasc Imaging.* (2018) 11:260–74. doi: 10.1016/J.JCMG.2017.11.017

36. Cikes M, Solomon SD. Beyond ejection fraction: an integrative approach for assessment of cardiac structure and function in heart failure. *Eur Heart J.* (2016) 37:1642–50. doi: 10.1093/EURHEARTJ/EHV510

37. Nesbitt GC, Mankad S, Oh JK. Strain imaging in echocardiography: methods and clinical applications. *Int J Cardiovasc Imaging.* (2009) 251:9–22. doi: 10.1007/S10554-008-9414-1

38. Kalam K, Otahal P, Marwick TH. Prognostic implications of global LV dysfunction: A systematic review and meta-analysis of global longitudinal strain and ejection fraction. *Heart.* (2014) 100:1673–80. doi: 10.1136/heartjnl-2014-305538

39. Pedrizzetti G, Claus P, Kilner PJ, Nagel E. Principles of cardiovascular magnetic resonance feature tracking and echocardiographic speckle tracking for informed clinical use. *J Cardiovasc Magn Reson.* (2016) 18:1–12. doi: 10.1186/s12968-016-0269-7

40. Ambale-Venkatesh B, Armstrong AC, Liu CY, Donekal S, Yoneyama K, Wu CO, et al. Diastolic function assessed from tagged MRI predicts heart failure and atrial fibrillation over an 8-year follow-up period: the multi-ethnic study of atherosclerosis. *Eur Heart J Cardiovasc Imaging.* (2014) 15:442–9. doi: 10.1093/ehjci/jet189

41. Neizel M, Lossnitzer D, Korosoglou G, Schäufele T, Lewien A, Steen H, et al. Strain-encoded (SENC) magnetic resonance imaging to evaluate regional heterogeneity of myocardial strain in healthy volunteers: comparison with conventional tagging. *J Magn Reson Imaging.* (2009) 29:99–105. doi: 10.1002/JMRI.21612

42. Korosoglou G, Giusca S, Hofmann NP, Patel AR, Lapinskas T, Pieske B, et al. Strain-encoded magnetic resonance: a method for the assessment of myocardial deformation. *ESC Hear Fail.* (2019) 6:584–602. doi: 10.1002/EHF2.12442

43. Lapinskas T, Zieschang V, Erley J, Stoiber L, Schnackenburg B, Stehning C, et al. Strain-encoded cardiac magnetic resonance imaging: a new approach for fast estimation of left ventricular function. *BMC Cardiovasc Disord.* (2019) 19:1–7. doi: 10.1186/S12872-019-1031-5/FIGURES/4

44. Pan L, Stuber M, Kraitchman DL, Fritzges DL, Gilson WD, Osman NF. Real-time imaging of regional myocardial function using fast-SENC. *Magn Reson Med.* (2006) 55:386–95. doi: 10.1002/MRM.20770

45. Petersen SE, Jung BA, Wiesmann F, Selvanayagam JB, Francis JM, Hennig J, et al. Myocardial tissue phase mapping with cine phase-contrast MR imaging: regional wall motion analysis in healthy volunteers. *Radiology.* (2006) 238:816–26. doi: 10.1148/radiol.2383041992

46. Kinno M, Nagpal P, Horgan S, Waller AH. Comparison of echocardiography, cardiac magnetic resonance, and computed tomographic imaging for the evaluation of left ventricular myocardial function: part 2 (diastolic and regional assessment). *Curr Cardiol Rep.* (2017) 19:1–13. doi: 10.1007/s11886-017-0816-3

47. Onishi T, Saha SK, Delgado-Montero A, Ludwig DR, Onishi T, Schelbert EB, et al. Global longitudinal strain and global circumferential strain by speckle-tracking echocardiography and feature-tracking cardiac magnetic resonance imaging: comparison with left ventricular ejection fraction. *J Am Soc Echocardiogr.* (2015) 28:587–96. doi: 10.1016/j.echo.2014.11.018

48. Kuetting D, Sprinkart AM, Doerner J, Schild H, Thomas D. Comparison of magnetic resonance feature tracking with harmonic phase imaging analysis (CSPAMM) for assessment of global and regional diastolic function. *Eur J Radiol.* (2015) 84:100–7. doi: 10.1016/j.ejrad.2014.10.011

49. Moody WE, Taylor RJ, Edwards NC, Chue CD, Umar F, Taylor TJ, et al. Comparison of magnetic resonance feature tracking for systolic and diastolic strain and strain rate calculation with spatial modulation of magnetization imaging analysis. *J Magn Reson Imaging.* (2015) 41:1000–12. doi: 10.1002/jmri.24623

50. Ito H, Ishida M, Makino W, Goto Y, Ichikawa Y, Kitagawa K, et al. Cardiovascular magnetic resonance feature tracking for characterization of patients with heart failure with preserved ejection fraction: correlation of global longitudinal strain with invasive diastolic functional indices. *J Cardiovasc Magn Reson.* (2020) 22:1–11. doi: 10.1186/s12968-020-00636-w

51. Romano S, Judd RM, Kim RJ, Kim HW, Klem I, Heitner JF, et al. Feature-tracking global longitudinal strain predicts death in a multicenter population of patients with ischemic and nonischemic dilated cardiomyopathy incremental to ejection fraction and late gadolinium enhancement. *JACC Cardiovasc Imaging.* (2018) 11:1419–29. doi: 10.1016/j.jcmg.2017.10.024

52. Kammerlander AA, Kraiger JA, Nitsche C, Donà C, Duca F, Zotter-Tufaro C, et al. Global longitudinal strain by CMR feature tracking is associated with outcome in HFPEF. *JACC Cardiovasc Imaging.* (2019) 12:1585–7. doi: 10.1016/j.jcmg.2019.02.016

53. Kowallick JT, Lamata P, Hussain ST, Kutty S, Steinmetz M, Sohns JM, et al. Quantification of left ventricular torsion and diastolic

recoil using cardiovascular magnetic resonance myocardial feature tracking. *PLoS ONE* (2014) 9:e0109164. doi: 10.1371/journal.pone.0109164

54. Nucifora G, Muser D, Morocutti G, Piccoli G, Zanuttini D, Gianfagna P, et al. Disease-specific differences of left ventricular rotational mechanics between cardiac amyloidosis and hypertrophic cardiomyopathy. *Am J Physiol Heart Circ Physiol.* (2014) 307:H680–8. doi: 10.1152/AJPHEART.00251.2014

55. Pritchett AM, Mahoney DW, Jacobsen SJ, Rodeheffer RJ, Karon BL, Redfield MM. Diastolic dysfunction and left atrial volume: a population-based study. *J Am Coll Cardiol.* (2005) 45:87–92. doi: 10.1016/J.JACC.2004.09.054

56. Tsang TSM, Abhayaratna WP, Barnes ME, Miyasaka Y, Gersh BJ, Bailey KR, et al. Prediction of cardiovascular outcomes with left atrial size: is volume superior to area or diameter? *J Am Coll Cardiol.* (2006) 47:1018–23. doi: 10.1016/J.JACC.2005.08.077

57. Souto Nacif M, Dias Barranhas A, Türkbey E, Marchiori E, Kawel N, Mello RAF, et al. Left atrial volume quantification using cardiac MRI in atrial fibrillation: Comparison of the Simpson's method with biplane area-length, ellipse, and three-dimensional methods. *Diagnostic Interv Radiol.* (2013) 19:213–20. doi: 10.5152/dir.2012.002

58. Kawel-Boehm N, Hetzel SJ, Ambale-Venkatesh B, Captur G, Francois CJ, Jerosch-Herold M, et al. Reference ranges ("normal values") for cardiovascular magnetic resonance (CMR) in adults and children: 2020 update. *J Cardiovasc Magn Reson.* (2020) 22:1–63. doi: 10.1186/S12968-020-00683-3

59. Khan MA, Yang EY, Zhan Y, Judd RM, Chan W, Nabi F, et al. Association of left atrial volume index and all-cause mortality in patients referred for routine cardiovascular magnetic resonance: a multicenter study 11 Medical and Health Sciences 1102 Cardiorespiratory Medicine and Haematology. *J Cardiovasc Magn Reson.* (2019) 21:1–12. doi: 10.1186/S12968-018-0517-0/FIGURES/5

60. Schuster A, Hor KN, Kowallick JT, Beerbaum P, Kutty S. Cardiovascular magnetic resonance myocardial feature tracking: concepts and clinical applications. *Circ Cardiovasc Imaging.* (2016) 9:1–9. doi: 10.1161/CIRCIMAGING.115.004077

61. Kanagala P, Arnold JR, Singh A, Khan JN, Gulsin GS, Gupta P, et al. Intra-study and inter-technique validation of cardiovascular magnetic resonance imaging derived left atrial ejection fraction as a prognostic biomarker in heart failure with preserved ejection fraction. *Int J Cardiovasc Imaging.* (2020) 36:921–8. doi: 10.1007/S10554-020-01785-W/FIGURES/3

62. Posina K, McLaughlin J, Rhee P, Li L, Cheng J, Schapiro W, et al. Relationship of phasic left atrial volume and emptying function to left ventricular filling pressure: a cardiovascular magnetic resonance study. *J Cardiovasc Magn Reson.* (2013) 15:1–8. doi: 10.1186/1532-429X-15-99

63. Nguyen J, Weber J, Hsu B, Mulyala RR, Wang L, Cao JJ. Comparing left atrial indices by CMR in association with left ventricular diastolic dysfunction and adverse clinical outcomes. *Sci Rep.* (2021) 11:1–10. doi: 10.1038/s41598-021-00596-w

64. Gupta S, Matulevicius SA, Ayers CR, Berry JD, Patel PC, Markham DW, et al. Left atrial structure and function and clinical outcomes in the general population. *Eur Heart J.* (2013) 34:278–85. doi: 10.1093/EURHEARTJ/EHS188

65. Markman TM, Habibi M, Venkatesh BA, Zareian M, Wu C, Heckbert SR, et al. Association of left atrial structure and function and incident cardiovascular disease in patients with diabetes mellitus : results from multi-ethnic study of atherosclerosis (MESA). *Eur Heart J.* (2017) 18:1138–44. doi: 10.1093/ehjci/jew332

66. Kanagala P, Arnold JR, Cheng ASH, Singh A, Khan JN, Gulsin GS, et al. Left atrial ejection fraction and outcomes in heart failure with preserved ejection fraction. *Int J Cardiovasc Imaging.* (2019) 36:101–10. doi: 10.1007/s10554-019-01684-9

67. Kowallick JT, Kutty S, Edelmann F, Chiribiri A, Villa A, Steinmetz M, et al. Quantification of left atrial strain and strain rate using Cardiovascular Magnetic Resonance myocardial feature tracking: a feasibility study. *J Cardiovasc Magn Reson.* (2014) 16:1–9. doi: 10.1186/s12968-014-0060-6

68. Chirinos JA, Sardana M, Ansari B, Satija V, Kuriakose D, Edelstein I, et al. Left atrial phasic function by cardiac magnetic resonance feature tracking is a strong predictor of incident cardiovascular events. *Circ Cardiovasc Imaging.* (2018) 11:e007512. doi: 10.1161/CIRCIMAGING.117.007512

69. Habibi M, Chahal H, Opdahl A, Gjesdal O, Helle-Valle TM, Heckbert SR, et al. Association of CMR-measured LA function with heart failure development: results from the MESA study. *JACC Cardiovasc Imaging.* (2014) 7:570–9. doi: 10.1016/j.jcmg.2014.01.016

70. Von Roeder M, Rommel KP, Kowallick JT, Blazek S, Besler C, Fengler K, et al. Influence of left atrial function on exercise capacity and left ventricular function in patients with heart failure and preserved ejection fraction. *Circ Cardiovasc Imaging.* (2017) 10:e005467. doi: 10.1161/CIRCIMAGING.116.005467

71. Kanagala P, Arnold JR, Singh A, Khan JN, Gulsin GS, Gupta P, et al. Prevalence of right ventricular dysfunction and prognostic significance in heart failure with preserved ejection fraction. *Int J Cardiovasc Imaging.* (2021) 37:255–66. doi: 10.1007/S10554-020-01953-Y/TABLES/5

72. Hur DJ, Sugeng L. Non-invasive multimodality cardiovascular imaging of the right heart and pulmonary circulation in pulmonary hypertension. *Front Cardiovasc Med.* (2019) 6:24. doi: 10.3389/FCVM.2019.00024/BIBTEX

73. Borlaug BA, Paulus WJ. Heart failure with preserved ejection fraction: pathophysiology, diagnosis, and treatment. *Eur Heart J.* (2011) 32:670–9. doi: 10.1093/eurheartj/ehq426

74. Neilan TG, Shah R V, Abbasi SA, Farhad H, Groarke JD, Dodson JA, et al. The incidence, pattern, and prognostic value of left ventricular myocardial scar by late gadolinium enhancement in patients with atrial fibrillation. *J Am Coll Cardiol.* (2013) 62:2205–14. doi: 10.1016/J.JACC.2013.07.067

75. Kwong RY, Sattar H, Wu H, Vorobiof G, Gandla V, Steel K, et al. Incidence and prognostic implication of unrecognized myocardial scar characterized by cardiac magnetic resonance in diabetic patients without clinical evidence of myocardial infarction. *Circulation.* (2008) 118:1011–20. doi: 10.1161/CIRCULATIONAHA.107.727826

76. Wong TC, Piehler KM, Zareba KM, Lin K, Phrampus A, Patel A, et al. Myocardial damage detected by late gadolinium enhancement cardiovascular magnetic resonance is associated with subsequent hospitalization for heart failure. *J Am Heart Assoc.* (2013) 2:e000416. doi: 10.1161/JAHA.113.000416

77. Azadani PN, King JB, Kheirkhahan M, Chang L, Marrouche NF, Wilson BD. Left atrial fibrosis is associated with new-onset heart failure in patients with atrial fibrillation. *Int J Cardiol.* (2017) 248:161–5. doi: 10.1016/j.ijcard.2017.07.007

78. Duca F, Kammerlander AA, Zotter-Tufaro C, Aschauer S, Schwaiger ML, Marzluf BA, et al. Interstitial fibrosis, functional status, and outcomes in heart failure with preserved ejection fraction. *Circ Cardiovasc Imaging.* (2016) 9:e005277. doi: 10.1161/CIRCIMAGING.116.005277/-/DC1

79. Messroghli DR, Moon JC, Ferreira VM, Grosse-Wortmann L, He T, Kellman P, et al. Clinical recommendations for cardiovascular magnetic resonance mapping of T1, T2, T2* and extracellular volume: a consensus statement by the Society for Cardiovascular Magnetic Resonance (SCMR) endorsed by the European Association for Cardiovascular Imaging (EACVI). *J Cardiovasc Magn Reson.* (2017) 19:1–24. doi: 10.1186/S12968-017-0389-8

80. Su MYM, Lin LY, Tseng YHE, Chang CC, Wu CK, Lin JL, et al. CMR-verified diffuse myocardial fibrosis is associated with diastolic dysfunction in HFpEF. *JACC Cardiovasc Imaging.* (2014) 7:991–7. doi: 10.1016/J.JCMG.2014.04.022

81. Rommel KP, Von Roeder M, Latuscynski K, Oberueck C, Blazek S, Fengler K, et al. Extracellular volume fraction for characterization of patients with heart failure and preserved ejection fraction. *J Am Coll Cardiol.* (2016) 67:1815–25. doi: 10.1016/J.JACC.2016.02.018

82. Omori T, Nakamori S, Fujimoto N, Ishida M, Kitagawa K, Ichikawa Y, et al. Myocardial native T 1 predicts load-independent left ventricular chamber stiffness in patients with HFpEF. *JACC Cardiovasc Imaging.* (2020) 13:2117–28. doi: 10.1016/J.JCMG.2020.05.030

83. Mordi IR, Singh S, Rudd A, Srinivasan J, Frenneaux M, Tzemos N, et al. Comprehensive echocardiographic and cardiac magnetic resonance evaluation differentiates among heart failure with preserved ejection fraction patients, hypertensive patients, and healthy control subjects. *JACC Cardiovasc Imaging.* (2018) 11:577–85. doi: 10.1016/J.JCMG.2017.05.022

84. Roy C, Slimani A, De Meester C, Amzulescu M, Pasquet A, Vancraeynest D, et al. Associations and prognostic significance of diffuse myocardial fibrosis by cardiovascular magnetic resonance in heart failure with preserved ejection fraction. *J Cardiovasc Magn Reson.* (2018) 20:1–12. doi: 10.1186/S12968-018-0477-4

85. Schelbert EB, Fridman Y, Wong TC, Abu Daya H, Piehler KM, Kadakkal A, et al. Temporal relation between myocardial fibrosis and heart failure with preserved ejection fraction: association with baseline disease severity and subsequent outcome. *JAMA Cardiol.* (2017) 2:995–1006. doi: 10.1001/JAMACARDIO.2017.2511

86. Mascherbauer J, Marzluf BA, Tufaro C, Pfaffenberger S, Graf A, Wexberg P, et al. Cardiac magnetic resonance postcontrast T1 time is associated with outcome in patients with heart failure and preserved ejection fraction. *Circ Cardiovasc Imaging.* (2013) 6:1056–65. doi: 10.1161/CIRCIMAGING.113.000633

87. Kanagala P, Cheng ASH, Singh A, Khan JN, Gulsin GS, Patel P, et al. Relationship between focal and diffuse fibrosis assessed by CMR and clinical outcomes in heart failure with preserved ejection fraction. *JACC Cardiovasc Imaging.* (2019) 12:2291–301. doi: 10.1016/J.JCMG.2018.11.031

88. Nitsche C, Kammerlander AA, Binder C, Duca F, Aschauer S, Koschutnik M, et al. Native T1 time of right ventricular insertion points by cardiac magnetic resonance: relation with invasive haemodynamics and outcome in heart failure

with preserved ejection fraction. *Eur Heart J Cardiovasc Imaging.* (2020) 21:683–91. doi: 10.1093/EHJCI/JEZ221

89. Guazzi M, Adams V, Conraads V, Halle M, Mezzani A, Vanhees L, et al. Clinical recommendations for cardiopulmonary exercise testing data assessment in specific patient populations. *Circulation.* (2012) 126:2261–74. doi: 10.1161/CIR.0b013e31826fb946

90. Obokata M, Kane GC, Reddy YNV, Olson TP, Melenovsky V, Borlaug BA. Role of diastolic stress testing in the evaluation for heart failure with preserved ejection fraction: a simultaneous invasive-echocardiographic study. *Circulation.* (2017) 135:825–38. doi: 10.1161/CIRCULATIONAHA.116.024822

91. Kato S, Nakamori S, Roujol S, Delling FN, Akhtari S, Jang J, et al. Relationship between native papillary muscle T1 time and severity of functional mitral regurgitation in patients with non-ischemic dilated cardiomyopathy. *J Cardiovasc Magn Reson.* (2017) 18:79. doi: 10.1186/s12968-016-0301-y

92. Rush CJ, Berry C, Oldroyd KG, Rocchiccioli JP, Lindsay MM, Touyz RM, et al. Prevalence of coronary artery disease and coronary microvascular dysfunction in patients with heart failure with preserved ejection fraction. *JAMA Cardiol.* (2021) 6:1130–43. doi: 10.1001/JAMACARDIO.2021.1825

93. Backhaus SJ, Lange T, George EF, Hellenkamp K, Gertz RJ, Billing M, et al. Exercise stress real-time cardiac magnetic resonance imaging for noninvasive characterization of heart failure with preserved ejection fraction: the HFpEF-stress trial. *Circulation* (2021) 143:1484–98. doi: 10.1161/CIRCULATIONAHA.120.051542

94. Löffler AI, Pan JA, Balfour PC, Shaw PW, Yang Y, Nasir M, et al. Coronary microvascular dysfunction and diffuse myocardial fibrosis measured by cardiovascular magnetic resonance are characteristic of HFpEF. *Am J Cardiol.* (2019) 124:1584. doi: 10.1016/J.AMJCARD.2019.08.011

95. Pezel T, Hovasse T, Sanguineti F, Kinnel M, Garot P, Champagne S, et al. Long-term prognostic value of stress CMR in patients with heart failure and preserved ejection fraction. *Cardiovasc Imaging.* (2021) 14:2319–33. doi: 10.1016/J.JCMG.2021.03.010

96. Arnold JR, Kanagala P, Budgeon CA, Jerosch-Herold M, Gulsin GS, Singh A, et al. Prevalence and prognostic significance of microvascular dysfunction in heart failure with preserved ejection fraction. *JACC Cardiovasc Imaging* (2022) 15:1001–11. doi: 10.1016/J.JCMG.2021.11.022

97. Diamant M, Lamb HJ, Groeneveld Y, Endert EL, Smit JWA, Bax JJ, et al. Diastolic dysfunction is associated with altered myocardial metabolism in asymptomatic normotensive patients with well-controlled type 2 diabetes mellitus. *J Am Coll Cardiol.* (2003) 42:328–35. doi: 10.1016/s0735-1097(03)00625-9

98. Burrage MK, Hundertmark M, Valkovič L, Watson WD, Rayner J, Sabharwal N, et al. Energetic basis for exercise-induced pulmonary congestion in heart failure with preserved ejection fraction. *Circulation.* (2021) 144:1664–78. doi: 10.1161/circulationaha.121.054858

99. Mahmod M, Pal N, Rayner J, Holloway C, Raman B, Dass S, et al. The interplay between metabolic alterations, diastolic strain rate and exercise capacity in mild heart failure with preserved ejection fraction: A cardiovascular magnetic resonance study. *J Cardiovasc Magn Reson.* (2018) 20:1–10. doi: 10.1186/S12968-018-0511-6/TABLES/3

100. Anker SD, Butler J, Filippatos G, Ferreira JP, Bocchi E, Böhm M, et al. Empagliflozin in heart failure with a preserved ejection fraction. *N Engl J Med.* (2021) 385:1451–61. doi: 10.1056/NEJMOA2107038/SUPPL_FILE/NEJMOA2107038_DATA-SHARING.PDF

101. Thirunavukarasu S, Jex N, Chowdhary A, Hassan IU, Straw S, Craven TP, et al. Empagliflozin treatment is associated with improvements in cardiac energetics and function and reductions in myocardial cellular volume in patients with type 2 diabetes. *Diabetes.* (2021) 70:2810–22. doi: 10.2337/DB21-0270

102. Rao VN, Fudim M, Mentz RJ, Michos ED, Felker GM. Regional adiposity and heart failure with preserved ejection fraction. *Eur J Heart Fail.* (2020) 22:1540–50. doi: 10.1002/EJHF.1956

103. Obokata M, Reddy YNV, Pislaru S V, Melenovsky V, Borlaug BA. Evidence supporting the existence of a distinct obese phenotype of heart failure with preserved ejection fraction. *Circulation.* (2017) 136:6–19. doi: 10.1161/CIRCULATIONAHA.116.026807/-/DC1

104. Mendoza D, Codella N, Wang Y, Prince M, Sethi S, Manoushagian S, et al. Impact of diastolic dysfunction severity on global left ventricular volumetric filling—assessment by automated segmentation of routine cine cardiovascular magnetic resonance. *J Cardiovasc Magn Reson.* (2010) 12:1–11. doi: 10.1186/1532-429X-12-46

105. Gao C, Tao Y, Pan J, Shen C, Zhang J, Xia Z, et al. Evaluation of elevated left ventricular end diastolic pressure in patients with preserved ejection fraction using cardiac magnetic resonance. *Eur Radiol.* (2019) 29:2360–8. doi: 10.1007/s00330-018-5955-4

106. Hieda M, Parker J, Rajabi T, Fujimoto N, Bhella PS, Prasad A, et al. Left ventricular volume-time relation in patients with heart failure with preserved ejection fraction. *Am J Cardiol.* (2018) 121:609–14. doi: 10.1016/j.amjcard.2017.11.033

107. Kawaji K, Codella NCF, Prince MR, Chu CW, Shakoor A, LaBounty TM, et al. Automated segmentation of routine clinical cardiac magnetic resonance imaging for assessment of left ventricular diastolic dysfunction. *Circ Cardiovasc Imaging.* (2009) 2:476–84. doi: 10.1161/CIRCIMAGING.109.879304

108. Reiter G, Reiter U, Kovacs G, Kainz B, Schmidt K, Maier R, et al. Magnetic resonance-derived 3-dimensional blood flow patterns in the main pulmonary artery as a marker of pulmonary hypertension and a measure of elevated mean pulmonary arterial pressure. *Circ Cardiovasc Imaging.* (2008) 1:23–30. doi: 10.1161/CIRCIMAGING.108.780247

109. Reiter U, Reiter G, Kovacs G, Stalder AF, Gulsun MA, Greiser A, et al. Evaluation of elevated mean pulmonary arterial pressure based on magnetic resonance 4D velocity mapping: comparison of visualization techniques. *PLoS ONE.* (2013) 8:e82212. doi: 10.1371/JOURNAL.PONE.0082212

110. Reiter G, Reiter U, Kovacs G, Olschewski H, Fuchsjäger M. Blood flow vortices along the main pulmonary artery measured with MR imaging for diagnosis of pulmonary hypertension. *Radiology.* (2015) 275:71–9. doi: 10.1148/RADIOL.14140849

111. Ramos JG, Fyrdahl A, Wieslander B, Reiter G, Reiter U, Jin N, et al. Cardiovascular magnetic resonance 4D flow analysis has a higher diagnostic yield than Doppler echocardiography for detecting increased pulmonary artery pressure. *BMC Med Genet.* (2020) 21:1–9. doi: 10.1186/S12880-020-00428-9

112. Shors SM, Cotts WG, Pavlovic-Surjancev B, François CJ, Gheorghiade M, Finn JP. Heart failure: evaluation of cardiopulmonary transit times with time-resolved. *MR Angiography.* (2003) 229:743–8. doi: 10.1148/RADIOL.2293021363

113. Cao JJ Li L, McLaughlin J, Passick M. Prolonged central circulation transit time in patients with HFpEF and HFrEF by magnetic resonance imaging. *Eur Heart J Cardiovasc Imaging.* (2018) 19:339–46. doi: 10.1093/ehjci/jex051

114. Khalique Z, Ferreira PF, Scott AD, Nielles-Vallespin S, Firmin DN, Pennell DJ. Diffusion tensor cardiovascular magnetic resonance imaging: a clinical perspective. *JACC Cardiovasc Imaging.* (2020) 13:1235–55. doi: 10.1016/J.JCMG.2019.07.016

115. Arani A, Arunachalam SP, Chang ICY, Baffour F, Rossman PJ, Glaser KJ, et al. Cardiac MR elastography for quantitative assessment of elevated myocardial stiffness in cardiac amyloidosis. *J Magn Reson Imaging.* (2017) 46:1361–7. doi: 10.1002/JMRI.25678

116. Raisi-Estabragh Z, Izquierdo C, Campello VM, Martin-Isla C, Jaggi A, Harvey NC, et al. Cardiac magnetic resonance radiomics: basic principles and clinical perspectives. *Eur Hear J - Cardiovasc Imaging.* (2020) 21:349–56. doi: 10.1093/EHJCI/JEAA028

frontiers | Frontiers in Cardiovascular Medicine

TYPE Systematic Review
PUBLISHED 22 July 2022
DOI 10.3389/fcvm.2022.895836

OPEN ACCESS

EDITED BY
Tong Liu,
Tianjin Medical University, China

REVIEWED BY
Jiang Bian,
University of Florida, United States
Kevin Sack,
Medtronic Inc, Ireland

*CORRESPONDENCE
Xizhou Guan
gxz301@126.com
Kunlun He
kunlunhe@301hospital.com.cn

†These authors have contributed equally to this work

SPECIALTY SECTION
This article was submitted to Heart Failure and Transplantation, a section of the journal Frontiers in Cardiovascular Medicine

RECEIVED 14 March 2022
ACCEPTED 04 July 2022
PUBLISHED 22 July 2022

CITATION
Sun J, Guo H, Wang W, Wang X, Ding J, He K and Guan X (2022) Identifying novel subgroups in heart failure patients with unsupervised machine learning: A scoping review. *Front. Cardiovasc. Med.* 9:895836. doi: 10.3389/fcvm.2022.895836

Identifying novel subgroups in heart failure patients with unsupervised machine learning: A scoping review

Jin Sun[1†], Hua Guo[1†], Wenjun Wang[2,3†], Xiao Wang[2,3], Junyu Ding[1], Kunlun He[2,3*] and Xizhou Guan[4*]

[1]Medical School of Chinese PLA, Beijing, China, [2]Key Laboratory of Ministry of Industry and Information Technology of Biomedical Engineering and Translational Medicine, Chinese PLA General Hospital, Beijing, China, [3]Medical Big Data Center, Chinese PLA General Hospital, Beijing, China, [4]Department of Pulmonary and Critical Care Medicine, The Eighth Medical Center, Chinese PLA General Hospital, Beijing, China

Background: Heart failure is currently divided into three main forms, HFrEF, HFpEF, and HFmrEF, but its etiology is diverse and highly heterogeneous. Many studies reported a variety of novel subgroups in heart failure patients, with unsupervised machine learning methods. The aim of this scoping review is to provide insights into how these techniques can diagnose and manage HF faster and better, thus providing direction for future research and facilitating its routine use in clinical practice.

Methods: The review was performed following PRISMA-SCR guideline. We searched the PubMed database for eligible publications. Studies were included if they defined new subgroups in HF patients using clustering analysis methods, and excluded if they are (1) Reviews, commentary, or editorials, (2) Studies not about defining new sub-types, or (3) Studies not using unsupervised algorithms. All study screening and data extraction were conducted independently by two investigators and narrative integration of data extracted from included studies was performed.

Results: Of the 498 studies identified, 47 were included in the analysis. Most studies (61.7%) were published in 2020 and later. The largest number of studies (46.8%) coming from the United States, and most of the studies were authored and included in the same country. The most commonly used machine learning method was hierarchical cluster analysis (46.8%), the most commonly used cluster variable type was comorbidity (61.7%), and the least used cluster variable type was genomics (12.8%). Most of the studies used data sets of less than 500 patients (48.9%), and the sample size had negative correlation with the number of clustering variables. The majority of studies (85.1%) assessed the association between cluster grouping and at least one outcomes, with death and hospitalization being the most commonly used outcome measures.

Conclusion: This scoping review provides an overview of recent studies proposing novel HF subgroups based on clustering analysis. Differences were

found in study design, study population, clustering methods and variables, and outcomes of interests, and we provided insights into how these studies were conducted and identify the knowledge gaps to guide future research.

KEYWORDS

heart failure, subtype, machine learning, clustering analysis, scoping review

Introduction

Heart failure (HF) is the serious manifestation and terminal stage of many cardiovascular diseases, with a high level of mortality and readmission rate (1). The global prevalence of HF is about 26 million, and with the aggravation of population aging and the increase of survival rate of acute coronary syndrome (ACS), the prevalence of HF is increasing continuously (2). However, the existing treatment measures are only symptomatic support treatments to improve symptoms, but cannot completely reverse the course of disease. One of the reasons for this phenomenon is that the current HF subpopulation cannot fully integrate the heterogeneity of HF clinical manifestations and progression, which further aggravates the serious consequences caused by inadequate or even inaccurate phenotypic classification.

In previous guidelines for heart failure, heart failure was classified according to the cut-off point of LVEF—heart failure with reduced ejection fraction (HFrEF): HF with LVEF $\leq$ 40%; Heart failure with preserved ejection fraction (HFpEF): HF with LVEF $\geq$ 50%; Heart failure with intermediate ejection fraction (HFmrEF): HF with LVEF $>$ 40% and L VEF $<$ 50% (3). The new guideline proposed a new and revised classification of HF according to LVEF: HF with improved ejection fraction (HFimpEF): symptomatic HF with a baseline LVEF $\leq$ 40%, a $\geq$ 10 points increase from baseline LVEF, and a second measurement of LVEF $>$ 40%. When classifying heart failure based on LVEF, previous guidelines have used HFrEF and HFpEF, but for the types of heart failure with EF values between 40 and 49%, there are different terms used, and there is no uniform standard. In the new classification, patients with normalized EF may have decreased EF after drug treatment was discontinued, meaning that although EF improved, cardiac structure and function did not (4). Although large number of studies have analyzed and summarized the structural and functional characteristics of cardiac cells, intercellular excitation conduction pathway, and cellular inflammation degree of patients in each subtype under this classic classification, there is still a situation of lack of effective treatment and limited personalized medical care, which urgently requires more accurate and detailed grouping strategies (5, 6). The complexity of the development of heart failure is difficult to explain with the emphasis on symptoms and signs in the previous diagnostic classification. We believe that the new subtype will give new directions in the interpretation of heterogeneity and treatment selection. The introduction of subgroups of patients with homogeneous characteristics is helpful to treat patients according to their clinical and pathophysiological characteristics, reduces the complexity of the cross influence of data characteristics of different dimensions during the treatment of patients, and plays a role in improving the treatment and prognosis (7).

Machine learning (ML) has achieved good accuracy in early diagnosis, clinical classification and risk factor prediction of patients with HF (8, 9). However, because of the black box feature of the algorithm, we cannot learn from the classification process of the algorithm. Unsupervised machine learning, specifically clustering analysis, is used to find the similar or different features between patients groups, and identify subgroups with homogeneous features. Clustering studies have certain advantages in characterizing, classifying or treating patients differently. Clustering algorithms commonly are performed in a static way with baseline data and/or outcome data. They are useful to answer descriptive questions (10, 11). In the early attempts, unsupervised clustering analysis algorithms were used on clinical laboratory indexes and demographic data characteristics of patients with heart failure to make homogeneous inductive groups (12, 13). In recent studies, researchers also used echocardiography, genomics and comorbidity characteristics to explore more grouping strategies (14). Without knowing the outcomes information (i.e., unsupervised learning), clustering analysis can comprehensively reflect the association between new subgroups and heart failure outcomes and other prognostic indicators.

There are wide variations in studies defining new heart failure subgroups, in study design, statistical methods, and reporting of outcomes, which makes comparing and summarizing results from different studies very difficult. Therefore, it is necessary to conduct a scope review to summarize the current practice in studies on the new subgroups of heart failure, clarify the limitations and provide direction and planning for the future research. At present, some researchers have discussed the application of machine learning in heart failure subtypes. Banerjee et al. included 15 studies published

up to 2015, and compared the symptoms of cardiovascular diseases such as ACS, myocardial infarction (MI) and heart failure (HF) (15); In addition, Banerjee and others evaluated the subtype definition and risk prediction of ML in HF, ACS and AF (Atrial Fibrillation), and systematically reviewed them (15). However, in their research, the definitions of heart failure and subgroups are only a part of the research, and the clustering variables concerned are not comprehensive, and the included research is up to December, 2019 at the latest. Therefore, it is necessary to define the scope with a specific focus on the subtype classification in heart failure, and fully incorporating the latest research reports. This scoping review will integrate the current evidence on subtype classification of heart failure reported in the existing literature to provide a reference for clinicians and community health care workers to manage HF better, and identify the knowledge gaps to point out the direction for future research.

Methods

This scoping review followed the Preferred Reporting Items for Systematic reviews and Meta-Analyses extension for Scoping Reviews (PRISMA-ScR) guideline (16), and a competed PRISMA-ScR checklist was provided in **Supplementary Material**. A study protocol was designed by a senior author and agreed by all authors, and this protocol was not registered or published.

Literature search

We performed a search in PubMed to identify primary studies on discovery of new HF sub-types by using clustering analysis. The search strategy contained 3 modules: the HF module, the algorithm module, and the sub-type module, and a filter of publication time till 31st December 2021 (see **Supplementary Material** Search Strategy).

Eligibility criteria

Studies were included if they defined new subgroups in HF patients using clustering analysis methods. Exclusion criteria were: (1) Reviews, commentary, or editorials, (2) Studies not about defining new sub-types, (3) Studies not using unsupervised algorithms.

Study selection

Titles and abstracts were independently scanned by one of the two authors and checked by the other, to identify potentially eligible articles, which were then assessed with full texts for final inclusion. Disagreements were resolved through discussion by the two reviewers, and a third author made the final decision when an agreement was not reached.

Data extraction

Data was collected on basic study characteristics including title, name of the first author, year of publication, country, and information and the analysis and results including study population, sample size, clustering method(s), types of clustering variables, and outcome(s). The data extraction form and data extracted in this study can be found in the **Supplementary Material**. All included articles were reviewed and extracted by one of the two authors and double checked by the other. Disagreements were resolved through discussion, if necessary the final judgment was from a third reviewer.

Data synthesis

Data synthesis was performed with descriptive statistics and data visualization. Categorical variables were presented as counts and proportions, and continuous variables were presented with median and IQR. All the statistical analyses were performed with R version 3.6.1 and RStudio version 1.2.5001, and packages ggplot2, networkD3 (sankey diagram), ggparliament (parliament diagram), UpSetR (upset plot) and scatterpie (bubble chart).

Results

Search finding

A total of 498 studies were identified by the search strategy, all of them were screened for titles and abstracts, of which 446 were excluded at this stage. Fifty-two studies entered the stage of full-text reading to assess their qualification, and five of them were excluded, for reasons shown in **Figure 1**. In the end, 47 studies were included in the review.

Characteristics of the included studies

Table 1 shows the basic characteristics of the included studies in this review. Among the 47 included studies, 23(48.9%) studies focused on patients with generalized HF (7, 13, 17–31), while the rest 24 studies focused on patients with specific categories of HF, among which 19 studies (40.4%) focused on patients with HFpEF (32–50), and the other 5 studies (14, 51–54) (10.6%) focused on HFrEF. Of these studies, only one

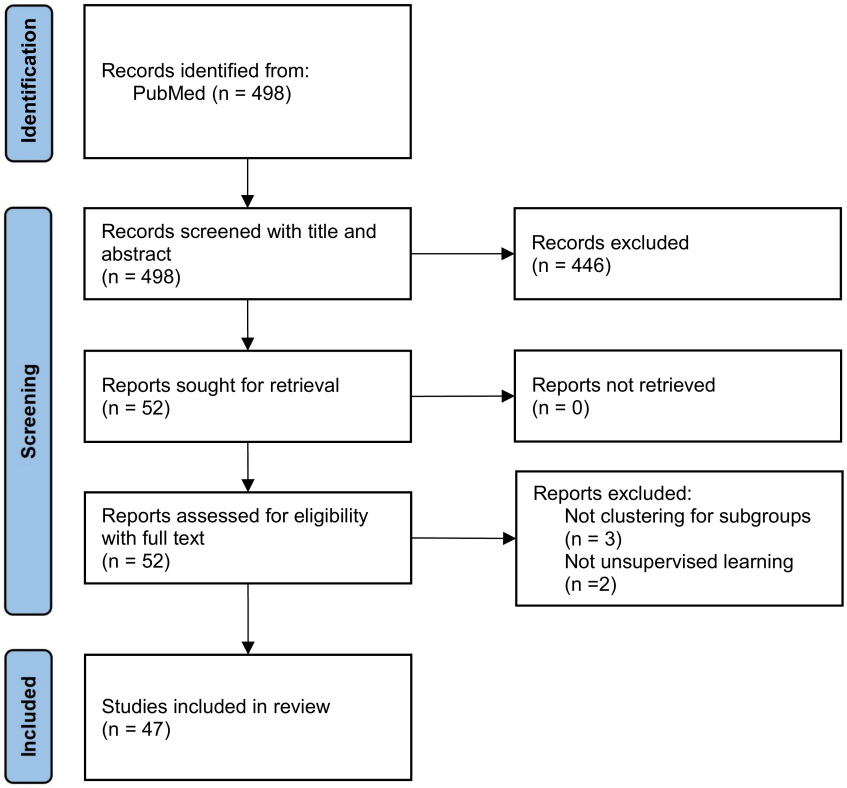

FIGURE 1
PRISMA flow diagram for study inclusion.

(2.1%) was published before 2010 (55) and four (8.5%) were published between 2010 and 2014 (19, 20, 54, 56). Most of the research was published after 2015, and the research after 2020 accounted for 61.7% (32, 34, 35, 37, 38, 40, 42–44), as shown in **Figure 2**.

In all the included studies, the corresponding authors were from 13 different countries, including the United States (22, 46.8%) (18–22, 24, 26–28, 33, 36, 37, 40, 41, 44, 48, 53, 54, 56–59), the Netherlands (5, 10.6%) (23, 45, 47, 55, 60), France (5, 10.6%) (13, 17, 32, 43, 51), Spain (3, 6.4%) (25, 34, 38), China (3, 6.4%) (7, 35, 49) and Japan (2, 4.3%) (31). Australia (52), Germany (30), Italy (14), Poland (39), Switzerland (46), Canada (50) and the United Kingdom (29) each had only one study (1, 2.1%). The research data were from a single country in 40 studies (85.1%), and the rest 7 studies (14.9%) were performed with multinational data (13, 17, 24, 28, 37, 43, 60). The relationship between data sources and corresponding authors is shown in **Figure 3**. We further classify them according to their continents, and find that the highest number of authors and participants are from America and Europe, followed by Asia and Oceania, as shown in **Table 1**.

We analyzed the types of data source, the results showed that in all included in the article, there are 24 articles (51.1%) using EHR data, 9 articles (19.1%) using RCT research data, 8 articles (17.0%) using disease registration data, 3 article (6.4%) using the observational data, 1 article (2.1%) using the claims data. In addition, one study used EHR data and Claims data simultaneously, and another study used EHR data, RCT data and registries data simultaneously.

In addition, of the 47 included studies, only 6 (12.8%) were externally validated, while the remaining 41 studies (87.2%) were not.

Types of clustering methods in the included studies

The clustering methods were categorized into six main types, and the usage of each type of methods in the included studies are shown in **Figure 4** and **Table 1**. The most commonly used ML method was hierarchical clustering method (32–33, 35, 38–41, 43, 44), accounting for 46.8% (22/47) of all studies, followed by latent class analysis (11, 23.4%) (7, 17, 24, 26, 29, 30, 32, 36, 37, 47, 55) and K-Means/Medoids (9, 19.1%) (13, 28, 31, 34, 42, 50, 52, 53, 60), and two studies used mixture model-based approach (4.3%) (46, 58). The least commonly used methods were spectral (49), self-organizing map (23) and composite of hierarchical and K-Means/Medoids (27).

TABLE 1 Descriptive statistics of study characteristics.

Characteristics	Studies, *n* (%)/M(Q1–Q3)
HF subtype	
HF	23 (48.9%)
HFpEF	19 (40.4%)
HFrEF	5 (10.6%)
Years published	
<2010	1 (2.1%)
2010–2014	4 (8.5%)
2015–2019	13 (27.7%)
≥2020	29 (61.7%)
Author country	
Asia	5 (10.6%)
Europe	18 (38.3%)
America	23 (48.9%)
Oceania	1 (2.1%)
Data source	
Asia	4 (8.5%)
Europe	14 (29.8%)
America	21 (44.7%)
Oceania	1 (2.1%)
Multinational	7 (14.9%)
Data types	
EHR	24 (51.1%)
RCT	9 (19.1%)
Disease registries	8 (17.0%)
Observational data	3 (6.4%)
Claims data	1 (2.1%)
EHR and claims data	1 (2.1%)
EHR, RCT, and registries data	1 (2.1%)
Method	
K-Means/Medoids	9 (19.1%)
LCA	11 (23.4%)
Hierarchical	22 (46.8%)
Hierarchical & K-Means/Medoids	1 (2.1%)
SOM	1 (2.1%)
Spectral	1 (2.1%)
Mixture model-based	2 (4.3%)
Sample size	480 (301–1619)
Number of variables	18 (11–47)
Number of clusters	3 (3–6)
Variable type	
Demographic	24 (51.1%)
Clinical	25 (53.2%)
Laboratory	21 (44.7%)
Imaging	24 (51.1%)
Genetic	6 (12.8%)
Symptoms and complaints	18 (38.3%)
Comorbidities	29 (61.7%)
Outcome	
Cross sectional	7 (14.9%)
Mortality	36 (76.6%)
Hospitalisation	27 (57.4%)
Other events	14 (29.8%)
External validation	
Yes	6 (12.8%)
No	41 (87.2%)

Types of clustering variables used in the included studies

We divide all the variables used by the institute for unsupervised cluster analysis into seven categories: demographic data (such as gender, age, education level, etc.), clinical data (such as heart rate, respiratory rate, etc.), laboratory data, image features (such as LEVF, etc.), genetic data, clinical symptoms and complications, and comorbidities. We have sorted out the frequency with which these variable types are used and whether they are jointly used in cluster analysis, as shown in **Table 1** and **Figure 5**. As far as the frequency of variable types is concerned, comorbidities are the most frequently used in these studies 29(61.7%), and the clinical data, imaging data, demographic data and laboratory data are almost the same, which are 25(53.2%), 24(51.1%), 24(51.1%) and 21(44.7%) respectively. Among them, gene data, symptoms and complications data, image data, laboratory data and complications data are used alone in the process of sub-grouping in some studies. Most studies combine multiple data types to make a new subgroup classification of heart failure.

Sample size, number of clustering variables, and number of clusters

The sample sizes in the derivation of subgroups ranged from 63 to 318,384. In all 47 studies, the median sample size was 480, of which 23 studies (48.9%) included data sets of more than 500 people, and only 2 studies (4.3%) had a sample size of less than 100 people. The number of clustering variables involved in the research also varies widely, the research with the least variables was using only 7 clinical, laboratory or imaging indicators, and the research with the most variables was using 13,000 genes for clustering analysis to determine their molecular subgroups. The number of clusters obtained in most studies ranged from 2 to 7 (97.9%), with a median of 3, of which 16 studies (34.0%) finally got 3 clusters, and only one study got 11 clusters. **Figure 6** shows the relationship between the number of variables (X-axis, in log scale) and the number of clusters (Y-axis) identified in each study, and the sample size (in log scale) is presented as the radius of the bubble. The Spearman correlation was −0.14

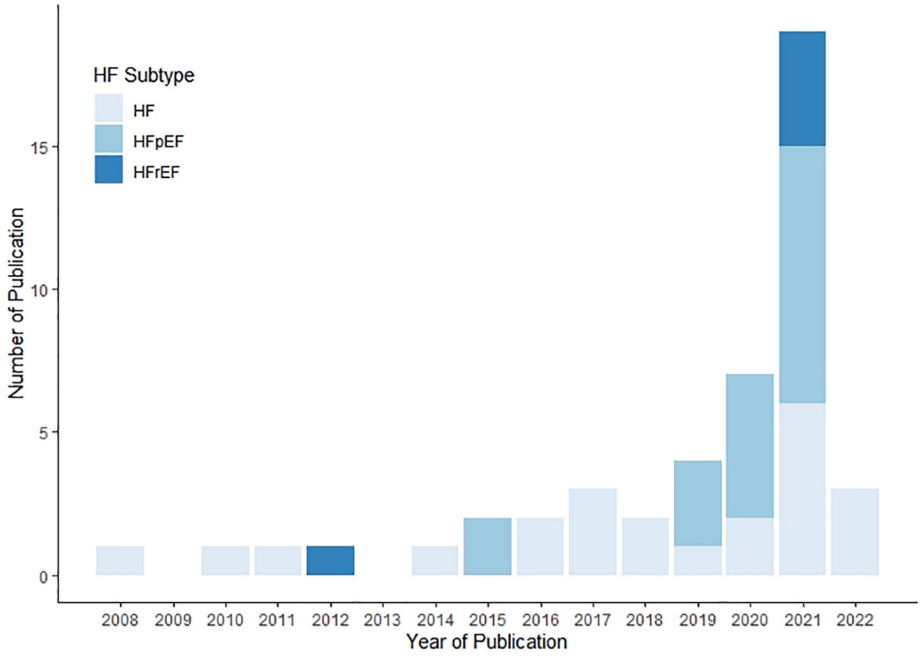

FIGURE 2
Number of publication per year by HF sub-types.

between sample size and number of clustering variables, 0.15 between sample size and number of clusters, and 0.13 between number of clustering variables and number of clusters.

Prognostic implications of the clusters proposed in the included studies

Many different outcomes were used to evaluate the prognostic implication of the identified new subgroups, thus they were classified into four categories: death, hospitalization, other events, and cross-sectional study (i.e., no prognostication was assessed). The most commonly used endpoints were death (36, 76.6%) and hospital (27, 57.4%) respectively, while in 7 studies (14.9%) no analysis was performed for prognostic implications. The outcomes evaluated in each study are shown in **Figure 6**.

Discussion

In this scoping review, we summarized the current research on identifying subgroups in HF patients with unsupervised machine learning methods. This type of studies increased quickly over past years, and there were 19 new publications in 2021. Differences were found in study design, study population, clustering methods and variables, and outcomes of interests, and we aimed to provide insights into how these studies were conducted and identify the knowledge gaps to guide future research.

Most of the studies were conducted by researchers from developed countries, or in geographic, from Europe and North America, which is not a surprising finding given their leading position in the field of biomedical and clinical researches. However, subgroups identified from these populations may have poor generalizability in other part of the world. Africa, South America, South and West Asia were under represented, since the data availability is limited in those areas. We also noticed that most researchers worked on data from their own country, and only a few studies were from multinational collaboration. Future research should consider combining datasets containing patients from different countries and regions, to investigate the potential application of the new subgroups worldwide.

With regarding to the clustering methods, in this scoping review, the most commonly used unsupervised machine learning algorithm is hierarchical clustering, followed by K-Means or K-Medoids. Hierarchical clustering has the advantage of not requesting predefined number of clusters, which is useful in exploring novel subgroups. Researchers have had long history in using K-Means or K-Medoids clustering in analyzing data, and these methods were considered as multivariate analysis before the term of machine learning getting its popularity (61, 62).

The novel HF subgroups can be defined with different types of variable, however, the application of subgroups also depends on how difficult these clustering variables can be

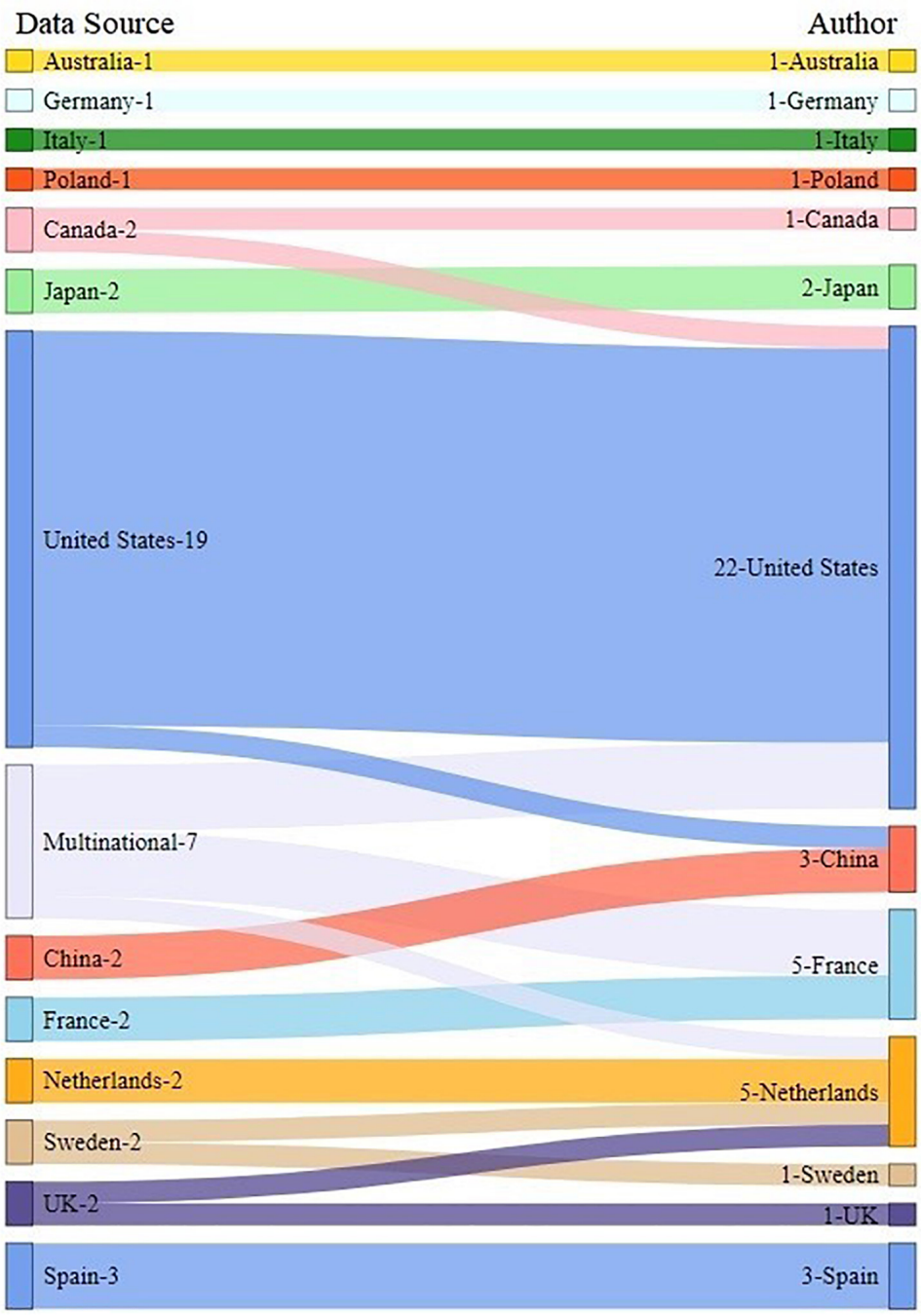

FIGURE 3
Relationship between data sources and corresponding authors.

collected. Obtaining demographic variables and underlying comorbidities is straightforward by asking the patient's medical history at admission, which made them as the most frequently used variables in clustering analysis, and laboratory data and imaging data can also be obtained in routine examination after admission. However, genomics or proteomics data may need extra special examination methods, which are less common compared with other data types, so that genomics or proteomics are rarely used in the included studies, but this also heralds the great potential of genomics in revealing the prognosis of heart failure patients.

The implementation of machine learning methods relay on data in a large degree. In the included studies, 23 studies used datasets of less than 500 patients and only 15 studies

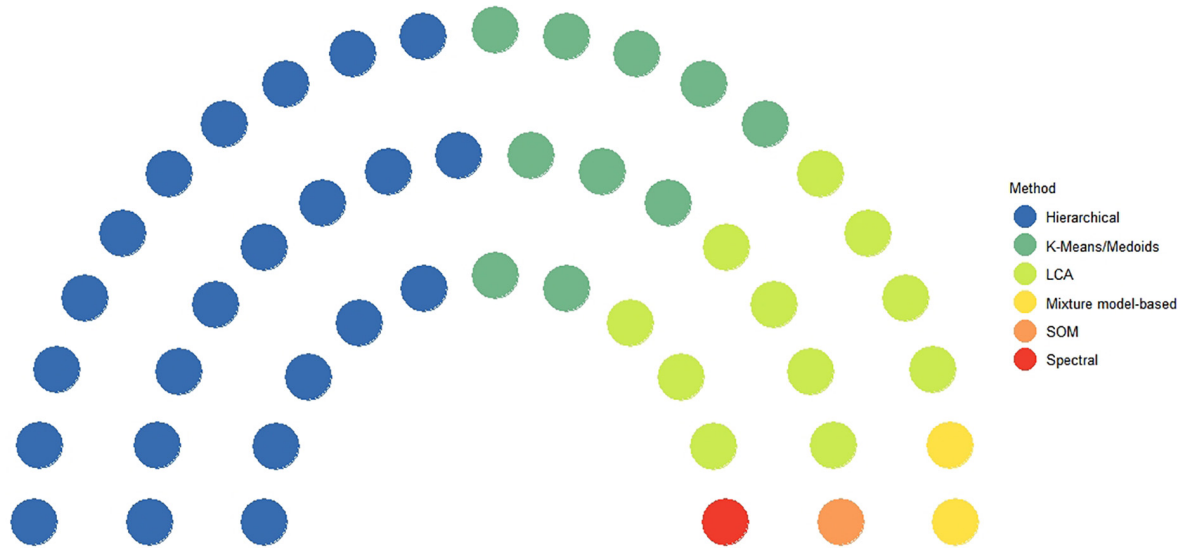

FIGURE 4
Types of machine learning methods used in identifying HF subgroups.

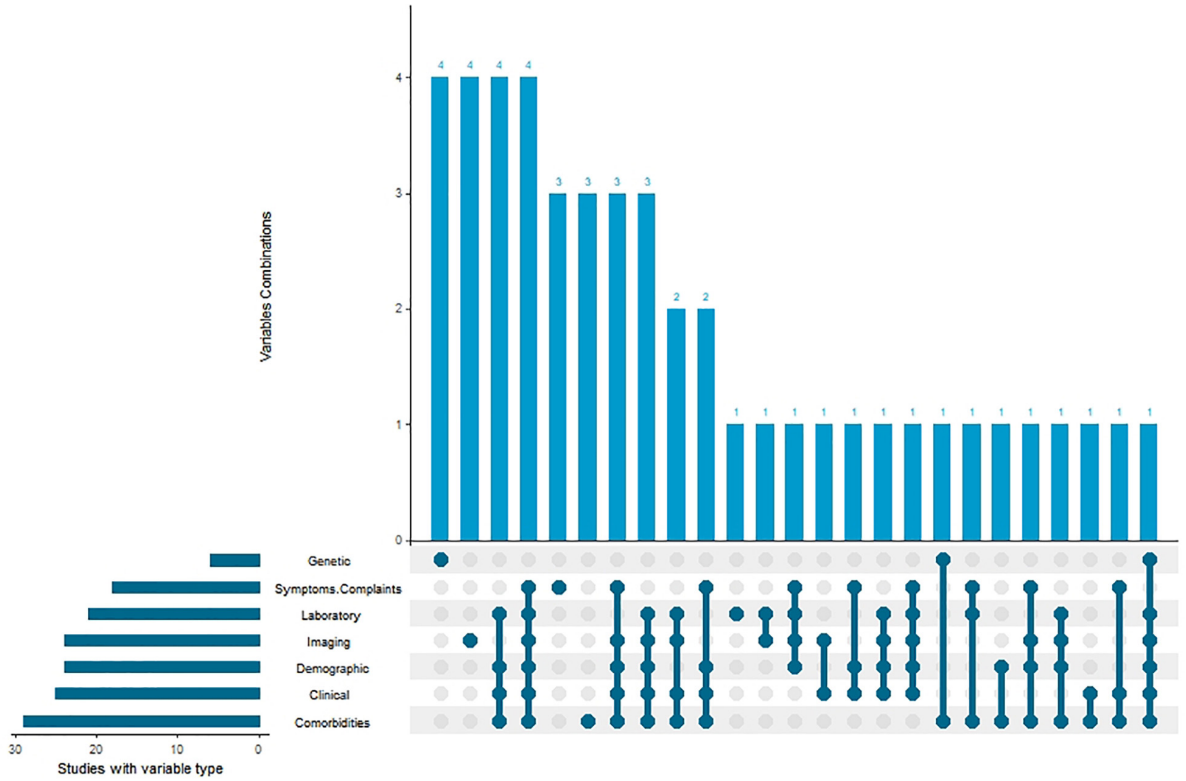

FIGURE 5
Types of clustering variables used in identifying HF subgroups.

used data sets of more than 1,000 patients. At the same time, the number of clustering variables is relatively big, sometime even higher than the sample size, which may lead to overfitting issues. A negative correlation was observed between the number of clustering variables and the sample size, which is not as expected. When more clustering variables are included in the

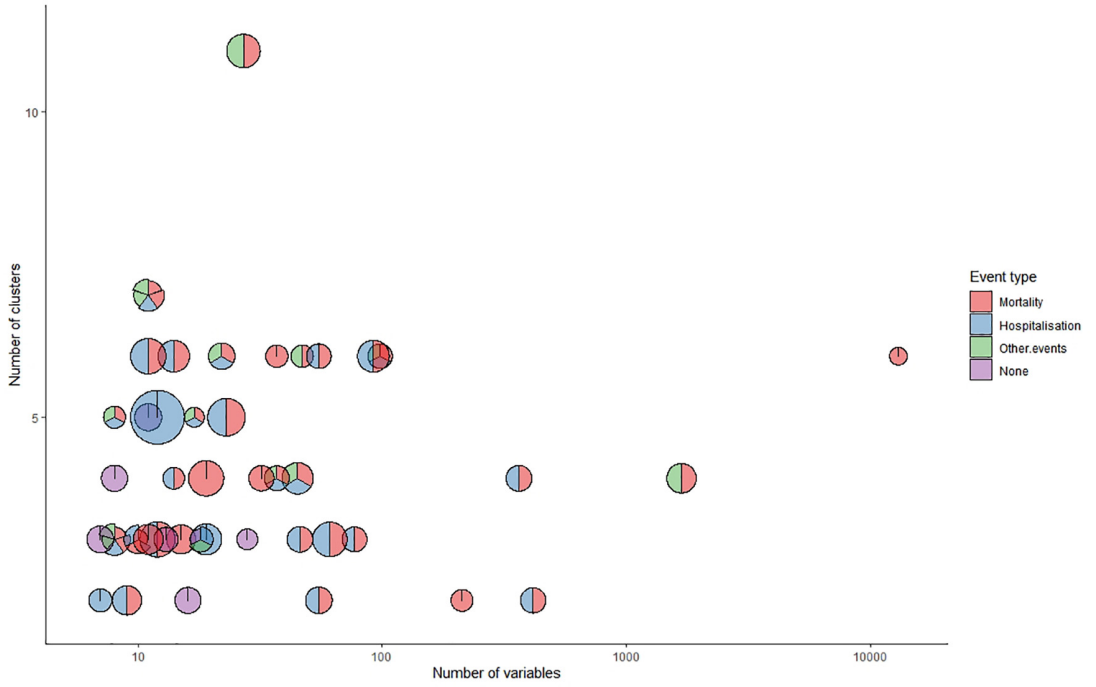

FIGURE 6
Features of the clusters identified in the included studies.

analyses, researchers need to make sure the sample size is sufficient to get reliable results.

Some included studies did not evaluate the prognostic implication of the proposed subgroups, and we marked these studies as cross-sectional studies. Unsupervised cluster analysis does have obvious advantages in finding out the heterogeneity among patients, and the new subgroup is also more accurate in describing the symptoms and complications of patients, but not connecting with the prognosis means that it is limited in clinical application, so we hope that more researches will make a clear plan for the clinical endpoint of patients. In addition, we found that few studies have set the quality of life or daily behavior ability as the research endpoint, which may be due to the fact that similar endpoints need more detailed evaluation scales or multi-dimensional evaluation indicators, which are quite different in the nature of easy access compared with the outcome endpoints such as death or readmission.

Unlike traditional prediction models, which pay more attention to the prediction accuracy and absolute probability of having a specific event, clustering analysis focused on classifying complex and heterogeneous diseases and identifying people with similar clinical characteristics. Thus, subgroups identified with clustering analysis may have better explanation and clinical meaning than prediction models. With these novel subgroups, patients can be more accurately risk stratified by more simple and easily available clinical indicators, and then targeted treatment schemes can be formulated.

With the development of coronary intervention technology, more patients with coronary heart disease survive and develop into heart failure. Coupled with the aggravation of population aging, the number of patients with heart failure is increasing year by year (63, 64), there is a higher proportion of elderly patients among them, and the existence mode of comorbidity is more complicated, which is followed by the increase of medical expenses, mortality and hospitalization rate (65). More and more researchers are aware of the importance of comorbidity management. The study on comorbidity of patients with heart failure found that the number of participants suffering from diabetes, chronic kidney disease and atrial fibrillation was higher (66), and other common comorbidities included hypertension and chronic obstructive pulmonary diseases. Some studies showed that some comorbidities would change the disease phenotype of patients with heart failure, and even become the main cause of heart failure (67), whereas some studies reported that the comorbidity of patients with heart failure was more serious, which might be caused by heart failure. Diabetes, hypertension, etc., are also associated with worse clinical outcomes in other diseases. Therefore, it is of great significance to carry out more personalized management for patients with heart failure under different comorbidity modes. These common comorbidities are important variables in our included studies, and the emergence of new subgroups and new treatment standards have also brought about the improvement of clinical prognosis in these studies. In addition to the elderly

patients with heart failure, recent studies have found that the prevalence of cardiovascular comorbidities in middle-aged patients with heart failure is also very high, compared with the elderly patients with heart failure (>85 years old) (68). In the included studies, the new grouping of patients based on comorbidity or combined with other types of data also provided reference for clinical treatment.

There are also some limitations of the current scoping review. First, when searching for eligible publications, we only performed the literature search in PubMed database. Some other databases such as scienceDirect, Embase, IEEE, Scopus, etc., were not searched specifically, since most of the relevant publications are covered by PubMed, and looking for more databases will only increase the duplicates and add unnecessary workload. Given this is a scope review rather than a systematic review, we strictly enforce this search strategy, and we are confident the results presented in this scoping review are not biased. Second, we only included publications in English, and excluded those in other languages, which may reduce the diversity of this scope review. Third, we did not evaluate the evaluation criteria and external validation of the novel subgroups, since they are seldom done in the included studies. We believe validation or replication of the proposed subgroups are essential before these subgroups will be used in clinical practice, and future studies should pay more attention to these analyses. At last, this scoping review is only a comprehensive description of the existing researches on subgroup identification in HF patients, thus no formal assessment on methodological quality (or risk of bias) or meta-analysis was performed in this review. These analyses are usually within a systematic review, and are beyond the scope of this scoping review. In future research, we plan to perform a systematic review on studies with similar subgroup definition and a meta-analysis on their prognostic performance.

Data availability statement

The original contributions presented in this study are included in the article/**Supplementary Material**, further inquiries can be directed to the corresponding authors.

Author contributions

JS and HG screened the publications, extracted data, and prepared the first draft. WW conducted a rigorous review of the first and final drafts. XW and JD participated in the revision of the research protocol and data extraction form. KH and XG designed and conceptualized the research project, rigorously revised and approved the final manuscript. All authors contributed to the article and approved the submitted version.

Funding

This work was supported by the Ministry of Industry and Information Technology of China (2020-01 03-3-1).

Conflict of interest

The authors declare that the research was conducted in the absence of any commercial or financial relationships that could be construed as a potential conflict of interest.

Publisher's note

Supplementary material

The Supplementary Material for this article can be found online at: https://www.frontiersin.org/articles/10.3389/fcvm.2022.895836/full#supplementary-material

References

1. Tomasoni D, Adamo M, Lombardi CM, Metra M. Highlights in heart failure. *ESC Heart Fail.* (2019) 6:1105–27. doi: 10.1002/ehf2.12555

2. Savarese G, Lund LH. Global public health burden of heart failure. *Cardiac Fail Rev.* (2017) 3:7–11. doi: 10.15420/cfr.2016:25:2

3. Bozkurt B, Coats AJS, Tsutsui H, Abdelhamid CM, Adamopoulos S, Albert N, et al. Universal definition and classification of heart failure: a report of the Heart Failure Society of America, Heart Failure Association of the European Society of Cardiology, Japanese Heart Failure Society and Writing Committee of the Universal Definition of Heart Failure: endorsed by the Canadian Heart Failure Society, Heart Failure Association of India, Cardiac Society of Australia and New Zealand, and Chinese Heart Failure Association. *Eur J Heart Fail.* (2021) 23:352–80. doi: 10.1002/ejhf.2115

4. Writing Committee Members, ACC/AHA Joint Committee Members. 2022 AHA/ACC/HFSA Guideline for the Management of Heart Failure. *J Card Fail.* (2022) 28:e1–167. doi: 10.1016/j.cardfail.2022.02.010

5. Warbrick I, Rabkin SW. Effect of the peptides relaxin, neuregulin, ghrelin and glucagon-like peptide-1, on cardiomyocyte factors involved in the molecular mechanisms leading to diastolic dysfunction and/or heart failure with preserved ejection fraction. *Peptides.* (2019) 111:33–41. doi: 10.1016/j.peptides.2018.05.009

6. Mishra S, Kass DA. Cellular and molecular pathobiology of heart failure with preserved ejection fraction. *Nat Rev Cardiol.* (2021) 18:400–23. doi: 10.1038/s41569-020-00480-6

7. Zheng C, Han L, Tian J, Li J, He H, Han G, et al. Hierarchical management of chronic heart failure: a perspective based on the latent structure of comorbidities. *ESC Heart Fail.* (2022) 9:595–605. doi: 10.1002/ehf2.13708

8. Sanchez-Martinez S, Duchateau N, Erdei T, Fraser AG, Bijnens BH, Piella G. Characterization of myocardial motion patterns by unsupervised multiple kernel learning. *Med Image Anal.* (2017) 35:70–82. doi: 10.1016/j.media.2016.06.007

9. Motwani M, Dey D, Berman DS, Germano G, Achenbach S, Al-Mallah MH, et al. Machine learning for prediction of all-cause mortality in patients with suspected coronary artery disease: a 5-year multicentre prospective registry analysis. *Eur Heart J.* (2017) 38:500–7. doi: 10.1093/eurheartj/ehw188

10. Liu Y, Li Z, Xiong H, Gao X, Wu J, Wu S. Understanding and enhancement of internal clustering validation measures. *IEEE Trans Cybern.* (2013) 43:982–94. doi: 10.1109/tsmcb.2012.2220543

11. Gravesteijn BY, Steyerberg EW, Lingsma HF. Modern learning from big data in critical care: primum non nocere. *Neurocrit Care.* (2022). [Epub ahead of print]. doi: 10.1007/s12028-022-01510-6

12. Omar AMS, Narula S, Abdel Rahman MA, Pedrizzetti G, Raslan H, Rifaie O, et al. Precision phenotyping in heart failure and pattern clustering of ultrasound data for the assessment of diastolic dysfunction. *JACC Cardiovasc Imaging.* (2017) 10:1291–303. doi: 10.1016/j.jcmg.2016.10.012

13. Stienen S, Ferreira JP, Kobayashi M, Preud'homme G, Dobre D, Machu JL, et al. Enhanced clinical phenotyping by mechanistic bioprofiling in heart failure with preserved ejection fraction: insights from the MEDIA-DHF study (The Metabolic Road to Diastolic Heart Failure). *Biomarkers.* (2020) 25:201–11. doi: 10.1080/1354750x.2020.1727015

14. Carluccio E, Pugliese NR, Biagioli P, Zuchi C, Lauciello R, Mengoni A, et al. Global longitudinal strain in heart failure with reduced ejection fraction: prognostic relevance across disease severity as assessed by automated cluster analysis. *Int J Cardiol.* (2021) 332:91–8. doi: 10.1016/j.ijcard.2021.02.072

15. Banerjee A, Chen S, Fatemifar G, Zeina M, Lumbers RT, Mielke J, et al. Machine learning for subtype definition and risk prediction in heart failure, acute coronary syndromes and atrial fibrillation: systematic review of validity and clinical utility. *BMC Med.* (2021) 19:85. doi: 10.1186/s12916-021-01940-7

16. Tricco AC, Lillie E, Zarin W, O'Brien KK, Colquhoun H, Levac D, et al. PRISMA extension for scoping reviews (PRISMA-ScR): checklist and explanation. *Ann Intern Med.* (2018) 169:467–73. doi: 10.7326/m18-0850

17. Tamisier R, Damy T, Bailly S, Davy JM, Verbraecken J, Lavergne F, et al. Adaptive servo ventilation for sleep apnoea in heart failure: the FACE study 3-month data. *Thorax.* (2022) 77:178–85. doi: 10.1136/thoraxjnl-2021-217205

18. Sethares KA, Chin E. Age and gender differences in physical heart failure symptom clusters. *Heart Lung.* (2021) 50:832–7. doi: 10.1016/j.hrtlng.2021.07.001

19. Vanburen P, Ma J, Chao S, Mueller E, Schneider DJ, Liew CC. Blood gene expression signatures associate with heart failure outcomes. *Physiol Genomics.* (2011) 43:392–7. doi: 10.1152/physiolgenomics.00175.2010

20. Ahmad T, Pencina MJ, Schulte PJ, O'Brien E, Whellan DJ, Piña IL, et al. Clinical implications of chronic heart failure phenotypes defined by cluster analysis. *J Am Coll Cardiol.* (2014) 64:1765–74. doi: 10.1016/j.jacc.2014.07.979

21. Ahmad T, Desai N, Wilson F, Schulte P, Dunning A, Jacoby D, et al. Clinical implications of cluster analysis-based classification of acute decompensated heart failure and correlation with bedside hemodynamic profiles. *PLoS One.* (2016) 11:e0145881. doi: 10.1371/journal.pone.0145881

22. Gevaert AB, Tibebu S, Mamas MA, Ravindra NG, Lee SF, Ahmad T, et al. Clinical phenogroups are more effective than left ventricular ejection fraction categories in stratifying heart failure outcomes. *ESC Heart Fail.* (2021) 8:2741–54. doi: 10.1002/ehf2.13344

23. Uszko-Lencer N, Janssen DJA, Gaffron S, Vanfleteren L, Janssen E, Werter C, et al. Clustering based on comorbidities in patients with chronic heart failure: an illustration of clinical diversity. *ESC Heart Fail.* (2022) 9:614–26. doi: 10.1002/ehf2.13704

24. Park J, Johantgen ME. A cross-cultural comparison of symptom reporting and symptom clusters in heart failure. *J. Transcult Nurs.* (2017) 28:372–80. doi: 10.1177/1043659616651673

25. Yun S, Enjuanes C, Calero-Molina E, Hidalgo E, José N, Calvo E, et al. Effectiveness of telemedicine in patients with heart failure according to frailty phenotypes: insights from the iCOR randomised controlled trial. *Eur J Intern Med.* (2022) 96:49–59. doi: 10.1016/j.ejim.2021.09.021

26. Park J, Moser DK, Griffith K, Harring JR, Johantgen M. Exploring symptom clusters in people with heart failure. *Clin Nurs Res.* (2019) 28:165–81. doi: 10.1177/1054773817729606

27. Bose E, Radhakrishnan K. Using unsupervised machine learning to identify subgroups among home health patients with heart failure using telehealth. *Comput Inform Nurs.* (2018) 36:242–8. doi: 10.1097/cin.0000000000000423

28. Cikes M, Sanchez-Martinez S, Claggett B, Duchateau N, Piella G, Butakoff C, et al. Machine learning-based phenogrouping in heart failure to identify responders to cardiac resynchronization therapy. *Eur J Heart Fail.* (2019) 21:74–85. doi: 10.1002/ejhf.1333

29. Gulea C, Zakeri R, Quint JK. Model-based comorbidity clusters in patients with heart failure: association with clinical outcomes and healthcare utilization. *BMC Med.* (2021) 19:9. doi: 10.1186/s12916-020-01881-7

30. Henneges C, Morbach C, Sahiti F, Scholz N, Frantz S, Ertl G, et al. Sex-specific bimodal clustering of left ventricular ejection fraction in patients with acute heart failure. *ESC Heart Fail.* (2022) 9:786–90. doi: 10.1002/ehf2.13618

31. Horiuchi Y, Tanimoto S, Latif A, Urayama KY, Aoki J, Yahagi K, et al. Identifying novel phenotypes of acute heart failure using cluster analysis of clinical variables. *Int J Cardiol.* (2018) 262:57–63. doi: 10.1016/j.ijcard.2018.03.098

32. Fayol A, Wack M, Livrozet M, Carves JB, Domengé O, Vermersch E, et al. Aetiological classification and prognosis in patients with heart failure with preserved ejection fraction. *ESC Heart Fail.* (2022) 9:519–30. doi: 10.1002/ehf2.13717

33. Kobayashi Y, Tremblay-Gravel M, Boralkar KA, Li X, Nishi T, Amsallem M, et al. Approaching higher dimension imaging data using cluster-based hierarchical modeling in patients with heart failure preserved ejection fraction. *Sci Rep.* (2019) 9:10431. doi: 10.1038/s41598-019-46873-7

34. Arévalo-Lorido JC, Carretero-Gómez J, Aramburu-Bodas O, Grau-Amoros J, Torres-Cortada G, Camafort-Babkowski M. Blood pressure, congestion and heart failure with preserved ejection fraction among patients with and without type 2 diabetes mellitus. A cluster analysis approach from the observational registry DICUMAP. *High Blood Press Cardiovasc Prev.* (2020) 27:399–408. doi: 10.1007/s40292-020-00405-x

35. Gu J, Pan JA, Lin H, Zhang JF, Wang CQ. Characteristics, prognosis and treatment response in distinct phenogroups of heart failure with preserved ejection fraction. *Int J Cardiol.* (2021) 323:148–54. doi: 10.1016/j.ijcard.2020.08.065

36. Kao DP, Lewsey JD, Anand IS, Massie BM, Zile MR, Carson PE, et al. Characterization of subgroups of heart failure patients with preserved ejection fraction with possible implications for prognosis and treatment response. *Eur J Heart Fail.* (2015) 17:925–35. doi: 10.1002/ejhf.327

37. Cohen JB, Schrauben SJ, Zhao L, Basso MD, Cvijic ME, Li Z, et al. Clinical phenogroups in heart failure with preserved ejection fraction: detailed phenotypes, prognosis, and response to spironolactone. *JACC Heart Fail.* (2020) 8:172–84. doi: 10.1016/j.jchf.2019.09.009

38. Arévalo-Lorido JC, Carretero-Gómez J, Gómez-Huelgas R, Llácer P, Manzano L, Quesada Simón MA, et al. Comorbidities and their implications in patients with and without type 2 diabetes mellitus and heart failure with preserved ejection fraction. Findings from the rica registry. *Int J Clin Pract.* (2021) 75:e13661. doi: 10.1111/ijcp.13661

39. Przewlocka-Kosmala M, Marwick TH, Dabrowski A, Kosmala W. Contribution of cardiovascular reserve to prognostic categories of heart failure with preserved ejection fraction: a classification based on machine learning. *J Am Soc Echocardiogr.* (2019) 32:604–15.e6. doi: 10.1016/j.echo.2018.12.002

40. Pandey A, Kagiyama N, Yanamala N, Segar MW, Cho JS, Tokodi M, et al. Deep-learning models for the echocardiographic assessment of diastolic dysfunction. *JACC Cardiovasc Imaging.* (2021) 14:1887–900. doi: 10.1016/j.jcmg.2021.04.010

41. Shah SJ, Katz DH, Selvaraj S, Burke MA, Yancy CW, Gheorghiade M, et al. Phenomapping for novel classification of heart failure with preserved ejection fraction. *Circulation.* (2015) 131:269–79. doi: 10.1161/circulationaha.114.010637

42. Harada D, Asanoi H, Noto T, Takagawa J. Different pathophysiology and outcomes of heart failure with preserved ejection fraction stratified by K-means clustering. *Front Cardiovasc Med.* (2020) 7:607760. doi: 10.3389/fcvm.2020.607760

43. Schrub F, Oger E, Bidaut A, Hage C, Charton M, Daubert JC, et al. Heart failure with preserved ejection fraction: a clustering approach to a heterogenous syndrome. *Arch Cardiovasc Dis.* (2020) 113:381–90. doi: 10.1016/j.acvd.2020.03.012

44. Casebeer A, Horter L, Hayden J, Simmons J, Evers T. Phenotypic clustering of heart failure with preserved ejection fraction reveals different rates of hospitalization. *J Cardiovasc Med.* (2021) 22:45–52. doi: 10.2459/jcm.0000000000001116

45. Woolley RJ, Ceelen D, Ouwerkerk W, Tromp J, Figarska SM, Anker SD, et al. Machine learning based on biomarker profiles identifies distinct subgroups of heart failure with preserved ejection fraction. *Eur J Heart Fai.* (2021) 23:983–91. doi: 10.1002/ejhf.2144

46. Hedman ÅK, Hage C, Sharma A, Brosnan MJ, Buckbinder L, Gan LM, et al. Identification of novel pheno-groups in heart failure with preserved ejection fraction using machine learning. *Heart.* (2020) 106:342–9. doi: 10.1136/heartjnl-2019-315481

47. Uijl A, Savarese G, Vaartjes I, Dahlström U, Brugts JJ, Linssen GCM, et al. Identification of distinct phenotypic clusters in heart failure with preserved ejection fraction. *Eur J Heart Fail.* (2021) 23:973–82. doi: 10.1002/ejhf.2169

48. Hahn VS, Knutsdottir H, Luo X, Bedi K, Margulies KB, Haldar SM, et al. Myocardial gene expression signatures in human heart failure with preserved ejection fraction. *Circulation.* (2021) 143:120–34. doi: 10.1161/circulationaha.120.050498

49. Wu Y, Wang H, Li Z, Cheng J, Fang R, Cao H, et al. Subtypes identification on heart failure with preserved ejection fraction via network enhancement fusion using multi-omics data. *Comput Struct Biotechnol J.* (2021) 19:1567–78. doi: 10.1016/j.csbj.2021.03.010

50. Nouraei H, Rabkin SW. A new approach to the clinical subclassification of heart failure with preserved ejection fraction. *Int J Cardiol.* (2021) 331:138–43. doi: 10.1016/j.ijcard.2021.01.052

51. Riolet C, Menet A, Verdun S, Altes A, Appert L, Guyomar Y, et al. Clinical and prognostic implications of phenomapping in patients with heart failure receiving cardiac resynchronization therapy. *Arch Cardiovasc Dis.* (2021) 114:197–210. doi: 10.1016/j.acvd.2020.07.004

52. Bartko PE, Heitzinger G, Spinka G, Pavo N, Prausmüller S, Kastl S, et al. Principal morphomic and functional components of secondary mitral regurgitation. *JACC Cardiovasc Imaging.* (2021) 14:2288–300. doi: 10.1016/j.jcmg.2021.05.020

53. Perry A, Loh F, Adamo L, Zhang KW, Deych E, Foraker R, et al. Unsupervised cluster analysis of patients with recovered left ventricular ejection fraction identifies unique clinical phenotypes. *PLoS One.* (2021) 16:e0248317. doi: 10.1371/journal.pone.0248317

54. Kao DP, Wagner BD, Robertson AD, Bristow MR, Lowes BD. A personalized BEST: characterization of latent clinical classes of nonischemic heart failure that predict outcomes and response to bucindolol. *PLoS One.* (2012) 7:e48184. doi: 10.1371/journal.pone.0048184

55. Smith OR, Gidron Y, Kupper N, Winter JB, Denollet J. Vital exhaustion in chronic heart failure: symptom profiles and clinical outcome. *J Psychosom Res.* (2009) 66:195–201. doi: 10.1016/j.jpsychores.2008.10.021

56. Lee KS, Song EK, Lennie TA, Frazier SK, Chung ML, Heo S, et al. Symptom clusters in men and women with heart failure and their impact on cardiac event-free survival. *J Cardiovasc Nurs.* (2010) 25:263–72. doi: 10.1097/JCN.0b013e3181cfbb88

57. Sabbah MS, Fayyaz AU, de Denus S, Felker GM, Borlaug BA, Dasari S, et al. Obese-inflammatory phenotypes in heart failure with preserved ejection fraction. *Circ Heart Fail.* (2020) 13:e006414. doi: 10.1161/circheartfailure.119.006414

58. Segar MW, Patel KV, Ayers C, Basit M, Tang WHW, Willett D, et al. Phenomapping of patients with heart failure with preserved ejection fraction using machine learning-based unsupervised cluster analysis. *Eur J Heart Fail.* (2020) 22:148–58. doi: 10.1002/ejhf.1621

59. Sethares KA, Viveiros JD, Ayotte B. Uncertainty levels differ by physical heart failure symptom cluster. *Appl Nurs Res.* (2021) 60:151435.

60. Tromp J, Ouwerkerk W, Demissei BG, Anker SD, Cleland JG, Dickstein K, et al. Novel endotypes in heart failure: effects on guideline-directed medical therapy. *Eur Heart J.* (2018) 39:4269–76. doi: 10.1093/eurheartj/ehy712

61. Zhao W-L, Deng C-H, Ngo C-W. k-means: a revisit. *Neurocomputing.* (2018) 291:195–206. doi: 10.1016/j.neucom.2018.02.072

62. Towards Machine Learning. *What is K-Means Algorithm and How It Works*. Available online at: https://towardsmachinelearning.org/k-means/

63. Benjamin EJ, Muntner P, Alonso A, Bittencourt MS, Callaway CW, Carson AP, et al. Heart disease and stroke statistics-2019 update: a report from the American heart association. *Circulation.* (2019) 139:e56–528. doi: 10.1161/cir.0000000000000659

64. Levy D, Kenchaiah S, Larson MG, Benjamin EJ, Kupka MJ, Ho KK, et al. Long-term trends in the incidence of and survival with heart failure. *N Engl J Med.* (2002) 347:1397–402. doi: 10.1056/NEJMoa020265

65. Jackson SL, Tong X, King RJ, Loustalot F, Hong Y, Ritchey MD. National burden of heart failure events in the United States, 2006 to 2014. *Circ Heart Fail.* (2018) 11:e004873. doi: 10.1161/circheartfailure.117.004873

66. Sharma A, Zhao X, Hammill BG, Hernandez AF, Fonarow GC, Felker GM, et al. Trends in noncardiovascular comorbidities among patients hospitalized for heart failure: insights from the get with the guidelines-heart failure registry. *Circ Heart Fail.* (2018) 11:e004646. doi: 10.1161/circheartfailure.117.004646

67. van Deursen VM, Urso R, Laroche C, Damman K, Dahlström U, Tavazzi L, et al. Co-morbidities in patients with heart failure: an analysis of the European Heart Failure Pilot Survey. *Eu J Heart Fail.* (2014) 16:103–11. doi: 10.1002/ejhf.30

68. Mogensen UM, Ersbøll M, Andersen M, Andersson C, Hassager C, Torp-Pedersen C, et al. Clinical characteristics and major comorbidities in heart failure patients more than 85 years of age compared with younger age groups. *Eur J Heart Fail.* (2011) 13:1216–23. doi: 10.1093/eurjhf/hfr116

frontiers | Frontiers in Cardiovascular Medicine

TYPE Mini Review
PUBLISHED 11 August 2022
DOI 10.3389/fcvm.2022.910957

OPEN ACCESS

EDITED BY
Tong Liu,
Tianjin Medical University, China

REVIEWED BY
Gani Bajraktari,
University of Pristina, Albania

*CORRESPONDENCE
Kiyotaka Fukamachi
fukamak@ccf.org

SPECIALTY SECTION
This article was submitted to Heart Failure and Transplantation, a section of the journal Frontiers in Cardiovascular Medicine

RECEIVED 27 April 2022
ACCEPTED 26 July 2022
PUBLISHED 11 August 2022

CITATION
Miyagi C, Kuroda T, Karimov JH and Fukamachi K (2022) Novel approaches for left atrial pressure relief: Device-based monitoring and management in heart failure. *Front. Cardiovasc. Med.* 9:910957. doi: 10.3389/fcvm.2022.910957

Novel approaches for left atrial pressure relief: Device-based monitoring and management in heart failure

Chihiro Miyagi[1], Taiyo Kuroda[1], Jamshid H. Karimov[1,2] and Kiyotaka Fukamachi[1,2]*

[1]Department of Biomedical Engineering, Cleveland Clinic, Lerner Research Institute, Cleveland, OH, United States, [2]Cleveland Clinic Lerner College of Medicine of Case Western Reserve University, Cleveland, OH, United States

The importance of the left atrium (LA) has been emphasized in recent years as the features of heart failure (HF), especially with regard to variability in patient and pathology phenotypes, continue to be uncovered. Of note, among the population with HF with preserved ejection fraction (HFpEF), pressure or size of the LA have become a target for advanced monitoring and a therapeutic approach. In the case of diastolic dysfunction or pulmonary hypertension, which are often observed in patients with HFpEF, a conventional approach with clinical symptoms and physical signs of decompensation turned out to have a poor correlation with LA pressure. Therefore, to optimize HF treatment for these populations, several devices that are applied directly to the LA have been developed. First, two LA pressure (LAP) sensors (Heart POD and V-LAP Device) were developed and may enable patient self-management remotely with LAP-guided and physician-directed style. Second, there are device-based approaches that aim to decompress the LA directly. These include: (1) interatrial shunt devices; (2) left ventricular assist devices with LA cannulation; and (3) the left atrial assist device. While these novel device-based therapies are not yet commercially available, there is expected to be a rise in the proposition and adoption of a wider range of choices for monitoring or treating LA using device-based options, based on LA dimensional reduction and optimization of the clinically significant pressure relief. Further development and evaluation are necessary to establish a more favorable management strategy for HF.

KEYWORDS

device-based treatment, mechanical circulatory support, left ventricular assist device (LVAD), interatrial shunt device, diastolic dysfunction (DD), heart failure with preserved ejection fraction (HFpEF), left atrial monitoring, left atrial assist

Introduction

In the treatment of chronic heart failure (HF), left atrial (LA) function has been identified as one of the most important parameters affecting the quality of life and potential deterioration or improvement of left atrial unloading. In ∼90% of hospitalizations for exacerbation of HF, there is pulmonary congestion related to

an increase in LA pressure (LAP) (1–3). In daily medical care, however, current management strategies for ambulatory HF patients generally rely on clinical symptoms and physical signs of decompensation, even though these indicators have a poor correlation with LAP (4).

For patients with HF with preserved ejection fraction (HFpEF) or pulmonary hypertension, diastolic dysfunction or right HF are the main pathophysiological elements responsible for the clinical representation and overall course of the disease. These types of HF tend to be resistant to simple volume reduction or vasodilators, since these approaches do not directly reduce the LAP in case left ventricular (LV) systolic function is preserved. Even though patients with HFpEF account for nearly half of the entire HF population (5), there is still an unmet need for effective therapeutic options.

To achieve more dedicated HF control for this population, it is essential to understand the specific clinical requirements in order to have effective options for monitoring LAP, and accurately adjusted, effective LA decompression. In this mini-review, we describe several novel devices that are currently in the development pipeline to treat HF that specifically address the LA function and parameters. The features, advantages and limitations of these device platforms are discussed.

Left atrial pressure sensors

Changes in volume status or ventricular function, followed by decompensation and severe symptoms in HF patients, often require hospitalization and invasive monitoring of the patient's clinical status to achieve optimal medication and volume control. To limit the number of hospitalizations, strong efforts have been made for several decades to develop an accurate and remote monitoring system for early detection of exacerbation of chronic HF conditions (6). The unprecedented era of the COVID-19 pandemic has emphasized the necessity of reliable remote monitoring of HF patients more than ever.

Currently, continuous and remote monitoring of pulmonary artery pressure (PAP) have been confirmed to be associated with a reduced number of hospitalizations and mortality rates in the HF with reduced ejection fraction (HFrEF) population (7, 8). Also, PAP-guided therapies (PAP sensors) are the only commercially available option for CHF management so far. However, PAP does not always reflect left-sided ventricular filling pressures (9, 10) as seen in advanced HF patients with increased pulmonary vascular resistance or patients with pulmonary hypertension or acute HF.

Under these circumstances, LAP direct monitoring systems (intra-cardiac pressure readings) were developed to provide more sensitive and important information, including the evaluation of diastolic function and atrial arrhythmias.

Heart POD device

The Heart POD (Abbott, Abbott Park, IL) was developed as the first attempt to place in a human a permanently implantable direct LAP monitoring device (11). This is a pacemaker-shaped device with a coil antenna implanted in the subcutaneous pocket and a sensor lead placed across the atrial septum (Figure 1A). A patient advisor module is used to communicate with the implanted sensor lead. In a prospective, multicenter, non-randomized, open-label feasibility clinical trial [the Hemodynamically Guided Home Self-Therapy in Severe Heart Failure Patients (HOMEOSTASIS) trial], the Heart POD was implanted in eight patients with established HF (11). At 12 weeks of follow-up, the device measurements were as accurate as within ±5 mm Hg of simultaneous pulmonary capillary wedge pressure readings, and no complications were reported.

As a follow-up to the HOMEOSTASIS trial, a prospective and observational study of a physician-directed patient self-management system targeting LAP was conducted, enrolling 40 patients with HFrEF and HFpEF and a history of acute decompensation (12). During pressure-guided therapy, mean daily LAP fell in the first 3 months from 17.6 to 14.8 mm Hg ($p = 0.003$), and the frequency of LAP elevation higher than 25 mm Hg was reduced by 67% ($p < 0.001$). In addition, improvements in New York Heart Association (NYHA) functional Class, LV ejection fraction, and pharmacological profiles were observed.

Following this, the Left Atrial Pressure Monitoring to Optimize Heart Failure Therapy (LAPTOP-HF) study was initiated (13). The LAPTOP-HF was a prospective, multicenter, randomized, controlled clinical trial, which was designed to enroll up to 730 patients with NYHA functional class II and either of a history of hospitalization for HF in past 12 months or an elevated B-type natriuretic peptide level, regardless of the LV ejection fraction. The enrollment was terminated early, however, because of a large number of procedure-related complications by trans-septal punctures. The analysis of 486 patients that were enrolled prior to the termination showed that the HF therapy, with LAP-guided, physician-directed, and patient self-management, was associated with a 41% reduction in HF hospitalizations at 12 months ($p = 0.005$) (14). These efforts were followed by the development of the V-LAP, a more advanced LAP sensor.

V-LAP remote monitoring system

The V-LAP System (Vectorious Medical Technologies, Tel Aviv, Israel), is a wireless remote monitoring system that measures LAP directly (2, 15). The system includes a sensory implant (Figure 1B) placed at the interatrial septum and an external unit (reader, Figure 1C). The implant is leadless, has no battery, and receives all its power from the reader. All procedures can be done percutaneously. A hermetically

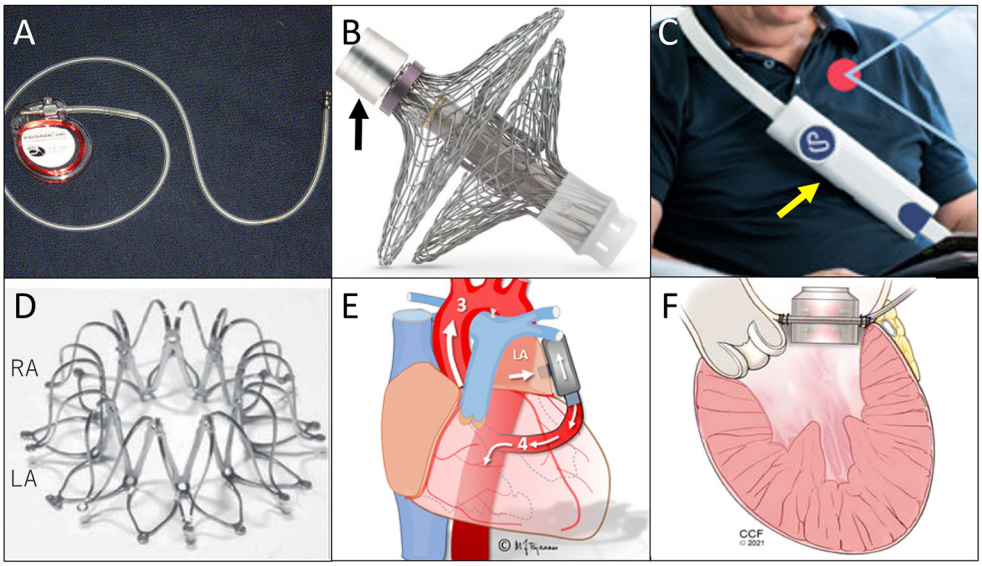

FIGURE 1
Illustrations of each device. **(A)** Heart POD, quoted from (6); **(B)** Sensory implant of V-LAP System (black arrow is the pressure-sensing assembly connected to electronic circuitry), quoted from (6); **(C)** Sensor of V-LAP (yellow arrow), quoted from (15); **(D)** Corvia Atrial Shunt Device, quoted from (19); **(E)** PulseVAD, quoted from (30), and; **(F)** Left Atrial Assist Device, quoted from (32).

sealed tube encases the sensing elements and electronics, and bidirectional communications with a reader is enabled.

After *ex vivo* and *in vivo* animal experiences (16), the V-LAP Left Atrium Monitoring system for Patients With Chronic sysTOlic & Diastolic Congestive heart Failure (VECTOR-HF) study (ClinicalTrials.gov: NCT3775161) was recently initiated. This is a prospective, multicenter, single-arm, and open-label, first-in-human clinical study that aims to assess the safety, performance, and usability of the device in patients with NYHA class III HF. So far, 24 patients have received the device implants, which are transmitting accurate pressure measurements of LAP with no device-related complications or sensor failure events (2).

In general, the most serious concern with these LAP sensors is a higher rate of procedure-related complication. The V-LAP system seems to have less risk of thrombosis than the Heart POD because of its shape, but information about long-term biocompatibility and effectiveness are still needed.

Depressurization of the left atrium

Decompression of the LA is the most ideal therapeutic approach to relief the symptoms and vicious circle of exacerbated HF. Especially in cases of HF with diastolic dysfunction, as represented by patients with HFpEF, pharmacological treatments have not been as feasible as they have been for HFrEF. Use of LV assist devices (LVADs) is also controversial because of limited experience and concerns over the risk of ventricular suction events. Although sodium glucose cotransporter 2 (SGLT2) inhibitors were recently suggested to be beneficial for HFpEF (17, 18), their efficacy is still unclear after fluid overload is appropriately managed. SGLT2 inhibitors brought a lower risk of hospitalization for HF, but there was no improvement in death rates. Therefore, new device-based therapies that address LA decompression have been getting more attention in the area of HFpEF treatment (19, 20).

There are three options for decompressing the LA with a device: (1) fenestrate the interatrial wall; (2) use LVADs with LA cannulation; and (3) pump blood directly from the LA to the LV. High LAP and large LA size are two of the most important features of HFpEF pathology, and reducing LA size and pressure have been set as important therapeutic targets (21, 22). Here, we summarize recent findings for each type of device.

Interatrial shunt devices

Interatrial shunt devices are the most widely applied option for the HFpEF population. There are three different devices, used as artificial interatrial shunts (23): the Corvia Atrial Shunt Device (IASD System II, Corvia Medical Inc., Tewksbury, MA), the V-Wave device (V-Wave Ltd., Caesarea, Israel), and the Atrial Flow Regulator (AFR, Occlutech, Helsingborg, Sweden). They employ the same concept of creating a shunt between the LA and the right atrium (RA) and reducing LAP by generating left-to-right flow artificially. Their materials and shapes vary, but typically, a 5-to-10 mm shunt is made and fixed at the interatrial

wall by a self-expanding prosthesis, and all procedures can be done percutaneously.

Among them, the Corvia Atrial Shunt Device (Figure 1D) has already undergone several randomized clinical trials. A randomized, multicentre (international), blinded, sham-controlled trial (REDUCE LAP-HF II) (24), enrolled 1,072 participants; 314 were assigned to the device-implanted group. The placement of an atrial shunt did not reduce the total HF event rates at 12 or 24 months after implantation. The authors stated that the strategy of excluding pulmonary vascular disease might have not been adequate. Thus, with better patient selection, atrial shunt devices still have a chance to be beneficial. Nevertheless, as an HF treatment, the efficacy of this device is limited to symptom relief, and it can never be used as a causal treatment nor to stop progression of the disease.

Left atrial cannulation of left ventricular assist devices

As noted, LVADs are not considered to be as beneficial for patients with HF with diastolic dysfunction as for those with systolic dysfunction, because the LV wall in diastolic dysfunction is often too thick and the LV cavity too narrow for the LVAD inflow cannulas. The concept of applying LVADs with LA cannulation emerged, and some case reports depicted the potential efficacy of LVAD implantation in hearts with diastolic dysfunction, such as hypertrophic cardiomyopathy (25–27).

There are some novel devices that employ a similar concept of drawing blood from the LA and returning it to the aorta or subclavian artery. For example, the CircuLite Synergy Micro-Pump Device (Medtronic, Minneapolis, MN) (28) is a micropump-based form of mechanical circulatory support device, with a pump the size of an AA battery (29). The implantation can be done with a right mini-thoracotomy without using cardiopulmonary bypass, and the outflow graft is anastomosed to the subclavian artery. Although the development of the Synergy Micro-Pump Device and related project had been abandoned several years ago, this concept was successfully migrated to the new pumps, such as the VADovations cardiac assist system (VADovations, Oklahoma City, OK) or the PulseVAD (Northern Development, Strandhaugen, Oslo).

These two devices are at the beginning of the development process, and very limited information is available. Briefly, VADovations is a small pump the size of a AAA battery and is placed between the LA and the ascending aorta without inflow/outflow cannulas. The experimental results have not yet been documented. The PulseVAD is a pulsatile heart assist device and pumps blood from the LA to the descending aorta with minimally invasive surgery without cardiopulmonary bypass (Figure 1E).

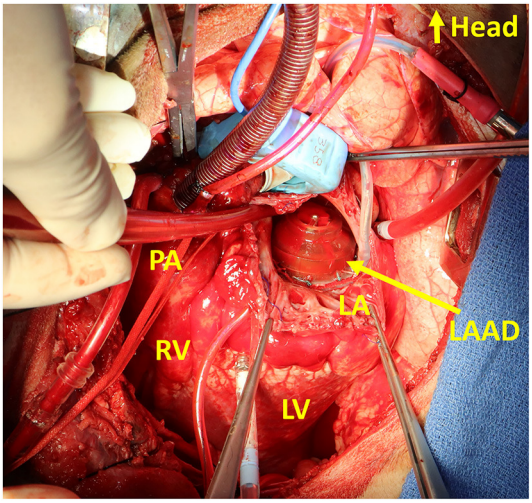

FIGURE 2
Intraoperative photo of the Left Atrial Assist Device (LAAD) implanted at the mitral position. LA, left atrium; LV, left ventricle; PA, pulmonary artery; RV, right ventricle.

Gude and Fiane recently published the results of *in vivo* studies with the PulseVAD using ovine, and reported survival for 11 days after implantation without any complication (30).

Draining blood directly from the LA seems to be the most reasonable method of decreasing LAP, but these devices make an alternative bloodstream by shortcutting the LV. Even if they are intended as partial circulatory support, stagnation in the LV and a risk of LV thrombosis are inevitable. Also, pulsatility should be decreased as the pump support becomes larger.

Left atrial assist device

Sharing the concept of draining blood from the LA, the Left Atrial Assist Device (LAAD) has a unique feature of being implanted at the mitral position and pumping blood directly to the LV (Figure 1F) (31). The target of this pump is mainly HFpEF or diastolic dysfunction with normal EF, since the systolic function of the heart needs to be maintained for the native LV to pump blood by itself. For use in hearts with preserved EF, the LAAD can decrease LAP and support the LV filling, maintaining physiological blood pathway and pulsatility.

Our progress with the LAAD was reported with *in vitro* and *in vivo* studies with calves (32, 33). The intraoperative image of the LAAD implanted at the mitral position is seen as Figure 2. The effect of reducing LAP has been successfully demonstrated with introduced diastolic HF models. The work on reduction of the device profile, which would

allow shrinking of the device dimensions and favor the implantability and technology footprint inside the heart, is ongoing. Driveline exteriorization strategies are pending evaluation, and would provide more information on the most appropriate anatomical considerations and surgical options for its pass through cardiac structures. The evaluation with long-term safety and efficacy is needed, as well as the development of animal models that can simulate diastolic HF with more fidelity.

Discussion

The importance of LA function has been gradually and steadily emphasized as the concept of diastolic dysfunction has become more popular in the HF field. Decreased LA compliance and mechanics are believed to be associated with an increased risk for new onset atrial fibrillation in HFpEF (34), and reducing the LA size and pressure has become the key treatment strategy. However, considering LA as a therapeutic target requires tremendous effort, since obtaining the precise value of LAP requires invasive catheterization in the hospital.

Whether performed percutaneously or surgically, there is an inevitable risk of systemic thrombosis when any prosthetic is introduced into the LA, and so anticoagulation and/or antiplatelet therapies are usually prescribed (6, 35). Therefore, for these LA devices, patient selection is very important. Patients with diastolic dysfunction as represented by HFpEF or right HF, including HF with pulmonary hypertension, would be good candidates, since LA function plays larger roles.

The devices introduced here are all in development, and none has obtained approval from the U.S. Food and Drug Administration (FDA). Their effects on early detection or prevention of LA arrhythmia have not been demonstrated, and it's also unclear if they have any therapeutic effect on presenting arrhythmia. However, under the social, medical, and economic crises brought on by the COVID-19 pandemic, a case was reported in which constant tele-monitoring of LAP and subsequent adjustment of medication prevented possible decompensation of HF and hospitalization in a patient who was in self-isolation (15). With more evidence and the need for remote care, continuous remote monitoring by invasive sensors is expected to play a larger role in HF care.

As for the LA decompression devices, the Corvia Atrial Shunt Device received FDA breakthrough device designation in 2019, but it failed to show a long-term efficacy in a randomized trial. The pump-based devices should have promise for decompressing LA, but their development is still at the animal experiment stage, and needs more time before a first-in-human trial. Also, pump devices-implantation tends to be more invasive.

Conclusion

With the new device-based options, there is a wider range of choices for monitoring or treating LAP. Further development and evaluation are required to establish a more favorable management strategy for HF.

Author contributions

CM performed the literature search, designed the study, and prepared the manuscript. KF, JK, and TK provided methodological support in the study design and revised the manuscript. All authors have read and approved the manuscript before submission.

Funding

The LAAD study was supported by funding from National Heart, Lung and Blood Institute, National Institutes of Health (NIH), NIH Center for Accelerated Innovation at Cleveland Clinic (NCAI-CC), (NIH-NHLBI 1UH54HL119810; NCAI-19-12-APP-CCF).

Conflict of interest

Authors KF and JK are co-inventors of the LAAD.

The remaining authors declare that the research was conducted in the absence of any commercial or financial relationships that could be construed as a potential conflict of interest.

Publisher's note

References

1. Adamson PB, Magalski A, Braunschweig F, Böhm M, Reynolds D, Steinhaus D, et al. Ongoing right ventricular hemodynamics in heart failure: clinical value of measurements derived from an implantable monitoring system. *J Am Coll Cardiol*. (2003) 41:565–71. doi: 10.1016/s0735-1097(02)02896-6

2. Perl L, Meerkin D, D'Amario D, Avraham BB, Gal TB, Weitsman T, et al. The V-LAP system for remote left atrial pressure monitoring of patients with heart failure: remote left atrial pressure monitoring. *J Card Fail*. (2022) 28:963–72. doi: 10.1016/j.cardfail.2021.12.019

3. Adams KF, Jr., Fonarow GC, Emerman CL, LeJemtel TH, Costanzo MR, Abraham WT, et al. Characteristics and outcomes of patients hospitalized for heart failure in the united states: rationale, design, and preliminary observations from the first 100,000 cases in the acute decompensated heart failure national registry (adhere). *Am Heart J*. (2005) 149:209–16. doi: 10.1016/j.ahj.2004.08.005

4. Stevenson LW, Perloff JK. The limited reliability of physical signs for estimating hemodynamics in chronic heart failure. *JAMA*. (1989) 261:884–8.

5. Xanthopoulos A, Triposkiadis F, Starling RC. Heart failure with preserved ejection fraction: classification based upon phenotype is essential for diagnosis and treatment. *Trends Cardiovasc Med*. (2018) 28:392–400. doi: 10.1016/j.tcm.2018.01.001

6. Radhoe SP, Veenis JF, Brugts JJ. Invasive devices and sensors for remote care of heart failure patients. *Sensors*. (2021) 21:2014. doi: 10.3390/s21062014

7. Abraham J, Bharmi R, Jonsson O, Oliveira GH, Artis A, Valika A, et al. Association of ambulatory hemodynamic monitoring of heart failure with clinical outcomes in a concurrent matched cohort analysis. *JAMA Cardiol*. (2019) 4:556–63. doi: 10.1001/jamacardio.2019.1384

8. Givertz MM, Stevenson LW, Costanzo MR, Bourge RC, Bauman JG, Ginn G, et al. Pulmonary artery pressure-guided management of patients with heart failure and reduced ejection fraction. *J Am Coll Cardiol*. (2017) 70:1875–86. doi: 10.1016/j.jacc.2017.08.010

9. Campbell P, Drazner MH, Kato M, Lakdawala N, Palardy M, Nohria A, et al. Mismatch of right- and left-sided filling pressures in chronic heart failure. *J Card Fail*. (2011) 17:561–8. doi: 10.1016/j.cardfail.2011.02.013

10. Drazner MH, Velez-Martinez M, Ayers CR, Reimold SC, Thibodeau JT, Mishkin JD, et al. Relationship of right- to left-sided ventricular filling pressures in advanced heart failure: insights from the escape trial. *Circ Heart Fail*. (2013) 6:264–70. doi: 10.1161/CIRCHEARTFAILURE.112.000204

11. Ritzema J, Melton IC, Richards AM, Crozier IG, Frampton C, Doughty RN, et al. Direct left atrial pressure monitoring in ambulatory heart failure patients: initial experience with a new permanent implantable device. *Circulation*. (2007) 116:2952–9. doi: 10.1161/CIRCULATIONAHA.107.702191

12. Ritzema J, Troughton R, Melton I, Crozier I, Doughty R, Krum H, et al. Physician-directed patient self-management of left atrial pressure in advanced chronic heart failure. *Circulation*. (2010) 121:1086–95. doi: 10.1161/CIRCULATIONAHA.108.800490

13. Maurer MS, Adamson PB, Costanzo MR, Eigler N, Gilbert J, Gold MR, et al. Rationale and design of the left atrial pressure monitoring to optimize heart failure therapy study (LAPTOP-HF). *J Card Fail*. (2015) 21:479–88. doi: 10.1016/j.cardfail.2015.04.012

14. Abraham WT, Adamson PB, Costanzo MR, Eigler N, Gold M, Klapholz M, et al. Hemodynamic monitoring in advanced heart failure: results from the LAPTOP-HF trial. *J Card Fail*. (2016) 22:940. doi: 10.1016/j.cardfail.2016.09.012

15. Feickert S, D'Ancona G, Murero M, Ince H. Intra-cardiac microcomputer allows for innovative telemedicine in chronic heart failure during coronavirus disease-2019 pandemic: a case report. *Eur Heart J Case Rep*. (2020) 4:1–6. doi: 10.1093/ehjcr/ytaa501

16. Perl L, Soifer E, Bartunek J, Erdheim D, Köhler F, Abraham WT, et al. A novel wireless left atrial pressure monitoring system for patients with heart failure, first *ex-vivo* and animal experience. *J Cardiovasc Transl Res*. (2019) 12:290–8. doi: 10.1007/s12265-018-9856-3

17. Anker SD, Butler J, Filippatos G, Ferreira JP, Bocchi E, Böhm M, et al. Empagliflozin in heart failure with a preserved ejection fraction. *N Engl J Med*. (2021) 385:1451–61. doi: 10.1056/NEJMoa2107038

18. Nassif ME, Windsor SL, Borlaug BA, Kitzman DW, Shah SJ, Tang F, et al. The sglt2 inhibitor dapagliflozin in heart failure with preserved ejection fraction: a multicenter randomized trial. *Nat Med*. (2021) 27:1954–60. doi: 10.1038/s41591-021-01536-x

19. Miyagi C, Miyamoto T, Karimov JH, Starling RC, Fukamachi K. Device-based treatment options for heart failure with preserved ejection fraction. *Heart Fail Rev*. (2021) 26:749–62. doi: 10.1007/s10741-020-10067-5

20. Burlacu A, Simion P, Nistor I, Covic A, Tinica G. Novel percutaneous interventional therapies in heart failure with preserved ejection fraction: an integrative review. *Heart Fail Rev*. (2019) 24:793–803. doi: 10.1007/s10741-019-09787-0

21. Issa O, Peguero JG, Podesta C, Diaz D, De La Cruz J, Pirela D, et al. Left atrial size and heart failure hospitalization in patients with diastolic dysfunction and preserved ejection fraction. *J Cardiovasc Echogr*. (2017) 27:1–6. doi: 10.4103/2211-4122.199064

22. Zile MR, Gottdiener JS, Hetzel SJ, McMurray JJ, Komajda M, McKelvie R, et al. Prevalence and significance of alterations in cardiac structure and function in patients with heart failure and a preserved ejection fraction. *Circulation*. (2011) 124:2491–501. doi: 10.1161/CIRCULATIONAHA.110.011031

23. Emani S, Burkhoff D, Lilly SM. Interatrial shunt devices for the treatment of heart failure. *Trends Cardiovasc Med*. (2021) 31:427–32. doi: 10.1016/j.tcm.2020.09.004

24. Shah SJ, Borlaug BA, Chung ES, Cutlip DE, Debonnaire P, Fail PS, et al. Atrial shunt device for heart failure with preserved and mildly reduced ejection fraction (REDUCE LAP-HR II): a randomised, multicentre, blinded, sham-controlled trial. *Lancet*. (2022) 399:1130–40. doi: 10.1016/S0140-6736(22)00016-2

25. Kiamanesh O, Rankin K, Billia F, Badiwala MV. Left ventricular assist device with a left atrial inflow cannula for hypertrophic cardiomyopathy. *JACC Case Reports*. (2020) 2:2090–4. doi: 10.1016/j.jaccas.2020.10.006

26. Topilsky Y, Pereira NL, Shah DK, Boilson B, Schirger JA, Kushwaha SS, et al. Left ventricular assist device therapy in patients with restrictive and hypertrophic cardiomyopathy. *Circ Heart Fail*. (2011) 4:266–75. doi: 10.1161/CIRCHEARTFAILURE.110.959288

27. Wynne E, Bergin JD, Ailawadi G, Kern JA, Kennedy JL. Use of a left ventricular assist device in hypertrophic cardiomyopathy. *J Card Surg*. (2011) 26:663–5. doi: 10.1111/j.1540-8191.2011.01331.x

28. Burkhoff D, Maurer MS, Joseph SM, Rogers JG, Birati EY, Rame JE, et al. Left atrial decompression pump for severe heart failure with preserved ejection fraction: theoretical and clinical considerations. *JACC Heart Fail*. (2015) 3:275–82. doi: 10.1016/j.jchf.2014.10.011

29. Mohite PN, Sabashnikov A, Simon AR, Weymann A, Patil NP, Unsoeld B, et al. Does circulite synergy assist device as partial ventricular support have a place in modern management of advanced heart failure? *Expert Rev Med Devices*. (2015) 12:49–60. doi: 10.1586/17434440.2015.985208

30. Gude E, Fiane AE. Can mechanical circulatory support be an effective treatment for hfpef patients? *Heart Fail Rev*. (2021). doi: 10.1007/s10741-021-10154-1

31. Fukamachi K, Horvath DJ, Karimov JH, Kado Y, Miyamoto T, Kuban BD, et al. Left atrial assist device to treat patients with heart failure with preserved ejection fraction: initial *in vitro* study. *J Thorac Cardiovasc Surg*. (2021) 162:120–6. doi: 10.1016/j.jtcvs.2019.12.110

32. Miyagi C, Fukamachi K, Kuban BD, Gao S, Miyamoto T, Flick CR, et al. Left atrial circulatory assistance in simulated diastolic heart failure model: first *in vitro* and *in vivo*. *J Card Fail*. (2022) 28:789–98. doi: 10.1016/j.cardfail.2021.11.024

33. Miyagi C, Kuban BD, Flick CR, Polakowski AR, Miyamoto T, Karimov JH, et al. Left atrial assist device for heart failure with preserved ejection fraction: initial results with torque control mode in diastolic heart failure model. *Heart Fail Rev*. (2021). doi: 10.1007/s10741-021-10117-6

34. Reddy YNV, Obokata M, Verbrugge FH, Lin G, Borlaug BA. Atrial dysfunction in patients with heart failure with preserved ejection fraction and atrial fibrillation. *J Am Coll Cardiol*. (2020) 76:1051–64. doi: 10.1016/j.jacc.2020.07.009

35. Kaye DM, Nanayakkara S. Interatrial shunt device for heart failure with preserved ejection fraction. *Front Cardiovasc Med*. (2019) 6:143. doi: 10.3389/fcvm.2019.00143

frontiers | Frontiers in Cardiovascular Medicine

TYPE Original Research
PUBLISHED 15 September 2022
DOI 10.3389/fcvm.2022.933532

OPEN ACCESS

EDITED BY
Ying Liu,
Dalian Medical University, China

REVIEWED BY
Cameron McAlpine,
Icahn School of Medicine at Mount Sinai, United States
Ruijing Zhang,
Second Hospital of Shanxi Medical University, China

*CORRESPONDENCE
Zhong Chen
zhongchen7498@hotmail.com

†These authors have contributed equally to this work and share first authorship

SPECIALTY SECTION
This article was submitted to Heart Failure and Transplantation, a section of the journal Frontiers in Cardiovascular Medicine

RECEIVED 01 May 2022
ACCEPTED 31 August 2022
PUBLISHED 15 September 2022

CITATION
Meng X, Xia G, Zhang L, Xu C and Chen Z (2022) T cell immunoglobulin and mucin domain-containing protein 3 is highly expressed in patients with acute decompensated heart failure and predicts mid-term prognosis. *Front. Cardiovasc. Med.* 9:933532. doi: 10.3389/fcvm.2022.933532

T cell immunoglobulin and mucin domain-containing protein 3 is highly expressed in patients with acute decompensated heart failure and predicts mid-term prognosis

Xin Meng†, Guofang Xia†, Lili Zhang, Congfeng Xu and Zhong Chen*

Department of Cardiology, The Affiliated Sixth People's Hospital, Shanghai Jiao Tong University School of Medicine, Shanghai, China

Background and aims: T cell immunoglobulin and mucin domain-containing protein 3 (Tim-3) is mainly expressed by immune cells and plays an immunomodulatory role in cardiovascular disease. However, the prognostic value of Tim-3 in acute decompensated heart failure (ADHF) is unclear. This study aimed to investigate the expression profile of Tim-3 on $CD4^+$ and $CD8^+$ T cells in patients with ADHF and its impact on their prognosis.

Methods: In this prospective study, 84 patients who were hospitalized with ADHF and 83 patients without heart failure were enrolled. Main clinical data were collected during patient visits. The Tim-3 expression on $CD4^+$ and $CD8^+$ T cells in peripheral blood samples was assayed by flow cytometry. Long-term prognosis of the patients with ADHF was evaluated by major adverse cardiac and cerebrovascular events (MACCE) over a 12-month follow-up period.

Results: We found that the Tim-3 expression on $CD4^+$ T cells [2.08% (1.15–2.67%) vs. 0.88% (0.56–1.39%), $p < 0.001$] and $CD8^+$ T cells [3.81% (2.24–6.03%) vs. 1.36% (0.76–3.00%), $p < 0.001$] in ADHF group were significantly increased vs. the non-ADHF group. Logistic analysis revealed that high levels of Tim-3 expressed on $CD4^+$ and $CD8^+$ T cells were independent risk factors of ADHF (OR: 2.76; 95% CI: 1.34–5.65, $p = 0.006$; OR: 2.58; 95% CI: 1.26–5.31, $p = 0.010$, respectively). ROC curve analysis showed that the high level of Tim-3 on $CD4^+$ or $CD8^+$ T cells as a biomarker has predictive performance for ADHF (AUC: 0.75; 95% CI: 0.68–0.83; AUC: 0.78, 95% CI: 0.71–0.85, respectively). During a median follow-up of 12 months, the Cox regression analysis revealed that higher Tim-3 on $CD4^+$ and $CD8^+$ T cells were strongly associated with increased risks of MACCE within 12 months after

ADHF (HR: 2.613; 95% CI: 1.11–6.13, p = 0.027; HR: 2.762, 95% CI: 1.15–6.63, p = 0.023; respectively).

Conclusion: Our research indicated that the expression level of Tim-3 on $CD4^+$ and $CD8^+$ T cells, elevated in patients with ADHF, was an independent predictor of MACCE within 12 months after ADHF. It suggests a potential immunoregulatory role of Tim-3 signaling system in the mechanism of ADHF.

KEYWORDS

acute decompensated heart failure, Tim-3, T-lymphocytes, prognosis, heart failure

Introduction

Acute decompensated heart failure (ADHF) has become a significant medical, social, and economic problem due to its high rehospitalization rate and mortality (1–3). It is well known that the occurrence and development of heart failure are mainly related to ventricular remodeling, including hypertrophy of cardiomyocytes, myocardial fibroblast proliferation, and myocardial fibrosis. These changes are inseparable from the inflammatory response, and it has been reported that the activation and infiltration of immune cells in the myocardium are directly involved in the pathogenesis of heart failure (4, 5). It is worth noting that with heart failure, a large number of T lymphocytes accumulate in myocardial tissue, and their ability to express inflammatory factors is significantly enhanced (6), which leads to a sustained inflammatory response and the progression of myocardial remodeling (7). Nevertheless, the immune regulatory mechanism of T lymphocytes involved in myocardial inflammation in ADHF is still unclear.

T cell immunoglobulin and mucin domain-containing protein 3 (Tim-3, encoded by hepatitis A virus-cellular receptor 2 [*HAVCR2*]) is a unique inhibitory co-receptor expressed restrictedly on the surface of immune cells and mediates immune tolerance by regulating the activity of immune cells like T cells (8). In recent years, numerous studies have examined the negative regulatory role of Tim-3-mediated immune responses in a variety of diseases (9–13). However, some scholars found that Tim-3 can convert to inflammatory and tissue injury phenotypes under acute stimulation (14–16). Currently, new advances have been made in the field of Tim-3-mediated regulation of immune inflammation in heart failure; Yu et al. (17) discovered that the proportion of Tim-3 on $CD4^+$ and $CD8^+$ T cells was significantly increased in patients with chronic heart failure, suggesting that Tim-3 may induce T cell dysfunction in patients with chronic heart failure, participate in the process of myocardial remodeling, and accelerate heart failure progression. Despite that, to our knowledge, the relationship between Tim-3 expression and ADHF remains unclear.

Consequently, we speculated that Tim-3 may be involved in the process of myocardial remodeling in ADHF by upregulating the activity and proliferation of $CD4^+$ and $CD8^+$ T cells, and affects the prognosis of ADHF patients. To test this hypothesis, we analyzed the characteristics of Tim-3 expression on peripheral $CD4^+$ and $CD8^+$ T cells in patients with ADHF and assessed its predictive value for major adverse cardiovascular and cerebrovascular events (MACCE) within 12 months after ADHF.

Abbreviations: Tim-3, T cell immunoglobulin and mucin domain-containing protein 3; ADHF, Acute decompensated heart failure; MACCE, Major adverse cardiac and cerebrovascular events; HAVCR2, Hepatitis A virus-cellular receptor 2; BNP, Brain natriuretic peptide; NT-proBNP, N-terminal pro-brain natriuretic peptide; Scr, Serum creatinine; CK-MB, Cardiac-specific enzymes such as creatine kinase-MB; TnI, Troponin I; LVEDD, Left ventricular end diastolic diameter; LVEF, Left ventricular ejection fraction; PBMCs, Peripheral blood mononuclear cells; OR, Odds ratio; AUC, Area under receiver operating characteristic curve; CI, Confidence interval.

Materials and methods

Study population and design

From December 2020 to February 2021, 84 consecutive patients with ADHF admitted to the Department of Cardiology, Affiliated Sixth People's Hospital, Shanghai Jiao Tong University School of Medicine were enrolled as the ADHF group. Inclusion criteria were as follows: patients with ADHF diagnosed according to the 2016 European Society of Cardiology guidelines for the diagnosis and treatment of acute heart failure and defined as rapid or chronic onset of decompensated HF or decompensation of chronic HF, with signs and symptoms of HF resulting in unplanned hospitalization (18). 83 patients with other diseases were also recruited as the non-HF group. The exclusion criteria were as follows: inflammatory diseases, autoimmune diseases, active infections or malignant tumors, and clinical data being incomplete.

Peripheral blood was collected from the patients on the day of admission. Peripheral blood mononuclear cells were isolated. The expression of Tim-3 on $CD4^+$ and

$CD8^+$ T cells were detected by flow cytometry. Other biochemical indicators including brain natriuretic peptide (BNP), N-terminal pro-brain natriuretic peptide (NT-proBNP), serum creatinine (Scr), cardiac-specific enzymes like creatine kinase-MB (CK-MB), cardiac troponin I (cTnI) and inflammatory indicators were also evaluated. All patients eligible for coronary heart disease underwent coronary angiography. Coronary angiography was performed by standard techniques, and significant coronary artery disease was visually diagnosed if there was ≥50% diameter stenosis in the major epicardial coronary arteries. Left main disease was counted as two-vessel disease, and the presence of more than two significant coronary artery lesions was considered multi-vessel disease.

Echocardiographic assessment was performed within 24 hours of admission. We measured echocardiographic parameters according to the current guidelines of the American Society of Echocardiography (19). Left atrial diameter and left ventricular end diastolic diameter (LVEDD) were routinely evaluated by two-dimensional ultrasound, and left ventricular ejection fraction (LVEF) was measured by modified Simpson method.

Each patient's baseline clinical data, biochemical and angiographic variables, and ultrasonic cardiogram results were recorded. All patients with acute heart failure were followed up by a cardiovascular physician.

This study was approved by the Ethics Committee of Shanghai Jiao Tong University Affiliated Sixth People's Hospital. All patients included in the study volunteered to participate in this clinical study and signed an informed consent form.

Peripheral blood mononuclear cells isolation

Peripheral blood was collected in tubes containing sodium heparin (BD Biosciences, NJ, USA) by venipuncture. Human peripheral blood mononuclear cells (PBMCs) were isolated from peripheral blood samples via density gradient centrifugation using Lymphoprep Solution (Axis-Shield, Dundee, Scotland). PBMCs were washed with 2% fetal bovine serum in cold phosphate-buffered saline and frozen in cryopreservation medium (20% fetal bovine serum and 10% dimethyl sulfoxide in Dulbecco's Modified Eagle Medium) until further use.

Flow cytometry

PBMCs (2×10^6/tube) were stained for 15 min on ice using Zombie NIR Fixable Viability Kit (Biolegend, CA, USA) to gate out dead cells. The cells were washed once, incubated for 30 min on ice with a cocktail composed of the following antibodies: anti-CD3 FITC antibody (UCHT1, Biolegend), anti-CD4 PerCP/Cyanine 5.5 antibody (OKT4, Biolegend), anti-CD8a APC antibody (RPA-T8, Biolegend) and anti-CD366 PE antibody (F38-2E2, Biolegend). To prepare Full Minus One (FMO) control, we added all other antibodies and Zombie NIR Fixable Viability dye except anti-CD366 PE antibody into each sample and stained in the same condition. Labeled cells were washed once with staining buffer and analyzed by BD Cantoplus Analyzer (BD Biosciences, NJ, USA) and FlowJo software (BD Biosciences, NJ, USA). Lymphocytes were selected based on FSC-A vs. side scatter area. We analyzed forward scatter area vs. forward scatter height to remove doublets. The analysis strategy for evaluating the proportion of Tim-3 on $CD4^+$ and $CD8^+$ T cells is presented in **Figure 1**. The precise gating bound of Tim-3 in each sample was determined according to corresponding Full Minus One control (**Supplementary Figure 1**).

Follow-up

Clinical follow-up data were obtained from the patient's inpatient medical records, regular outpatient visits, and telephone interviews. 84 patients with ADHF were followed up for 12 months. The primary clinical endpoint was MACCE during follow-up (12 months from ADHF). MACCE were defined as rehospitalization for heart failure, unplanned coronary lesion revascularization, acute coronary syndrome at follow-up, ischemic cerebrovascular accident, and cardiac death within 12 months. All potential endpoint events were adjudicated by an assessment committee whose members were blind to patient characteristics.

Statistical analysis

Continuous variables are presented as mean ± standard deviation (SD) for normally distributed variables, otherwise, median (25th–75th percentile) for non-normally distributed variables. Categorical parameters, such as enumeration data, are expressed as percentages (%). Comparisons of continuous variables were performed by two-sample Student's *t*-test or Mann-Whitey-U test (for significantly skewed variables). The chi-square test was used to assess differences in categorical data. Logistic multivariate regression analysis was performed for indicators with $p < 0.05$ in univariate analysis to calculate odds ratio (OR) and 95% confidence interval (95%Cl). Spearman correlation analysis was used to calculate correlation coefficient. The area under the receiver operating characteristic curve (AUC) was used to analyze the prediction of Tim-3 for the risk of ADHF; the effect of Tim-3 expression on $CD4^+$ and $CD8^+$ T cells on the incidence of MACCE

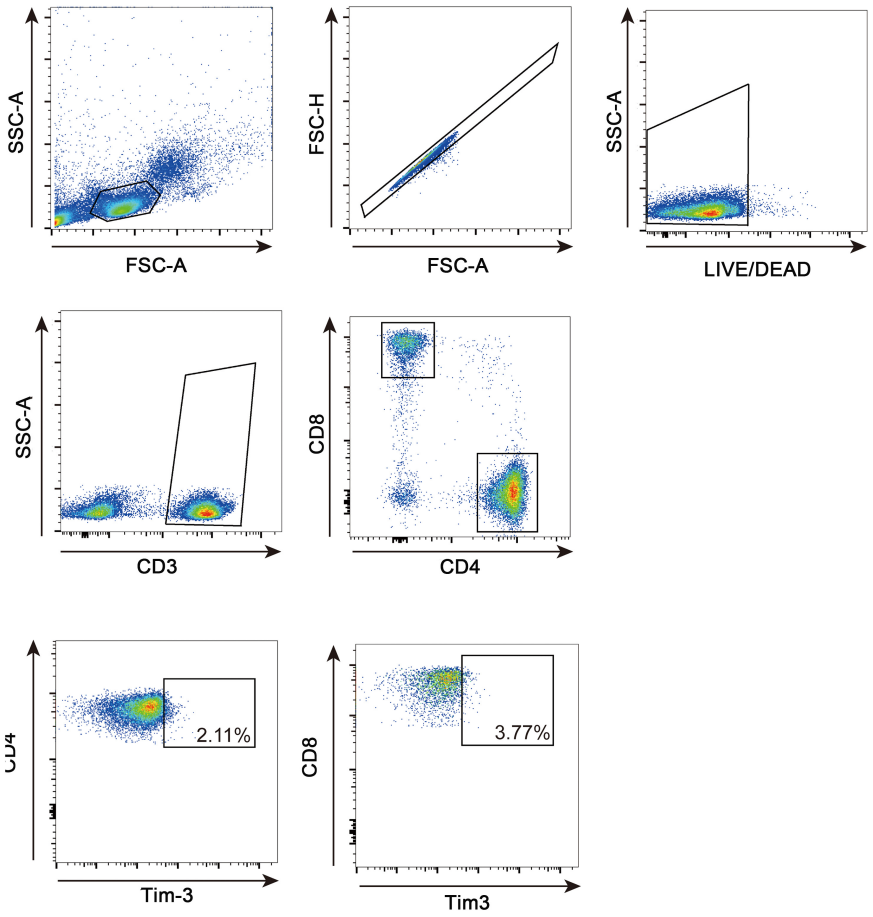

FIGURE 1
FACS gating strategy for lymphocytes. Representative flow cytometric dot plots to determine $CD4^+$ and $CD8^+$ lymphocytes in human PBMCs. PBMC were gated as lymphocytes on forward and side scatter density plots. Then, singlets were gated on FSC-A and FSC-H plots, and live cells were gated for subsequent analysis. $CD4^+$ and $CD8^+$ T cells were identified from the positive population for CD3. $CD4^+$ Tim-3^+ and $CD8^+$Tim-3^+ subpopulation were gated on $CD4^+$ and $CD8^+$ T cells, respectively.

within 12 months after ADHF was evaluated with Cox regression analysis, and expressed as hazard ratio (HR) and respective 95% confidence interval (CI) for each standard deviation (1-SD) increase in continuous variables, and adjusted for potential confounders in a multivariate model. In this analysis, high Tim-3 expression on $CD4^+$ and $CD8^+$ T cells was defined as the mean Tim-3 expression within the 2 highest quartiles (Q3-Q4), whereas low Tim-3 expression on $CD4^+$ and $CD8^+$ T cells was defined as the first to second quartile (Q1–Q2), and stratified by high (Q3–Q4) and low (Q1–Q2) expression of Tim-3 on $CD4^+$ and $CD8^+$ T cells. Kaplan-Meier survival curves were used to estimate the survival status of patients with high and low Tim-3 expression on $CD4^+$ and $CD8^+$ T cells within 12 months after ADHF and compared using the log-rank test. Statistical significance was defined as $p < 0.05$. All analyses were performed using IBM SPSS software (version 22.0 for Windows; SPSS, Inc., Chicago, IL, USA). The ROC curve and Kaplan-Meier survival curves were plotted using GraghPadPrism7.0.

Results

Baseline characteristics

Eighty-four patients with ADHF and 83 patients without HF were enrolled in this study. The baseline clinical data, biochemical and angiographic variables, and echocardiographic parameter results are shown in **Table 1**.

We dichotomized patients into two groups, the ADHF and non-HF group. Compared with those in the non-HF group, the patients in the ADHF group were older [69 years (55–82 years) vs. 61 years (54–69 years), $p = 0.001$] and had no gender difference (71.4 vs. 62.7%, $p = 0.228$). The initial-presented levels of BNP and NT-proBNP, as well-known markers of ADHF,

TABLE 1 Clinical characteristics of patients.

Parameters	Overall (n = 167)	ADHF group (n = 84)	Non-HF group (n = 83)	P-value
Age (years)	66 (54–73)	69 (55–82)	61 (54–69)	0.001
Male, n (%)	112 (67.10%)	60 (71.40%)	52 (62.70%)	0.228
Hypertension, n (%)	78 (46.70%)	45 (53.60%)	33 (39.80%)	0.074
Diabetes, n (%)	36 (21.60%)	22 (26.20%)	14 (16.90%)	0.143
Atrial fibrillation, n (%)	23 (13.80%)	19 (22.60%)	4 (4.80%)	0.001
DCM, n (%)	16 (9.60%)	16 (19.00%)	0 (0)	–
CHD, n (%)	60 (35.90%)	39 (46.40%)	21 (25.30%)	0.004
AMI, n (%)	32 (19.20%)	32 (38.10%)	0 (0)	–
Target vessel				
LAD, n (%)	52 (31.10%)	33 (39.30%)	19 (22.90%)	0.022
LCX, n (%)	24 (14.40%)	17 (20.20%)	7 (8.40%)	0.030
RCA, n (%)	24 (14.40%)	14 (16.70%)	10 (12.00%)	0.395
Single-vessel disease, n (%)	32 (19.20%)	17 (20.20%)	15 (18.10%)	0.722
Multi-vessel disease, n (%)	31 (18.60%)	23 (27.40%)	8 (9.60%)	0.003
LA (mm)	39.20±6.65	42.21±6.93	35.75±4.22	<0.001
LVEDD (mm)	49.96±7.30	53.23±7.95	46.19±3.95	<0.001
LVEF (%)	59 (46.0–64.0)	47 (36.5–55.5)	64 (62.0–67.0)	<0.001
BNP (pg/mL)	125.5 (29.0–1254.8)	1,160 (472.5–1931.5)	29 (17.0–44.0)	<0.001
NT-proBNP (pg/mL)	184 (59.4–5090)	5,090 (2660.0–14200.0)	59.4 (39.2–85.8)	<0.001
D-Dimer (mg/L)	0.41 (0.22–1.04)	0.86 (0.41–1.91)	0.24 (0.15–0.41)	<0.001
Lac (mmol/L)	1.80 (1.35–2.85)	1.80 (1.40–2.90)	1.50 (0.60–2.40)	0.437
Scr (μmol/L)	81.5 (66.8–110.5)	95.5 (73.0–126.0)	71.0 (62.8–85.3)	<0.001
cTnI (μg/L)	0.02 (0.004–0.335)	0.34 (0.04–7.98)	0.005 (0.003–0.006)	<0.001
CRP (mg/L)	5.03 (0.5–12.85)	10.91 (4.59–31.49)	0.5 (0.49–5.55)	<0.001
ESR (mm/h)	8.0 (2.0–19.0)	17.0 (6.0–33.0)	4.0 (2.0–11.0)	<0.001
PCT (ng/mL)	0.66 (0.04–0.16)	0.07 (0.04–0.61)	0.06 (0.03–0.09)	0.305
$CD4^+$ T cells (%)	61.6 (52.1–78.7)	63.7 (53.8–84.3)	59.3 (43.5–70.8)	0.015
$CD8^+$ T cells (%)	19.6 (6.4–33.6)	26.9 (15.3–37.8)	11.5 (4.0–31.4)	<0.001

DCM, Dilated cardiomyopathy; CHD, Coronary heart disease; AMI, Acute myocardial infarction; LAD, Left anterior descending branch; LCX, Left circumflex branch; RCA, Right coronary artery; LA, Left atrium; LVEDD, End diastolic diameter of left ventricle; LVEF, Left ventricular ejection fraction; BNP, Brain natriuretic peptide; NT-proBNP, N-terminal pro-brain natriuretic peptide; Lac, Lactic acid; Scr, Serum creatinine; cTnI, cardiac Troponin I; CRP, C-reactive protein; ESR, Erythrocyte sedimentation rate; PCT, Procalcitonin.

were significantly different between the two groups ($p < 0.001$). The angiographic results suggested that the ADHF group had considerably more multi-vessel disease and anterior descending branch (LAD) coronary lesions than the non-HF group had. In echocardiographic parameters, the baseline LVEF of the ADHF group was lower than those of the non-HF group [47% (36.5–55.5%) vs. 64% (62.0–67.0%), $p < 0.001$], and the levels of LVEDD were significantly higher in the HF group than in the non-HF group (53.2 ± 7.9 mm vs. 46.2 ± 3.9 mm, $p < 0.001$). Intriguingly, the values of Scr [95.5 μmol/L (73.0–126.0 μmol/L) vs. 71.0 μmol/L (62.8 μmol/L −85.3 μmol/L), $p < 0.001$] tended to be higher in patients with ADHF. Notably, we found that the frequencies of both $CD4^+$ ($p = 0.015$) and $CD8^+$ ($p < 0.001$) T cells were significantly increased in the ADHF group compared with the non-HF group (Table 1).

Tim-3 levels in the acute decompensated heart failure and non-HF groups

We analyzed the expression of Tim-3 on $CD4^+$ and $CD8^+$ T cells in both ADHF and non-HF group by flow cytometry (Figures 2A,C). As shown in Figure 2B, we observed that the expression of Tim-3 on $CD4^+$T cells was increased in the ADHF group [2.08% (1.15–2.67%) vs. 0.88% (0.56–1.39%), $p < 0.001$] than those in the non-HF group. Similarly, the expression of Tim-3 on $CD8^+$ T cells showed a tendency to be higher than those in the non-HF group [3.81% (2.24–6.03%) vs. 1.36% (0.76–3.00%), $p < 0.001$; Figure 2D].

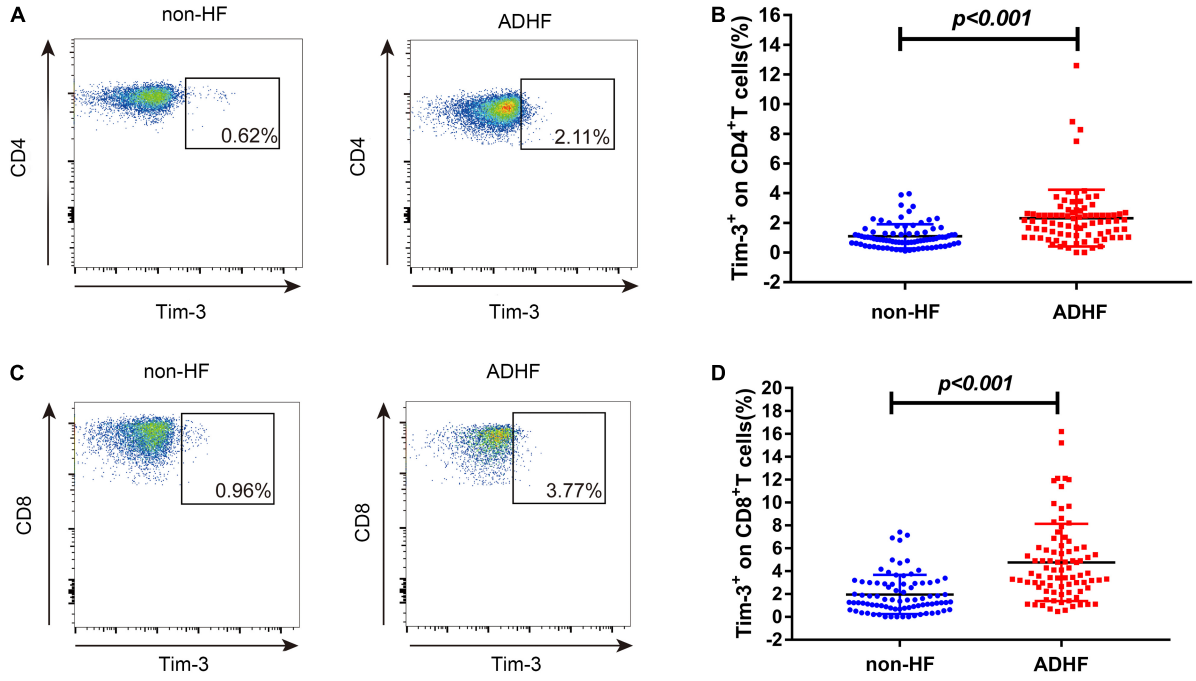

FIGURE 2
The expression of Tim-3 on $CD4^+$ T cells and $CD8^+$ T cells in non-HF and ADHF groups. Peripheral blood mononuclear cells (PBMCs) were isolated from ADHF group (n = 84) and the non-HF group (n = 83). **(A)** Flow cytometry analysis of Tim-3 expression on $CD4^+$ T cells. **(B)** The statistical graph of Tim-3 expression on $CD4^+$ T cells is shown for ADHF group [n = 84, 2.08% (1.15–2.67%)] and non-HF group [n = 83, 0.88% (0.56–1.39%)]. **(C)** Flow cytometry analysis of Tim-3 expression on $CD8^+$ T cells. **(D)** The statistical graph of Tim-3 expression on $CD8^+$ T cells is shown for ADHF group [n = 84, 3.81% (2.24–6.03%)] and non-HF group [n = 83, 1.36% (0.76–3.00%)].

Correlation between Tim-3 expression and different heart failure indexes

As illustrated in Table 2, the expression of Tim-3 on $CD4^+$ T cells was positively correlated with NT-proBNP (ρ = 0.426, $p < 0.001$) and BNP (ρ = 0.428, $p < 0.001$), whereas it was negatively correlated with LVEF (ρ = -0.370, $p < 0.001$). Similarly, the expression of Tim-3 on $CD8^+$ T cells was positively correlated with NT-proBNP (ρ = 0.423, $p < 0.001$); BNP (ρ = 0.362, $p < 0.001$) and LVEDD (ρ = 0.250, p = 0.003), and negatively correlated with LVEF (ρ = -0.377, $p < 0.001$).

TABLE 2 Correlation between Tim-3 expression and different heart failure indexes.

Variable		Tim-3$^+$ on CD4$^+$ T cells(%)	Tim-3$^+$ on CD8$^+$ T cells(%)
NT-proBNP (pg/mL)	ρ	0.426	0.423
	p	<0.001	<0.001
BNP (pg/mL)	ρ	0.428	0.362
	p	<0.001	<0.001
LVEDD (mm)	ρ	0.157	0.250
	p	0.061	0.003
LVEF (%)	ρ	−0.370	−0.377
	p	<0.001	<0.001

Spearman's coefficient of rank correlation was used in calculation. BNP, Brain natriuretic peptide; NT-proBNP, N-terminal pro-brain natriuretic peptide; LVEDD, End diastolic diameter of left ventricle; LVEF, Left ventricular ejection fraction; ρ, correlation coefficient; p, calculated probability.

Logistic regression analysis of specific markers as risk factors for the assessment of acute decompensated heart failure

As Table 3 indicates, univariate analysis showed that the high Tim-3 expression on $CD4^+$ and $CD8^+$T cells were associated with ADHF events (OR 3.72; 95% CI: 1.96–7.06, $p < 0.001$; OR 3.35; 95% CI: 1.78–6.32, $p < 0.001$, respectively). Interestingly, advanced age (OR 1.03; 95% CI: 1.01–1.06, p = 0.002), coronary artery disease (OR 2.56: 95% CI: 1.33–4.93, p = 0.005), LAD lesions (OR 2.18; 95% CI: 1.11–4.28, p = 0.023), and multi-vessel coronary lesions (OR 3.54; 95% CI: 1.48–8.46, p = 0.005) were also associated with ADHF events.

By using multivariate logistic regression analysis, after adjustment for potential confounders, we found that high level of Tim-3 expressed on $CD4^+$ and $CD8^+$T cells remained

TABLE 3 Logistic regression analysis of the correlation between specific markers, risk factors and ADHF events.

Variables	Univariate analysis		Multivariate analysis	
	OR(95% CI)	*P*-value	OR(95% CI)	*P*-value
Male	1.49 (0.78–2.85)	0.229	–	–
Age	1.03 (1.01–1.06)	0.002	1.04 (1.01-1.06)	0.002
Hypertension	1.75 (0.95–3.23)	0.075	–	–
Diabetes	1.75 (0.82–3.71)	0.146	–	–
CHD	2.56 (1.33–4.93)	0.005	2.56 (0.62-10.64)	0.197
Target vessel				
LAD	2.18 (1.11–4.28)	0.023	0.85 (0.19-3.88)	0.833
LCX	2.76 (1.08–7.05)	0.135	–	–
RCA	1.46 (0.61–3.50)	0.397	–	–
Single-vessel disease	1.15 (0.53–2.49)	0.722	–	–
Multi-vessel disease	3.54 (1.48–8.46)	0.005	1.47 (0.45-4.82)	0.528
$CD4^+$ $Tim\text{-}3^+$ high level	3.72 (1.96–7.06)	<0.001	2.76 (1.34-5.65)	0.006
$CD8^+$ $Tim\text{-}3^+$ high level	3.35 (1.78–6.32)	<0.001	2.58 (1.26-5.31)	0.010

CHD, Coronary heart disease; LAD, Left anterior descending branch; LCX, Left circumflex branch; RCA, Right coronary artery; $CD4^+Tim\text{-}3^+$ high level, The highest quartile (Q3–Q4) of Tim-3 expression on $CD4^+$T cells; $CD8^+Tim\text{-}3^+$ high level, The highest quartile (Q3–Q4) of Tim-3 expression on $CD8^+$T cells.

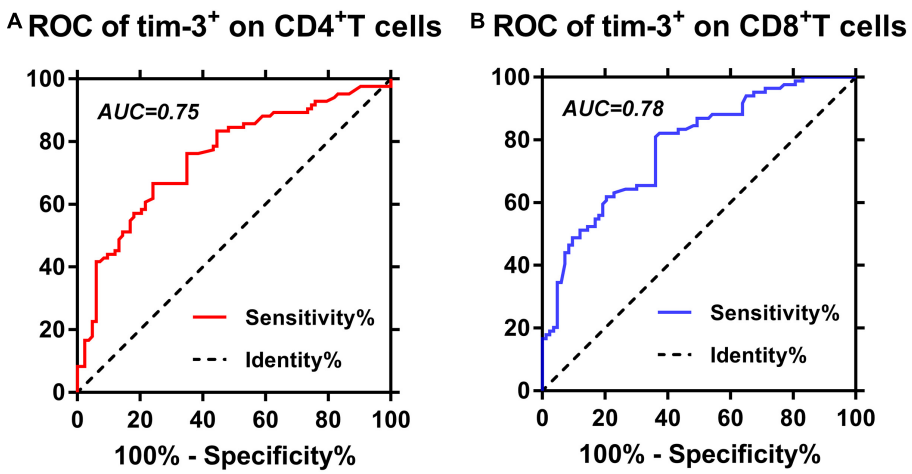

FIGURE 3
Predictive performances of Tim-3 expression on $CD4^+$ and $CD8^+$ T cells. **(A)** ROC curves for Tim-3 expression on $CD4^+$ T cells. **(B)** ROC curves for Tim-3 expression on $CD8^+$ T cells.

TABLE 4 Predictive values of each biomarker.

Makers	AUC (95% CI)	Cut-off	Sensitivity	Specificity	PPV	NPV	PLR	NLR
$Tim\text{-}3^+$ on $CD4^+$ cells	0.75 (0.68, 0.83)	1.400	71.3%	71.3%	73.7%	69.2%	2.48	0.40
$Tim\text{-}3^+$ on $CD8^+$ cells	0.78 (0.71, 0.85)	1.965	72.50%	72.3%	69.4%	76.8%	2.62	0.38

PPV, Positive predictive value; NPV, Negative predictive value; PLR, Positive likelihood radio; NLR, Negative likelihood ratio.

independent predictors of ADHF (OR 2.76; 95% CI: 1.34–5.65, $p = 0.006$; OR 2.58; 95% CI: 1.26–5.31, $p = 0.010$, respectively).

Predictive performances of Tim-3 expressed on CD4$^+$ and CD8$^+$ T cells for acute decompensated heart failure

We further investigated the predictive performance and optimal cutoff value of Tim-3 expression for ADHF events by ROC curve analysis. As reflected in **Figure 3** and **Table 4**, the ROC curve analysis showed that AUC for Tim-3 expressed on CD4$^+$ T cells was 0.75 (95% CI: 0.68–0.83), with a sensitivity of 71.3% and a specificity of 71.3% at the optimal cutoff value of 1.400%. The positive likelihood ratio (PLR) and negative likelihood ratio (NLR) values were 2.48 and 0.40, respectively. The AUC for Tim-3 expression on CD8$^+$ T cells was 0.78 (95% CI: 0.71–0.85) with a sensitivity of 72.5% and a specificity of 72.3% at the cutoff value of 1.965%. The PLR and NLR values were 2.62 and 0.38, respectively.

Survival analysis

Kaplan-Meier survival curves

After a median follow-up of 12 months in patients with ADHF, a total of 37 (44%) patients had MACCE (5 cardiac deaths, 22 readmissions due to HF, and 10 readmissions due to acute coronary syndrome). Patients with ADHF were divided into high (Q3–Q4) and low (Q1–Q2) expression of Tim-3 on CD4$^+$ and CD8$^+$T cells groups according to the quartiles. The Kaplan-Meier curve depicted the follow-up without MACCE (MACCE-free) survival by comparing high and low expression of Tim-3 on CD4$^+$ and CD8$^+$ T cells in ADHF patients, followed by comparison of survival curves using log-rank test. As presented in **Figure 4**, Kaplan-Meier survival curves showed that ADHF patients with higher Tim-3 expression on CD4$^+$ T cells ($p = 0.007$; **Figure 4A**) and CD8$^+$ T cells ($p = 0.010$; **Figure 4B**) had shorter survival times without MACCE.

Univariate and multivariate cox proportional hazard regression analyses for the risk of major adverse cardiac and cerebrovascular events within 12 months after acute decompensated heart failure

According to **Table 5**, the incidence of MACCE within 12 months was higher in patients with LVEF < 50% (HR: 3.936; 95% CI:1.71–9.07; $p = 0.001$) and LVEDD > 50 mm (HR: 2.531; 95% CI: 1.18–5.43; $p = 0.017$). Analysis of individuals presenting with DCM showed an association with MACCE (HR: 2.968; 95% CI: 1.48–5.97; $p = 0.002$). Noteworthy, high expression of Tim-3 on CD4$^+$ T cells demonstrated a strong association with MACCE in the entire study cohort with a

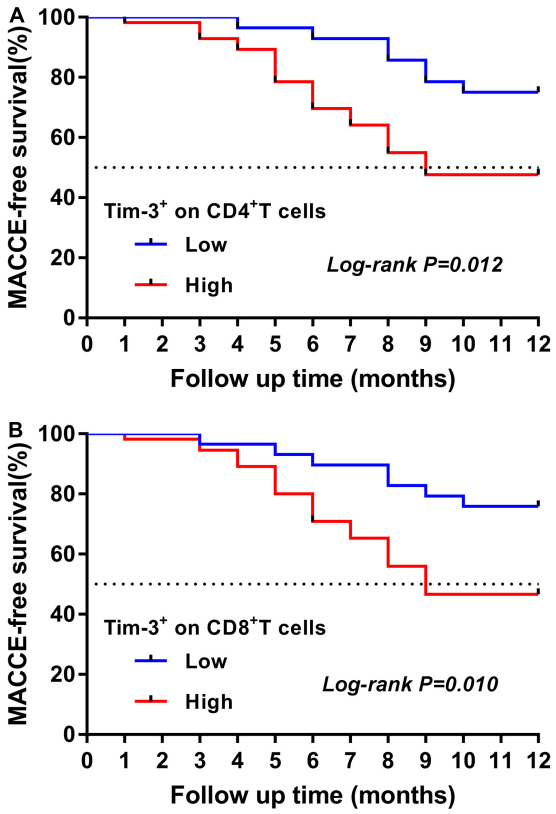

FIGURE 4
Kaplan-Meier curve for the 12-month MACCE-free survival in patients with ADHF. **(A)** Time-to-event curves for the highest quartile (Q3–Q4) of Tim-3 expression on CD4$^+$ T cells vs. the lowest quartiles (Q1–Q2) measured in ADHF patients according to the primary endpoints. The log rank test was used to compare the survival curves. **(B)** Time-to-event curves for the highest quartile (Q3–Q4) of Tim-3 expression on CD8$^+$ T cells vs. the lowest quartiles (Q1–Q2) measured in ADHF patients according to the primary endpoints. The log rank test was used to compare the survival curves.

crude HR per 1-SD of 2.685 (95% CI: 1.17–6.14, $p = 0.019$). In addition, high expression of Tim-3 on CD8$^+$ T cells correlated strongly with MACCE with an HR per 1-SD of 2.730 (95% CI: 1.19–6.24, $p = 0.017$). After adjustment for confounders, high Tim-3 expression on CD4$^+$ and CD8$^+$ T cells were independent predictors of MACCE at 12 months after ADHF (HR: 2.613, 95% CI: 1.11–6.13, $p = 0.027$; HR: 2.762, 95% CI: 1.15–6.63, $p = 0.023$; respectively).

Discussion

In the present study, we demonstrated that Tim-3 was up-regulated on both CD4$^+$ and CD8$^+$ T cells in patients with ADHF, and its expression correlated positively with NT-proBNP levels and BNP levels. High expression of Tim-3 on CD4$^+$ and CD8$^+$ T cells were independent predictors of ADHF

TABLE 5 Univariate and multivariate cox proportional hazard regression analyses for the risk of MACCE within 12 months among patients with ADHF.

Variables	Univariate analysis			Multivariate analysis		
	HR	95% CI	*P*	HR	95% CI	*P*
Age	0.986	0.97–1.00	0.171	–	–	–
Male	0.908	0.44–1.89	0.796	–	–	–
Hypertension	0.920	0.48–1.77	0.803	–	–	–
Diabetes	1.010	0.49–2.10	0.979	–	–	–
CHD	0.953	0.49–1.84	0.886	–	–	–
Target vessel						
LAD	1.051	0.54–2.05	0.885	–	–	–
Multi-vessel disease	1.327	0.65–2.70	0.435	–	–	–
Atrial fibrillation	1.038	0.49–2.21	0.923	–	–	–
DCM	2.968	1.48–5.97	0.002	1.443	0.64–3.24	0.374
LVEDD > 50 mm	2.531	1.18–5.43	0.017	1.213	0.47–3.11	0.688
LVEF < 50%	3.936	1.71–9.07	0.001	3.873	1.44–10.42	0.007
BNP > 500 pg/mL	1.638	1.79–3.41	0.187	–	–	–
NT-proBNP > 1,200 pg/mL	3.410	0.56–20.76	0.183	–	–	–
$CD4^+$ $Tim\text{-}3^+$ high level	2.685	1.17–6.14	0.019	2.613	1.11–6.13	0.027
$CD8^+$ $Tim\text{-}3^+$ high level	2.730	1.19–6.24	0.017	2.762	1.15–6.63	0.023

DCM, Dilated cardiomyopathy; CHD, Coronary heart disease; LAD, Left anterior descending branch; LVEDD, End diastolic diameter of left ventricle; LVEF, Left ventricular ejection fraction; $CD4^+$ $Tim\text{-}3^+$ high level, The highest quartile (Q3–Q4) of Tim-3 expression on $CD4^+$T cells; $CD8^+$$Tim\text{-}3^+$ high level, The highest quartile (Q3–Q4) of Tim-3 expression on $CD8^+$T cells.

events. COX analysis suggested that the up-regulation of Tim-3 expression on $CD4^+$ and $CD8^+$ T cells was significantly associated with MACCE events within 12 months after ADHF.

Over recent years, scholars have found that the immune inflammatory response plays an important role in ventricular remodeling. Epelman et al. (20) proposed that inflammatory cytokines were up-regulated in cardiac tissue of heart failure model cells. Immune regulatory receptors on the surface of inflammatory cells also regulate left ventricular hypertrophy (21). The current experimental results in animal models show that $CD4^+$ T cells accumulated in the left ventricular tissue of mice with congestive heart failure (22) and participate in collagen production through proliferation and activation (5). Under cardiac pressure overload, dendritic cells induced $CD4^+$ T cell proliferation by accumulating immunoregulatory signaling proteins (23), and on the other hand, the involvement of chemokines promotes the activation of $CD4^+$ T cells and cardiac infiltration, promote myocardial fibrosis and left ventricular dysfunction (24). Notably, recent studies have revealed the relationship between specific subpopulation of $CD8^+$ T cells and myocardial remodeling. In the early stage of heart failure, the frequency of $CD8^+$ T cells in the myocardium is significantly increased (25). The dynamic interaction between myocardial infiltrating $CD8^+$ T cells and macrophages promotes myocardial hypertrophy and plays an important role in the occurrence of adaptive myocardial remodeling (26). In our study, the frequency of $CD4^+$ and $CD8^+$ T cells in ADHF group was significantly increased. Our data suggest that $CD4^+$ and $CD8^+$ T cells under myocardial overload in ADHF patients may be influenced by immune regulation to proliferate and activate participating in myocardial fibrosis and heart failure progression.

Tim-3 is an immunomodulatory and tolerogenic regulator that is expressed in innate and adaptive immune cells. Accumulating evidence suggests that abnormal expression of Tim-3 on peripheral $CD4^+$ and $CD8^+$ T cells is closely associated with autoimmune diseases, viral infections, and cancers. It has been previously reported that Tim-3 often acts as a negative regulator to mediate T cell exhaustion (27). The results of studies published so far mostly support the conclusion that Tim-3 inhibits T cell responses, especially when chronic stimuli are involved (28–30). In contrast, several reports provided evidence that Tim-3 could promote both T-lymphocyte proliferation and proinflammatory cytokine production under acute stimulation (14–16). These results suggest that the immunomodulatory function of Tim-3 may be reversed in the presence of its different ligands. In our data, ADHF patients exhibit an increased expression of Tim-3 on $CD4^+$ and $CD8^+$ T cells. It depicts that the up-regulation of Tim-3 expression on $CD4^+$ and $CD8^+$ T cells in ADHF patients may increase the number of specific subpopulations of $CD4^+$ and $CD8^+$ T cells. Notably, we show that the high expression of Tim-3 on $CD4^+$ and $CD8^+$T cells is an independent predictor

of ADHF. Further ROC analysis revealed the expression of Tim-3 on $CD4^+$ and $CD8^+$T cells provides a good diagnosis of ADHF (**Figure 3**). Our study indicated that Tim-3 seems to be a structural positive regulator of T cell function during ADHF episodes. It can be speculated that in these patients, Tim-3 positively regulates T lymphocyte function by binding to HLA-B–associated transcript 3 (31) in response to acute myocardial injury stimulus (15). It expands the infiltration and accumulation of $CD4^+$ and $CD8^+$ T cells in the myocardium and promotes the release of myocarditis factors (such as IL-2, IL-6, etc.). Also, it induces the production of cytotoxic T cells and releases perforin and granzyme, thereby aggravating myocardial inflammatory injury and pathological hypertrophy (32). However, studies are still needed to confirm the potential biological role of Tim-3 in the development of ADHF.

Based on the relationship between T cells and acute heart failure (33), recent studies have continuously confirmed that the inflammatory response mediated by specific subpopulations of $CD4^+$ and $CD8^+$ T cells significantly affects the progression and prognosis of heart failure (34). Animal studies have shown that the proportion of $CD4^+$ T cells and the production of activating factors are significantly increased in patients with acute heart failure, which is associated with the clinical outcome of acute heart failure (35). Clinically, it was also found that the high expression of $CD4^+$ T cells in patients with heart failure is a strong predictor of all-cause and cardiovascular mortality in patients with heart failure and a potential marker for the progression of heart failure (36). Moreover, a significant increase in the proportion of $CD8^+$ T cells was associated with deteriorating cardiac function and long-term MACCE (37, 38). Therefore, it is particularly important to explore the immunomodulatory mechanisms of T cells by specific immunomodulatory factors in ADHF patients. Notably, Tim-3 influenced the development of most diseases through immunomodulatory functions (9, 34, 39, 40). Our data show that ADHF patients with high expression of Tim-3 on $CD4^+$ and $CD8^+$ T cells had a higher incidence of MACCE by Kaplan-Meier analysis (**Figure 4**). In particular, the predictive performance of high expression of Tim-3 on $CD4^+$ and $CD8^+$ T cells remained in multivariate Cox proportional hazards regression analysis after adjusting for potential confounders (**Table 5**). Our study indicates that high co-expression of Tim-3 on $CD4^+$ and $CD8^+$ T cells is an independent predictor of the occurrence of MACCE in patients with ADHF, and its upregulation is associated with poor survival in ADHF patients. It has the potential utility to help identify patients at high risk of MACCE early.

Study limitations

Our study has the following limitations. First, the number of samples included in this study is relatively small, and the expression of Tim-3 may reflect multiple diseases. To eliminate this selection bias, we excluded patients with inflammatory diseases, autoimmune diseases, active infections, or malignancies during case collection; however, potential selection bias could not be fully excluded in this study. Further large-scale prospective studies are needed to determine whether these deficiencies affect the results. Second, in this study, we only recorded Tim-3 expression of $CD4^+$ and $CD8^+$ T cells on the day of admission for ADHF, and no information was reported about the changes in Tim-3 expression on $CD4^+$ and $CD8^+$ T cells after ADHF improved with treatment and its impact on the prognosis of ADHF. Third, no antibody intervention for Tim-3 was performed in this study, and further studies are still needed to confirm the effect of immunomodulation therapy targeting Tim-3 on ADHF.

Conclusion

The results of this study show that Tim-3 is highly expressed on both $CD4^+$ and $CD8^+$ T cells in ADHF, and it might be an independent predictor of MACCE incidence within 12 months after ADHF. Consequently, these findings suggest a potential immunoregulatory role of a Tim-3 signaling system in the pathogenesis of ADHF and might be used as a novel biomarker to assess the prognosis of ADHF. Targeted regulation of Tim-3 expression would be a new strategy for the treatment of ADHF, and this needs to be confirmed by further studies.

Data availability statement

The raw data supporting the conclusions of this article will be made available by the authors, without undue reservation.

Ethics statement

The studies involving human participants were reviewed and approved by the Independent Ethics Committee of Shanghai Sixth People's Hospital. The patients/participants provided their written informed consent to participate in this study.

Author contributions

XM and GX designed the research study, wrote the manuscript, performed data management, data analysis, all cell processing, and flow cytometry analysis. LZ, ZC, and CX edited and revised the article. All authors contributed to the article and approved the submitted version.

Funding

This study was supported by the Hospital Scientific Research Fund of Shanghai Sixth People's Hospital East (DY2020011) to XM and National Nature Science Foundation of China (82171812) to CX.

Conflict of interest

The authors declare that the research was conducted in the absence of any commercial or financial relationships that could be construed as a potential conflict of interest.

Publisher's note

Supplementary material

The Supplementary Material for this article can be found online at: https://www.frontiersin.org/articles/10.3389/fcvm.2022.933532/full#supplementary-material

References

1. O'Connor CM, Miller AB, Blair JE, Konstam MA, Wedge P, Bahit MC, et al. Causes of death and rehospitalization in patients hospitalized with worsening heart failure and reduced left ventricular ejection fraction: results from efficacy of vasopressin antagonism in heart failure outcome study with tolvaptan (EVEREST) program. *Am Heart J.* (2010) 159:841–849.e1. doi: 10.1016/j.ahj.2010.02.023

2. Chun S, Tu JV, Wijeysundera HC, Austin PC, Wang X, Levy D, et al. Lifetime analysis of hospitalizations and survival of patients newly admitted with heart failure. *Circ Heart Fail.* (2012) 5:414–21. doi: 10.1161/CIRCHEARTFAILURE.111.964791

3. Dharmarajan K, Hsieh AF, Lin Z, Bueno H, Ross JS, Horwitz LI, et al. Diagnoses and timing of 30-day readmissions after hospitalization for heart failure, acute myocardial infarction, or pneumonia. *JAMA.* (2013) 309:355–63.

4. Carrillo-Salinas FJ, Ngwenyama N, Anastasiou M, Kaur K, Alcaide P. Heart inflammation: immune cell roles and roads to the heart. *Am J Pathol.* (2019) 189:1482–94. doi: 10.1016/j.ajpath.2019.04.009

5. Bansal SS, Ismahil MA, Goel M, Patel B, Hamid T, Rokosh G, et al. Activated T lymphocytes are essential drivers of pathological remodeling in ischemic heart failure. *Circ Heart Fail.* (2017) 10:e003688. doi: 10.1161/CIRCHEARTFAILURE.116.003688

6. Nevers T, Salvador AM, Grodecki-Pena A, Knapp A, Velázquez F, Aronovitz M, et al. Left ventricular T-cell recruitment contributes to the pathogenesis of heart failure. *Circ Heart Fail.* (2015) 8:776–87. doi: 10.1161/CIRCHEARTFAILURE.115.002225

7. Bansal SS, Ismahil MA, Goel M, Zhou G, Rokosh G, Hamid T, et al. Dysfunctional and proinflammatory regulatory T-lymphocytes are essential for adverse cardiac remodeling in ischemic cardiomyopathy. *Circulation.* (2019) 139:206–21. doi: 10.1161/CIRCULATIONAHA.118.036065

8. Das M, Zhu C, Kuchroo VK. Tim-3 and its role in regulating anti-tumor immunity. *Immunol Rev.* (2017) 276:97–111.

9. Pu F, Chen F, Zhang Z, Qing X, Lin H, Zhao L, et al. TIM-3 expression and its association with overall survival in primary osteosarcoma. *Oncol Lett.* (2019) 18:5294–300.

10. Yan WJ, Sun P, Wei DD, Wang SX, Yang JJ, Li YH, et al. T cell immunoglobulin and mucin domain-containing molecule 3 on CD14(+) monocytes serves as a novel biological marker for diabetes duration in type 2 diabetes mellitus. *J Diabetes Invest.* (2016) 7:867–73. doi: 10.1111/jdi.12523

11. Qiu MK, Wang SC, Dai YX, Wang SQ, Ou JM, Quan ZW. PD-1 and Tim-3 pathways regulate CD8+ T cells function in atherosclerosis. *PLoS One.* (2015) 10:e0128523. doi: 10.1371/journal.pone.0128523

12. Qiu MK, Wang SC, Tang Y, Pan C, Wang Y, Wang SQ, et al. Tim-3 inhibits low-density lipoprotein-induced atherogenic responses in human umbilical vein endothelial cells. *Oncotarget.* (2017) 8:61001–10. doi: 10.18632/oncotarget.17720

13. Zhang Y, Zhang M, Li X, Tang Z, He L, Lv K. Expansion of CD11b(+)Ly-6C(+) myeloid-derived suppressor cells (MDSCs) driven by galectin-9 attenuates CVB3-induced myocarditis. *Mol Immunol.* (2017) 83:62–71. doi: 10.1016/j.molimm.2017.01.013

14. Guo Y, Zhang J, Lai X, Chen M, Guo Y. Tim-3 exacerbates kidney ischaemia/reperfusion injury through the TLR-4/NF-κB signalling pathway and an NLR-C4 inflammasome activation. *Clin Exp Immunol.* (2018) 193:113–29. doi: 10.1111/cei.13126

15. Avery L, Filderman J, Szymczak-Workman AL, Kane LP. Tim-3 co-stimulation promotes short-lived effector T cells, restricts memory precursors, and is dispensable for T cell exhaustion. *Proc Natl Acad Sci U S A.* (2018) 115:2455–60. doi: 10.1073/pnas.1712107115

16. Qiu Y, Chen J, Liao H, Zhang Y, Wang H, Li S, et al. Tim-3-expressing CD4+ and CD8+ T cells in human tuberculosis (TB) exhibit polarized effector memory phenotypes and stronger anti-TB effector functions. *PLoS Pathogens.* (2012) 8:e1002984. doi: 10.1371/journal.ppat.1002984

17. Yu HW, Dong YY, Dang YH. [The modulatory activity of T cell immunoglobulin and mucin domain-containing protein 3 on T lymphocytes in patients with chronic heart failure]. *Zhonghua Yi Xue Za Zhi.* (2020) 100:1315–9.

18. Ponikowski P, Voors AA, Anker SD, Bueno H, Cleland JG, Coats AJ, et al. 2016 ESC guidelines for the diagnosis and treatment of acute and chronic heart failure: the task force for the diagnosis and treatment of acute and chronic heart failure of the European society of cardiology (ESC). developed with the special contribution of the heart failure association (HFA) of the ESC. *Eur J Heart Fail.* (2016) 18:891–975.

19. Lang RM, Bierig M, Devereux RB, Flachskampf FA, Foster E, Pellikka PA, et al. Recommendations for chamber quantification: a report from the American society of echocardiography's guidelines and standards committee and the chamber quantification writing group, developed in conjunction with the European association of echocardiography, a branch of the European society of cardiology. *J Am Soc Echocardiogr.* (2005) 18:1440–63. doi: 10.1016/j.echo.2005.10.005

20. Epelman S, Liu PP, Mann DL. Role of innate and adaptive immune mechanisms in cardiac injury and repair. *Nat Rev Immunol.* (2015) 15:117–29.

21. Shang L, Yue W, Wang D, Weng X, Hall ME, Xu Y, et al. Systolic overload-induced pulmonary inflammation, fibrosis, oxidative stress and heart failure progression through interleukin-1β. *J Mol Cell Cardiol.* (2020) 146:84–94. doi: 10.1016/j.yjmcc.2020.07.008

22. El-Menyar AA. Cytokines and myocardial dysfunction: state of the art. *J Cardiac Fail.* (2008) 14:61–74.

23. Ngwenyama N, Kirabo A, Aronovitz M, Velázquez F, Carrillo-Salinas F, Salvador AM, et al. Isolevuglandin-modified cardiac proteins drive CD4+ T-cell activation in the heart and promote cardiac dysfunction. *Circulation.* (2021) 143:1242–55. doi: 10.1161/CIRCULATIONAHA.120.051889

24. Ngwenyama N, Salvador AM, Velázquez F, Nevers T, Levy A, Aronovitz M, et al. CXCR3 regulates CD4+ T cell cardiotropism in pressure overload-induced cardiac dysfunction. *JCI Insight.* (2019) 4:e125527. doi: 10.1172/jci.insight.125527

25. Gröschel C, Sasse A, Monecke S, Röhrborn C, Elsner L, Didié M, et al. CD8(+)-T cells with specificity for a model antigen in cardiomyocytes can become activated after transverse aortic constriction but do not accelerate progression to heart failure. *Front Immunol.* (2018) 9:2665. doi: 10.3389/fimmu.2018.02665

26. Komai K, Ito M, Nomura S, Shichino S, Katoh M, Yamada S, et al. Single-cell analysis revealed the role of CD8(+) effector T cells in preventing cardioprotective macrophage differentiation in the early phase of heart failure. *Front Immunol.* (2021) 12:763647. doi: 10.3389/fimmu.2021.763647

27. Lee J, Oh JM, Hwang JW, Ahn JK, Bae EK, Won J, et al. Expression of human TIM-3 and its correlation with disease activity in rheumatoid arthritis. *Scand J Rheumatol.* (2011) 40:334–40.

28. Holderried TAW, de Vos L, Bawden EG, Vogt TJ, Dietrich J, Zarbl R, et al. Molecular and immune correlates of TIM-3 (HAVCR2) and galectin 9 (LGALS9) mRNA expression and DNA methylation in melanoma. *Clin Epigen.* (2019) 11:161. doi: 10.1186/s13148-019-0752-8

29. Mohsenzadegan M, Bavandpour P, Nowroozi MR, Amini E, Kourosh-Arami M, Momeni SA, et al. The potential of T cell immunoglobulin and mucin-domain containing-3 (Tim-3) in designing novel immunotherapy for bladder cancer. *Endocr Metab Immune Disord Drug Targets.* (2021) 21:2131–46. doi: 10.2174/1871530321666210310142141

30. Liu Y, Gao LF, Liang XH, Ma CH. Role of Tim-3 in hepatitis B virus infection: an overview. *World J Gastroenterol.* (2016) 22:2294–303. doi: 10.3748/wjg.v22.i7.2294

31. Tang R, Rangachari M, Kuchroo VK. Tim-3: a co-receptor with diverse roles in T cell exhaustion and tolerance. *Sem Immunol.* (2019) 42:101302. doi: 10.1016/j.smim.2019.101302

32. Meléndez GC, McLarty JL, Levick SP, Du Y, Janicki JS, Brower GL. Interleukin 6 mediates myocardial fibrosis, concentric hypertrophy, and diastolic dysfunction in rats. *Hypertension.* (2010) 56:225–31. doi: 10.1161/HYPERTENSIONAHA.109.148635

33. Frieler RA, Mortensen RM. Immune cell and other noncardiomyocyte regulation of cardiac hypertrophy and remodeling. *Circulation.* (2015) 131:1019–30. doi: 10.1161/CIRCULATIONAHA.114.008788

34. Kallikourdis M, Martini E, Carullo P, Sardi C, Roselli G, Greco CM, et al. T cell costimulation blockade blunts pressure overload-induced heart failure. *Nat Commun.* (2017) 8:14680. doi: 10.1038/ncomms14680

35. Youn JC, Jung MK, Yu HT, Kwon JS, Kwak JE, Park SH, et al. Increased frequency of CD4(+)CD57(+) senescent T cells in patients with newly diagnosed acute heart failure: exploring new pathogenic mechanisms with clinical relevance. *Sci Rep.* (2019) 9:12887. doi: 10.1038/s41598-019-49332-5

36. Koller L, Blum S, Korpak M, Richter B, Goliasch G, Zorn G, et al. Predictive power of the fractalkine receptor CX3CR1 on CD4 T cells in patients with chronic heart failure. *Int J Cardiol.* (2014) 171:96–7. doi: 10.1016/j.ijcard.2013.11.082

37. Tae YH, Youn JC, Lee J, Park S, Chi HS, Lee J, et al. Characterization of CD8(+)CD57(+) T cells in patients with acute myocardial infarction. *Cell Mol Immunol.* (2015) 12:466–73. doi: 10.1038/cmi.2014.74

38. Zhang L, Wang Z, Wang D, Zhu J, Wang Y. CD8(+)CD28(+) T cells might mediate injury of cardiomyocytes in acute myocardial infarction. *Mol Immunol.* (2018) 101:74–9. doi: 10.1016/j.molimm.2018.05.015

39. Piao Y, Jin X. Analysis of Tim-3 as a therapeutic target in prostate cancer. *Tumour Biol.* (2017) 39:1010428317716628.

40. Li YM, Li Y, Yan L, Tang JT, Wu XJ, Bai YJ, et al. Assessment of serum Tim-3 and Gal-9 levels in predicting the risk of infection after kidney transplantation. *Int Immunopharmacol.* (2019) 75:105803. doi: 10.1016/j.intimp.2019.105803

frontiers | Frontiers in Cardiovascular Medicine

TYPE Original Research
PUBLISHED 27 September 2022
DOI 10.3389/fcvm.2022.933597

OPEN ACCESS

EDITED BY
Tong Liu,
Tianjin Medical University, China

REVIEWED BY
Serban Mihai Balanescu,
Carol Davila University of Medicine and Pharmacy, Romania
Juan-Juan Qin,
Renmin Hospital of Wuhan University, China

*CORRESPONDENCE
Hang Yu
yuhang@xjtu.edu.cn
Fengwei Guo
guofengwei@xjtu.edu.cn

†These authors have contributed equally to this work and share first authorship

SPECIALTY SECTION
This article was submitted to Heart Failure and Transplantation, a section of the journal Frontiers in Cardiovascular Medicine

RECEIVED 01 May 2022
ACCEPTED 29 August 2022
PUBLISHED 27 September 2022

CITATION
Zhong L, Quan X, Dang P, Tang M, Yu H and Guo F (2022) Clinical characteristics and risk factors of in-hospital gastrointestinal bleeding in patients with acute myocardial infarction.
Front. Cardiovasc. Med. 9:933597.
doi: 10.3389/fcvm.2022.933597

Clinical characteristics and risk factors of in-hospital gastrointestinal bleeding in patients with acute myocardial infarction

Liang Zhong[1†], Xingpu Quan[2†], Peizhu Dang[3], Manyun Tang[3], Hang Yu[3*] and Fengwei Guo[1*]

[1]Department of Cardiovascular Surgery, The First Affiliated Hospital of Xi'an Jiaotong University, Xi'an, China, [2]Department of Gastroenterology, The First Affiliated Hospital of Xi'an Jiaotong University, Xi'an, China, [3]Department of Cardiovascular Medicine, The First Affiliated Hospital of Xi'an Jiaotong University, Xi'an, China

Background: Gastrointestinal bleeding (GIB) is one of the most serious complications of acute myocardial infarction (AMI) and is correlated with poor outcomes.

Objective: To evaluate the prevalence, risk factors and in-hospital mortality of GIB in patients with AMI.

Methods: This observational case-control study retrospectively enrolled consecutive patients with AMI from the Department of Cardiovascular Medicine and Cardiovascular Surgery of the First Affiliated Hospital of Xi'an Jiaotong University from January 2015 to December 2020. GIB after AMI was identified by International Classification of Diseases (ICD) codes from inpatient medical settings and validated by medical record review. AMI patients without GIB were accordingly classified as the control group. Propensity score matching (PSM) was used to match with the GIB group and the control group. All anonymized clinical data were provided by the Biobank of the First Affiliated Hospital of Xi'an Jiaotong University.

Results: A total of 5,868 AMI patients were enrolled, 0.87% (51/5,868) of whom developed GIB after AMI. On the univariate analysis, history of diabetes, chronic kidney disease, Killip IV, a lower hemoglobin concentration, a higher serum level of creatinine, blood urea nitrogen and D-dimer were closely associated with the risk of GIB ($P < 0.05$). On the multivariable analysis, a lower hemoglobin concentration (OR: 0.93, 95% CI: 0.89–0.96, $P < 0.001$) was independently associated with the risk of GIB. Patients with GIB had a much higher in-hospital mortality rate than those without GIB (14.3 vs. 2.1%, $P = 0.047$). In-hospital mortality among patients with GIB after AMI appeared to be associated with a decreased hemoglobin concentration (OR: 0.93, 95% CI: 0.86–0.99, $P = 0.045$) and Killip IV (OR: 51.59, 95% CI: 2.65–1,005.30, $P = 0.009$).

Conclusion: The history of diabetes, poor renal function and heart failure were associated with the high risk of GIB in patients experiencing AMI. The in-hospital mortality in patients with AMI complicating GIB was higher than

that in patients without GIB and was associated with a decreased hemoglobin concentration and high Killip classification.

KEYWORDS

acute myocardial infarction, heart failure, gastrointestinal bleeding, risk stratification, propensity score matching

Introduction

Acute myocardial infarction (AMI) is a serious increasing global health problem due to its high mortality and morbidity rates (1). The emphasis of treatment for AMI is prompt myocardial reperfusion, including the application of thrombolytic therapy or primary percutaneous coronary intervention (PCI) (2). Antithrombotic (anticoagulant or antiplatelet) effects are important mechanisms of PCI, which can reduce even prevent perioperative and long-term ischemic cardiovascular events, including stent thrombosis and recurrent myocardial infarction (3, 4). Substantial progress has been made in myocardial infarction treatment, such as early reperfusion therapy, which has extensively decreased the mortality rate in patients with AMI (5).

However, bleeding is one of the most serious complications of AMI which directly associated with an increased mortality (6). Gastrointestinal bleeding (GIB) is a joint adverse drug reaction that occurs in patients receiving dual antiplatelet medication, with an incidence of 5% to more than 10% (7). Bleeding events after PCI are related to increasement of short- and long-term morbidity and mortality (8, 9). GIB can affect the prognosis of AMI patients and increase the risk of major adverse cardiac events (MACEs) in the early stage (during hospitalization and within 30 days after discharge) and late stage (10–12). GIB is associated with markedly increased mortality and morbidity and can be life-threatening in patients with acute coronary syndromes (ACSs) (13). However, there is no systematic report on the risk factors and prognosis of GIB in AMI patients in China. Here, we conducted a real-world study to evaluate the risk factors and in-hospital outcomes of GIB in AMI patients in a Chinese population.

Methods

Study design

This was an observational, case-control study. Anonymized clinical data were collected from the Biobank of the First Affiliated Hospital of Xi'an Jiaotong University. The Ethics Committee of the First Affiliated Hospital of Xi'an Jiaotong University approved this study (no. XJTU1AF2021LSK116), and informed consent was obtained. All methods were carried out in accordance with relevant guidelines and regulations and the principles of the Declaration of Helsinki.

Participants

A total of 5,868 consecutive patients hospitalized for the first time for AMI were enrolled between January 2015 and December 2020 at the First Affiliated Hospital of Xi'an Jiaotong University (Shaanxi, China). AMI was defined based on the universal definition criteria established by the American College of Cardiology (14). GIB was defined as clinical events of bleeding (coffee ground emesis, hematemesis, melena, or hematochezia) diagnosed by a physician or the presence of blood in the upper or lower gastrointestinal tract on endoscopic evaluation (15).

The inclusion criterion was a diagnosis of AMI, including non-ST-segment elevation myocardial infarction (NSTEMI) and ST-segment elevation myocardial infarction (STEMI). The exclusion criteria were prior history of bleeding within 1 month and baseline data missing.

Data collection

Collected data included demographic characteristics, medical history, clinical information, laboratory results, and oral medications within 24 h after admission. Venous blood was analyzed in the Core Laboratory of the First Affiliated Hospital of Xi'an Jiaotong University for examinations of blood biochemistry, hemoglobin, blood urea nitrogen (BUN), serum creatinine, and D-dimer. Coronary angiography data were also collected and the angiographic burden of AMI patients was quantified by the modified Gensini Score (16).

Propensity score matching

A propensity score-matching (PSM) analysis adjusted to sex, age, myocardial infarction type (including STEMI and NSTEMI), and hospital stay was performed in order to reduce bias. The subjects were matched in a 1:1 ratio and the caliper value was 0.002. Through the application

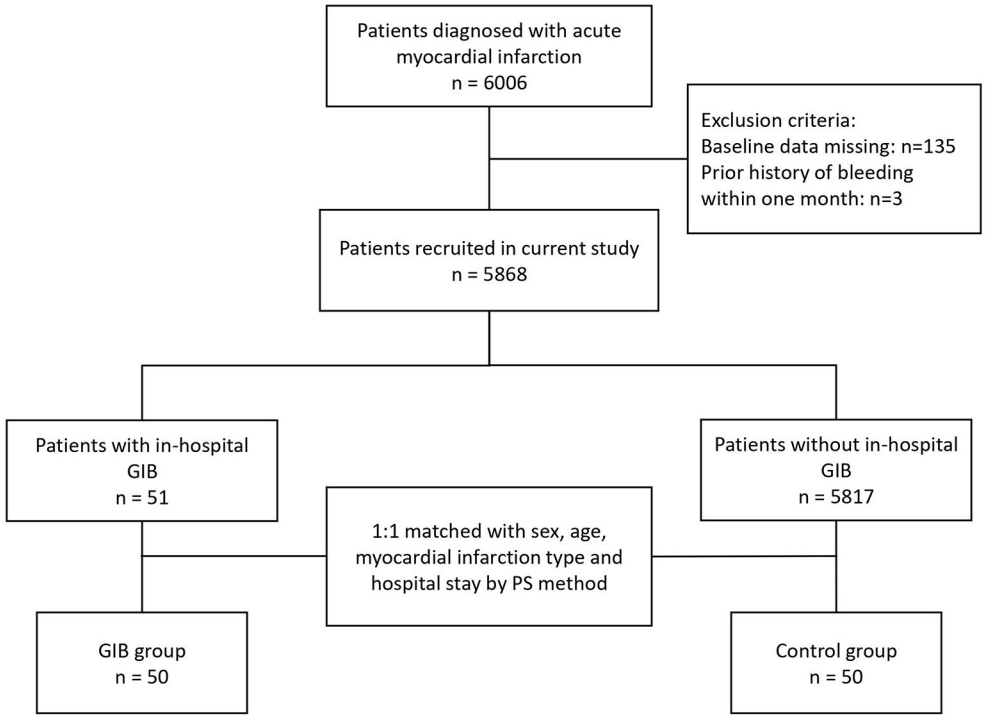

FIGURE 1
Flowchart of the selection process of the current study. AMI, acute myocardial infarction; GIB, gastrointestinal bleeding.

of PSM, the participants of the GIB group and the control group were paired for the factors mentioned above. This statistical approach reduced the possibility of introducing confounding factors by providing a balanced distribution of selected characteristics of the two groups.

Statistical analysis

Statistical analysis was performed using SPSS version 26.0 (SPSS Inc., Chicago, IL, USA). Mean values with standard deviations (SDs) and counts with percentages were used to describe clinical characteristics and factors related to GIB. Differences were evaluated with a paired *T*-test or Wilcoxon test for continuous variables and a chi-square test or Fisher's exact test for categorical variables. Univariate and multivariate logistic regressions were used to determine possible factors influencing the prevalence and in-hospital outcomes of GIB. Odds ratios (ORs) and 95% confidence intervals (CIs) were calculated. All *P*-values were two-sided, and $P < 0.05$ was considered statistically significant.

Results

A total of 5,868 AMI patients were enrolled, and the occurrence of in-hospital GIB was clinically confirmed in 51 patients (51/5868, 0.87%). Before PSM, 80.5% were males. Among the GIB patients, 22/51 (43.1%) had STEMI, and 29/51 (56.9%) had NSTEMI. After PSM, 50 patients who developed in-hospital GIB were finally assigned to the GIB group and 50 patients pair matched with sex, age, myocardial infarction type and hospitalization time were assigned to the control group (Figure 1).

Population comparison before and after PSM

The original demographics and characteristics of all enrolled patients are shown in Table 1. Before PSM, the average age in the GIB group was significantly higher than that in the control group (67.67 ± 10.35 vs. 61.49 ± 12.15, $P < 0.001$), and the mean hospitalization time in the GIB group was significantly longer than that in the control group (10.53 ± 12.07 vs. 5.69 ± 5.15, $P < 0.001$). Moreover, there were more STEMI patients

in the GIB group (43.1 vs. 28.5%, $P < 0.05$). Then, after PSM, all matched factors were well-balanced and comparable between the two groups, and there were no significant differences in sex, age, myocardial infarction type and mean hospitalization time (Table 1).

Baseline characteristics

Table 2 showed the differences in demographic and clinical characteristics of AMI patients with and without in-hospital GIB after PSM. Compared with patients without in-hospital GIB, patients who developed in-hospital GIB were more likely to have a much lower hemoglobin count (99.38 ± 24.06 vs. 129.64 ± 15.82, $P < 0.001$), and a higher serum level of D-dimer (3.31 ± 6.78 vs. 1.47 ± 2.65, $P = 0.001$), BUN (8.36 ± 6.05 vs. 5.58 ± 3.91, $P = 0.028$) and creatinine (116.69 ± 130.51 vs. 80.60 ± 56.34, $P = 0.038$). Moreover, history of diabetes, Killip level IV and chronic kidney disease (CKD) were also more common in the GIB group ($P < 0.05$).

Risk factors of AMI patients with in-hospital GIB

According to the analysis of differences in demographic and clinical characteristics between the GIB group and the control group, factors used to predict in-hospital GIB were identified as hemoglobin concentration, serum level of creatinine, BUN, D-dimer, and history of diabetes and Killip IV. All these factors were then assessed by multivariable regression analysis, and lower hemoglobin concentration was found to be an independent risk factor for in-hospital GIB following AMI (OR: 0.92, 95% CI: 0.89–0.96, $P < 0.001$; Table 3). The receiver operating characteristic (ROC) curve was plotted with hemoglobin concentration. The area under the curve was 0.86 (95% CI: 0.78–0.94, $P = 0.039$) with a sensitivity of 0.84 and a specificity of 0.80, indicating that hemoglobin had a high discriminative ability for in-hospital GIB after AMI (Figure 2).

Factors affecting in-hospital outcomes in AMI patients with in-hospital GIB

The in-hospital outcome of interest was all-cause death related or not related to in-hospital bleeding. Univariate and multivariate analyses were performed to evaluate the risk factors of outcomes, and the results are shown in Table 4. On the univariate analysis, a lower hemoglobin concentration (OR: 0.95, 95% CI: 0.90–1.00, $P = 0.049$), a higher BUN concentration (OR: 1.16, 95% CI: 1.01–1.33, $P = 0.030$) and Killip IV (OR: 13.67, 95% CI: 1.88–99.35, $P = 0.010$) were associated with the in-hospital death of AMI patients with GIB. After adjusted for confounding factors on the multivariable analysis, a lower hemoglobin concentration (OR: 0.93, 95% CI: 0.86–0.99, $P = 0.045$) and Killip IV (OR: 51.59, 95% CI: 2.65–1,005.30, $P = 0.009$) were found to independently associate with the in-hospital death of AMI patients with GIB.

Discussion

In this single center, retrospective analysis study, patients with AMI complicated with GIB were enrolled and analyzed. The independent risk factors for GIB in AMI patients during hospitalization included history of diabetes, heart failure (Killip IV) and poor renal function. Moreover, AMI patients with GIB had an increased risk of death compared to AMI patients without GIB, which was associated with a lower hemoglobin concentration and heart failure (Killip IV).

The incidence and mortality rates of GIB after AMI have progressively declined over the past decades (17). The patients enrolled in this study were from one of the most prestigious medical centers in Western China. In this study, among the AMI patients, the GIB prevalence was 0.87%, which was lower than that in previous investigations ranging from 1.1 to 3.0% (18). In the ACUITY (Acute Catheterization and Urgent Intervention Triage Strategy) trial, GIB served as the second major common source of non-coronary artery bypass graft (CABG)-related bleeding in the entire study population, which ranked only after access site bleeding (8). A temporal trend study for GIB indicated that despite aggressive treatment for ACS, the incidence of GIB associated with PCI decreased over a decade, which may explain the results in our research (19). In addition, Chinese physicians tend to prevent GIB by applying proton-pump inhibitors, which could also explain the reduced incidence of GIB.

Risk factors of gastrointestinal hemorrhage after AMI, such as older age, history of diabetes, high Killip classification and chronic renal insufficiency, have been documented (20–22). Our results demonstrated that the occurrence of GIB in patients with AMI was closely associated with history of diabetes, high Killip classification and chronic renal insufficiency. Moscucci et al. (23) conducted a large observational study in patients with AMI enrolled in the GRACE (Global Acute Coronary Events Registry) and observed that older age, female sex, history of bleeding, and renal insufficiency were independent predictors of major bleeding Sarajlic et al. (24) also found that blood glucose, smoking status, and previous GIB were predictors of major bleeding among 149,447 patients with AMI enrolled in the SWEDEHEART (Swedish Web-system for Enhancement and Development of Evidence-based care in Heart disease Evaluated According to Recommended Therapies) registry. Although most of these factors are immutable, their recognition allows for better risk stratification and more active management to reduce associated morbidity and mortality.

TABLE 1 Clinical characteristics of in-hospital GIB in AMI patients before and after PSM.

Characteristics	Before PSM ($N = 5,868$)				After PSM ($N = 100$)			
	GIB group ($N = 51$)	Control group ($N = 5,817$)	SMD	*P*-value	GIB group ($N = 50$)	Control group ($N = 50$)	SMD	*P*-value
Male (*n*, %)	44 (86.3)	4,677 (80.4)	0.158	0.381	43 (86.0)	41 (82.0)	0.109	0.785
Age (years)	67.67 ± 10.35	61.49 ± 12.15	0.547	<0.001	67.46 ± 10.35	63.36 ± 12.65	0.355	0.079
Myocardial infarction type (*n*, %)			0.310	0.031			0.206	0.412
STEMI	22 (43.1)	1,655 (28.5)			22 (44.0)	17 (34.0)		
NSTEMI	29 (56.9)	4,162 (71.5)			28 (56.0)	33 (66.0)		
Mean hospitalization time (days)	10.53 ± 12.07	5.69 ± 5.15	0.522	<0.001	9.84 ± 11.13	6.86 ± 9.07	0.294	0.145

GIB, gastrointestinal bleeding; AMI, acute myocardial infarction; PSM, propensity score matching; SMD, standardized mean difference; STEMI, ST-elevation myocardial infarction; NSTEMI, non-ST-segment elevation myocardial infarction.

TABLE 2 Differences in demographic and clinical characteristics of AMI patients with and without in-hospital GIB.

Patients	In total ($N = 100$)	GIB group ($N = 50$)	Control group ($N = 50$)	*P*-value
Smoker (*n*, %)	51 (56.7)	22 (53.7)	29 (59.2)	0.598
Drinker (*n*, %)	9 (9.2)	5 (10.2)	4 (8.2)	1.000
SBP (mmHg)	126.09 ± 27.27	127.24 ± 27.86	125.00 ± 26.95	0.432
DBP (mmHg)	77.61 ± 15.55	75.20 ± 15.18	79.88 ± 15.71	0.301
Blood biochemistry				
Hb (g/L)	114.51 ± 25.33	99.38 ± 24.06	129.64 ± 15.82	<0.001
WBC ($\times 10^9$/L)	8.08 ± 3.45	8.16 ± 3.25	8.00 ± 3.67	0.721
Platelet ($\times 10^9$/L)	212.55 ± 106.99	214.36 ± 123.28	210.74 ± 89.01	0.567
BUN (mmol/L)	6.94 ± 5.23	8.36 ± 6.05	5.58 ± 3.91	0.028
Creatinine (μmol/L)	98.28 ± 100.92	116.69 ± 130.51	80.60 ± 56.34	0.038
D-dimer (mg/L)	2.31 ± 5.03	3.31 ± 6.78	1.47 ± 2.65	0.001
Medications				
Aspirin (*n*, %)	79 (88.8)	34 (82.9)	45 (93.8)	0.177
P2Y12 inhibitors (*n*, %)	83 (93.3)	36 (87.8)	47 (97.9)	0.091
Anticoagulant (*n*, %)	36 (40.4)	11 (26.8)	25 (52.1)	0.016
PPI (*n*, %)	83 (93.3)	38 (92.7)	45 (93.8)	1.000
PCI (*n*, %)	66 (73.3)	23 (56.1)	43 (87.8)	0.001
Killip classification (*n*, %)				
I	62 (66.7)	25 (58.1)	37 (74.0)	0.115
II	17 (18.3)	8 (18.6)	9 (18.0)	1.000
III	5 (5.4)	3 (7.0)	2 (4.0)	1.000
IV	7 (7.5)	6 (14.0)	1 (2.0)	0.031
Comorbidities				
Hypertension (*n*, %)	48 (92.0)	23 (54.8)	25 (50.0)	0.649
Diabetes (*n*, %)	25 (25.0)	18 (36.0)	7 (14.0)	0.002
Stroke (*n*, %)	13 (14.1)	7 (16.7)	6 (12.0)	0.522
CKD (*n*, %)	9 (9.0)	8 (16.0)	1 (2.0)	0.010
Tumor (*n*, %)	9 (9.0)	5 (10.0)	4 (8.0)	0.727
Gensini score	62.50 ± 36.53	69.31 ± 42.25	58.48 ± 32.54	0.747
In-hospital death (*n*, %)	7 (7.8)	6 (14.3)	1 (2.1)	0.047

AMI, acute myocardial infarction; GIB, gastrointestinal bleeding; SBP, systolic blood pressure; DBP, diastolic blood pressure; Hb, hemoglobin; WBC, white blood cell; BUN, blood urea nitrogen; PPI, proton pump inhibitors; PCI, percutaneous coronary intervention; CKD, chronic kidney disease.

The mechanisms of in-hospital bleeding in patients with AMI are multifactorial. It has been assumed that the presence of local vascular changes is a common cause of the increased incidence of bleeding complications in elderly and diabetic patients (25). In addition, insufficient tissue perfusion adversely affects the coagulation system and platelet function, which may lead to gastritis or ulcers that increase the risk of upper gastrointestinal bleeding (23). Moreover, the "over-administration" effect, which results in high blood concentration, is the main mechanism of the increased risk of bleeding due to renal insufficiency (26). To reduce the risk of bleeding, all antithrombotic and antiplatelet drug agents should be administered in combination with renal function (27).

The outcomes of patients presenting with AMI have improved over time due to improvements in systems of care (e.g., symptom recognition, door-to-balloon time, etc.), advances in primary PCI techniques and their widespread adoption (28). However, in previous studies, gastrointestinal hemorrhage in AMI patients during hospitalization have been shown to be associated with increased short-and long-term mortality (17, 29). Our results supported this opinion. Patients with in-hospital GIB had a much higher in-hospital mortality rate than those without (2.1 vs. 14.3%). GIB complicating AMI leads to increased mortality, but there're still many unknowns about what and how factors affect the in-hospital outcomes of GIB. We sought to examine clinical and procedural factors associated with GIB. Compared with the survivors, patients who died in the hospital had a lower level of hemoglobin, a higher level of BUN, and a higher Killip classification.

TABLE 3 Logistic regression analysis of AMI patients with in-hospital GIB.

Characteristics	OR	95% CI	*P*-value
Hb	0.92	0.89–0.96	<0.001
Creatinine	1.00	0.99–1.01	0.453
BUN	0.99	0.83–1.17	0.877
D-dimer	1.08	0.96–1.22	0.212
Diabetes	4.10	0.92–18.15	0.063
Killip IV	12.57	0.62–255.99	0.100

OR, odd ratio; CI, confidence interval. Other abbreviations as in Table 2.

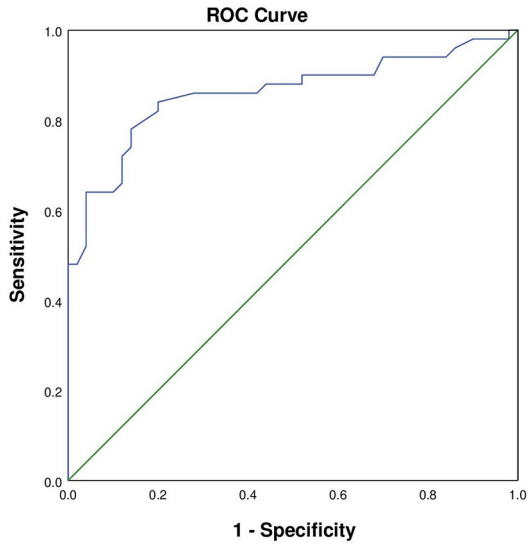

FIGURE 2
The ROC curve of AMI patients with in-hospital GIB. The area under the curve was 0.860 (95% CI: 0.78–0.94, $P = 0.039$). The sensitivity was 0.84 and the specificity was 0.80.

TABLE 4 Factors affecting in-hospital outcomes in AMI patients with in-hospital GIB.

Characteristics	Univariate model		Multivariate model	
	OR (95% CI)	*P*-value	OR (95% CI)	*P*-value
Age	1.04 (0.96–1.14)	0.352		
Hb	0.95 (0.90–1.00)	0.049	0.93 (0.86–0.99)	0.045
WBC	1.14 (0.89–1.47)	0.311		
Platelet	0.99 (0.98–1.00)	0.170		
BUN	1.16 (1.01–1.33)	0.030	1.08 (0.91–1.29)	0.372
Creatinine	1.00 (0.99–1.01)	0.741		
D-dimer	1.00 (0.86–1.16)	0.973		
Diabetes	4.29 (0.70–26.24)	0.115		
Killip IV	13.67 (1.88–99.35)	0.010	51.59 (2.65–1,005.301)	0.009
Hypertension	1.20 (0.22–6.61)	0.834		

Abbreviations as in Tables 2, 3.

Eikelboom et al. (30) found that the severity of GIB was associated with increased mortality. The mechanisms linking GIB with mortality are probably multifactorial. Massive GIB can lead to hemodynamic compromise, which results in death. While mild to moderate GIB can cause systemic inflammation with a prothrombic state, which in turn may lead to recurrent ischemic events. In addition to these direct effects, some indirect effects also affect the prognosis of AMI patients. For example, blood transfusion may increase oxidative stress and lead to a paradoxical decrease in oxygen delivery, all of which could contribute to worse outcomes (31). Moreover, even mild bleeding that does not require transfusion may lead to discontinuation of antithrombotic therapy, which indirectly affects prognosis.

Due to the widespread application of PCI and its clinical benefits over thrombolytic therapy, the majority of AMI patients admitted to our hospital have undergone PCI, excluding those who had economic difficulties. In this study, the use of anticoagulants and PCI treatment rates were significantly lower in patients with AMI combined GIB than those in the control group. This was due to the higher PCI risk and contraindications of anticoagulant therapy in AMI patients with GIB, which led to a statistical bias in this study.

There are some limitations that need to be noted. First, this was a single-center, retrospective study, and the cohort of patients was not large enough. A relatively small number of female AMI patients were enrolled in the present study. Second, the sample size in this study was relatively small because of the low incidence of GIB. Follow-up research based on a larger cohort is warranted to further explore the prognosis of and preventive factors associated with GIB.

Conclusion

In summary, in this single center, retrospective analysis, we identified that diabetes, heart failure (Killip IV) and poor renal function were associated with the risk of GIB. Moreover, AMI patients with GIB had a higher risk of all-cause death during hospitalization and a decreased hemoglobin concentration and heart failure were found to contribute to this increased mortality. The present study provides new evidence, allowing a better understanding of GIB and providing guidance for its clinical management.

Data availability statement

The raw data supporting the conclusions of this article will be made available by the authors, without undue reservation.

Ethics statement

The studies involving human participants were reviewed and approved by the Ethics Committee of the First Affiliated Hospital of Xi'an Jiaotong University (No. XJTU1AF2021LSK116). The patients/participants provided their written informed consent to participate in this study.

Author contributions

FG and HY designed and supervised the study. LZ, XQ, and MT wrote and revised the paper. PD collected the clinical data, obtained informed consent from the patients, and analyzed the data. All authors contributed to the article and approved the final version for submission.

Acknowledgments

We are grateful to the Biobank of The First Affiliated Hospital of Xi'an Jiaotong University for providing clinical data. We also thank Dr. Chaofeng Sun and Yang Yan in our department for critically reading and editing the manuscript.

Conflict of interest

The authors declare that the research was conducted in the absence of any commercial or financial relationships that could be construed as a potential conflict of interest.

Publisher's note

References

1. Zhang YM, Zhang ZY, Wang RX. Protective mechanisms of quercetin against myocardial ischemia reperfusion injury. *Front Physiol.* (2020) 11:956. doi: 10.3389/fphys.2020.00956

2. Seropian IM, Toldo S, Van Tassell BW, Abbate A. Anti-inflammatory strategies for ventricular remodeling following ST-segment elevation acute myocardial infarction. *J Am Coll Cardiol.* (2014) 63:1593–603. doi: 10.1016/j.jacc.2014.01.014

3. Krackhardt F, Waliszewski M, Kočka V, Toušek P, Janek B, Hudec M, et al. Real-world dual antiplatelet therapy following polymer-free sirolimus-eluting stent implantations to treat coronary artery disease. *Cardiovasc Drugs Ther.* (2020) 34:335–44. doi: 10.1007/s10557-020-06963-5

4. Saito Y, Kobayashi Y. Update on antithrombotic therapy after percutaneous coronary intervention. *Intern Med.* (2020) 59:311–21. doi: 10.2169/internalmedicine.3685-19

5. Davidson SM, Ferdinandy P, Andreadou I, Bøtker HE, Heusch G, Ibáñez B, et al. Multitarget strategies to reduce myocardial ischemia/reperfusion injury: JACC review topic of the week. *J Am Coll Cardiol.* (2019) 73:89–99. doi: 10.1016/j.jacc.2018.09.086

6. Tersalvi G, Biasco L, Cioffi GM, Pedrazzini G. Acute coronary syndrome, antiplatelet therapy, and bleeding: a clinical perspective. *J Clin Med.* (2020) 9:2064. doi: 10.3390/jcm9072064

7. Wolska N, Rozalski M. Blood platelet adenosine receptors as potential targets for anti-platelet therapy. *Int J Mol Sci.* (2019) 20:5475. doi: 10.3390/ijms20215475

8. Costa F, Tijssen JG, Ariotti S, Giatti S, Moscarella E, Guastaroba P, et al. Incremental value of the CRUSADE, ACUITY, and HAS-BLED risk scores for the prediction of hemorrhagic events after coronary stent implantation in patients undergoing long or short duration of dual antiplatelet therapy. *J Am Heart Assoc.* (2015) 4:e002524. doi: 10.1161/JAHA.115.002524

9. Secemsky EA, Butala NM, Kartoun U, Mahmood S, Wasfy JH, Kennedy KF, et al. Use of chronic oral anticoagulation and associated outcomes among patients undergoing percutaneous coronary intervention. *J Am Heart Assoc.* (2016) 5:e004310. doi: 10.1161/JAHA.116.004310

10. Cantor WJ, Mehta SR, Yuan F, DŽavík V, Worthley M, Niemelä K, et al. Radial versus femoral access for elderly patients with acute coronary syndrome undergoing coronary angiography and intervention: insights from the RIVAL trial. *Am Heart J.* (2015) 170:880–6. doi: 10.1016/j.ahj.2015.08.011

11. Rao SV, Dai D, Subherwal S, Weintraub WS, Brindis RS, Messenger JC, et al. Association between periprocedural bleeding and long-term outcomes following percutaneous coronary intervention in older patients. *JACC Cardiovasc Interv.* (2012) 5:958–65. doi: 10.1016/j.jcin.2012.05.010

12. Kosmidou I, Mintz GS, Jatene T, Embacher M, Redfors B, Wong SC, et al. Impact of bleeding assessment and adjudication methodology on event rates and clinical trial outcomes: insights from the HORIZONS-AMI trial. *EuroIntervention.* (2018) 14:e580–7. doi: 10.4244/EIJ-D-18-00131

13. Reilev M, Damkier P, Rasmussen L, Olesen M, Thomsen Ernst M, Rishøj RM, et al. Use of beta-blockers and risk of serious upper gastrointestinal bleeding: a population-based case-control study. *Therap Adv Gastroenterol.* (2017) 10:919–29. doi: 10.1177/1756283X17734116

14. Levine GN, Bates ER, Bittl JA, Brindis RG, Fihn SD, Fleisher LA, et al. 2016 ACC/AHA guideline focused update on duration of dual antiplatelet therapy in patients with coronary artery disease: a report of the American college of cardiology/American heart association task force on clinical practice guidelines: an update of the 2011 ACCF/AHA/SCAI guideline for percutaneous coronary intervention, 2011 ACCF/AHA guideline for coronary artery bypass graft surgery, 2012 ACC/AHA/ACP/AATS/PCNA/SCAI/STS guideline for the diagnosis and management of patients with stable ischemic heart disease, 2013 ACCF/AHA guideline for the management of ST-elevation myocardial infarction, 2014 AHA/ACC guideline for the management of patients with non-ST-elevation acute coronary syndromes, and 2014 ACC/AHA guideline on perioperative cardiovascular evaluation and management of patients undergoing noncardiac surgery. *Circulation.* (2016) 134:e123–55. doi: 10.1161/CIR.0000000000000404

15. Sehested TSG, Carlson N, Hansen PW, Gerds TA, Charlot MG, Torp-Pedersen C, et al. Reduced risk of gastrointestinal bleeding associated with proton pump inhibitor therapy in patients treated with dual antiplatelet therapy after myocardial infarction. *Eur Heart J.* (2019) 40:1963–70. doi: 10.1093/eurheartj/ehz104

16. Gensini GG. A more meaningful scoring system for determining the severity of coronary heart disease. *Am J Cardiol.* (1983) 51:606. doi: 10.1016/S0002-9149(83)80105-2

17. Albeiruti R, Chaudhary F, Alqahtani F, Kupec J, Balla S, Alkhouli M. Incidence, predictors, and outcomes of gastrointestinal bleeding in patients admitted with ST-elevation myocardial infarction. *Am J Cardiol.* (2019) 124:343–8. doi: 10.1016/j.amjcard.2019.05.008

18. Nikolsky E, Stone GW, Kirtane AJ, Dangas GD, Lansky AJ, McLaurin B, et al. Gastrointestinal bleeding in patients with acute coronary syndromes: incidence, predictors, and clinical implications: analysis from the ACUITY (acute catheterization and urgent intervention triage strategy) trial. *J Am Coll Cardiol.* (2009) 54:1293–302. doi: 10.1016/j.jacc.2009.07.019

19. Shivaraju A, Patel V, Fonarow GC, Xie H, Shroff AR, Vidovich MI. Temporal trends in gastrointestinal bleeding associated with percutaneous coronary intervention: analysis of the 1998–2006 nationwide inpatient sample (NIS) database. *Am Heart J.* (2011) 162:1062–1068.e5. doi: 10.1016/j.ahj.2011.09.009

20. Gupta K, Khan A, Kumar M, Sawalha K, Abozenah M, Singhania R. Readmissions rates after myocardial infarction for gastrointestinal bleeding: a national perspective. *Dig Dis Sci.* (2021) 66:751–9. doi: 10.1007/s10620-020-06315-1

21. Wu CJ, Lin HJ, Weng SF, Hsu CC, Wang JJ, Su SB, et al. Acute myocardial infarction risk in patients with coronary artery disease doubled after upper gastrointestinal tract bleeding: a nationwide nested case-control study. *PLoS ONE.* (2015) 10:e0142000. doi: 10.1371/journal.pone.0142000

22. Hoedemaker NPG, Damman P, Ottervanger JP, Dambrink JHE, Gosselink ATM, Kedhi E, et al. Trends in cardiovascular and bleeding outcomes in acute coronary syndrome patients treated with or without proton-pump inhibitors during the introduction of novel P2Y12 inhibitors: a 5-year experience from a single-centre observational registry. *Eur Heart J Cardiovasc Pharmacother.* (2019) 5:127–38. doi: 10.1093/ehjcvp/pvy030

23. Moscucci M, Fox KA, Cannon CP, Klein W, López-Sendón J, Montalescot G, et al. Predictors of major bleeding in acute coronary syndromes: the global registry of acute coronary events (GRACE). *Eur Heart J.* (2003) 24:1815–23. doi: 10.1016/S0195-668X(03)00485-8

24. Sarajlic P, Simonsson M, Jernberg T, Back M, Hofmann R. Incidence, associated outcomes, and predictors of upper gastrointestinal bleeding following acute myocardial infarction: a SWEDEHEART-based nationwide cohort study. *Eur Heart J Cardiovasc Pharmacother.* (2022) 8:483–91. doi: 10.1093/ehjcvp/pvab059

25. Matić DM, Ašanin MR, Stanković S, Mrdović IB, Marinković JM, Kočev NI, et al. Incidence, predictors and prognostic implications of bleeding complicating primary percutaneous coronary intervention. *Vojnosanit Pregl.* (2015) 72:589–95. doi: 10.2298/VSP140223064M

26. Becattini C, Giustozzi M, Ranalli MG, Bogliari G, Cianella F, Verso M, et al. Variation of renal function over time is associated with major bleeding in patients treated with direct oral anticoagulants for atrial fibrillation. *J Thromb Haemost.* (2018) 16:833–41. doi: 10.1111/jth.13985

27. Cavender MA, Rao SV. Bleeding associated with current therapies for acute coronary syndrome: what are the mechanisms? *J Thromb Thrombolysis.* (2010) 30:332–9. doi: 10.1007/s11239-010-0487-z

28. Szummer K, Wallentin L, Lindhagen L, Alfredsson J, Erlinge D, Held C, et al. Improved outcomes in patients with ST-elevation myocardial infarction during the last 20 years are related to implementation of evidence-based treatments: experiences from the SWEDEHEART registry 1995–2014. *Eur Heart J.* (2017) 38:3056–65. doi: 10.1093/eurheartj/ehx515

29. Ndrepepa G, Berger PB, Mehilli J, Seyfarth M, Neumann FJ, Schömig A, et al. Periprocedural bleeding and 1-year outcome after percutaneous coronary interventions: appropriateness of including bleeding as a component of a quadruple end point. *J Am Coll Cardiol.* (2008) 51:690–7. doi: 10.1016/j.jacc.2007.10.040

30. Eikelboom JW, Mehta SR, Anand SS, Xie C, Fox KA, Yusuf S. Adverse impact of bleeding on prognosis in patients with acute coronary syndromes. *Circulation.* (2006) 114:774–82. doi: 10.1161/CIRCULATIONAHA.106.612812

31. Al-Mallah M, Bazari RN, Jankowski M, Hudson MP. Predictors and outcomes associated with gastrointestinal bleeding in patients with acute coronary syndromes. *J Thromb Thrombolysis.* (2007) 23:51–5. doi: 10.1007/s11239-006-9005-8

frontiers | Frontiers in Cardiovascular Medicine

TYPE Original Research
PUBLISHED 29 September 2022
DOI 10.3389/fcvm.2022.907997

OPEN ACCESS

EDITED BY
Aggeliki Gkouziouta,
Onassis Cardiac Surgery Center, Greece

REVIEWED BY
Zeneng Wang,
Cleveland Clinic, United States
Fabiana Lucà,
Grande Ospedale Metropolitano Bianchi Melacrino Morelli, Italy

*CORRESPONDENCE
Qin Fan
fanqin125@163.com
Rong Tao
rongtao@hotmail.com

†These authors have contributed equally to this work

SPECIALTY SECTION
This article was submitted to Heart Failure and Transplantation, a section of the journal Frontiers in Cardiovascular Medicine

RECEIVED 30 March 2022
ACCEPTED 14 September 2022
PUBLISHED 29 September 2022

CITATION
Zong X, Fan Q, Yang Q, Pan R, Zhuang L, Xi R, Zhang R and Tao R (2022) Trimethyllysine, a trimethylamine N-oxide precursor, predicts the presence, severity, and prognosis of heart failure. *Front. Cardiovasc. Med.* 9:907997. doi: 10.3389/fcvm.2022.907997

Trimethyllysine, a trimethylamine N-oxide precursor, predicts the presence, severity, and prognosis of heart failure

Xiao Zong[1,2†], Qin Fan[1*†], Qian Yang[1,2†], Roubai Pan[1], Lingfang Zhuang[1,2], Rui Xi[1], Ruiyan Zhang[1] and Rong Tao[1*]

[1]Department of Cardiovascular Medicine, Ruijin Hospital, Shanghai Jiao Tong University School of Medicine, Shanghai, China, [2]Shanghai Jiao Tong University School of Medicine, Institution of Cardiovascular Diseases, Shanghai, China

Background and aims: Intestinal flora metabolites are associated with cardiovascular (CV) diseases including heart failure (HF). The carnitine precursor trimethyllysine (TML), which participates in the generation of the atherogenic-related metabolite trimethylamine N-oxide (TMAO), was found to be related to poor prognosis in patients with CV diseases. The aim of the present study was to examine the relationship between TML and stable chronic HF.

Methods and results: In total, 956 subjects including 471 stable chronic HF and 485 non-HF patients were enrolled in the present cohort study and subjects with stable HF were followed up for 2.0 ± 1.1 years. Serum levels of TML and TMAO were measured by liquid chromatography mass spectrometry in tandem. TML levels were significantly elevated in patients with HF compared with non-HF patients and were positively correlated with N-terminal pro-brain natriuretic peptide (NTproBNP) levels (r = 0.448, $P < 0.001$). TML was associated with the presence of HF after adjusting for age, sex, complications, traditional clinical factors, and TMAO (tertile 3 (T3), adjusted odds ratio (OR) 1.93, 95% confidence interval (CI) 1.19–3.13, and P = 0.007). In patients with HF, increased TML levels were associated with a composite endpoint of CV death and HF hospitalization during follow-up (T3, adjusted hazard ratio (HR) 1.93, 95% CI 1.27–2.93, and P = 0.002). Increased TML levels indicated a higher risk of CV death, re-hospitalization, and all-cause mortality.

Conclusion: Serum TML levels were associated with the presence and severity of HF in all subjects. High levels of TML can indicate complications and poor prognosis in HF patients.

KEYWORDS

trimethyllysine, heart failure, prognosis, gut microbiota, metabolite

Introduction

Heart failure (HF) is a complex clinical syndrome that results from any structural or functional impairment of ventricular filling or ejection of blood (1). Intestinal flora can serve as an endocrine organ that contributes to the pathogenesis of HF through its metabolites (2–4). In particular, trimethylamine N-oxide (TMAO), which is an intestine-derived metabolite of the choline/carnitine metabolic pathway, has been proven to be a metabolite potentially linking intestinal flora to cardiovascular (CV) disease (5, 6). Recent studies have also found that increased TMAO levels can predict poor prognosis in patients with both acute (6) and chronic HF (7, 8).

However, nowadays the exploration between intestinal flora metabolites and HF mainly concentrated on TMAO. Within the TMAO-related intestinal flora pathway, other metabolites also showed significant association with CV risk and CV diseases, including trimethyllysine (TML) (9, 10).

The amino acid TML, which is introduced by various animal- and plant-derived dietary sources, can work as a precursor for intestinal flora-dependent generation of TMAO (11) as well as a regulator of carnitine biosynthesis (12). Since increased TML levels were determined to be related to higher CV risk in subjects who were taken cardiac risk evaluation (11), several studies have probed into the association between TML and CV diseases. TML was found to be related to an increased risk of mortality in patients with evidence of carotid artery atherosclerosis in one small study (9). It is associated with the progression of atherosclerosis (13) and is involved a variety of different pathways potentially leading to atherogenesis (14). TML could also independently predict the risk of acute myocardial infarction among patients with suspected angina pectoris (15), and predict adverse CV prognosis among patients presenting with acute coronary syndrome (10). Recent research found a relationship between TML and the risk of mortality in subjects with acute HF (16); however, at present, whether serum TML levels are associated with disease severity in stable chronic HF has not been well discovered.

Therefore, the present study was to examine the relationship between systemic TML levels and the presence as well as prognosis of patients with stable chronic HF.

Materials and methods

Study population

The present study was a prospective cohort study designed to investigate the intestinal microbiota metabolite levels in patients with HF. A total of 956 including 471 stable chronic HF and 485 non-HF patients hospitalized in the Department of Cardiovascular Medicine, Ruijin Hospital, were included consecutively. Patients with severe concomitant diseases, such as infections, connective tissue diseases, autoimmune diseases, malignancies, and gastrointestinal disorders were excluded. Patients with acute myocardial infarction and cerebrovascular events during the last 6 months were also excluded. However, no information was available from patients with the probability of excessive intake of antioxidants, vitamins, micronutrients, or fish oils. The study was conducted in accordance with the Declaration of Helsinki and was approved by the Ethics Committee of Ruijin Hospital, Ethics Committee reference number: 2016-019. All patients were explained about the study and provided informed consent before enrollment.

Follow-up and outcomes

The present study included the primary outcome and three secondary outcomes. A composite endpoint including CV death and first re-hospitalization because of HF was defined as the primary outcome. The secondary outcomes consisted of CV death, hospitalization due to HF, and all-cause mortality. Follow-up survey was conducted by hospital visits or through telephone. All endpoints were confirmed by independent cardiologists intensively. Recurrent HF was diagnosed on account of signs and symptoms, abnormal laboratory parameters, as well as imageological examination.

Detection of trimethyllysine and trimethylamine N-oxide

Fasting serum blood samples were collected and frozen at −80°C until analysis to avoid oxidation or modification. None of the participants performed any exercise prior to blood collection. Levels of TML and TMAO in serum were detected by liquid chromatography-mass spectrometry (LC-MS). Isotopically labeled TML-d9 (sc-475693, Santa Cruz Biotechnology, Santa Cruz, CA, USA) and TMAO-d9 (sc-475042, Santa Cruz Biotechnology, Santa Cruz, CA, USA) were used as internal standards. 150 μl of TML-d9 (20 μg/ml, dissolved in ultrapure water) and 500 μl of TMAO-d9 (1 ug/ml, dissolved in ultrapure water) were added to 200 ml of pure methanol, then vortexed and mixed to obtain the internal standard dilution working solution (ISWS). 50 μl of serum sample was placed in a 96-well plate, and 400 μl of ISWS was added to each sample, vortexed and mixed for 15 min, followed by centrifugation at 3,000 g for 15 min at 4°C. 150 μl supernatant was then transferred to the 96-well plate and tested on the machine.

Samples were separated on a 1.7 μm (2.1 × 50 mm) column (ACQUITY UPLC BEH Amide, Waters, Milford, MA, USA) through the high-performance liquid chromatography (UltiMate 3000, Dionex, Sunnyvale, CA, USA) using an elution gradient of two mobile phases (A) 10 mM ammonium acetate 0.1% formic acid and (B) 10 mM ammonium acetate 95% acetonitrile 0.1% formic acid. Quantification was

performed with a triple quadrupole mass spectrometry (TSQ Vantage, Thermo Scientific, Waltham, MA, USA) with positive electrospray ionization in the multiple reaction monitoring mode where the precursor ion (parent ion) of the target substance was first screened by the quadrupole and the fragment ions of the precursor ion were filtered through QQQ to select a desired characteristic fragment ion for quantification. The retention times of TML and TMAO were 2.54 and 1.5 min, respectively. The MRM-transitions monitored were for TML m/z 189 > 84, for TML-d9 m/z 198 > 84, for TMAO m/z 76 > 58, and for TMAO-d9 m/z 85 > 66. The peak area of each analyte was corrected by the peak area of the internal standards compound, and the concentrations of TML and TMAO in the serum sample were calculated semi-quantitatively by the ratio of the peak area of each analyte to the internal standards compound, and further quantified according to the standard concentration.

The same volume of serum was drawn from each sample, pooled and mixed, which is the quality control (QC) sample. During the testing process, every 12 samples were followed by a QC sample. The samples and the machine can be considered stable if the relative standard deviation (RSD) of QC samples were below 15%. And the RSD of TMAO and TML in the QC sample was 6.51 and 3.71%, respectively.

Echocardiographic measurements

Echocardiography was conducted by experienced cardiac sonographers and analyzed by independent cardiologists. M-mode echocardiography was used to assess left atrial diameter (LAD), left ventricular end diastolic diameter (LVEDD), and left ventricular end systolic diameter (LVESD). And the biplanar Simpson's method was performed to determine the cardiac function as measured by left ventricular ejection fraction (LVEF).

Statistical analyses

Continuous variables were shown as mean ± standard deviation (SD), and expressed per SD for regression. Log transformation was performed before analysis if it was not normally distributed. The comparison between two groups was conducted by unpaired *t*-test, while trends over tertiles were tested by one-way ANOVA analysis. Categorical variables are presented as counts (%) and significant differences between groups were determined using the chi-square test or Fisher's exact test.

Simple correlation analyses were performed to investigate the relationship between TML and different clinical features. Logistic regression models were used to determine the association between TML and the presence of HF. Odds ratios (ORs) with 95% CIs for HF were obtained for both univariable and multivariable analyses. The adjusted model 1 consisted of both age and sex. The full adjustment model 2 contained age, sex, body mass index (BMI), hypertension, diabetes mellitus (DM), hemoglobin, albumin, creatinine, glycosylated hemoglobin, low-density lipoprotein cholesterol, high-sensitivity C-reactive protein (hsCRP), and TMAO.

For follow-up data, the relationship between TML (as shown by tertiles) and the primary endpoint and secondary endpoints were visualized using Kaplan–Meier plots and assessed by log-rank tests. Cox regression models in univariate, model 1 (age and sex) adjusted, and model 2 adjusted analyses were performed to calculate hazard ratios (HRs) and 95% CIs. In regression analyses, results were presented according to per 1 SD increment of log-transformed TML concentrations and the 3rd versus 1st tertile. Patients who were lost during follow-up were analyzed according to the censored data. Statistical analyses were performed using SPSS version 22.0 software, and the two-sided P-value < 0.05 was defined as statistically significant.

Results

Baseline characteristics

A total of 956 subjects participated in the present study including 471 stable chronic HF and 485 non-HF patients. In all subjects, the average age was 61.4 ± 10.9 years, 62.8% were men, 55.4% had hypertension, 25.1% had DM, 15.4% had dyslipidemia, and 16.0% had renal dysfunction.

Baseline demographic, clinical, and laboratory characteristics of all participants was shown in **Table 1** (grouped by TML tertile) and **Supplementary Table 1** (grouped by HF or non-HF). Patients in the higher TML level group were more possible to have complicating diseases such as hypertension, DM, and renal dysfunction. There was a positive association between incremental TML levels and the increase in HbA1c, creatinine, uric acid, hsCRP, and N-terminal pro-brain natriuretic peptide (NTproBNP). Patients with higher TML levels had lower albumin levels as well as estimated glomerular filtration rates (eGFR). TML serum concentrations were also significantly correlated with TMAO levels ($r = 0.395$, $P < 0.001$).

Trimethyllysine levels were associated with the presence and severity of heart failure

Initial examination of the distribution of TML levels showed remarkably higher TML levels (0.9 ± 0.5 vs. 0.6 ± 0.3 μM, $P < 0.001$) among subjects with HF (**Figure 1A**). TML concentrations were significantly correlated to NTproBNP levels ($r = 0.448$, $P < 0.001$, **Figure 1B**), LAD ($r = 0.322$,

TABLE 1 Baseline characteristics of all subjects.

	TML < 0.54 μM (n = 318)	0.54 μM ≤ TML < 0.75 μM (n = 319)	TML ≥ 0.75 μM (n = 319)	P-value
Demographic characteristics				
Age (years)	60.1 ± 9.5	61.3 ± 11.7	62.7 ± 11.4	0.014
Male	135 (42.5)	226 (70.8)	239 (74.9)	<0.001
Current smoking	65 (20.4)	115 (36.1)	134 (42.0)	<0.001
Current drinking	57 (17.9)	77 (24.1)	77 (24.1)	0.092
Body mass index (kg/m^2)	24.4 ± 3.3	25.2 ± 3.7	24.9 ± 3.8	0.015
Systolic blood pressure (mmHg)	132.3 ± 18.7	130.3 ± 20.2	131.1 ± 20.6	0.435
Diastolic blood pressure (mmHg)	76.6 ± 11.4	76.0 ± 13.4	76.2 ± 13.2	0.802
Heart rate (beats/min)	78.7 ± 11.2	79.9 ± 13.4	79.8 ± 15.2	0.438
Family history	37 (11.6)	50 (15.7)	51 (16.0)	0.219
Medical history				
Hypertension	150 (47.2)	177 (55.5)	203 (63.6)	<0.001
Diabetes mellitus	58 (18.2)	88 (27.6)	94 (29.5)	0.002
Dyslipidemia	47 (14.8)	50 (15.7)	50 (15.7)	0.937
Renal dysfunction	8 (2.5)	44 (13.8)	101 (31.7)	<0.001
Stroke	24 (7.5)	16 (5.0)	44 (13.8)	<0.001
Lab. examination				
WBC (*10^9/L)	6.1 ± 1.9	6.5 ± 2.0	6.7 ± 2.0	0.001
Hemoglobin (g/L)	135.7 ± 13.8	138.3 ± 15.7	135.7 ± 20.3	0.069
Platelet (*10^9/L)	191.5 ± 52.9	182.7 ± 50.6	181.5 ± 54.9	0.034
HbA1c (%)	6.0 ± 1.0	6.2 ± 1.1	6.3 ± 1.1	0.005
ALT (IU/L)	30.5 ± 86.1	33.0 ± 55.6	31.5 ± 40.7	0.883
Albumin (g/L)	39.6 ± 3.6	38.6 ± 3.7	38.0 ± 4.7	<0.001
Creatinine (μmol/L)	69.6 ± 14.2	82.2 ± 27.3	118.3 ± 120.5	<0.001
Uric acid (μmol/L)	322.7 ± 90.4	373.4 ± 110.2	403.3 ± 124.9	<0.001
eGFR (ml/min/1.73 m^2)	88.2 ± 16.5	81.3 ± 18.8	68.9 ± 24.5	<0.001
Triglyceride (mmol/L)	1.5 ± 0.9	1.6 ± 1.0	1.6 ± 1.3	0.341
Total cholesterol (mmol/L)	4.4 ± 1.8	4.1 ± 1.1	4.1 ± 1.5	0.021
LDL-C (mmol/L)	2.5 ± 0.9	2.5 ± 1.0	2.4 ± 0.9	0.207
HDL-C (mmol/L)	1.2 ± 0.3	1.1 ± 0.3	1.1 ± 0.3	<0.001
Tropnin I (ng/ml)	0.6 ± 4.2	1.0 ± 6.3	1.5 ± 8.5	0.228
hsCRP (mg/L)	3.7 ± 11.4	5.6 ± 16.5	10.2 ± 28.3	0.001
NTproBNP (pg/ml)	528.8 ± 1232.8	1358.7 ± 3282.8	3732.3 ± 7777.7	<0.001
D-dimer (mg/L)	0.5 ± 1.4	0.6 ± 1.4	0.7 ± 1.1	0.161
TMAO (μM)	0.9 ± 1.0	1.2 ± 1.5	2.2 ± 4.1	<0.001
LAD (mm)	37.8 ± 6.2	40.9 ± 6.8	42.9 ± 7.0	<0.001
LVEDD (mm)	50.6 ± 8.1	54.9 ± 9.8	58.0 ± 9.5	<0.001
LVESD (mm)	34.5 ± 10.3	39.9 ± 12.0	43.6 ± 12.1	<0.001
LVEF (%)	59.1 ± 14.8	51.9 ± 16.7	46.4 ± 16.4	<0.001
Medications				
ACEI/ARB/ARNI	128 (40.3)	186 (58.3)	212 (66.5)	<0.001
β-blocker	169 (53.1)	207 (64.9)	224 (70.2)	<0.001
Spironolactone	42 (13.2)	94 (29.5)	132 (41.4)	<0.001
Statins	224 (70.4)	248 (77.7)	239 (74.9)	0.104
Hypoglycemic drugs	47 (14.8)	69 (21.6)	69 (21.6)	0.041

ACEI, angiotensin-converting enzyme inhibitor; ALT, alanine transaminase; ARB, angiotensin receptor blocker; ARNI, angiotensin receptor enkephalin inhibitor; eGFR, estimated glomerular filtration rates; HbA1c, glycosylated hemoglobin; HDL-C, high-density lipoprotein cholesterol; hsCRP, high sensitivity C reactive protein; LAD, left atrial diameter; LDL-C, low-density lipoprotein cholesterol; LVEDD, left ventricular end diastolic diameter; LVEF, left ventricular ejection fraction; LVESD, left ventricular end systolic diameter; NTproBNP, N-terminal pro-brain natriuretic peptide; TMAO, trimethylamino oxide; TML, trimethyllysine; WBC, white blood cells.
*Means multiply.

P < 0.001), LVEDD (r = 0.361, P < 0.001), and LVESD (r = 0.323, P < 0.001), and negatively associated with LVEF (r = –0.324, P < 0.001).

Patients belonging to the highest tertile of TML concentrations had a significantly higher risk of HF compared with participants in the lowest tertile (Table 2). After adjusting for age, sex, BMI, hypertension, DM, hemoglobin, albumin, creatinine, LDL, HbA1c, hsCRP, and TMAO, increased TML levels remained associated with significantly increased odds for HF (tertile 3 (T3) vs. tertile 1, OR: 1.93, 95% CI: 1.19–3.13, P = 0.007). As a continuous variable, TML levels could also predict the presence of HF at baseline after full adjustment

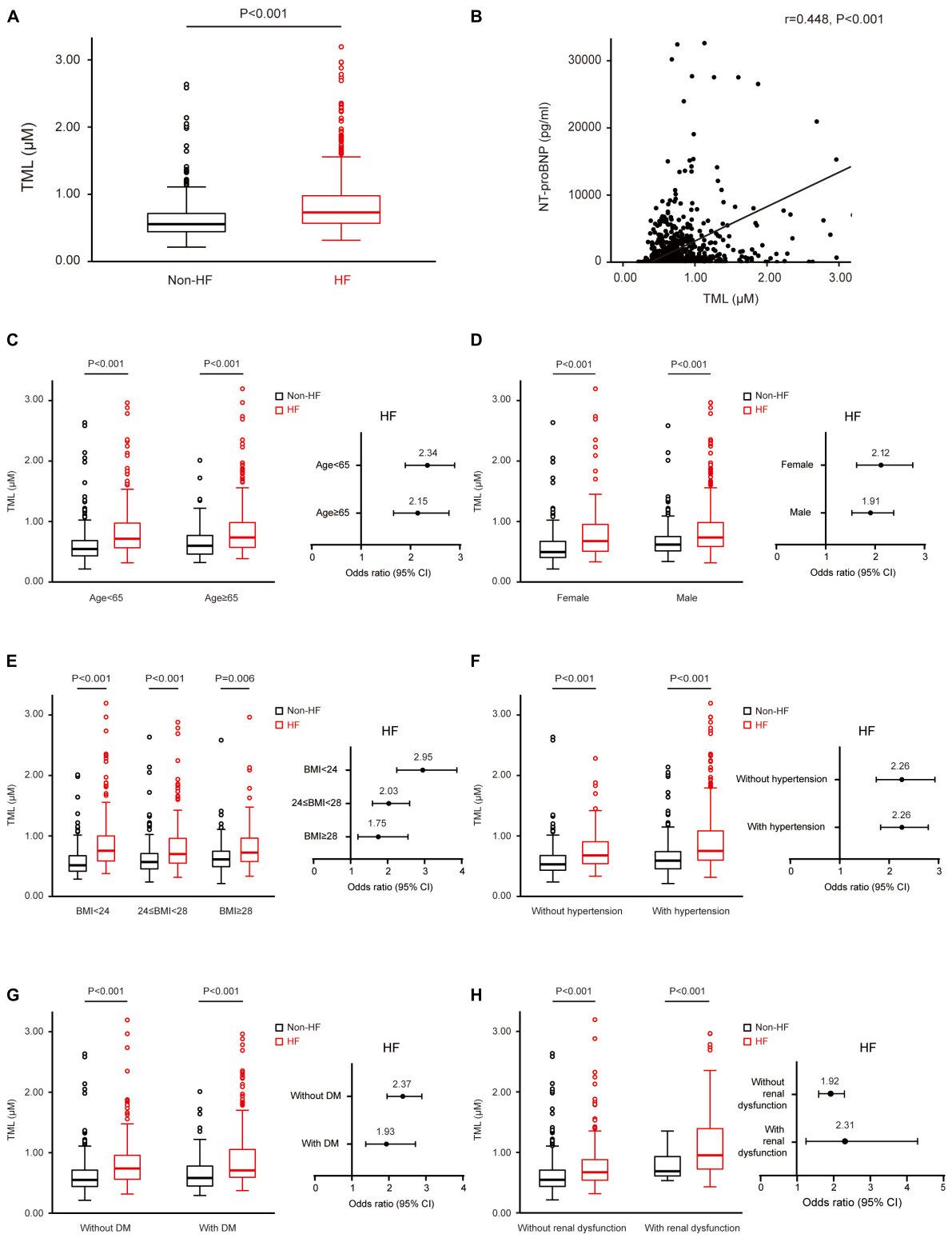

FIGURE 1
Trimethyllysine (TML) levels are associated with the presence and severity of heart failure (HF) in all subjects and different subgroups. **(A)** TML levels are increased in patients with HF compared with the non-HF group in all subjects at baseline. **(B)** Simple correlation analysis between serum levels of TML and N-terminal pro-brain natriuretic peptide (NTproBNP). Box–Whisker plots of TML levels among patients with and without HF in different subgroups, including ages <65 and ≥65 **(C)**; male and female **(D)**; normal, overweight, and obesity **(E)**; with and without hypertension **(F)**; with and without DM **(G)**; as well as with and without dyslipidemia **(H)**. Forest plots illustrate the odds of the presence of HF according to TML levels in these subgroups **(C–G)**. Symbols represent odds ratios (ORs) and the 95% confidence intervals are shown by line length.

TABLE 2 Trimethyllysine (TML) was associated with the presence of heart failure (HF) in all subjects.

	Unadjusted OR	*P*-value	Adjusted for model 1 OR	*P*-value	Adjusted for model 2 OR	*P*-value
log TML per SD	2.31 (1.96–2.72)	<0.001	1.93 (1.63–2.29)	<0.001	1.28 (1.02–1.61)	0.037
TML tertiles	2.32 (1.96–2.75)	<0.001	1.88 (1.56–2.27)	<0.001	1.39 (1.10–1.77)	0.007
Tertile 1	1 (ref)		1 (ref)		1 (ref)	
Tertile 2	2.57 (1.86–3.57)	<0.001	1.68 (1.17–2.42)	0.005	1.25 (0.79–1.96)	0.344
Tertile 3	5.38 (3.84–7.56)	<0.001	3.53 (2.44–5.11)	<0.001	1.93 (1.19–3.13)	0.007

OR, odds ratio; SD, standard deviation; TML, trimethyllysine. Model 1: adjusted for age and sex. Model 2: adjusted for age, sex, body mass index (BMI), hypertension, diabetes mellitus (DM), hemoglobin, albumin, creatinine, low-density lipoprotein cholesterol, glycosylated hemoglobin, high sensitivity C reactive protein (hsCRP), and trimethylamino oxide.

(per 1 SD, OR: 1.28, 95% CI: 1.02–1.61, $P = 0.037$) (Table 2). The receiver operating characteristic (ROC) curve of TML in predicting HF was 0.71 (0.67–0.74, $P < 0.01$), and the predictive cut-off value of TML was 0.7 μM.

Trimethyllysine levels could predict the presence of heart failure in different subgroups

We also analyzed age- and sex-specific associations of circulating TML concentrations with the presence of HF. In both patients aged <65 and ≥65 years, those with HF had higher levels of TML, and TML could predict HF in both groups (Figure 1C). Increased TML levels were correlated with elevated odds of HF more remarkably in women than in men (Figure 1D). TML was more significantly correlated with HF in subjects with normal weight than in those who were overweight or obese (Figure 1E). Moreover, subgroup analyses demonstrated that increased TML levels could predict the presence of HF among patients with or without a history of hypertension, DM, and renal dysfunction, respectively, more remarkably in those without DM and in those with renal dysfunction (Figures 1F–H).

Trimethyllysine levels were associated with the complications and poor prognosis in patients with heart failure

Among all subjects, 471 were diagnosed with stable systolic HF. TML levels were higher among those with hypertension, DM, renal dysfunction, and stroke in the HF patients. TML was also associated with the presence of these complications after adjustment (Figure 2).

During a mean follow-up of 2.0 ± 1.1 years, outcomes consisted of all-cause mortality in 66 patients (14.0%) including CV death in 57 patients (12.1%), re-admission because of HF in 111 patients (23.6%), and the composite primary endpoint in 154 patients (32.7%). Therefore, we first investigated the association between TML levels and primary as well as secondary outcomes in patients with HF.

Patients who experienced the primary endpoint were more likely to have higher serum TML levels at presentation (1.0 ± 0.7 vs. 0.8 ± 0.4 μM, $P = 0.004$). Kaplan–Meier analyses and survival curves illustrated enhanced rates of the primary endpoint with elevating TML levels (log-rank $P < 0.001$, Figure 3A). Similarly, patients in the higher TML level group had a higher risk of experiencing CV death, HF re-admission, and all-cause mortality during follow-up (Figures 3B–D).

Following multivariable cox regression analyses adjusting for conventional risk factors including age, sex, BMI, hypertension, DM, hemoglobin, albumin, creatinine, LDL, HbA1c, and TMAO, elevated (tertile 3 vs. tertile 1) serum TML remained independently correlated to increased risk of the primary endpoint (HR: 1.93, 95% CI: 1.27–2.93, $P = 0.002$) (Table 3). Furthermore, patients in the highest tertile of TML levels demonstrated a significantly elevated risk of CV death (HR: 3.96, 95% CI: 1.80–8.72, $P = 0.001$), HF hospitalization (HR: 1.75, 95% CI: 1.09–2.80, $P = 0.019$), and all-cause mortality (HR: 3.34, 95% CI: 1.68–6.64, $P = 0.001$), compared with those in the lowest tertile after full adjustment (Table 3). TML concentrations could also predict the primary endpoint in HF patients belonging to different subgroups (Figure 3E).

Discussion

The present study probed into the potential impact of TML on the presence and prognosis of HF. The major findings are as follows: First, patients with HF had significantly increased serum levels of TML compared with those without HF. Second, higher serum TML concentrations are independently associated with HF. Higher TML levels could also significantly predict the complications and poor prognosis in patients with HF, including CV death and HF re-admission. The proposed interaction between TML and HF was summarized in Figure 4. These results indicate that detection of serum TML may provide further value for making out patients at risk for HF and long-term poor prognosis.

A healthy intestinal barrier prevents intestinal bacteria and harmful substances from entering the bloodstream. As a result of HF, the intestine becomes congested and edematous, the intestinal barrier is damaged, and intestinal flora and

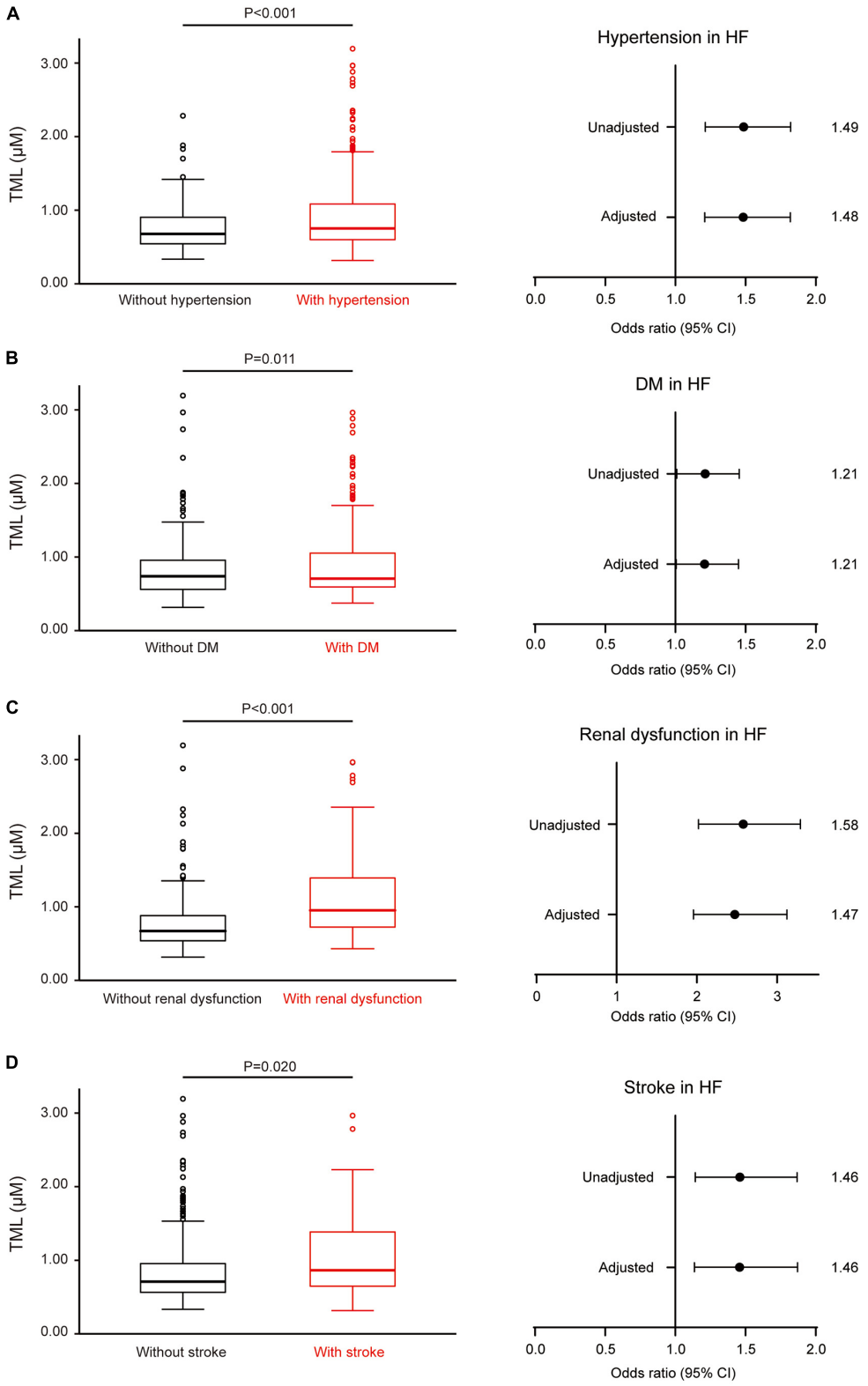

FIGURE 2
Trimethyllysine (TML) levels are associated with several complications in patients with heart failure (HF). **(A)** In HF patients, serum levels of TML are elevated in those with hypertension than those without it. The forest plot at right illustrates the odds of the presence of hypertension according to TML levels in patients with HF, both unadjusted and adjusted for age, sex, and body mass index (BMI). Similar results were found regarding diabetes mellitus (DM) **(B)**, renal dysfunction **(C)**, and stroke **(D)**.

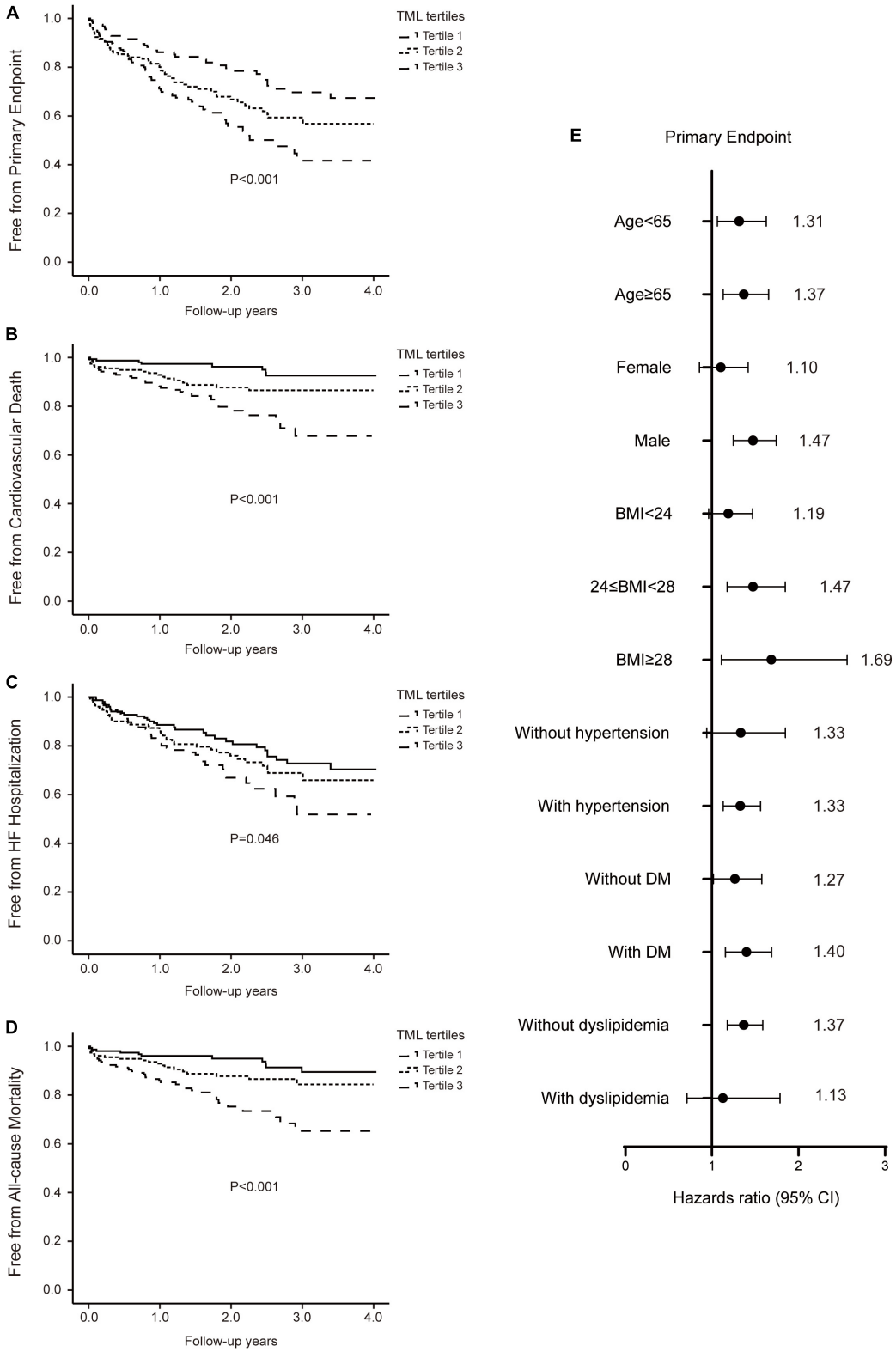

FIGURE 3
Increased trimethyllysine (TML) levels are associated with poor prognosis in patients with heart failure (HF). Kaplan–Meier curves and log-rank analyses illustrating the risks of the primary endpoint **(A)**, cardiovascular (CV) death **(B)**, hospitalization due to HF **(C)**, and all-cause mortality **(D)**, stratified by the tertiles of TML levels in patients with HF. **(E)** Forest plots indicating the risks of the primary endpoint in different subgroups according to TML levels in patients with HF. Symbols represent hazard ratios (HRs) and line length indicates the 95% confidence intervals.

TABLE 3 Trimethyllysine (TML) was associated with poor prognosis in patients with heart failure (HF).

	Unadjusted HR	*P*-value	Adjusted for model 1 HR	*P*-value	Adjusted for model 2 HR	*P*-value
Primary endpoint						
log TML per SD	1.35 (1.17–1.55)	<0.001	1.33 (1.16–1.53)	<0.001	1.20 (1.03–1.39)	0.018
TML tertiles	1.49 (1.22–1.82)	<0.001	1.51 (1.24–1.85)	<0.001	1.37 (1.12–1.68)	0.002
Tertile 1	1 (ref)		1 (ref)		1 (ref)	
Tertile 2	1.60 (1.05–2.44)	0.03	1.66 (1.09–2.54)	0.019	1.62 (1.06–2.47)	0.026
Tertile 3	2.25 (1.49–3.39)	<0.001	2.33 (1.54–3.52)	<0.001	1.93 (1.27–2.93)	0.002
Cardiovascular death						
log TML per SD	1.66 (1.34–2.06)	<0.001	1.64 (1.32–2.02)	<0.001	1.41 (1.13–1.76)	0.002
TML tertiles	2.10 (1.47–3.01)	<0.001	2.15 (1.50–3.08)	<0.001	1.94 (1.35–2.78)	<0.001
Tertile 1	1 (ref)		1 (ref)		1 (ref)	
Tertile 2	2.27 (0.99–5.23)	0.053	2.212 (0.96–5.12)	0.064	2.24 (0.97–5.16)	0.059
Tertile 3	4.56 (2.09–9.96)	<0.001	4.67 (2.13–10.21)	<0.001	3.96 (1.80–8.72)	0.001
HF hospitalization						
log TML per SD	1.22 (1.02–1.45)	0.028	1.21 (1.02–1.44)	0.028	1.17 (0.99–1.40)	0.073
TML tertiles	1.34 (1.06–1.69)	0.014	1.36 (1.08–1.71)	0.01	1.32 (1.05–1.67)	0.019
Tertile 1	1 (ref)		1 (ref)		1 (ref)	
Tertile 2	1.31 (0.81–2.11)	0.267	1.36 (0.84–2.19)	0.212	1.33 (0.82–2.15)	0.243
Tertile 3	1.79 (1.12–2.85)	0.015	1.84 (1.16–2.94)	0.01	1.75 (1.09–2.80)	0.019
All-cause mortality						
log TML per SD	1.62 (1.32–1.98)	<0.001	1.59 (1.30–1.94)	<0.001	1.41 (1.14–1.73)	0.002
TML tertiles	2.02 (1.45–2.80)	<0.001	2.05 (1.47–2.86)	< 0.001	1.85 (1.33–2.57)	<0.001
Tertile 1	1 (ref)		1 (ref)		1 (ref)	
Tertile 2	1.77 (0.84–3.71)	0.134	1.71 (0.81–3.61)	0.162	1.73 (0.82–3.64)	0.150
Tertile 3	3.88 (1.97–7.66)	<0.001	3.96 (2.00–7.82)	<0.001	3.34 (1.68–6.64)	0.001

Model 1: adjusted for age and sex. Model 2: adjusted for age, sex, body mass index (BMI), hypertension, diabetes mellitus (DM), hemoglobin, albumin, creatinine, low-density lipoprotein cholesterol, glycosylated hemoglobin, and trimethylamino oxide.

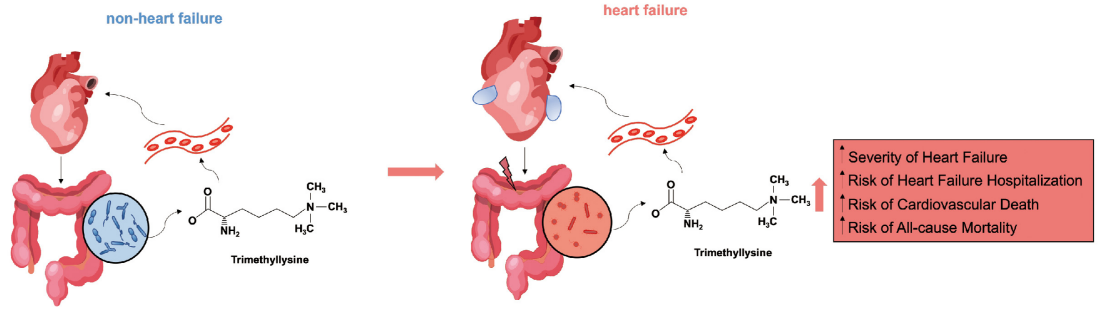

FIGURE 4
Summary diagram outlining the proposed relationship between trimethyllysine (TML) and heart failure (HF). In non-HF conditions, TML synthesis and blood entry are minimal under the protection of the balanced intestinal flora and a healthy intestinal barrier. When HF occurs, the heart's ability to pump blood decreases, the gut becomes congested and edematous, and the prevalent harmful bacteria, as well as the impaired intestinal barrier together, make TML easier to enter the bloodstream. Elevated circulating levels of TML are independently associated with the severity and poor prognosis of HF.

metabolites enter the bloodstream, aggravating inflammation and cardiac dysfunction (4). Many intestinal flora metabolites are associated with HF, particularly TMAO (7, 17). A study analyzing some TMAO-carnitine/choline pathway metabolic products found a relationship between TML and poor prognosis in patients with acute HF (16). Another small study investigating carnitine metabolism and HF also detected increased levels of L-carnitine and its precursor TML in patients with HF (18). TML levels were positively related to NTproBNP and CRP levels and negatively associated with cardiac index and eGFR (18), which was in accordance with the results of the present study. Nonetheless, it is the first study to indicate the predictive

value of TML in patients with stable HF with a relatively large population.

In spite of the discovered association between TML and incident HF risks as well as poor prognosis, the underlying mechanisms interpreting the strong relationship have not been fully elucidated. On the one hand, a recent study found that trimethyl-5-aminovaleric acid, a derivative of TML, inhibits fatty acid metabolism in cardiac myocytes and exacerbates myocardial hypertrophy, and HF (19), which could be a possible way in which TML plays a role in HF. On the other hand, TML is also an intermediate, rate-limiting factor for carnitine biosynthesis (20), and carnitine may play a role in HF pathophysiology. Carnitine is an important transporter to carry fatty acid into mitochondria (21, 22). However, there is a shift in energy metabolism in the pathological heart during HF, indicated by the reduced utilization of fatty acids and the increased utilization of glucose and ketone bodies (23). As a probably compensatory mechanism to rescue fatty acid metabolism, thus improving cardiac function, circulating carnitine levels are found to increase during HF (16, 18). Thus, our observations suggest that measuring TML levels, as an intermediate in carnitine biosynthesis, may discover patients with severe cardiac metabolic dysfunction, thereby causing HF, and poor prognosis. The current study also found that TML was correlated with hsCRP, which indicates that TML may also play a part in the inflammatory process during HF.

Another mechanism is the potential function of TML to form TMA and TMAO, the prothrombotic and atherogenic metabolite (11). Gut microbiota-derived metabolite TMAO plasma levels have been found to be positively correlated to increased CV risk and mortality (24). It can modulate cholesterol and sterol metabolism in multiple compartments and enhance atherosclerosis (25). Previous studies have also found a relationship between TML and atherosclerosis (9, 13). In patients with acute coronary syndrome, TML is a predictor of future major adverse CV events (10, 11). However, elevated TAMO was not associated with cardiac systolic dysfunction, although high TMAO was observed in HF patients and portended long-term mortality risk (7), while our study found a relationship between TML and systolic dysfunction. The present study also investigated the relationship between TML and TMAO levels. In line with recent studies (10, 11, 15), a strong association between serum levels of TML and TMAO was observed at baseline. However, different from other TMAO-producing dietary sources, such as carnitine, choline, or betaine, whose prognostic value was abolished following the inclusion of TMAO into regression models (26, 27), TML could predict the presence of HF in all subjects as well as the poor prognosis in HF patients independent of TMAO. Thus, alternative mechanisms to TMAO may also explain the observed relationship between TML and HF, which needs to be explored in future studies.

On the other hand, the major sources of TML in the human body involve both exogenous and endogenous mechanisms. Exogenous assumptions from both animal-and plant-based foods, such as meat, seafood, and vegetables, are an important dietary source of TML, where TML is widely present in the protein-bound form (11, 28, 29). Endogenous production of TML is a portion of the post-translational modification of proteins in mammals. It took part in the process of the modification in histone during chromatin remodeling as well as gene expression regulation (30–32). The identification of the contributions of microbial versus eukaryotic cells in TML production will have an important impact in exploring the function of TML in CV diseases including HF.

In the present study, we indicated a significant relationship between TML and the complications of HF, including hypertension, DM, renal dysfunction, and stroke. At baseline, elevated TML levels were discovered among participants with a medical history of hypertension, DM, or renal dysfunction, which is in accordance with the findings of other cohorts (15). Another study also demonstrated that in patients with coronary artery disease, serum TML levels can predict the risk of type 2 DM independently of traditional risk factors (33), partly due to dysfunctional acid metabolism. Although the specific mechanisms underlying each complication need to be explored in future studies, these complications, which are related to increased TML levels, could further influence the overall state of patients with HF and lead to a high mortality rate and poor prognosis.

Among all these processes, which one is the major underlying mechanism accounting for the association between serum TML levels and HF has not been identified, and it is debated whether increased TML concentration is the cause or result of HF, which needs further exploration. Nevertheless, TML may help identify patients with a high risk of HF and poor prognosis, and promotion in preventive risk-reducing efforts in HF.

Study limitations

First, this was a single-center study, and data about dietary intake which could affect metabolite levels were not available. The present study also did not specifically differentiate the etiologies of HF and compared TML levels in each group. Furthermore, our study measured circulating TML levels at a single time point, and the changes in TML levels as time goes on need to be examined in future studies. Some unidentified confounding effects might not have been evaluated, and the study was not designed to detect other carnitine/choline metabolites besides TMAO. The mechanisms underlying the relationship between TML and HF will be explored in further studies. Nonetheless, our study provides novel insights which provide clinical links between intestinal flora-associated metabolite TML and the pathophysiology of HF with application prospects and research value.

Conclusion

In conclusion, serum levels of TML provide independent clinical value for the presence and severity of chronic HF. It could also provide clinical value for poor prognosis and mortality among patients with chronic HF.

Data availability statement

The raw data supporting the conclusions of this article will be made available by the authors, without undue reservation.

Ethics statement

The studies involving human participants were reviewed and approved by the Ethics Committee of Ruijin Hospital, Ethics Committee reference number: 2016-019. The patients/participants provided their written informed consent to participate in this study.

Author contributions

XZ, QF, QY, and RT contributed to all stages including the conception and design of this study and interpretation of the data. XZ, RP, QY, and LZ were integral to the design of the study and the data collection. QF and RX took charge of the statistical analysis. RX and RZ also assisted with the interpretation of the data. QF contributed to drafting the article, together with RZ and RT participating in revising the version to be submitted. All authors assisted with preparing the manuscript itself as well as revising the manuscript for important intellectual content, and they also had read and approved the manuscript.

Funding

This study was supported by the National Nature Science Foundation of China (81970327 to RT and 82000368 to QF); "Chen Guang" project supported by the Shanghai Municipal Education Commission and Shanghai Education Development Foundation (KY20211453 to QF).

Acknowledgments

We wish to thank all the participants in the study for their patience and understanding. We also wish to acknowledge all the doctors and researchers in the Department of Cardiovascular Medicine, Ruijin Hospital who contributed to the data collection. Particularly, we thank Simin Yang, Meng Liu, and Yong Zuo of Core Facility of Basic Medical Sciences, Shanghai Jiao Tong University School of Medicine for their technical support of LC-MS.

Conflict of interest

The authors declare that the research was conducted in the absence of any commercial or financial relationships that could be construed as a potential conflict of interest.

Publisher's note

Supplementary material

The Supplementary Material for this article can be found online at: https://www.frontiersin.org/articles/10.3389/fcvm.2022.907997/full#supplementary-material

SUPPLEMENTARY FIGURE 1
Receiver operating characteristic (ROC) curve for predicting the presence of heart failure (HF).

References

1. Yancy CW, Jessup M, Bozkurt B, Butler J, Casey DE Jr, Drazner MH, et al. 2013 ACCF/AHA guideline for the management of heart failure: executive summary: a report of the American college of cardiology foundation/American heart association task force on practice guidelines. *Circulation.* (2013) 128:1810–52. doi: 10.1161/CIR.0b013e31829e8807

2. Salzano A, Cassambai S, Yazaki Y, Israr MZ, Bernieh D, Wong M, et al. The gut axis involvement in heart failure: focus on trimethylamine N-oxide. *Heart Fail Clin.* (2020) 16:23–31. doi: 10.1016/j.hfc.2019.08.001

3. Busnelli M, Manzini S, Chiesa G. The gut microbiota affects host pathophysiology as an endocrine organ: a focus on cardiovascular disease. *Nutrients.* (2019) 12:79. doi: 10.3390/nu12010079

4. Tang WHW, Li DY, Hazen SL. Dietary metabolism, the gut microbiome, and heart failure. *Nat Rev Cardiol.* (2019) 16:137–54. doi: 10.1038/s41569-018-0108-7

5. Tang WHW, Backhed F, Landmesser U, Hazen SL. Intestinal microbiota in cardiovascular health and disease: JACC state-of-the-art review. *J Am Coll Cardiol.* (2019) 73:2089–105. doi: 10.1016/j.jacc.2019.03.024

6. Suzuki T, Heaney LM, Bhandari SS, Jones DJ, Ng LL. Trimethylamine N-oxide and prognosis in acute heart failure. *Heart.* (2016) 102:841–8. doi: 10.1136/heartjnl-2015-308826

7. Tang WH, Wang Z, Fan Y, Levison B, Hazen JE, Donahue LM, et al. Prognostic value of elevated levels of intestinal microbe-generated metabolite trimethylamine-N-oxide in patients with heart failure: refining the gut hypothesis. *J Am Coll Cardiol.* (2014) 64:1908–14. doi: 10.1016/j.jacc.2014.02.617

8. Hayashi T, Yamashita T, Watanabe H, Kami K, Yoshida N, Tabata T, et al. Gut microbiome and plasma microbiome-related metabolites in patients with decompensated and compensated heart failure. *Circ J.* (2018) 83:182–92. doi: 10.1253/circj.CJ-18-0468

9. Skagen K, Troseid M, Ueland T, Holm S, Abbas A, Gregersen I, et al. The carnitine-butyrobetaine-trimethylamine-N-oxide pathway and its association with cardiovascular mortality in patients with carotid atherosclerosis. *Atherosclerosis.* (2016) 247:64–9. doi: 10.1016/j.atherosclerosis.2016.01.033

10. Li XS, Obeid S, Wang Z, Hazen BJ, Li L, Wu Y, et al. Trimethyllysine, a trimethylamine N-oxide precursor, provides near- and long-term prognostic value in patients presenting with acute coronary syndromes. *Eur Heart J.* (2019) 40:2700–9. doi: 10.1093/eurheartj/ehz259

11. Li XS, Wang Z, Cajka T, Buffa JA, Nemet I, Hurd AG, et al. Untargeted metabolomics identifies trimethyllysine, a TMAO-producing nutrient precursor, as a predictor of incident cardiovascular disease risk. *JCI Insight.* (2018) 3:e99096. doi: 10.1172/jci.insight.99096

12. Hulse JD, Ellis SR, Henderson LM. Carnitine biosynthesis. beta-Hydroxylation of trimethyllysine by an alpha-ketoglutarate-dependent mitochondrial dioxygenase. *J Biol Chem.* (1978) 253:1654–9. doi: 10.1016/S0021-9258(17)34915-3

13. Loland KH, Bleie O, Borgeraas H, Strand E, Ueland PM, Svardal A, et al. The association between progression of atherosclerosis and the methylated amino acids asymmetric dimethylarginine and trimethyllysine. *PLoS One.* (2013) 8:e64774. doi: 10.1371/journal.pone.0064774

14. Schiattarella GG, Trimarco B. Microbial metabolites as predictive biomarkers: a paradigm shift for cardiovascular risk stratification. *Eur Heart J.* (2019) 40:2710–2. doi: 10.1093/eurheartj/ehz377

15. Bjornestad EO, Olset H, Dhar I, Loland K, Pedersen EKR, Svingen GFT, et al. Circulating trimethyllysine and risk of acute myocardial infarction in patients with suspected stable coronary heart disease. *J Intern Med.* (2020) 288:446–56. doi: 10.1111/joim.13067

16. Israr MZ, Bernieh D, Salzano A, Cassambai S, Yazaki Y, Heaney LM, et al. Association of gut-related metabolites with outcome in acute heart failure. *Am Heart J.* (2021) 234:71–80. doi: 10.1016/j.ahj.2021.01.006

17. Suzuki T, Yazaki Y, Voors AA, Jones DJL, Chan DCS, Anker SD, et al. Association with outcomes and response to treatment of trimethylamine N-oxide in heart failure: results from BIOSTAT-CHF. *Eur J Heart Fail.* (2019) 21:877–86. doi: 10.1002/ejhf.1338

18. Ueland T, Svardal A, Oie E, Askevold ET, Nymoen SH, Bjorndal B, et al. Disturbed carnitine regulation in chronic heart failure–increased plasma levels of palmitoyl-carnitine are associated with poor prognosis. *Int J Cardiol.* (2013) 167:1892–9. doi: 10.1016/j.ijcard.2012.04.150

19. Zhao M, Wei H, Li C, Zhan R, Liu C, Gao J, et al. Gut microbiota production of trimethyl-5-aminovaleric acid reduces fatty acid oxidation and accelerates cardiac hypertrophy. *Nat Commun.* (2022) 13:1757. doi: 10.1038/s41467-022-29060-7

20. Vaz FM, Wanders RJ. Carnitine biosynthesis in mammals. *Biochem J.* (2002) 361(Pt 3):417–29. doi: 10.1042/bj3610417

21. Calvani M, Reda E, Arrigoni-Martelli E. Regulation by carnitine of myocardial fatty acid and carbohydrate metabolism under normal and pathological conditions. *Basic Res Cardiol.* (2000) 95:75–83. doi: 10.1007/s003950050167

22. Ussher JR, Lopaschuk GD, Arduini A. Gut microbiota metabolism of L-carnitine and cardiovascular risk. *Atherosclerosis.* (2013) 231:456–61. doi: 10.1016/j.atherosclerosis.2013.10.013

23. Ritterhoff J, Tian R. Metabolism in cardiomyopathy: every substrate matters. *Cardiovasc Res.* (2017) 113411–21.

24. Schiattarella GG, Sannino A, Toscano E, Giugliano G, Gargiulo G, Franzone A, et al. Gut microbe-generated metabolite trimethylamine-N-oxide as cardiovascular risk biomarker: a systematic review and dose-response meta-analysis. *Eur Heart J.* (2017) 38:2948–56. doi: 10.1093/eurheartj/ehx342

25. Bennett BJ, de Aguiar Vallim TQ, Wang Z, Shih DM, Meng Y, Gregory J, et al. Trimethylamine-N-oxide, a metabolite associated with atherosclerosis, exhibits complex genetic and dietary regulation. *Cell Metab.* (2013) 17:49–60. doi: 10.1016/j.cmet.2012.12.011

26. Koeth RA, Wang Z, Levison BS, Buffa JA, Org E, Sheehy BT, et al. Intestinal microbiota metabolism of L-carnitine, a nutrient in red meat, promotes atherosclerosis. *Nat Med.* (2013) 19:576–85. doi: 10.1038/nm.3145

27. Wang Z, Tang WH, Buffa JA, Fu X, Britt EB, Koeth RA, et al. Prognostic value of choline and betaine depends on intestinal microbiota-generated metabolite trimethylamine-N-oxide. *Eur Heart J.* (2014) 35:904–10. doi: 10.1093/eurheartj/ehu002

28. Servillo L, Giovane A, Cautela D, Castaldo D, Balestrieri ML. Where does N(epsilon)-trimethyllysine for the carnitine biosynthesis in mammals come from? *PLoS One.* (2014) 9:e84589. doi: 10.1371/journal.pone.0084589

29. Fischer M, Hirche F, Kluge H, Eder K. A moderate excess of dietary lysine lowers plasma and tissue carnitine concentrations in pigs. *Br J Nutr.* (2009) 101:190–6. doi: 10.1017/S0007114508994770

30. Handy DE, Castro R, Loscalzo J. Epigenetic modifications: basic mechanisms and role in cardiovascular disease. *Circulation.* (2011) 123:2145–56. doi: 10.1161/CIRCULATIONAHA.110.956839

31. Greer EL, Maures TJ, Hauswirth AG, Green EM, Leeman DS, Maro GS, et al. Members of the H3K4 trimethylation complex regulate lifespan in a germline-dependent manner in C. elegans. *Nature.* (2010) 466:383–7. doi: 10.1038/nature09195

32. Rhein VF, Carroll J, He J, Ding S, Fearnley IM, Walker JE. Human METTL20 methylates lysine residues adjacent to the recognition loop of the electron transfer flavoprotein in mitochondria. *J Biol Chem.* (2014) 289:24640–51. doi: 10.1074/jbc.M114.580464

33. Strand E, Rebnord EW, Flygel MR, Lysne V, Svingen GFT, Tell GS, et al. Serum carnitine metabolites and incident type 2 diabetes mellitus in patients with suspected stable angina pectoris. *J Clin Endocrinol Metab.* (2018) 103:1033–41. doi: 10.1210/jc.2017-02139

Frontiers in
Cardiovascular Medicine

Innovations and improvements in cardiovascular treatment and practice

Focuses on research that challenges the status quo of cardiovascular care, or facilitates the translation of advances into new therapies and diagnostic tools.

Discover the latest Research Topics

See more →

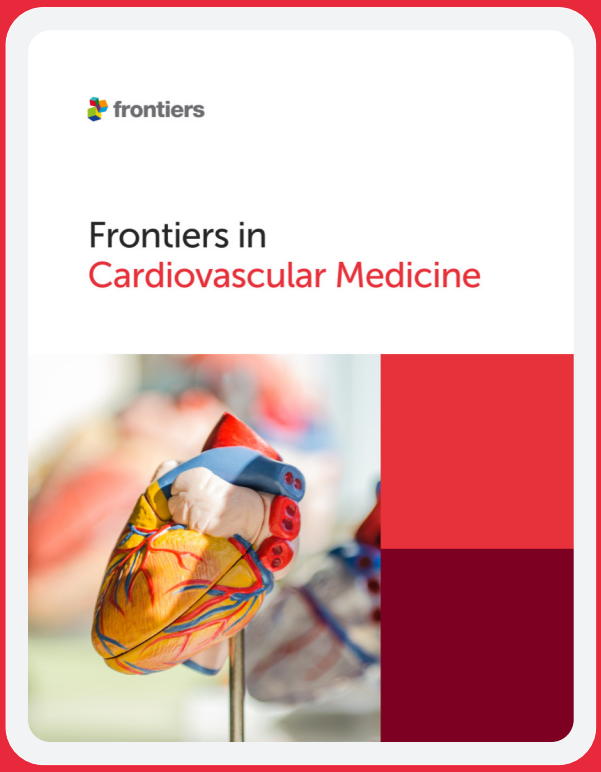

Frontiers

Avenue du Tribunal-Fédéral 34
1005 Lausanne, Switzerland
frontiersin.org

Contact us

+41 (0)21 510 17 00
frontiersin.org/about/contact